Engineering ionic liquid tolerant enzymes

A thesis submitted to the

Faculty of the Graduate School of the

University of Colorado

By

Erik M. Nordwald

B.S., University of Missouri, Columbia, 2010

In Partial Fulfillment of the

Requirements for the Degree of

Doctor of Philosophy

Department of Chemical and Biological Engineering

2015

This thesis entitled:
Engineering ionic liquid tolerant enzymes
written by Erik M. Nordwald
Has been approved for the Department of Chemical and Biological Engineering

_____
(Dr. Joel L. Kaar)

_____
(Dr. Theodore W. Randolph)

Date _____

The final copy of this thesis has been examined by the signatories, and we find that both the content and the form meet acceptable presentation standards of scholarly work in the above mentioned discipline

Nordwald, Erik M. (Ph.D., University of Colorado, Chemical and Biological Engineering)

Engineering ionic liquid tolerant enzymes

Thesis directed by Dr. Joel L. Kaar

As media for biocatalysis, imidazolium based ionic liquids (ILs) have many applications, including improving enzyme refolding, selectivity, and replacing organic solvents as either the bulk media or cosolvent for biocatalysis. Despite their potential as media for biocatalysis, however, ILs have received underwhelming results due to the broad inactivation of enzymes in this media. Activity profiles of enzymes in increasing concentrations of the ionic liquid 1-butyl-3-methylimidazolium chloride ([BMIM][Cl]) show increasing deactivation over time. The deactivation appears unrelated to protein solubility losses but correlated with unfolding based on ultra-violet spectroscopy and fluorescence measurements, respectively. Additionally, equilibrium dialysis measurements show increased IL-enzyme binding at higher concentrations where the enzyme is thought to be unfolded. Increased binding to the denatured state will favor unfolding. Crystallographic studies further shed light on enzyme-IL binding by finding the binding modes of [BMIM][Cl] with enzymes tend to be based on cation-π stacking and hydrophobic interactions. Aromatic and hydrophobic groups are typically in the core of proteins. Unfolding will therefore expose these binding sites allowing for increased binding, as seen in the equilibrium dialysis results.

Our approach to stabilize enzymes in ILs was to mediate preferential IL-enzyme binding. There is a non-specific and site-specific mechanism by which enzymes are proposed to be stabilized. The non-specific approach is based on mutating residues to negatively charged amino acids. The negative charge is thought to repel the anion, [Cl], more than it attracts the cation,

[BMIM], resulting in a net preferential exclusion of the IL. This non-specific preferential exclusion will, hypothetically, drive native state formation based on surface tension effects around the negative charge much like trehalose or other non-specifically excluded osmolytes. Alternatively, specific "high-affinity" sites where [BMIM][Cl] binds may be targeted such as tyrosines. If a tyrosine is exposed in the native state, it can likely still only bind one [BMIM] molecule from the exposed side. In the unfolded state, the tyrosine can now bind two [BMIM] molecules (one on either side). In theory, mutation of this high affinity residue will result in stabilization by eliminating one binding site in the folded protein and two binding sites in the unfolded protein.

Non-specific chemical modification approaches to model enzymes found that, in four cases, removing positively charged residues for a neutral moiety improved enzyme activity retention. Meanwhile, in all four cases, removing negatively charged residues for a neutral moiety was deleterious for enzyme stability. Certainly, this observation is a result of the total stability of the enzyme, which is the sum of its intrinsic stability (i.e. in buffer alone) and its ability to favorably mediate IL-solvent interactions. However, it was found that the intrinsic stability, measured via urea unfolding midpoint in buffer, was lower for all variants than the wild-type for two enzymes (the other two were not measured). While enzyme stabilization in ionic liquids may not be achieved via this chemical modification with every enzyme, it provides support for surface charge as a tool to non-specifically alter enzyme stability in ILs.

A site-specific approach to mediating binding interactions was employed using 2D HSQC NMR. [BMIM][Cl] was titrated into the enzyme sample, and perturbations in the resonance values of various peaks were observed. These peaks were interpreted as binding sites. In support of this, soaking enzyme crystals in [BMIM][Cl] resulted in resolution of [BMIM] and

[Cl] molecules surrounding the residues with the largest resonance perturbations. Mutation to a glutamic acid at the location with the largest perturbations resulted in decreased chemical shift perturbations of the amino acids surrounding the mutation upon titration of the mutant enzyme with [BMIM][Cl]. Mutagenesis also resulted in an enhanced activity retention profile in [BMIM][Cl]. Moreover, two highly exposed positive charges on the enzyme were mutated to a glutamic acid in attempt to non-specifically exclude [BMIM][Cl]. Both mutations resulted in enhanced activity retention of the enzyme in [BMIM][Cl], although to varying degrees. Combination of stabilizing mutations around the surface of the enzyme provided an additive effect on stability. The mutations did not, however, improve the melting temperature of the enzyme in the absence of IL, suggesting the intrinsic stability of the enzyme in buffer was not enhanced. Moreover, activity retention profiles in [BMIM][Cl] show an equilibrium being achieved which is higher for the mutant enzyme than the wild-type, suggesting thermodynamic stabilization, and not purely a kinetic effect based on altering the unfolding barrier. Crystallographic studies of the mutant and wild-type enzymes showed a [BMIM] molecule resolved at tyrosine 49 for the wild-type enzyme, but not at glutamic acid 49 in the mutant. Also, equilibrium dialysis suggested decreased binding of [BMIM][Cl] to the mutant relative to the wild-type enzyme, consistent with the proposed mechanism of stabilization via reducing IL-enzyme binding, which would be stronger (and therefore more reduced by mutation) in the denatured state.

For my father, Michael Nordwald, mother, Anne Nordwald, sister, Sarah Beers, and brother, David Nordwald, for their encouragement and support, without which this thesis would not exist.

Acknowledgements

I would like to thank my thesis adviser, Joel Kaar, for providing funding, support, and guidance throughout this project. He has provided me with the opportunity to be successful.

I would also like to thank the Kaar-group members, David Fallon, Sam Summers, James Weltz, Nuria Codina, Garrett Chado, Alaksh Choudhury and Navdeep Grover for their support. After myself, Kelsey MacConaghey has been here the longest and has been integral in building the lab. Joseph Plaks has provided excellent ideas, discussion, and work on this project. Sean YuMcloughlin has aided in my understanding and execution of molecular biology techniques. Lauren Woodruff and Sean Lynch were instrumental in helping me start my project and learning about molecular biology in general.

Dr. Michael Himmel has provided me a great deal of support and training as a researcher. Dr. Roman Brunecky has been extremely helpful in developing ideas and testing them. I would like to thank Dr. Ryan Gill for offering his laboratory when I first began, as well as advice throughout my thesis. I would like to thank Dr. Marcelo Sousa for his time and patience in teaching me the basics of crystallography. Thanks to Dr. Geoffrey Armstrong for his time and insight on NMR studies. Thanks to Dr. Randolph for discussions on thermodynamics.

I would also like to thank C2B2 and the GAANN fellowship for funding on my project for one year and one semester, respectively.

I would like to acknowledge my friends from graduate and undergraduate school for the support and advice to get through graduate school, which is a test of many things. A special thanks to Arezou Seifpour for her help.

I would like to thank my family for the support that allowed me to continue through graduate school. My father's advice is what preserved my focus and resolve through this all.

Contents

Tables

Figures

Chapter 1 Introduction

1.1 Biocatalysis in non-conventional solvents

Altering the solvent environment of a protein has the ability to tune enzyme substrate and product selectivity,[1] reduce microbial contamination, solubilize hydrophobic substrates,[2] reduce side reactions,[3] and reverse reaction equilibrium in some cases.[4, 5] For example, in the polar solvent, water, chymotrypsin is specific for the hydrophobic substrate N-acetyl-phenylalanine ethyl ester by 50,000 fold over the polar substrate N-acetyl-serine-ethyl ester. However, in the hydrophobic solvent, octane, the serine substrate is roughly 3-fold more reactive than the hydrophobic phenylalanine one.[4] Chirality and enantiomeric selectivity is also affected. Based on steric constraints, the S or R form of a substrate may become more desolvated upon binding to an enzyme and this desolvation may or may not be favorable depending on solvent polarity. In the absence of water, chymotrypsin can acetylate chiral dimethoxybenzyl propanedial to give the S product in hydrophobic solvents, or the R product in hydrophilic solvents. For similar reasons, regioselectivity and chemoselectivity of an enzyme can also be altered by tuning the environment.[4] Halling[6] does an excellent job giving a thermodynamic explanation of these results. In short, the solvent environment affects the solvation energy of the substrate. Phenylalanine, has a higher energy of solvation in a polar environment like water, driving binding to the more hydrophobic active site of chymotrypsin. Conversely, in a hydrophobic solvent, like octane, the hydrophobic force driving binding is reduced while a more

polar substrate, like a serine based one, now has a propensity to bind. Interestingly, due to the conformational rigidity of enzyme aggregates in non-aqueous solvents, enzymes have a molecular memory based on the aqueous conditions from which the enzyme was lyophilized (i.e. pH, ligands present).[7] On the point of enzyme rigidity, it is interesting to consider the conformational and kinetic stability of the enzyme in this un-natural environment. In water (although the exact contribution of various forces is still a debate) there is evidence that the major contributors are hydrophobic bonding and hydrogen bonding.[8] But in a non-natural environment like octane what are the major contributors? The hydrophobic effect cannot contribute to conformational stability in octane. To this point, Klibanov has suggested that proteins are conformationally unstable in such media, but kinetically trapped.[9] On the other hand, Pace[10] suggests that in octane, proteins would be stable due to the increased stabilization provided by hydrogen bonds as a result of octane not being able to hydrogen bond and the increased contribution of each hydrogen bond due to the lower dielectric of the media. Nonetheless, many interesting non-conventional solvent systems, such as aqueous-[BMIM][Cl], have propensities to inactivate enzymes by reportedly unfolding enzymes.[11-15] Therefore, making enzymes more robust in unnatural environments will certainly expand the scope of enzymology in general.

1.1.1 Properties of ionic liquids

Ionic liquids (ILs) are a highly interesting class of solvents that can open up new reactions and, in some cases, replace organic solvents as biocatalytic media. ILs are solvents with, by definition, a melting temperature < 100 °C.[16] ILs are very thermostable (typically above 300 °C)[2] and have negligible vapor pressure,[17] allowing high recyclability. Perhaps most interestingly, the properties of ionic liquids such as polarity,[18] hydrophobicity,[19] and

miscibility[20] (for co-solvents, substrates, or products) can be tailored by appropriate modification and combination of the cation and anion.[21] In fact, over 1,000 have been reported.[22] The miscibility behavior is very peculiar. For example, [BMIM][PF_6] is miscible with methanol but not ethanol, yet is soluble with propanol. Moreover, it is soluble with certain hydrophobic solvents such as toluene, but not hexane.[23] To believe this peculiar result, the author had to personally mix this IL with each of these solvents.

Owing to their unique miscibility behavior, ionic liquids show potential to reform reaction technology. For example, in the production of biodiesel from polar methanol and hydrophobic fatty acids, Ha et al.[24] showed that several ionic liquids have the ability to increase reaction rates by solubilizing the fatty acid and methanol substrates together. More intriguingly, at the end of the reaction, there is a phase separation of product oil and fatty acids from IL and methanol, allowing easy extraction of the product. ILs also have oddly high solubility of gasses such as H_2, CO, and O_2 making them attractive solvents for catalytic hydrogenations, carbonylations, hydroformylations, and aerobic oxidations.[2]

One of the most impressive features of imidazolium ILs like 1-butyl-3-methylimidazolium chloride ([BMIM][Cl]) is the ability to solubilize biomass to improve enzymatic breakdown of cellulose[25-29] by disrupting intermolecular hydrogen bonding.[30] In processing biomass, ILs can be used as a pretreatment before enzymatic hydrolysis of cellulose or in a single step breakdown of cellulose with cellulases in ionic liquids.[31] Due to the inactivating effects of ILs on cellulases,[13, 32-35] likely an industrial setup will involve solubilizing biomass in a neat ionic liquid, selectively removing undesired components such as lignin,[21] then diluting the ionic liquid with water to allow for enzymatic hydrolysis. Adding water will aggregate the cellulose, but the cellulose will be much more amorphous than before

dissolution. The process of dissolving biomass and re-aggregating the cellulose has been shown to improve enzymatic reaction rates more than 50-fold.[36] Another method, gaining attention, would be to dissolve biomass in an ionic liquid, then add acid as an initial step to hydrolyze the cellulose, then wash the IL away and finish the breakdown enzymatically.[37, 38] The enzymatic breakdown is necessary as it does not produce side-products like furfural and can give higher conversions than acid hydrolysis of cellulose. Although, even small amounts of IL tend to inactivate cellulases, making even the pretreatment approach difficult without engineering a robust, IL-tolerant enzyme.

1.1.2 Ionic liquids as biocatalytic media: possible reactions and current limitations

As media for biocatalysis, ionic liquids (ILs) have many applications, including improving enzyme refolding,[39-45] stability,[46, 47] selectivity,[3, 43] and replacing organic solvents as either the bulk media or cosolvent for biocatalysis.[19] For example, cytochrome C catalyzes a wide range of reactions with applications in pharmaceuticals.[48, 49] However, the substrates exhibit poor solubility in plain aqueous environments. ILs may be added as co-solvents to improve substrate solubility and reaction rates.[50] Also, as mentioned, some ILs can dissolve high amounts of cellulose and lignin,[21] creating a new opportunity to break down biomass with cellulases and laccases.[33, 36, 51-54] Remarkably, certain proteases and lipases have been used in anhydrous conditions to catalyze esterification, transesterification, and ammonolysis reactions of industrial significance. For instance, lipases can catalyze the production of biodiesel through the transesterification of triglycerides or the esterification of free fatty acids.[55] However, the reaction is limited by the solubility of short chain alcohols in the milieu. Using ILs as the media can solubilize free fatty acids with the alcohol and thus improve biodiesel yields.[56-58]

The production of sugar esters[22] in ionic liquid (IL) media is very auspicious, especially due to high sugar solubility in imidazolium ionic liquids. The transformation of galactosyl lactose, which sells for ~$100/mg and only requires two lactose molecules as substrates, was reported using a cellulase, CelB, and required 45 vol % of the IL 1-methyl-3-methylimidazolium methylsulfate ([MMIM][$MeSO_4$]) to inhibit the competing hydrolysis reaction. Without the IL present, the hydrolysis reaction dominated, but even with the IL yields were only ~30 %. Similarly, the production of N-acetyllactosamine ($7/mg from lactose and acetylglucosamine) was produced in 25 vol% [MMIM][$EtSO_4$].[3] The ionic liquid was proposed to have decreased the water activity of the solution, deterring the hydrolysis reaction. A saturated solution of NaCl was also used to try and eliminate the hydrolysis reaction, but reduced the enzyme's activity to a greater extent while not mitigating the hydrolysis reaction as much as [MMIM][$EtSO_4$]. Various salidrosides (worth ~$6/mg pure) have been synthesized in the presence of 1-butyl-3-methylimidazolium tetrafluoroborate ([BMIM][BF_4]) with a glucosidase.[59] The lipase catalyzed production of cis-pellitorine ($90/mg, substrates at < $0.01/mg), an anti-cancer lead compound,[60] can be made in anhydrous media through amidation of isobutylamine and (2E, 4E) decadienoic acid.[61] The enzymatic production of pellitorine has few side reactions allowing simple purification of the product and the reaction is far more simple and green than the corresponding chemical synthesis.[62]

However, although some ILs have actually been used for enzyme stabilization[63] (even on a multi-year timescale[64]), many ILs (i.e. ILs that dissolve sugars) inactivate enzymes.[65] Accordingly, despite the potential applications, biocatalysis in ILs has received underwhelming results due to the broad inactivation of enzymes in this media.[66, 67] To exploit the immense potential of ILs as solvents for biocatalysis for producing pharmaceuticals,[3, 22, 50] biofuels,[24, 33,

[36] and other fine chemicals,[52] rational approaches to improve enzyme tolerance to ILs are inherently needed. Biocatalytic reactions in neat ILs as well as aqueous-IL mixtures are reported to be limited due to the denaturation of enzymes by ILs, thus negating the excellent solvent properties of ILs.[68-71] While many approaches to improve the stability of enzymes in ILs have been investigated including immobilization, polyethylene glycol modification, and chemical crosslinking have been, in virtually all cases, unsuccessful in expanding the scope of biocatalysis in IL media.[72-78]

1.2 Industrial applications of biocatalysis in non-conventional solvent-systems

There are many examples of industrial biocatalysis in the presence of non-natural solvents, as aqueous mixtures or in anhydrous conditions. **Table 1-1** presents a list of chemicals produced enzymatically at the industrial scale either in neat anhydrous solvents or aqueous-cosolvent mixtures. Of particular interest is the recently launched production of 2-ethylhexyl palmitate (EHP) using lipase. This is uniquely interesting because, typically, the products need to be pharmaceuticals or fine chemicals of high value in order to justify biocatalytic production in anhydrous media. This cosmetic, EHP, on the other hand has rather low margins and sells for ~$15/kg. The ability to label the product as "natural" by making the good enzymatically likely also helps.[79] Of note, the non-aqueous solvents for these potential reactions are organic solvents, not ionic liquids.

Table 1-1. Industrial biocatalysis in non-aqueous solvents or aqueous-cosolvent mixtures.

Company	Product	Enzyme	Scale	Ref
Chemie Linz AG	Enatiopure propionic acids	lipase	kg	[80]
Schering-Plough	Azole antifungal agent	lipase	100kg	[81]
BASF	Enantiopure amines	lipase/esterase	ton	[82]
Enzymol Int. Inc.	Polyphenols	lipase	kg	[83]
BASF	Chiral amines	amidase/lipase	ton	[84]
Pfizer	Ibuprofen	lipase	kg	[85]
Bristol-Myers Squib	Saxagliptin	lipase	kg	[86]
Bristol-Myers Squib	Paclitaxel	lipase	kg	[85]
Eastman	2-ethylhexylpalmitate	lipase	ton	[79]
Evonik Industries	Myristyl myristate	lipase	ton	[79]

1.3 Protein-salt effects

1.3.1 Salt effects on protein solubility

Salts alter the solubility of proteins and are arranged according to their ability to increase or decrease solubility by the Hofmeister series (**Figure 1.1**).[87] Anions that decrease protein solubility are termed kosmotropes, or structure makers, as opposed to chaotropes, or structure breakers. Meanwhile, kosmotropic cations actually increase protein solubility, typically. Kosmotropic anions are excluded from protein surfaces as they prefer to remain hydrated in solution, creating a zone of exclusion, decreasing solubility.[88, 89] Meanwhile, kosmotropic cations like guandinium (Gn^+) or chaotropic anions like thiocyanate (SCN^-) tend to bind to proteins, increasing solubility.[90-92] Interestingly, it seems that anion variation has a larger impact on protein solubility than cation variation. Perhaps this has to do with water structure,[93] and anions being able to hydrate more strongly than cations of roughly the same radius, meaning the hydrogen from water can approach an anion more closely than the oxygen can approach a cation.[94]

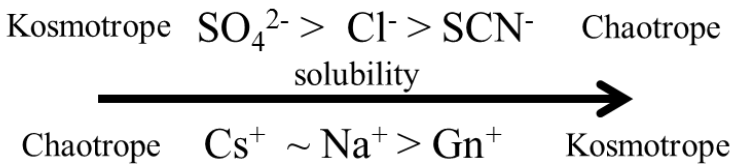

Figure 1.1. Hofmeister series of selected anions and cations. Kosmotropic anions decrease protein solubility while kosmotropic cations increase protein solubility.

Increasing concentration of salts with kosmotropic anions will decrease protein solubility, driving native state aggregation (**Figure 1.2**). This effect has been explained in the context of surface tension around the enzyme.[91] Increasing the surface tension around the enzyme by adding salt promotes aggregation, which minimizes the surface area. Thermodynamically, this can be expressed with the Gibbs free energy as $dG = \gamma dA$. Here G is the Gibbs free energy, γ is surface tension, and A is surface area. An increase in surface tension requires that the surface area is decreased to minimize dG (at constant temperature, pressure, moles). **Figure 1.2** describes the decrease in solubility of proteins in the presence of a salting-out ion, sulfate. The sulfate ion prefers to interact with water rather than protein. This creates a zone of exclusion which is minimized in the aggregated state. Specifically, the surface area of three aggregated proteins is smaller than three proteins in solution.

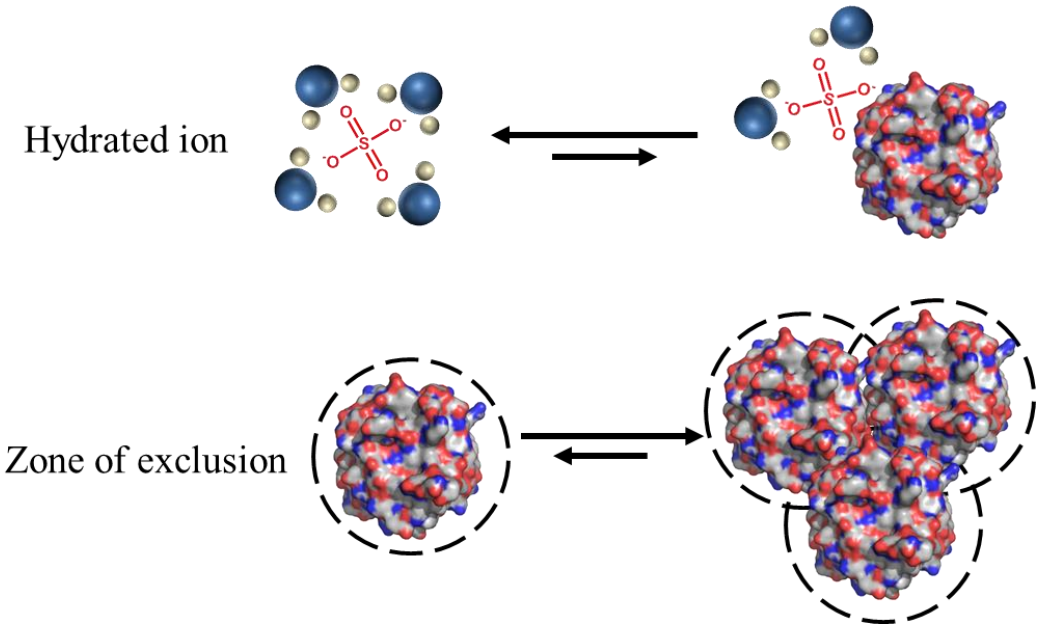

Figure 1.2. (A) Kosmotropic sulfate anion prefers to interact with water than the protein surface. (B) This creates a zone of exclusion which is minimized in the aggregated state. Blue and white spheres represent water.

1.3.2 Salt effects on protein stability

Von Hippel and Wong[95, 96] explored the effect of salts on protein stability[97-99] (**Figure 1.3**). In their seminal science paper, they added increasing molarity of various salts to ribonuclease A and performed differential scanning calorimetry to measure the melting temperature. They found that, as a function of salt concentration, protein melting temperature increases with salting-out ions and decreases with salting-in ions. They also found that, like with solubility, anions seem to have a bigger effect on altering protein thermostability than cations. **Figure 1.3** shows a select few of the salts they used to measure the melting temperature as a function of salt concentration. Their overall observations, which have been repeated and expanded by many others,[100-102] were that some ions, such as chloride, sodium, and potassium seem to be relatively inert in effecting protein stability. Other ions, such as SO_4, are excluded

from protein surfaces and increase protein stability with increasing concentration. Salting-in ions, however, like thiocyanate and guanidinium ions tend to decrease the melting temperature.

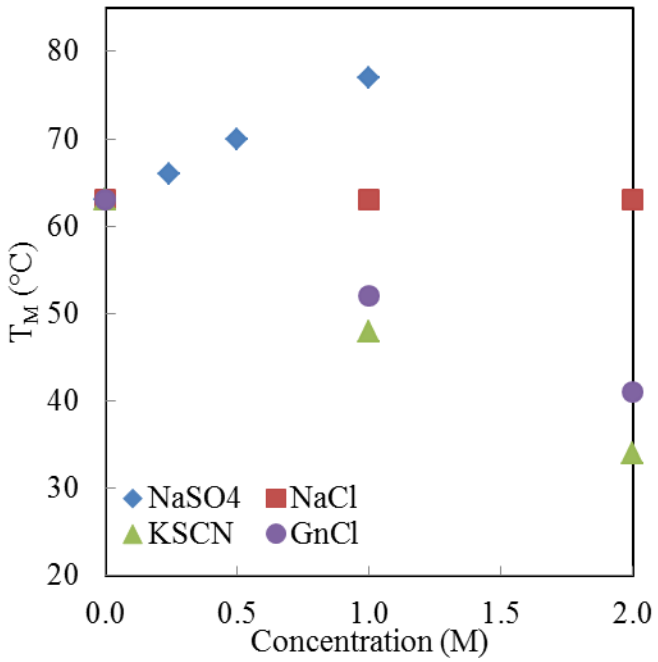

Figure 1.3. The melting temperature of ribonuclease A with the addition of various salts, sodium sulfate ($NaSO_4$), sodium chloride (NaCl), sodium thiocyanate (NaSCN), and guanidinium chloride (GnCl). The figure has been adapted from Von Hippel et al.[96]

Salts alter the stability of proteins based on a non-specific surface and specific binding effects, illustrated by **Figure 1.4**. Stabilizing ions, like sulfates, increase the surface tension around the macromolecule. Upon protein unfolding, there is an increase in surface area, which becomes more unfavorable as the surface tension is raised. In an interesting work by Lin and Timasheff[103] on the change in melting temperature of ribonuclease A with added solutes, they found a close correlation between the surface tension of water and the protein's melting temperature. The surface tension of water decreases at elevated temperatures while adding trehalose to water increases surface tension. Adding trehalose to a solution of ribonuclease A causes an increase in the protein's T_m by roughly the amount required to lower the surface

tension of water to that of a solution without trehalose. Many salts increase the surface tension around a macromolecule. This increase in surface tension drives compact, native states over unfolded polypeptides with large surface areas.

Solutes that are non-specifically excluded from proteins often promote the native state based on surface tension effects.[104] However, deviations occur based on specific binding interactions in the folded or unfolded states. For example, while a sulfate ion prefers hydration to a polar protein surface, it most certainly prefers hydration to the hydrophobic residues that reside in a protein interior. This is another, perhaps even larger, force driving proteins to remain in the native state and not expose their hydrophobic groups to the charged SO_4 anion. Conversely, Gn cations bind to peptide groups which are more exposed in the denatured state, driving unfolding. As will be discussed in the following background section, protein-salt effects on stability and solubility can be best understood in terms of *binding*, which can be positive (preferential binding) or negative (preferential hydration, or exclusion). To this point, for non-specifically excluded solutes, increased surface area of the denatured state creates a larger zone of exclusion for the excluded solute, resulting in more unfavorable negative binding. Also, whether describing stability in terms of binding, or surface tension, one is speaking about topics that are directly related through the Gibbs adsorption isotherm.

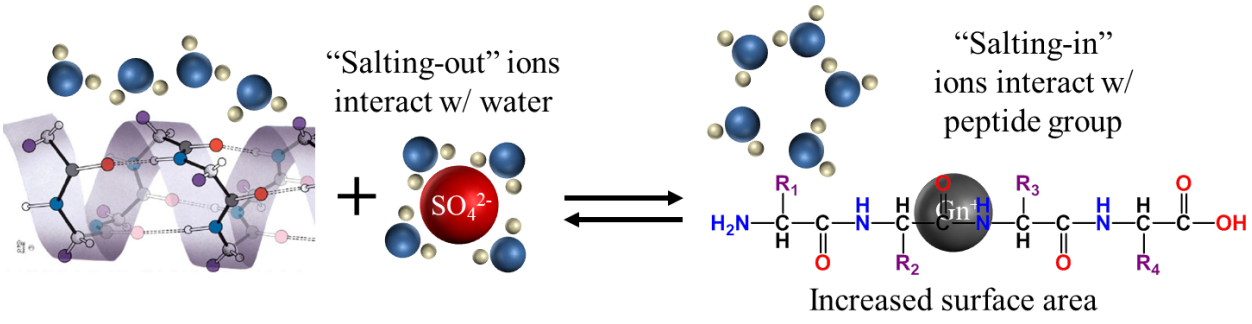

Figure 1.4. Water (blue sphere with white hydrogens) interacts with a protein exterior. A sulfate anion prefers to remain hydrated in solution than interact with the protein. Sulfates, therefore, favor native state proteins, which have smaller surface area. The unfolded polypeptide exposes

more peptide groups for the guanidinium cation to bind, favoring the unfolded state. Far left protein structure reproduced from Fundamentals of Biochemistry, 3rd Ed.[105]

1.3.3 Protein-salt binding

Traditional binding is typically thought of as site occupancy. That is if a ligand is present, it is bound. This works for ligands with strong affinities (i.e. K_d < μM) where the concentrations of ligand are low enough that the probability of a ligand being present without binding is extremely low. However, in the case of salt binding, often times there are multi-molar quantities of ligand present in solution that can, in some cases, take up 50 vol % or more of the solution.[106, 107] In this situation, if there is no protein-solvent binding, there is a high chance of finding that ligand at a particular spot. Therefore, we define binding as an excess quantity $\Gamma_{2,3} \equiv \left(\frac{\partial m_3}{\partial m_2}\right)_{\mu_3,T.P} = -\left(\frac{\partial \mu_2}{\partial \mu_3}\right)_{m_2,T,P}$.[108-112] In this equation, $\Gamma_{2,3}$ is the preferential binding parameter, m_3 is the molality of component 3 (ligand), m_2 is the molality of component 2 (protein), μ_3 is the chemical potential of ligand, μ_2 is the chemical potential of protein, T is temperature and P is pressure.[113] This expression can be thought of as how many molecules of component 3 must be added to a solution to restore its chemical potential upon adding a molecule of protein (component 2).[114] This definition of binding is purely thermodynamic and, importantly, based on the previous sentence shows that "…a molecule does not have to be in contact with a macromolecule to be bound to it…"[115, 116] Tanford suggests that a protein may, in fact, influence binding over as much as a few solvation layers.[111] This may especially be true in the context of synergistic ligand binding where ligands may have more affinity for themselves than principal solvent, water. If ligands have a certain affinity for themselves, perhaps one binding location on a protein surface actually binds two or more ligands. **Figure 1.5** attempts to illustrate

this concept of protein domain binding. Compared to the bulk solution there can either be an excess of salt molecules or a deficiency meaning preferential binding or hydration, respectively, which have opposite thermodynamic consequences on the thermodynamic stability of that particular state. Binding decreases the Gibbs free energy of that particular state (native state shown) whereas exclusion raises the Gibbs free energy.[117]

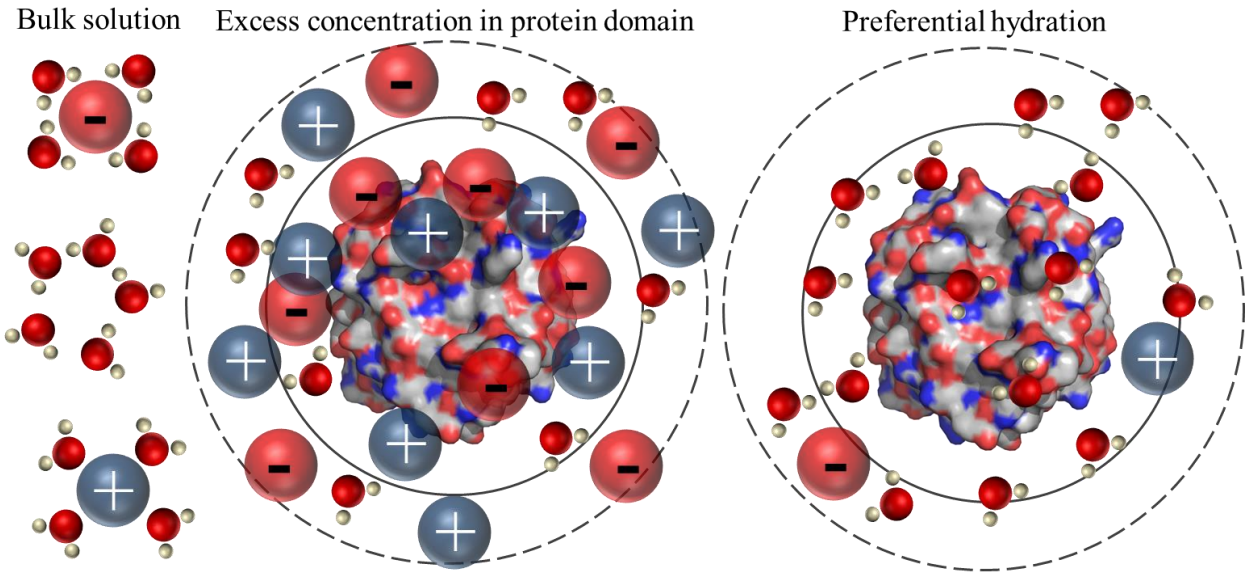

Figure 1.5. Preferential binding and preferential exclusion. Compared to bulk solution, the domain of the protein can contain either excess quantities or deficiencies of ligand. The domain of the protein is anywhere the protein exerts an influence on the solvent and consists of a solvent layer immediately adjacent to the protein (solid line) and potentially beyond into the solvent (dashed line). Waters are represented by a small red sphere (oxygen) with white spheres (hydrogens).

There are a few techniques to measure preferential binding: isopiestic distillation, vapor pressure osmometry, or equilibrium dialysis.[118] Equilibrium dialysis is probably the most easily accessible to the researcher. Here, protein is dialyzed against a solution containing ligand. At equilibrium in a membrane experiment, the chemical potential of diffusible components is the same on either side of the membrane (μ_3, μ_1). Therefore, measuring the amount of ligand in

different dialysis bags gives the excess ligand in solution as a function of protein concentration with all the data points having the same μ_3, μ_1. The slope of this plot (ligand vs. protein concentration) gives $\left(\frac{\partial m_3}{\partial m_2}\right)_{\mu_3,\mu_1,T}$ a slightly different binding parameter which is roughly equivalent to $\Gamma_{2,3}$.[119] Note that the osmotic pressure from the dialysis experiments makes the constant pressure assumption invalid. Also, typically infinite dilution of macromolecule is assumed in these assays such that non-idealities from protein-protein interactions are small.[120, 121] Equilibrium dialysis of salts with various proteins has been studied extensively by Timasheff and co-workers.[122, 123] The result of his, and others',[119, 124] work is that binding of salts to proteins is what mediates solubility and stability. Salts that decrease the solubility of proteins are preferentially excluded. This is explained clearly by the Gibbs adsorption isotherm, $\Gamma_i = -\frac{1}{RT}\frac{\partial \gamma}{\partial \ln(C_i)}$. This relates the excess of component 'i', Γ_i, at a surface to the surface tension, γ, and concentration of ligand, C_i (more accurately, the activity). This shows that if increasing the concentration of ligand increases the surface tension, there will be a deficiency (negative excess) of component 'i' at the surface. However, if increasing the concentration of ligand decreases the surface tension, then there will be ligand binding. Recalling section 1.3.1, increasing the surface tension drives minimizing surface area ($dG = \gamma dA$), thus favoring the aggregated state. Therefore, preferential exclusion favors aggregation via surface tension effects that lower protein solubility.[104] Conversely, binding will increase the solubility of that state in solution.

In terms of stability, there are two things that need be considered in relation to binding, the folded and unfolded states. In the Appendix, there is a derivation of the Wyman linkage relation,[125] $\frac{-1}{RT}\frac{\partial \Delta G}{\partial ln a_x} = \frac{\partial \ln(K)}{\partial ln a_x} = \upsilon_D - \upsilon_N = \Delta\upsilon$. Here, subscripts D and N designate the denatured and native state, ν is the total number of ligands bound to a particular state, a_x is the

activity of ligand x, and K is the protein unfolding equilibrium constant. We see that as ligand is added, if the number of molecules bound to the denatured state is larger than the number of molecules bound to the native state, the equilibrium constant increases, or the ΔG of $N \leftrightarrow D$ decreases, favoring the unfolded state. Therefore, something can bind tightly to the native state, but still destabilize a protein by binding more tightly to the unfolded state. For example, guanidinium cations bind to peptide groups, some of which are exposed in the native state. This creates some binding (increasing protein solubility) to the native state. However, as the protein unfolds more peptides are exposed (see **Figure 1.4**) meaning a larger number of cations are bound to the unfolded state.

Another note about salt binding, elucidated by Timasheff, is that the nature of the cation *and* anion seems to be important, and somewhat additive.[126] In an interesting study,[127] Timasheff and co-workers measured the binding of GnCl to BSA and found, as expected, preferential binding to the protein, correlating with a decrease in melting temperature. However, $GnSO_4$ was actually preferentially excluded from the domain of the protein correlating with an increase in melting temperature. It appears the SO_4 anion, which is known to be preferentially excluded, overcomes Gn binding. As shown here, the binding of salt-pairs is important. Moreover, as was observed for salt effects on the solubility measurements of Hofmeister[87] and the stability measurements of Von Hippel,[96] anion variation, apparently, has a larger impact on determining whether a salt binds to or is excluded from a protein domain. In light of the binding of salt-pairs, we have a condition of electroneutrality in bulk solution and in the domain of the protein.[128, 129] Shown in **Figure 1.5** is a counter-ion to balance every charge in the bulk and domain of the protein. Of course, this electroneutrality includes the charged groups on the protein surface, meaning the colloid in **Figure 1.5** must have equal positive and negative

charges. In light of Timasheff's result and electroneutrality, perhaps the SO_4 anion, which has negative affinity for the protein domain, recruits Gn cations away from the protein domain despite the positive affinity Gn ions have for proteins in order to maintain an electroneutral state. Equally, the Cl (from GnCl) must be in the domain of the protein to counterbalance excess Gn cations bound to the protein.

1.3.4 Solvent denaturation and protein stability

Since Pace and Green,[130] often people measure the conformational stability of a protein via linear extrapolation method, $\Delta G = m[Denaturant] + \Delta G^o$.[131] The ΔG of a protein is obtained accurately in various concentrations of denaturant where there are significant populations of denatured and native protein (transition region of unfolding curve), then the ΔG^o or stability in the absence of denaturant is obtained by back extrapolating to zero concentration of denaturant.[130, 132] This linearity falls out of application of the binding polynomial (see Appendix), which shows that the m-value can be related to the increase in molecules that bind to the protein upon denaturation.[133-136]

How does ν_N and ν_D from the Wyman linkage relation change with denaturant concentration? The Appendix shows hypothetical binding isotherms (analogous to traditional binding isotherms of Θ, occupancy, vs. ligand concentration) for weak and moderate binding for up to five binding sites. This expresses approximately how ν_N and ν_D may change with denaturant concentration. If there is one molecule that can bind to the native state and five that can bind to the unfolded state, you would get an increasing Δν with ligand concentration for weak binding (K_d ~ mM) but not for even moderate binding (K_d ~ μM) at ligand concentrations around ~1 M. This is because the binding sites are completely saturated at 1 M for strong binding, in both the unfolded and folded states. Under the strong binding condition, and at molar

concentrations, because the Δν is not changing, the ΔG for protein stability (see Wyman linkage relation) would not be changing linearly with ligand concentration. Mathematically this is described by Equation 1.26, $\Delta\nu = \frac{-x}{RT}\frac{d\Delta G}{dx}$ (Appendix, also Wyman linkage relation). Here x is the activity of ligand. If Δν is not a function of ligand concentration (x), as would be the case for saturation of binding in the native and denatured states, integrating Equation 1.26 shows that the ΔG would decrease with ln(x). These types of plots that deviate from linearity have been observed by Fersht et al.[137] However, if Δν increases roughly linearly with ligand concentration, as in the case of very weak binding, integration of Equation 1.26 shows that the ΔG changes linearly with ligand concentration. An example of ΔG as a function of ligand activity for very weak and moderate binding is shown using the independent site binding model in **Figure 12.1**. The binding must be very weak (~mM K_d values) to be consistent with the experimentally observed ΔG values around molar quantities of ligand.[102, 117, 118] This also tells us (**Figure 12.1**) that the binding in the native and unfolded states may still be increasing at, even, molar concentrations. This interpretation is more complicated when considering multiple, strong and weak, binding modes, and this model, itself, is not without flaw. Nonetheless, this knowledge is important for practical consideration of experimental design as well as data interpretation of ionic liquid effects on protein stability throughout the thesis. For example, is binding non-specific at many sites, resulting in a linear decrease in ΔG with ionic liquid concentration? Or is binding mostly from highly specific modes, resulting in a quick decrease in stability followed by a leveling off (assuming this is denatured state binding)? Answering these questions about ILs should give insight into non-specific and site-specific ways binding can be mediated to stabilize enzymes.

1.4 References

1. Ke, T., C.R. Wescott, and A.M. Klibanov, *Prediction of the solvent dependence of enzymatic prochiral selectivity by means of structure-based thermodynamic calculations.* Journal of the American Chemical Society, 1996. **118**(14): p. 3366-3374.
2. Sheldon, R., *Catalytic reactions in ionic liquids.* Chemical Communications, 2001(23): p. 2399-2407.
3. Kaftzik, N., P. Wasserscheid, and U. Kragl, *Use of ionic liquids to increase the yield and enzyme stability in the beta-galactosidase catalysed synthesis of N-acetyllactosamine.* Organic Process Research & Development, 2002. **6**(4): p. 553-557.
4. Klibanov, A.M., *Improving enzymes by using them in organic solvents.* Nature, 2001. **409**(6817): p. 241-246.
5. Schmid, A., et al., *Industrial biocatalysis today and tomorrow.* Nature, 2001. **409**(6817): p. 258-268.
6. Halling, P.J., *Thermodynamic Predictions for Biocatalysis in Nonconventional Media - Theory, Tests, and Recommendations for Experimental-Design and Analysis.* Enzyme and Microbial Technology, 1994. **16**(3): p. 178-206.
7. Klibanov, A.M., *Enzyme Memory - What Is Remembered and Why.* Nature, 1995. **374**(6523): p. 596-596.
8. Pace, C.N., *Energetics of protein hydrogen bonds.* Nature Structural & Molecular Biology, 2009. **16**(7): p. 681-682.
9. Koskinen, A. and A.M. Klibanov, *Enzymatic reactions in organic media*1996.
10. Pace, C.N., et al., *Protein structure, stability and solubility in water and other solvents.* Philosophical Transactions of the Royal Society of London Series B-Biological Sciences, 2004. **359**(1448): p. 1225-1234.
11. Griebenow, K. and A.M. Klibanov, *On protein denaturation in aqueous-organic mixtures but not in pure organic solvents.* Journal of the American Chemical Society, 1996. **118**(47): p. 11695-11700.
12. Nordwald, E.M., G.S. Armstrong, and J.L. Kaar, *NMR-Guided Rational Engineering of an Ionic-Liquid-Tolerant Lipase.* Acs Catalysis, 2014. **4**(11): p. 4057-4064.
13. Nordwald, E.M., et al., *Charge Engineering of Cellulases Improves Ionic Liquid Tolerance and Reduces Lignin Inhibition.* Biotechnology and Bioengineering, 2014. **111**(8): p. 1541-1549.
14. Nordwald, E.M. and J.L. Kaar, *Stabilization of Enzymes in Ionic Liquids Via Modification of Enzyme Charge.* Biotechnology and Bioengineering, 2013. **110**(9): p. 2352-2360.
15. Nordwald, E.M. and J.L. Kaar, *Mediating Electrostatic Binding of 1-Butyl-3-methylimidazolium Chloride to Enzyme Surfaces Improves Conformational Stability.* Journal of Physical Chemistry B, 2013. **117**(30): p. 8977-8986.
16. Zhao, H., *Methods for stabilizing and activating enzymes in ionic liquids - a review.* Journal of Chemical Technology and Biotechnology, 2010. **85**(7): p. 891-907.
17. Pinkert, A., et al., *Ionic Liquids and Their Interaction with Cellulose.* Chemical Reviews, 2009. **109**(12): p. 6712-6728.
18. Sheldon, R.A., et al., *Biocatalysis in ionic liquids.* Green Chemistry, 2002. **4**(2): p. 147-151.

19. van Rantwijk, F. and R.A. Sheldon, *Biocatalysis in ionic liquids.* Chemical Reviews, 2007. **107**(6): p. 2757-2785.
20. Freire, M.G., et al., *An overview of the mutual solubilities of water-imidazolium-based ionic liquids systems.* Fluid Phase Equilibria, 2007. **261**(1-2): p. 449-454.
21. Brandt, A., et al., *The effect of the ionic liquid anion in the pretreatment of pine wood chips.* Green Chemistry, 2010. **12**(4): p. 672-679.
22. Galonde, N., et al., *Use of ionic liquids for biocatalytic synthesis of sugar derivatives.* Journal of Chemical Technology and Biotechnology, 2012. **87**(4): p. 451-471.
23. Carda-Broch, S., A. Berthod, and D.W. Armstrong, *Solvent properties of the 1-butyl-3-methylimidazolium hexafluorophosphate ionic liquid.* Analytical and Bioanalytical Chemistry, 2003. **375**(2): p. 191-199.
24. Ha, S.H., et al., *Lipase-catalyzed biodiesel production from soybean oil in ionic liquids.* Enzyme and Microbial Technology, 2007. **41**(4): p. 480-483.
25. Alvira, P., et al., *Pretreatment technologies for an efficient bioethanol production process based on enzymatic hydrolysis: A review.* Bioresource Technology, 2010. **101**(13): p. 4851-4861.
26. Groff, D., et al., *Acid enhanced ionic liquid pretreatment of biomass.* Green Chemistry, 2013. **15**(5): p. 1264-1267.
27. Klein-Marcuschamer, D., B.A. Simmons, and H.W. Blanch, *Techno-economic analysis of a lignocellulosic ethanol biorefinery with ionic liquid pre-treatment.* Biofuels Bioproducts & Biorefining-Biofpr, 2011. **5**(5): p. 562-569.
28. Li, Q., et al., *Improving enzymatic hydrolysis of wheat straw using ionic liquid 1-ethyl-3-methyl imidazolium diethyl phosphate pretreatment.* Bioresource Technology, 2009. **100**(14): p. 3570-3575.
29. Shill, K., et al., *Ionic Liquid Pretreatment of Cellulosic Biomass: Enzymatic Hydrolysis and Ionic Liquid Recycle.* Biotechnology and Bioengineering, 2011. **108**(3): p. 511-520.
30. Zhang, J.M., et al., *NMR spectroscopic studies of cellobiose solvation in EmimAc aimed to understand the dissolution mechanism of cellulose in ionic liquids.* Physical Chemistry Chemical Physics, 2010. **12**(8): p. 1941-1947.
31. Fu, D.B. and G. Mazza, *Optimization of processing conditions for the pretreatment of wheat straw using aqueous ionic liquid.* Bioresource Technology, 2011. **102**(17): p. 8003-8010.
32. Turner, M.B., et al., *Ionic liquid salt-induced inactivation and unfolding of cellulase from Trichoderma reesei.* Green Chemistry, 2003. **5**(4): p. 443-447.
33. Bose, S., C.A. Barnes, and J.W. Petrich, *Enhanced stability and activity of cellulase in an ionic liquid and the effect of pretreatment on cellulose hydrolysis.* Biotechnology and Bioengineering, 2012. **109**(2): p. 434-443.
34. Datta, S., et al., *Ionic liquid tolerant hyperthermophilic cellulases for biomass pretreatment and hydrolysis.* Green Chemistry, 2010. **12**(2): p. 338-345.
35. Park, J.I., et al., *A Thermophilic Ionic Liquid-Tolerant Cellulase Cocktail for the Production of Cellulosic Biofuels.* Plos One, 2012. **7**(5).
36. Li, C.L., et al., *Comparison of dilute acid and ionic liquid pretreatment of switchgrass: Biomass recalcitrance, delignification and enzymatic saccharification.* Bioresource Technology, 2010. **101**(13): p. 4900-4906.
37. Rinaldi, R., et al., *An Integrated Catalytic Approach to Fermentable Sugars from Cellulose.* Chemsuschem, 2010. **3**(10): p. 1151-1153.

38. Uju, et al., *Peracetic acid-ionic liquid pretreatment to enhance enzymatic saccharification of lignocellulosic biomass.* Bioresource Technology, 2013. **138**: p. 87-94.
39. Akdogan, Y. and D. Hinderberger, *Solvent-Induced Protein Refolding at Low Temperatures.* Journal of Physical Chemistry B, 2011. **115**(51): p. 15422-15429.
40. Buchfink, R., et al., *Ionic liquids as refolding additives: Variation of the anion.* Journal of Biotechnology, 2010. **150**(1): p. 64-72.
41. Constatinescu, D., C. Herrmann, and H. Weingartner, *Patterns of protein unfolding and protein aggregation in ionic liquids.* Physical Chemistry Chemical Physics, 2010. **12**(8): p. 1756-1763.
42. Noritomi, H., et al., *Thermal stability of proteins in the presence of aprotic ionic liquids.* Journal of biomedical science and engineering, 2011. **4**: p. 94-99.
43. Attri, P., P. Venkatesu, and A. Kumar, *Activity and stability of alpha-chymotrypsin in biocompatible ionic liquids: enzyme refolding by triethyl ammonium acetate.* Physical Chemistry Chemical Physics, 2011. **13**(7): p. 2788-2796.
44. Lange, C., G. Patil, and R. Rudolph, *Ionic liquids as refolding additives: N '-alkyl and N '-(omega-hydroxyalkyl) N-methylimidazolium chlorides.* Protein Science, 2005. **14**(10): p. 2693-2701.
45. Summers, C.A. and R.A. Flowers, *Protein renaturation by the liquid organic salt ethylammonium nitrate.* Protein Science, 2000. **9**(10): p. 2001-2008.
46. Weaver, K.D., et al., *Structure and function of proteins in hydrated choline dihydrogen phosphate ionic liquid.* Physical Chemistry Chemical Physics, 2012. **14**(2): p. 790-801.
47. Rodrigues, J.V., et al., *Protein stability in an ionic liquid milieu: on the use of differential scanning fluorimetry.* Physical Chemistry Chemical Physics, 2011. **13**(30): p. 13614-13616.
48. Kuper, J., et al., *The role of active-site Phe87 in modulating the organic co-solvent tolerance of cytochrome P450 BM3 monooxygenase.* Acta Crystallographica Section F-Structural Biology and Crystallization Communications, 2012. **68**: p. 1013-1017.
49. Munro, A.W., et al., *P450 BM3: the very model of a modern flavocytochrome.* Trends in biochemical sciences, 2002. **27**(5): p. 250-257.
50. Tee, K.L., et al., *Ionic liquid effects on the activity of monooxygenase P450BM-3.* Green Chemistry, 2008. **10**(1): p. 117-123.
51. Liu, H.F., et al., *Directed laccase evolution for improved ionic liquid resistance.* Green Chemistry, 2013. **15**(5): p. 1348-1355.
52. Park, S. and R.J. Kazlauskas, *Biocatalysis in ionic liquids - advantages beyond green technology.* Current Opinion in Biotechnology, 2003. **14**(4): p. 432-437.
53. Fu, D.B. and G. Mazza, *Aqueous ionic liquid pretreatment of straw.* Bioresource Technology, 2011. **102**(13): p. 7008-7011.
54. Kamiya, N., et al., *Enzymatic in situ saccharification of cellulose in aqueous-ionic liquid media.* Biotechnology Letters, 2008. **30**(6): p. 1037-1040.
55. Hwang, H.T., et al., *Lipase-catalyzed process for biodiesel production: Protein engineering and lipase production.* Biotechnology and Bioengineering, 2013.
56. De Diego, T., et al., *A recyclable enzymatic biodiesel production process in ionic liquids.* Bioresource Technology, 2011. **102**(10): p. 6336-6339.
57. Zhang, K.P., et al., *Penicillium expansum lipase-catalyzed production of biodiesel in ionic liquids.* Bioresource Technology, 2011. **102**(3): p. 2767-2772.

58. Lozano, P., et al., *One-Phase Ionic Liquid Reaction Medium for Biocatalytic Production of Biodiesel.* Chemsuschem, 2010. **3**(12): p. 1359-1363.
59. Yang, R.L., N. Li, and M.H. Zong, *Using ionic liquid cosolvents to improve enzymatic synthesis of arylalkyl beta-D-glucopyranosides.* Journal of Molecular Catalysis B-Enzymatic, 2012. **74**(1-2): p. 24-28.
60. Ee, G.C.L., et al., *Pellitorine, a Potential Anti-Cancer Lead Compound against HL60 and MCT-7 Cell Lines and Microbial Transformation of Piperine from Piper Nigrum.* Molecules, 2010. **15**(4): p. 2398-2404.
61. Ley, J.P., et al., *Stereoselective enzymatic synthesis of cis-pellitorine, a taste active alkamide naturally occurring in tarragon.* European Journal of Organic Chemistry, 2004(24): p. 5135-5140.
62. Jacobson, M., *Pellitorine Isomers .2. The Synthesis of N-Isobutyl-Trans-2,Trans-4-Decadienamide.* Journal of the American Chemical Society, 1953. **75**(11): p. 2584-2586.
63. Weingartner, H., C. Cabrele, and C. Herrmann, *How ionic liquids can help to stabilize native proteins.* Physical Chemistry Chemical Physics, 2012. **14**(2): p. 415-426.
64. Byrne, N., et al., *Reversible folding-unfolding, aggregation protection, and multi-year stabilization, in high concentration protein solutions, using ionic liquids.* Chemical Communications, 2007(26): p. 2714-2716.
65. Yang, Z., *Hofmeister effects: an explanation for the impact of ionic liquids on biocatalysis.* Journal of Biotechnology, 2009. **144**(1): p. 12-22.
66. Engel, P., et al., *Point by point analysis: how ionic liquid affects the enzymatic hydrolysis of native and modified cellulose.* Green Chemistry, 2010. **12**(11): p. 1959-1966.
67. Singh, T., et al., *Ionic Liquids Induced Structural Changes of Bovine Serum Albumin in Aqueous Media: A Detailed Physicochemical and Spectroscopic Study.* Journal of Physical Chemistry B, 2012. **116**(39): p. 11924-11935.
68. Baker, G.A. and W.T. Heller, *Small-angle neutron scattering studies of model protein denaturation in aqueous solutions of the ionic liquid 1-butyl-3-methylimidazolium chloride.* Chemical Engineering Journal, 2009. **147**(1): p. 6-12.
69. Baker, S.N., et al., *Fluorescence energy transfer efficiency in labeled yeast cytochrome c: a rapid screen for ion biocompatibility in aqueous ionic liquids.* Physical Chemistry Chemical Physics, 2011. **13**(9): p. 3642-3644.
70. Heller, W.T., et al., *Characterization of the Influence of the Ionic Liquid 1-Butyl-3-methylimidazolium Chloride on the Structure and Thermal Stability of Green Fluorescent Protein.* Journal of Physical Chemistry B, 2010. **114**(43): p. 13866-13871.
71. Kaar, J.L., et al., *Impact of ionic liquid physical properties on lipase activity and stability.* Journal of the American Chemical Society, 2003. **125**(14): p. 4125-4131.
72. Nakashima, K., et al., *Comb-shaped poly(ethylene glycol)-modified subtilisin Carlsberg is soluble and highly active in ionic liquids.* Chem Commun, 2005. **34**(34): p. 4297-4299.
73. Persson, M. and U.T. Bornscheuer, *Increased stability of an esterase from Bacillus stearothermophilus in ionic liquids as compared to organic solvents.* J Mol Catal B: Enzym, 2003. **22**(1-2): p. 21-27.
74. Schofer, S.H., et al., *Enzyme catalysis in ionic liquids: lipase catalysed kinetic resolution of 1-phenylethanol with improved enantioselectivity.* Chem Commun, 2001. **5**(5): p. 425-426.
75. Toral, A.R., et al., *Cross-linked Candida antarctica lipase B is active in denaturing ionic liquids.* Enzyme Microb Technol, 2007. **40**(5): p. 1095-1099.

76. Vafiadi, C., et al., *Feruloyl esterase-catalysed synthesis of glycerol sinapate using ionic liquids mixtures.* J Biotechnol, 2009. **139**(1): p. 124-129.
77. van Rantwijk, F., F. Secundo, and R.A. Sheldon, *Structure and activity of Candida antarctica lipase B in ionic liquids.* Green Chem, 2006. **8**(3): p. 282-286.
78. Zhao, H., C.L. Jones, and J.V. Cowins, *Lipase dissolution and stabilization in ether-functionalized ionic liquids.* Green Chem, 2009. **11**(8): p. 1128-1138.
79. Ansorge-Schumacher, M.B. and O. Thum, *Immobilised lipases in the cosmetics industry.* Chemical Society Reviews, 2013. **42**(15): p. 6475-6490.
80. Kirchner, G., M.P. Scollar, and A.M. Klibanov, *Resolution of Racemic Mixtures Via Lipase Catalysis in Organic-Solvents.* Journal of the American Chemical Society, 1985. **107**(24): p. 7072-7076.
81. Zaks, A. and D.R. Dodds, *Application of biocatalysis and biotransformations to the synthesis of pharmaceuticals.* Drug Discovery Today, 1997. **2**(12): p. 513-531.
82. Carrea, G. and S. Riva, *Properties and synthetic applications of enzymes in organic solvents.* Angewandte Chemie-International Edition, 2000. **39**(13): p. 2226-2254.
83. Akkara, J.A., M.S.R. Ayyagari, and F.F. Bruno, *Enzymatic synthesis and modification of polymers in nonaqueous solvents.* Trends in Biotechnology, 1999. **17**(2): p. 67-73.
84. Karl, U. and A. Simon, *BASF's ChiPros (R) chiral building blocks The cornerstones of your API syntheses!* Chimica Oggi-Chemistry Today, 2009. **27**(5): p. 66-69.
85. Solano, D.M., et al., *Industrial biotransformations in the synthesis of building blocks leading to enantiopure drugs.* Bioresource Technology, 2012. **115**: p. 196-207.
86. Gill, I. and R. Patel, *Biocatalytic ammonolysis of (5S)-4,5-dihydro-1H-pyrrole-1,5-dicarboxylic acid, 1-(1,1-dimethylethyl)-5-ethyl ester: Preparation of an intermediate to the dipeptidyl peptidase IV inhibitor Saxagliptin.* Bioorganic & Medicinal Chemistry Letters, 2006. **16**(3): p. 705-709.
87. Hofmeister, F., *Zur Lehre von der Wrikung der Salze. Zweite Mittheilung.* Archiv for Expermentelle Pathologie und Pharmakologie, 1888. **24**: p. 247-260.
88. Timasheff, S.N., *Solvent effects on protein stability.* Current Opinion in Structural Biology, 1992. **2**(1): p. 35-39.
89. Pegram, L.M. and M.T. Record, *Hofmeister salt effects on surface tension arise from partitioning of anions and cations between bulk water and the air-water interface.* Journal of Physical Chemistry B, 2007. **111**(19): p. 5411-5417.
90. Baldwin, R.L., *How Hofmeister ion interactions affect protein stability.* Biophysical Journal, 1996. **71**(4): p. 2056-2063.
91. Pegram, L.M. and M.T. Record, *Thermodynamic origin of Hofmeister ion effects.* Journal of Physical Chemistry B, 2008. **112**(31): p. 9428-9436.
92. Nandi, P.K. and D.R. Robinson, *Effects of Urea and Guanidine-Hydrochloride on Peptide and Nonpolar Groups.* Biochemistry, 1984. **23**(26): p. 6661-6668.
93. Moelbert, S., B. Normand, and P.D. Rios, *Kosmotropes and chaotropes: modelling preferential exclusion, binding and aggregate stability.* Biophysical Chemistry, 2004. **112**(1): p. 45-57.
94. Plumridge, T.H. and R.D. Waigh, *Water structure theory and some implications for drug design.* Journal of Pharmacy and Pharmacology, 2002. **54**(9): p. 1155-1179.
95. Von Hippel, P.H. and K.Y. Wong, *On the conformational stability of globular proteins. The effects of various electrolytes and nonelectrolytes on the thermal ribonuclease transition.* The Journal of biological chemistry, 1965. **240**(10): p. 3909-23.

96. Von Hippel, P.H. and K.Y. Wong, *Neutral Salts: The Generality of Their Effects on the Stability of Macromolecular Conformations.* Science, 1964. **2**: p. 577-580.
97. Becktel, W.J. and J.A. Schellman, *Protein Stability Curves.* Biopolymers, 1987. **26**(11): p. 1859-1877.
98. Schellman, J.A. and R.B. Hawkes, *Protein Stability from Thermal and Solvent Denaturation Curves.* Hoppe-Seylers Zeitschrift Fur Physiologische Chemie, 1979. **360**(8): p. 1015-1015.
99. Pace, C.N. and K.L. Shaw, *Linear extrapolation method of analyzing solvent denaturation curves.* Proteins-Structure Function and Genetics, 2000: p. 1-7.
100. Tadeo, X., M. Pons, and O. Millet, *Influence of the Hofmeister anions on protein stability as studied by thermal denaturation and chemical shift perturbation.* Biochemistry, 2007. **46**(3): p. 917-23.
101. Bye, J.W. and R.J. Falconer, *Thermal stability of lysozyme as a function of ion concentration: A reappraisal of the relationship between the Hofmeister series and protein stability.* Protein Science, 2013. **22**(11): p. 1563-1570.
102. Courtenay, E.S., M.W. Capp, and M.T. Record, *Thermodynamics of interactions of urea and guanidinium salts with protein surface: Relationship between solute effects on protein processes and changes in water-accessible surface area.* Protein Science, 2001. **10**(12): p. 2485-2497.
103. Lin, T.Y. and S.N. Timasheff, *On the role of surface tension in the stabilization of globular proteins.* Protein Science, 1996. **5**(2): p. 372-381.
104. Arakawa, T., R. Bhat, and S.N. Timasheff, *Why Preferential Hydration Does Not Always Stabilize the Native Structure of Globular-Proteins.* Biochemistry, 1990. **29**(7): p. 1924-1931.
105. Donald Voet, Judith G. Voet, and C.W. Pratt, *Fundamentals of Biochemistry*. 3rd ed2008.
106. Schellman, J.A., *Solvent Denaturation.* Biopolymers, 1978. **17**(5): p. 1305-1322.
107. Schellman, J.A., *Selective binding and solvent denaturation.* Biopolymers, 1987. **26**(4): p. 549-59.
108. Timasheff, S.N., *In disperse solution, "osmotic stress" is a restricted case of preferential interactions.* Proceedings of the National Academy of Sciences of the United States of America, 1998. **95**(13): p. 7363-7367.
109. Timasheff, S.N., *Protein-solvent preferential interactions, protein hydration, and the modulation of biochemical reactions by solvent components.* Proceedings of the National Academy of Sciences of the United States of America, 2002. **99**(15): p. 9721-9726.
110. Arakawa, T. and S.N. Timasheff, *Preferential Interactions of Proteins with Salts in Concentrated-Solutions.* Biochemistry, 1982. **21**(25): p. 6545-6552.
111. Tanford, C., *Protein denaturation. C. Theoretical models for the mechanism of denaturation.* Advances in protein chemistry, 1970. **24**: p. 1-95.
112. Casassa, E.F. and H. Eisenberg, *Thermodynamic Analysis of Multicomponent Solutions.* Advances in protein chemistry, 1964. **19**: p. 287-395.
113. Scatchard, G., *Physical chemistry of protein solutions; derivation of the equations for the osmotic pressure.* Journal of the American Chemical Society, 1946. **68**(11): p. 2315-9.
114. Schellman, J.A., *A Simple-Model for Solvation in Mixed-Solvents - Applications to the Stabilization and Destabilization of Macromolecular Structures.* Biophysical Chemistry, 1990. **37**(1-3): p. 121-140.

115. Schellman, J.A., *The Relation between the Free-Energy of Interaction and Binding.* Biophysical Chemistry, 1993. **45**(3): p. 273-279.
116. Timasheff, S.N., *Thermodynamic binding and site occupancy in the light of the Schellman exchange concept.* Biophysical Chemistry, 2002. **101**: p. 99-111.
117. Timasheff, S.N., *Water as Ligand - Preferential Binding and Exclusion of Denaturants in Protein Unfolding.* Biochemistry, 1992. **31**(41): p. 9857-9864.
118. Courtenay, E.S., et al., *Vapor pressure osmometry studies of osmolyte-protein interactions: Implications for the action of osmoprotectants in vivo and for the interpretation of "osmotic stress" experiments in vitro.* Biochemistry, 2000. **39**(15): p. 4455-4471.
119. Anderson, C.F., E.S. Courtenay, and M.T. Record, *Thermodynamic expressions relating different types of preferential interaction coefficients in solutions containing two solute components.* Journal of Physical Chemistry B, 2002. **106**(2): p. 418-433.
120. Timasheff, S.N., *Protein hydration, thermodynamic binding, and preferential hydration.* Biochemistry, 2002. **41**(46): p. 13473-13482.
121. Arakawa, T., R. Bhat, and S.N. Timasheff, *Preferential Interactions Determine Protein Solubility in 3-Component Solutions - the Mgcl2 System.* Biochemistry, 1990. **29**(7): p. 1914-1923.
122. Noelken, M.E. and Timashef.Sn, *Preferential Solvation of Bovine Serum Albumin in Aqueous Guanidine Hydrochloride.* Journal of Biological Chemistry, 1967. **242**(21): p. 5080-&.
123. Arakawa, T. and S.N. Timasheff, *Mechanism of Protein Salting in and Salting out by Divalent-Cation Salts - Balance between Hydration and Salt Binding.* Biochemistry, 1984. **23**(25): p. 5912-5923.
124. Anderson, C.F., et al., *Generalized derivation of an exact relationship linking different coefficients that characterize thermodynamic effects of preferential interactions.* Biophysical Chemistry, 2002. **101**: p. 497-511.
125. Wyman, J., *Linked Functions and Reciprocal Effects in Hemoglobin - a 2nd Look.* Advances in protein chemistry, 1964. **19**: p. 223-286.
126. Timasheff, S.N., *Control of protein stability and reactions by weakly interacting cosolvents: The simplicity of the complicated.* Advances in Protein Chemistry, Vol 51, 1998. **51**: p. 355-432.
127. Arakawa, T. and S.N. Timasheff, *Protein Stabilization and Destabilization by Guanidinium Salts.* Biochemistry, 1984. **23**(25): p. 5924-5929.
128. Lopez-Garcia, J.J., C. Grosse, and J. Horno, *On the use of the hypothesis of local electroneutrality in colloidal suspensions for the calculation of their dielectric properties.* Journal of Physical Chemistry B, 2005. **109**(12): p. 5808-5815.
129. Hill, T.L., *A. Fundamental studies on the theory of the Donnan membrane equilibrium.* Discussions of the Faraday Society, 1955. **21**: p. 31-45.
130. Greene, R.F. and C.N. Pace, *Urea and Guanidine-Hydrochloride Denaturation of Ribonuclease, Lysozyme, Alpha-Chymotrypsin, and Beta-Lactoglobulin.* Journal of Biological Chemistry, 1974. **249**(17): p. 5388-5393.
131. Pace, C.N., *Measuring and Increasing Protein Stability.* Trends in Biotechnology, 1990. **8**(4): p. 93-98.
132. Pace, C.N., *Determination and analysis of urea and guanidine hydrochloride denaturation curves.* Methods in enzymology, 1986. **131**: p. 266-80.

133. Schellman, J.A., *Fifty years of solvent denaturation.* Biophysical Chemistry, 2002. **96**(2-3): p. 91-101.
134. Schellman, J.A., *The Thermodynamic Stability of Proteins.* Annual Review of Biophysics and Biophysical Chemistry, 1987. **16**: p. 115-137.
135. Schellman, J.A., *Macromolecular Binding.* Biopolymers, 1975. **14**(5): p. 999-1018.
136. Schellman, J.A., *The Thermodynamics of Solvent Exchange.* Biopolymers, 1994. **34**(8): p. 1015-1026.
137. Johnson, C.M. and A.R. Fersht, *Protein Stability as a Function of Denaturant Concentration - the Thermal-Stability of Barnase in the Presence of Urea.* Biochemistry, 1995. **34**(20): p. 6795-6804.

Chapter 2 Outline of manuscript: hypothesis and experimental aims

2.1 Part I. Determining the mechanism of ionic liquid induced enzyme inactivation

Recalling the work by Von Hippel[96] et al. as well as Timasheff[109] showing that salts alter protein stability in a concentration dependent manner based on binding, it is interesting to consider if organic salts (ILs) work in a similar manner. To this point, it has been shown that imidazolium based ionic liquids, such as [BMIM][Cl] can unfold enzymes[69] and that [BMIM][Cl] reduces the melting temperature of RnaseA in a similar manner as GnCl.[138] From the potential applications of imidazolium ILs as well as to build off the current knowledge on [BMIM][Cl], the effect of this IL, and similar imidazolium based ionic liquids, on enzymes will be studied.

Hypothesis: ionic liquids inactivate enzymes by inducing unfolding as a result of preferential binding.

There are two aims I propose to understand the mechanism IL-induced enzyme inactivation.

Aim 1: Explore the cause of enzyme inactivation in [BMIM][Cl] and the role of folding state on activity. (**Chapter 3**)

Aim 2: Study the binding modes of [BMIM][Cl] with enzymes. (**Chapter 3** and **Chapter 8**)

2.2 Engineering an ionic liquid tolerant enzyme: a hypothesis towards mediating *specific* binding to enhance enzyme function in ionic liquids

The amount of molecules bound to the unfolded and folded state is linked to the effect of that ligand on the equilibrium constant for unfolding based on the Wyman linkage relation $\frac{dln(K)}{dlnx} = \Delta\nu$. In this equation, K is the equilibrium constant, x is the activity of ligand, and $\Delta\nu$ is the difference in molecules bound to the unfolded vs. folded state. As will be shown, equilibrium dialysis shows [BMIM][Cl] binding to enzymes and more so in the denatured state, resulting in an unfavorable decrease in ΔG as a function of ligand concentration. So how does one mitigate binding based on denaturation, or make $\Delta\nu$ more favorable? There are three methods listed below.

Chapter 1 Decrease denatured state binding, ν_D

Perhaps mutating the residues with high [BMIM][Cl] affinity in the core could accomplish this. However, it is likely that modifying internal packing residues will also reduce the intrinsic stability of the enzyme, if not eliminate its ability to fold altogether.

Chapter 2 Increase native state binding, ν_N

Altering an exposed reside may be better than a drastic mutation to a buried residue. However, in order for this to work, the binding must be *specific* for the native state. Likely all single mutations in the native state that [BMIM][Cl] has an affinity for will also be available for binding in the denatured state. Typically when people mention binding to the native state, it is ligand binding to an active site evolved for a substrate, and in the unfolded state, this binding pocket does not exist.

Chapter 3 Decrease overall binding in both states, favorably alter $\Delta\nu$

If the binding is weak in the native state and strong in the denatured state, eliminating binding would result in relative stabilization. The easiest situation to imagine would be a residue that is partially exposed in the folded state and has some affinity for the IL, then upon unfolding, the

residue becomes completely exposed allowing stronger binding. Perhaps this binding can be reduced, in both states, by mutating an adjacent, highly exposed residue for which [BMIM][Cl] has low affinity. Also, by mutating a highly exposed residue, we are less likely to disrupt the intrinsic stability of the enzyme. A hypothetical example of decreasing binding in both the native and denatured states is depicted in **Figure 2.1**. [BMIM] is proposed to have a high affinity to stack with a tyrosine residue (which will be studied via crystallography). In the unfolded state, [BMIM] can stack on either side of the amino acid, and also with newly exposed hydrophobic groups like leucine. [Cl] is required to bind in the domain to maintain electroneutrality, and likely binds near the backbone. Based on the literature of various [Cl] salts dating back to Hofmiester,[87] it is unlikely [Cl] has a strong affinity to bind to proteins and alter their stability by itself. Mutating the tyrosine lowers the affinity of the IL for the native state of the protein. Shown is 1 [BMIM] binding for electroneutrality, but in real solution conditions perhaps this is actually a sodium ion or an H_3O^+ (this does not change the overall point). In the denatured state, less [BMIM][Cl] molecules bind to the protein, particularly over the range of its influence, shown as a red dotted circle. Here, eliminating a *specific* binding site that becomes stronger in the unfolded state is the primary cause for stabilization. The net result of this hypothetical situation is that $\Delta\nu$ may be more favorable in the situation with the glutamic acid than with the tyrosine. The amount bound to each state, ν, shown in **Figure 2.1**, is simply the sum of [BMIM] and [Cl] bound. Of note, at this point we do not know whether a positive or negative charge will be more favorable for mutagenesis. A negative mutation was chosen as it may also provide stabilization via *non-specific* exclusion. Because most mutations will likely lower the intrinsic stability of the enzyme, and the total enzyme stability in ILs is what we are interested in, the most IL-sensitive locations on an enzyme surface may need to be targeted.

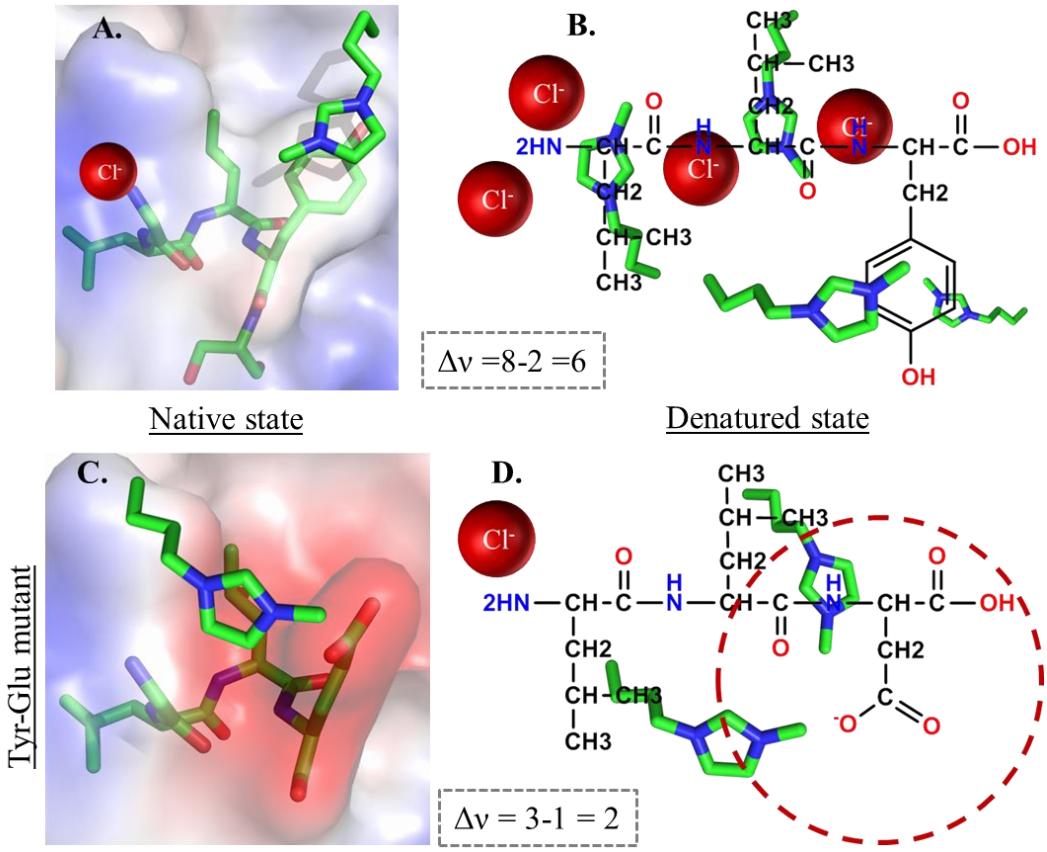

Figure 2.1. Hypothetical alterations in binding to the folded in unfolded states by mutating an exposed residue with high [BMIM][Cl] affinity. (A) Native state binding of a [BMIM] to a tyrosine, a [Cl] binds nearby to satisfy electroneutrality. (B) Unfolding of situation A. results in two [BMIM] molecules being able to cation-π stack with the tyrosine (top and bottom of residue). Also, the leucines which were buried are now exposed and can bind with the butyl chain of the [BMIM]. [Cl] does not necessarily have a high affinity for the backbone, but is recruited by [BMIM] in order to satisfy electroneutrality. (C) Native state binding in the same region as A., except that the tyrosine was mutated to an aspartic acid. (D) The unfolded state of situation C. results in less total binding of the salt [BMIM][Cl] than in B. because [BMIM] has lower affinity for glutamic acid than tyrosine. The difference in molecules bound to the native and denatured states (Δν) is more favorable for situation C-D.

2.3 A hypothesis towards mediating *non-specific* binding to enhance enzyme function in ionic liquids

Perhaps the binding of ILs can be mediating by engineering the charge of the enzyme. If [BMIM] binding is denaturing, perhaps large amounts of positive charge can repel the molecule.

Although, we will find that [BMIM] does not seem to have an affinity for charged, or highly polar, residues but rather hydrophobic residues.[139] Also, salt-pair binding is important.[127] For example, guanidinium ions preferentially bind to protein backbones, like in GnCl. However, when paired with a highly excluded anion, like SO_4, the salt $GnSO_4$ is excluded from the protein, and, as a consequence, is stabilizing to the protein structure.[127]

By mediating this electrostatic and/or hydrophobic[139] binding, enzyme stability in ionic liquids may be enhanced. Interestingly, nature's salt-tolerant proteins, halophiles, have been evolved to contain many acidic amino acids on their surfaces.[140-142] Perhaps one strategy to broadly improve enzyme utility, and mechanistically explore the forces causing enzyme inactivation in ILs, is to alter the surface charge of enzymes. Noting that many IL anions, such as [Cl], are small molecules of high charge density whereas cations usually are bulky hydrophobic compounds with a dispersed charge (such as [BMIM]), engineering enzyme charge could potentially mediate electrostatic interactions between enzymes and anions as well as hydrophobic interactions between the enzymes and the cation. Altering the surface properties of enzymes should provide minimal effects on the internal packing of the enzyme while, ideally, affecting enzyme-IL interactions in a beneficial manner. A situation depicting why modifying surface charged groups could be beneficial is depicted in **Figure 2.2**. Upon unfolding, increased [BMIM] bind to the protein and recruit more [Cl] molecules which cluster around a positive charge primarily. Mutating this residue to a negative amino acid eliminates all [Cl] binding over its influence (red circle) resulting in only 1 [Cl] binding site available. To maintain electroneutrality, only 2 [BMIM] molecules can therefore bind. The binding between the unfolded and folded states ($\Delta\nu$) which defines the impact of ligand on folding equilibrium, is more favorable in the case where the lysine is mutated to a glutamic acid. The reason for the

decreased binding is, essentially, within the influence of the amino acid, the decreased affinity of [Cl] is greater than any marginal increases in affinity [BMIM] gains for the negatively charged residue. Based on the results of this thesis [BMIM] apparently has very little electrostatic attraction or repulsion. Moreover, in the native state there is less surface area of adjacent residues for the glutamic acid to influence than in the denatured state, resulting in a bigger decrease in binding due to the residue with a hypothetical *total* negative affinity for [BMIM][Cl]. To this point, compounds that are nonspecifically excluded from protein surfaces, such as some sugars, typically increase protein stability (**Figure 1.4**).[104]

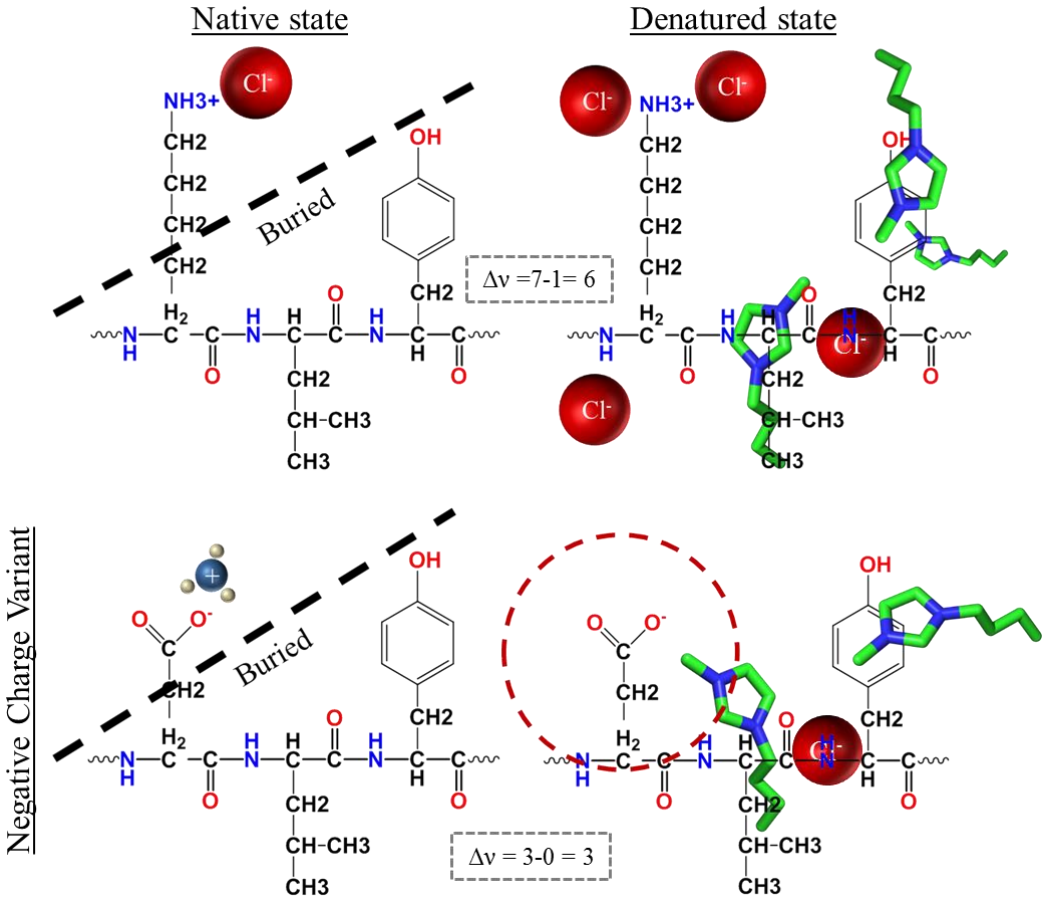

Figure 2.2. Hypothetical preferential binding interactions of a peptide in the native state (A, C) and denatured state (B, D) for where the only change was that a positively charged lysine (A, B) was replaced with an aspartic acid (C, D). The mutation results in a favorable alteration of binding between the unfolded and folded states (Δν). The positive blue sphere with three white spheres is a hydronium ion.

2.4 Part II: Enzyme stabilization via mediating ionic liquid-enzyme binding

Hypothesis: Macromolecule surface charge can favorably alter preferential binding ($\Delta\nu$), resulting in enzyme stabilization

Aim 3: Investigate non-specific and site-specific approaches to improve activity retention by altering [BMIM][Cl] binding.

- **Chapter 4**: The impact of systematic chemical modifications that alter macromolecule charge on kinetic activity will be studied for a few model enzymes.
- **Chapter 5**: The mechanism of stabilization by charge variation will be probed. Specifically, the interaction of the enzyme with the IL as a result of modification and if the modifications resulted in a generic increase in stability will be studied.
- **Chapter 6:** Charge engineering will be applied to a cellulase in an effort to improve the potential for biomass processing in ILs.
- **Chapter 7:** [NMR] will be used to find specific enzyme-IL interaction sites via chemical shift perturbations. The effect of mitigating chemical shift perturbation on activity retention profiles will be explored.
- **Chapter 8:** The mechanism of IL-stabilization of the mutant lipase from Chapter 7 will be explored.

2.5 References

69. Baker, S.N., et al., *Fluorescence energy transfer efficiency in labeled yeast cytochrome c: a rapid screen for ion biocompatibility in aqueous ionic liquids.* Physical Chemistry Chemical Physics, 2011. **13**(9): p. 3642-3644.
87. Hofmeister, F., *Zur Lehre von der Wrikung der Salze. Zweite Mittheilung.* Archiv for Expermentelle Pathologie und Pharmakologie, 1888. **24**: p. 247-260.
96. Von Hippel, P.H. and K.Y. Wong, *Neutral Salts: The Generality of Their Effects on the Stability of Macromolecular Conformations.* Science, 1964. **2**: p. 577-580.
104. Arakawa, T., R. Bhat, and S.N. Timasheff, *Why Preferential Hydration Does Not Always Stabilize the Native Structure of Globular-Proteins.* Biochemistry, 1990. **29**(7): p. 1924-1931.
109. Timasheff, S.N., *Protein-solvent preferential interactions, protein hydration, and the modulation of biochemical reactions by solvent components.* Proceedings of the National Academy of Sciences of the United States of America, 2002. **99**(15): p. 9721-9726.

127. Arakawa, T. and S.N. Timasheff, *Protein Stabilization and Destabilization by Guanidinium Salts.* Biochemistry, 1984. **23**(25): p. 5924-5929.
138. Constantinescu, D., H. Weingartner, and C. Herrmann, *Protein denaturation by ionic liquids and the Hofmeister series: A case study of aqueous solutions of ribonuclease A.* Angewandte Chemie-International Edition, 2007. **46**(46): p. 8887-8889.
139. Klahn, M., et al., *On the different roles of anions and cations in the solvation of enzymes in ionic liquids.* Physical Chemistry Chemical Physics, 2011. **13**(4): p. 1649-1662.
140. Elcock, A.H. and J.A. McCammon, *Electrostatic contributions to the stability of halophilic proteins.* Journal of Molecular Biology, 1998. **280**(4): p. 731-748.
141. Frolow, F., et al., *Insights into protein adaptation to a saturated salt environment from the crystal structure of a halophilic 2Fe-2S ferredoxin (vol 3, pg 452, 1996).* Nature Structural Biology, 1996. **3**(12): p. 1055-1055.
142. Rao, J.K.M. and P. Argos, *Structural Stability of Halophilic Proteins.* Biochemistry, 1981. **20**(23): p. 6536-6543.

Chapter 3 A mechanistic understanding of imidazolium-ionic liquid inactivation lends way towards rational enzyme design

This chapter will be submitted to the Journal of Physical Chemistry B

3.1 Introduction

Understanding protein-salt effects, which are ubiquitous in biocatalysis, will accelerate the growth of biotechnology and protein design. The delicate balance of protein stability, especially in the context of unique solvents, is of interest from an academic as well as practical standpoint. Since Tanford,[111] people have been seeking to understand solvent-denaturation and have made enormous strides in understanding urea, GnCl, and the perturbation of protein thermodynamic stability caused by various salts and co-solvents. It has been explored theoretically and experimentally by Timasheff,[109] Schellman,[133] and others,[99, 112, 113, 124, 125] the close relationship that binding plays in altering protein stability.

Imidazolium based ionic liquids (ILs) are a class of organic salts with unique properties containing the potential to open up additional biocatalytic reactions (production of biofuels,[24, 57] pharmaceuticals,[3, 22, 50] and fine chemicals[52]). However, many imidazolium ionic liquids greatly inactivate enzymes. Part of this inactivation is strictly activity loss due to inhibition,[143] increasing ionic strength, decreasing water activity (for hydrolases), and viscosity changes.[66] In addition to activity decreases with increasing IL concentration, at high IL conditions, the activity over time often decreases.[12-15, 33, 144-146] This activity loss is thought to be due to enzyme unfolding. In support of this, [BMIM][Cl] is reported to unfold various proteins at high concentrations,[68, 69, 147] and lower the melting temperature of RnaseA in a concentration

dependent manner.[138] Also, imidazolium ionic liquids have been used to prevent aggregation and as refolding additives, similar to GnCl, which suggests solubility is not an issue.[41] In fact, reportedly, Cytochrome C was dissolved in neat [BMIM][Cl] in concentrations up to 10 mM.[148]

In order to realize the full potential of ionic liquids as media for biocatalysis, enzymes must be made more robust in this milieu. Here, we explore the cause for inactivation using chymotrypsin from *Bos Taurus* (CT) as a model. In the context of salt-effects on proteins, perturbations in the solubility[87] and conformational stability[112] as a result of preferential binding[120] are the primary effects. Herein, we will specifically examine the effect of protein solubility and folding state in relation to the activity retention profile of CT in aqueous [BMIM][Cl]. Moreover, we will try to understand this in terms of preferential binding and explore possible mechanisms of [BMIM][Cl]-enzyme binding. A mechanistic understanding of [BMIM][Cl] inactivation can lend way towards rational enzyme design for imidazolium IL tolerance.

Folding of proteins in ILs is difficult to measure for a variety of reasons,[149] particularly at such high IL concentrations. Imidazolium swamps circular dichroism signal, even at low concentrations (< 5 vol %). Fourier-transformed infra-red spectroscopy signal is also convoluted by the IL in the amide I region. Also, very high concentrations of protein are necessary for reliable signal even in the absence of IL (> 10 mg/ml) and small amounts of noise make deconvolution of the amide I region difficult (whether by 2nd derivative analysis or Gaussian curve fitting). Raman spectroscopy fails for reasons similar to FTIR (in fact, even higher protein concentrations are needed). Moreover, when examining the influence of folding state and solubility on activity loss, it would be ideal to perform experiments near the same concentration of protein as activity retention experiments. Intrinsic tryptophan fluorescence, however, can

report on enzyme folding state by examining the wavelength at maximum intensity.[150-154] In a low-dielectric environment such as the protein interior, tryptophans have a maximum in fluoresce around ~310 nm.[153, 155-157] However, in a higher dielectric environment such as water, tryptophans have a maximum in fluorescence around 355 nm.[155] Therefore, tryptophan fluorescence can be used as an indicator of solvent exposure, which is related to folding state. Additionally, [BMIM] can quench tryptophan fluorescence.[15, 158-161] This allows us to use the magnitude in fluorescence as an indicator for folding state. In the folded state where an enzyme's tryptophans are more buried, its fluorescence will be quenched to a smaller degree by the [BMIM] molecule than when the enzyme is unfolded and the tryptophans are highly exposed.[162, 163] Moreover, if a two state model for unfolding is applicable, the magnitude of fluorescence can be used to determine fraction of enzyme folded or unfolded.[164] As a practical note, when performing biophysical and spectroscopic studies with ionic liquids, the highest purity is necessary as even small impurities can have large absorbances as well as fluorescence. Ionic liquids should appear colorless.[165] For example, a lower purity batch of ionic liquid (>95%) had fluorescence values ~1-2 orders of magnitude higher than the high purity batch (>98%).

3.2 Materials and methods

3.2.1 Materials

Dialysis membrane with a 12,000 to 16,000 MWCO was purchased from fisher scientific. All other chemicals, including [BMIM][Cl] (>98%), N-succinyl-alanine-alanine-proline-phenylalanine paranitroanalide, urea, and chymotrypsin (CT) from bovine pancreas, were purchased from Sigma Aldrich (St. Louis, MO) and used as supplied.

3.2.2 Chymotrypsin stability in [BMIM][Cl]

CT was incubated in an aqueous-IL solution containing 0-40 vol % [BMIM][Cl] at 30 °C. Enzyme inactivation was followed by removing aliquots periodically and assaying residual enzyme activity in the presence of ILs upon the addition of substrate. To assay residual activity, 975 µL of the enzyme-containing IL solution was added to 25 µL of substrate, stored in dimethylsulfoxide at 10 mg/ml.

3.2.3 Chymotrypsin solubility and fluorescence measurements

At 0.5 mg/ml the optical density at 280 nm and fluorescence of chymotrypsin was followed for up to 30 hours. The temperature for optical density and fluorescence experiments was 30 °C. For optical density measurements, a Thermo Fisher Scientific Evolution 260 Bio UV/Vis spectrophotometer was used. For fluorescence measurements, chymotrypsin was excited at 291 nm and emission recorded from 320 to 370 nm. At concentrations of [BMIM][Cl] < 40 vol %, to determine the spectra of the unfolded protein, the temperature was increased to denature the protein, allowed to equilibrate for 15mins, then the fluorescence measured. To determine the influence of temperature on fluorescence, the fluorescence spectra of chymotrypsin was measured every 5 °C from 60 to 45 °C with 10 min equilibrations at each interval. This data was used to back-extrapolate from 45 °C to 30 °C. Cooling to 30 °C caused an unusually large increase in fluorescence, which we believe is due to CT refolding. To this point, CT does regain activity as well. Of note, the 40 vol % [BMIM][Cl] does not have any activity at the end of the experiment, therefore this melting procedure to get the unfolded spectra was not necessary. At the end of all fluorescence experiments, the optical density was checked to ensure the protein was still soluble.

3.2.4 Equilibrium dialysis

Equilibrium dialysis was performed by placing 0-10 mg/ml concentrations of CT in a 12,000 to 16,000 MWCO dialysis bag under mixing at 30 rpm in 0 – 2.5 M concentrations of [BMIM][Cl]. The sample was equilibrated for 5 days to allow both transport and enzyme unfolding equilibrium to be achieved. After which, the concentration of [BMIM][Cl] in the dialysate as well as inside the dialysis bags, associated with the protein, was measured spectrophotometrically at an optically density of 211 nm. The concentration of [BMIM][Cl] was then converted to a molar concentration using a calibration curve. The concentration of protein was also checked at the end of the experiment by monitoring the absorbance at 280 nm, then converted to a molar concentration using an extinction coefficient of 51,840 (M^{-1},cm^{-1}) for CT. Plotting the molar concentration of [BMIM][Cl] against the molar concentration of protein, the slope is the preferential binding parameter, or the excess moles of IL per mole of protein.

3.2.5 Crystallization of chymotrypsin

This portion of the chapter was conducted by the National Renewable Energy Lab, and the specific details will be added before publication.

3.3 Results and discussion

3.3.1 Chymotrypsin solubility over time in [BMIM][Cl]

The optical density at 280 nm is known to correlate with protein concentration due to the absorbance of strained aromatic amino acids, particularly tryptophan. Therefore, to measure the solubility of CT in [BMIM][Cl], the optical density at 280 nm was measured over time. **Figure 3.1** shows how the solubility of a 0.5 mg/ml solution of CT in 40 vol % [BMIM][Cl] changes with time. This concentration of enzyme and IL was chosen to have high signal and to understand the solubility of the fluorescence and activity experiments presented later. In

particular, we wanted to understand why 0.04 mg/ml of CT in 40 vol % [BMIM][Cl] loses all its activity and that the cause for fluorescent loss at 0.5 mg/ml was not due to solubility. Based on **Figure 3.1**, the activity loss is not related to solubility loss. To this point, solubility should be more of an issue at 0.5 mg/ml (where we observed no decrease in solubility) than at 0.04 mg/ml (where the activity experiments were performed).

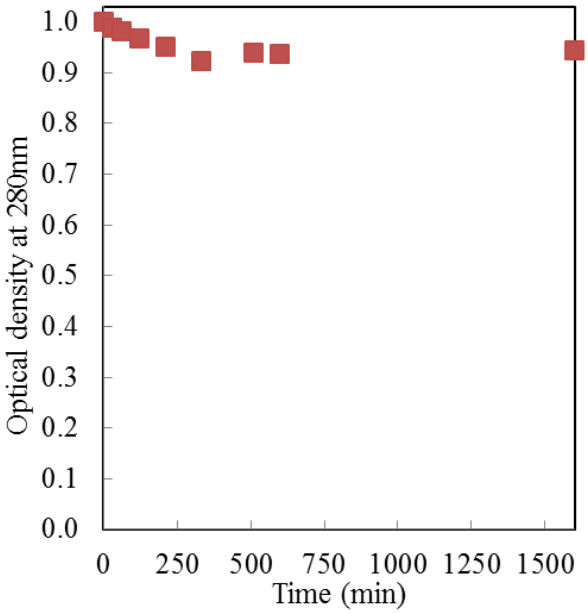

Figure 3.1. Optical density at 280 nm for chymotrypsin (CT) showing little to no decrease in solubility over time in 40 vol % [BMIM][Cl].

3.3.2 Unfolding of chymotrypsin in [BMIM][Cl]

CT has 8 tryptophans scattered throughout the protein (**Figure 3.2A**), which can report on the environment surrounding those residues. If the protein unfolds around one of the tryptophans, its fluorescence will red shift and decrease in aqueous [BMIM][Cl]. The red shift is a result of going from a low dielectric environment in a buried protein to a high dielectric in solution. An example of this is shown in **Figure 3.2C**, where we induced CT to unfold by adding

7.5 M urea. As one can see, there is indeed a red shift from about 335 nm to 355 nm. Note that in the absence of ILs, there is no decrease in signal, only a redshift. The decrease in signal upon unfolding would result from increased quenching from the [BMIM] molecules. An example, of [BMIM] quenching is shown in **Figure 3.2B**, where higher concentrations of [BMIM] quench the intrinsic fluorescence to a higher degree. As a final control to help us understand unfolding in the presence of [BMIM][Cl], we unfolded the enzyme using urea while in the presence of 10 vol % [BMIM][Cl]. **Figure 3.2D** shows exactly what we predicted, a red-shift due to exposure to a higher dielectric environment and a decrease in fluorescence from higher accessibility of [BMIM] to the tryptophan residues. It is convenient to have many (8) tryptophans scattered throughout CT, this gives us a hint as to whether there is a local unfolding event around one of the tryptophans, which would not result in a complete red shift, or a more global change exposing all the tryptophans.

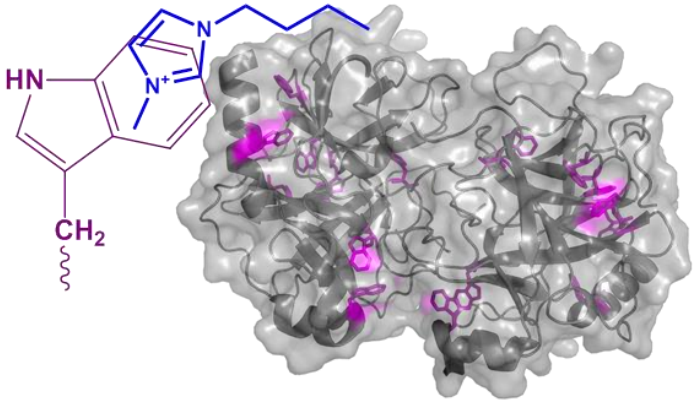

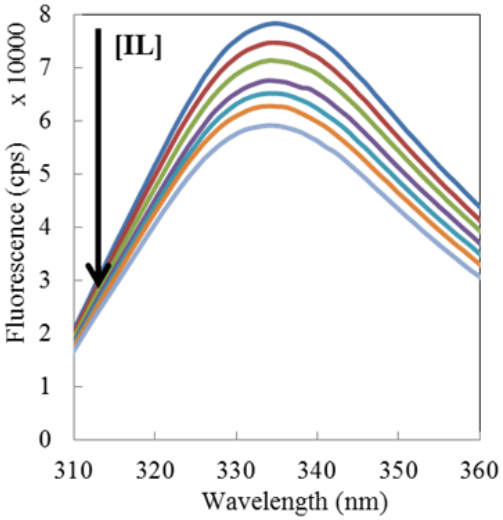

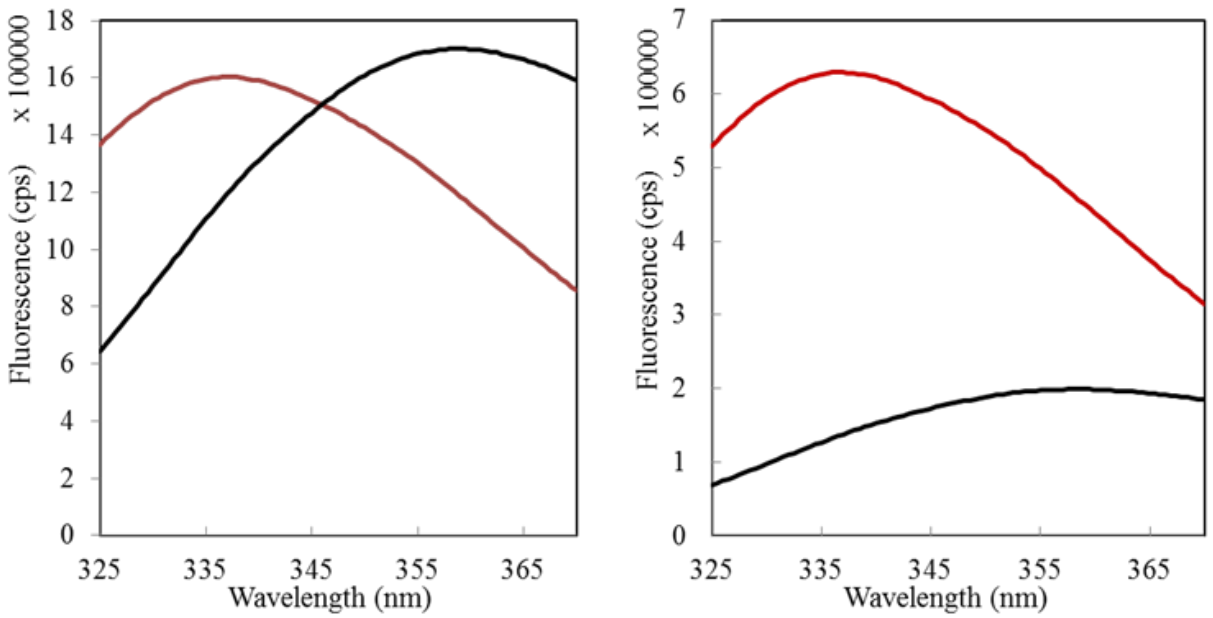

Figure 3.2. (A) Chymotrypsin (1YPH) contains 8 tryptophan residues (magenta) scattered throughout the enzyme. [BMIM] quenches fluorescence through short-range interactions that are increased with increased tryptophan exposure. (B) Quenching of chymotrypsin intrinsic fluorescence by adding [BMIM][Cl]. (C) Red-shift in chymotrypsin fluorescence as a result of urea (7.5 M) induced unfolding (native red, unfolded black). (D) Red shift and increased quenching as a result of urea induced unfolding in the presence of 10 vol % [BMIM][Cl].

To understand the effect of folding state on activity retention, we incubated CT under the same conditions as the activity experiment (40 vol % [BMIM][Cl], 30 °C) but at a higher concentration, 0.5 mg/ml vs. 0.04 mg/ml, required to get reliable signal to noise. In **Figure 3.3D** the signal decreases with time until a point where the fluorescence stops decreasing. After 30 hours the solution was allowed to incubate for an additional 24 hours, and one last fluorescence measurement recorded, this was used as the unfolded state fluorescence. We see that the fluorescence both decreases greatly and red shifts as time proceeds, indicating unfolding. It has been shown that the magnitude of native fluorescence is proportional to the fraction of enzyme folded, assuming a two-state unfolding mechanism.[164] Therefore, the fraction of fluorescence at 335 nm (native state maximum) between the time 0 data point and the final 54 hour sample was taken in attempt to follow the folding state of the enzyme with time. Overlaying this fraction of

fluorescence as a function of time with the fraction of activity as a function of time (**Figure 3.4**) shows a very good correlation between relative fluorescence and activity. This is taken as an indication that activity loss is directly related to unfolding. The fluorescence does decrease a little bit faster than the activity does. It, of course, does not make sense that an enzyme would retain activity longer than it retains its native structure. Aside from experimental error, one reason for quicker fluorescent loss than activity may be due to higher concentration of protease used for the fluorescence experiments. Because, proteases, like CT, can cleave themselves, higher concentration of protein represents higher substrate concentration or faster cleavage rates. Using higher concentrations of protein, while necessary for accurate fluorescence measurements, may cause faster proteolysis rates, resulting in faster relative fluorescent loss (or ~unfolding) than in the activity experiments at lower CT concentration (by > 10-fold). This effect may be magnified in light of enzyme unfolding, exposing more cleavage sites for proteolysis. Another reason could be that assuming perfect two state unfolding is likely not a perfect assumption. Nonetheless, the activity and fluorescence data correlate quite well.

A similar experiment was performed for 10, 20, and 30 vol % [BMIM][Cl] (**Figure 3.3A-C**). At the lower concentrations of [BMIM][Cl], as expected, we see a slower rate of fluorescence loss for CT with the slowest rate of fluorescence loss being the 10 vol % [BMIM][Cl] sample. Because CT does not lose all its activity over the time course of activity experiments in concentrations ≤ 30 vol % [BMIM][Cl], the final fluorescent value is not a good approximation for the unfolded state fluorescence. In order to obtain the unfolded state fluorescence, the enzyme was melted at 60 °C, allowed to equilibrate, and the fluorescence measured. Then the temperature was decreased in 5 °C increments and the fluorescence measured down to 45 °C as it was known that CT has no activity at 45 °C and 10, 20, or 30 vol

% [BMIM][Cl]. The dependence of fluorescence on temperature appears linear between 60 and 45 °C (supplemental). Further decreases in temperature cause deviations from this linearity, which we believe to be due to refolding of the enzyme which would rebury the tryptophans. Notably, CT does regain some of its activity when cooled back to 30 °C (more so for the lower IL concentrations). To avoid this, the fluorescence was back extrapolated from 45 °C, where CT is completely inactivated, to 30 °C by using the linear dependence of fluorescence on temperature determined between 60 and 45°C. The unfolded state fluorescence can also be achieved by back-extrapolating from the unfolded state with 7.5 M urea to 0 M urea using the dependence of fluorescence on urea concentration to achieve a similar result (supplemental). The temperature method was used as it can more accurately be programmed into the fluorimeter and does not require a separate solution be made. Also, a tryptophan in a polypeptide may not follow the exact same dependence on urea as free tryptophan in solution. Additionally, a temperature scan from 60 to 30 °C at 40 vol % [BMIM][Cl] appears linear over the entire range due to the enzyme being unfolded still at 30 °C, validating the linear extrapolation of fluorescence from 45 to 30 °C for the 10, 20, and 30 vol % IL samples.

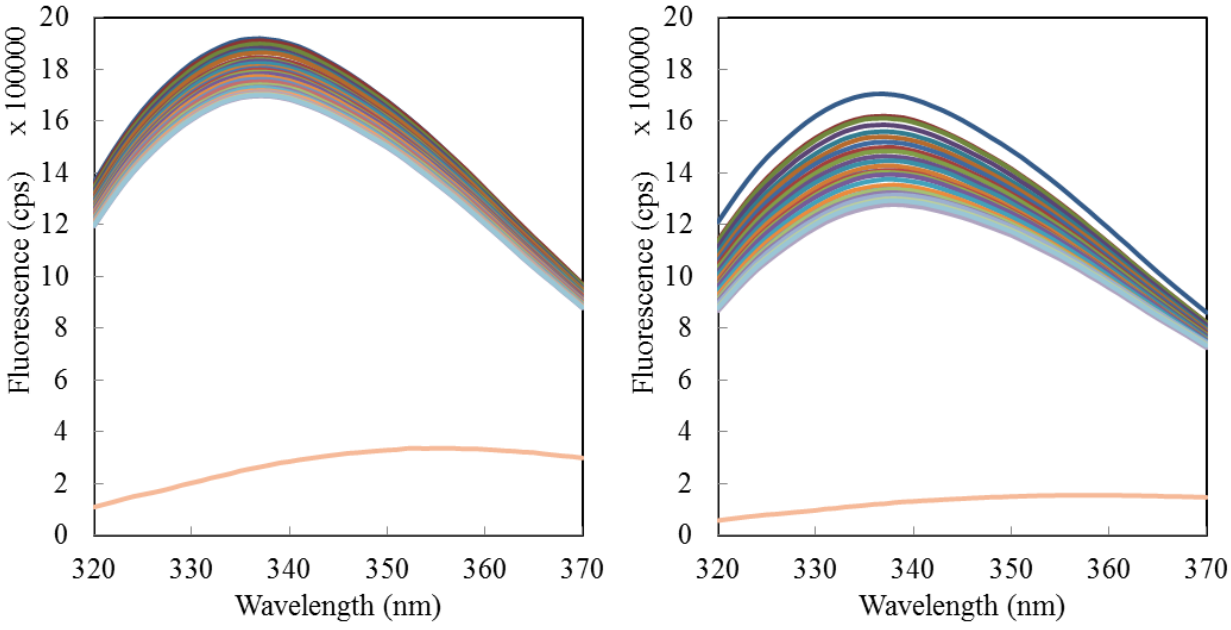

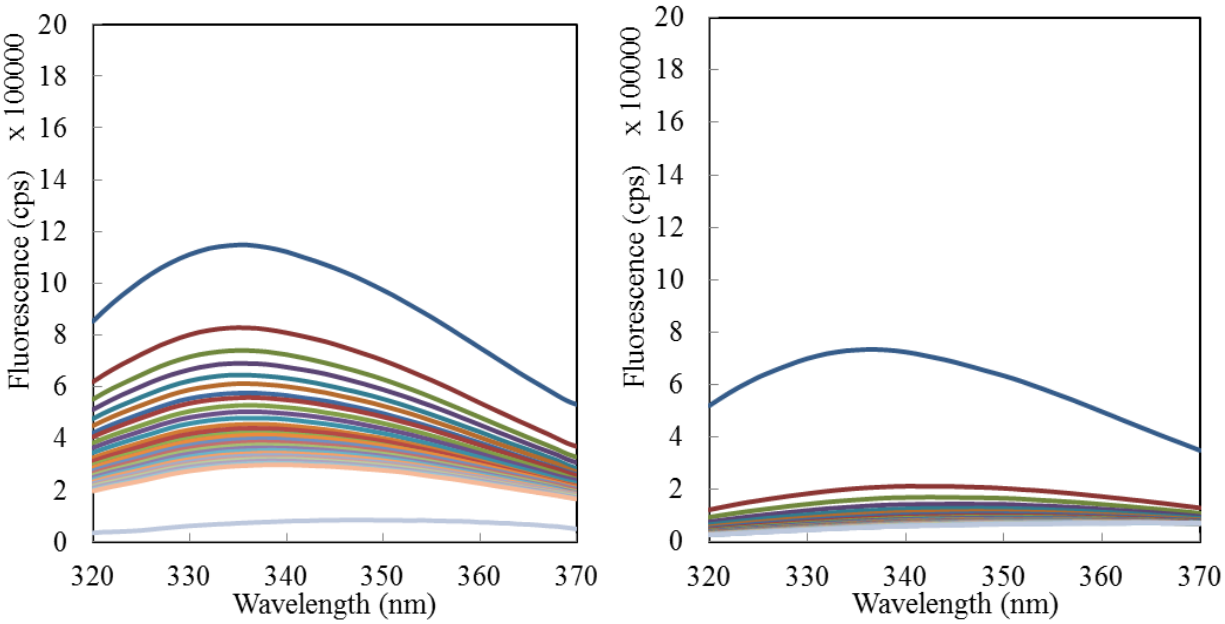

Figure 3.3. Change in fluorescent profile of chymotrypsin (CT) with time in (A) 10, (B) 20, (C) 30, and (D) 40 vol % [BMIM][Cl] and 30 °C. Fluorescence red shifts and decreases with time as a result of increased exposure from unfolding of the 8 Trp residues scattered across CT (increasing dielectric causes red shift, increasing exposure to [BMIM] results in increased quenching). For 10, 20, and 30 vol % concentrations, the unfolded state was determined by increasing the temperature to induce unfolding, see text and supplemental. However, the 40 % sample (D) was only allowed to equilibrate for one more day with no temperature increase.

The relative fluorescence over time at each condition, 10-40 vol % IL, overlay quite nicely with the relative activity of the enzyme over time at the corresponding IL concentration. However, the fluorescent profiles consistently decrease slightly more quickly than the activity profiles. Nonetheless, the same trend is observed for the activity and fluorescence as a function of IL concentration. Specifically, there is high retention of fluorescence and activity at 10 vol % IL, complete loss at 40 vol % IL, and intermediate loss of fluorescence and activity at intermediate concentrations. Given the difficulty of direct measurements of protein structure under the similar conditions of activity assay, this is taken as best attainable evidence that activity loss is directly related to enzyme unfolding. As shown in the supplemental (**Figure 3.10**), upon enhancing or reducing the activity retention profile of CT via chemical modification,

this relates to enhancing or reducing, respectively, the retention of fluorescence, which we interpret as retaining native structure.

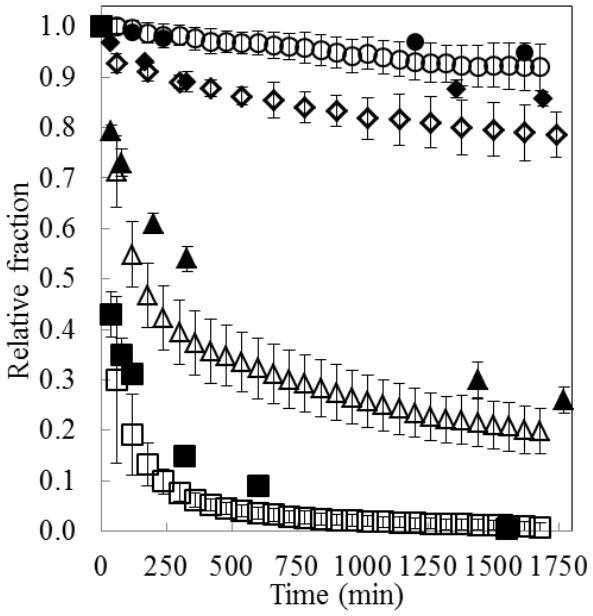

Figure 3.4. Fluorescent decrease (open symbols) resulting from unfolding correlates with enzyme activity decrease (closed symbols) at 10 (●), 20 (♦), 30 (▲), and 40 (■) vol % (0.6 - 2.3 M) [BMIM][Cl] and 30 °C.

3.3.3 Preferential binding of chymotrypsin with [BMIM][Cl]

The preferential interaction parameter, $\Gamma_{2,3} = (\frac{\partial m_3}{\partial m_2})_{\mu_3,\mu_1,T}$, represents the excess amount of ligand bound to the protein over what would be there statistically. Scatchard notation is used here where component 3 is ligand, 2 is protein, and 1 is principal solvent, or water.[113] In a concentrated solution of ligand, as is the case here, there may be, hypothetically, a 25% chance of finding a ligand at a particular spot.[113] A 10% excess of ligand would then mean 35% of the protein surface is covered with ligand. In an equilibrium membrane experiment the chemical potential of all diffusible species (in this case water and IL, ligand), is the same on all sides of the membrane. Assuming, equilibrium has been achieved, the data points for concentration of

[BMIM][Cl] as a function of protein concentration are all at the same chemical potential of diffusible components (μ_3, μ_1). Because the temperature is also the same for each data point, the derivative of the resulting line represents the preferential interaction parameter, $(\frac{\partial m_3}{\partial m_2})_{\mu_3,\mu_1,T}$. Similarly, it can also be thought of as the additional amount of [BMIM][Cl] required to restore its chemical potential upon addition of macromolecule.[114] Because the chemical potential is the same for diffusible components on either side of a membrane, having dialysis tubing with increasing concentration of protein (and increasing chemical potential) results in [BMIM][Cl] diffusing in or out of a membrane to maintain its chemical potential throughout the solution. Mathematically this is represented as $-\left(\frac{\partial \mu_2}{\partial \mu_3}\right)_{m_2,T,P} = \left(\frac{\partial m_3}{\partial m_2}\right)_{\mu_3,T.P}$.[109] For binding (positive $\left(\frac{\partial m_3}{\partial m_2}\right)$), an increase in chemical potential of ligand results in a decrease in protein chemical potential, and vice-versa. As such, to restore the chemical potential of ligand upon addition of macromolecule, additional ligand must be added inside the dialysis bag.

Figure 3.5 gives the thermodynamic binding parameter at 0.7, 1.2, and 2.5 M [BMIM][Cl] (12-43 vol % [BMIM][Cl]). As we can see, at lower concentrations where the proteins are expected to be folded, there is very little to no binding. As the concentration is increased to a point where we expect CT to unfold (and have data indicating so), there is a large excess of bound molecules. At the highest concentration of [BMIM][Cl], the experiment indicates about ~900 molecules of IL per molecule of protein are in excess. For CT, which has 245 amino acids, this represents about 3.7 molecules per residue. For reference, guanidine chloride binds in an excess of 100-200 molecules per molecule of BSA at 6 M GnCl.[122] It is interesting to compare this to the surface of CT which has a diameter of 45 Å. Pymol calculates a solvent accessible surface area of 10,100 $Å^2$ in the native state. Based on the calculations of Pace et al. the unfolded

state would have a surface area of roughly ~29,000 Å^2 in the unfolded state.[166] A [BMIM] molecule has a ~2.3 Å imidazolium head and a butyl tail that is ~5 Å. The molecule can be laid flat as a conservative approach (7 Å X 2 Å box) to fit ~720 molecules in the native state and ~2,100 in the unfolded state. Instead, the [BMIM] molecule can also point down onto the protein as a ~1.5 Å X 2 Å box and fit ~3,400 molecules in the native state or 14,500 molecules in the denatured state. Also, keep in mind that **Figure 3.5** reports *excess* molecules bound to the protein, over that in the bulk. Given this, why such large numbers for binding? Perhaps more than a monolayer of [BMIM] molecules may be binding in a particular region. For example, if the [BMIM] molecule is pointing down onto protein, feasibly the butyl chain of this [BMIM] may attract the butyl chain of another [BMIM] molecule. Likely the hydrophobic tail would rather interact with another butyl tail than be hydrated in solution. This is in line with Tanford's suggestion that binding can potentially occur over a few solvent layers.[111]

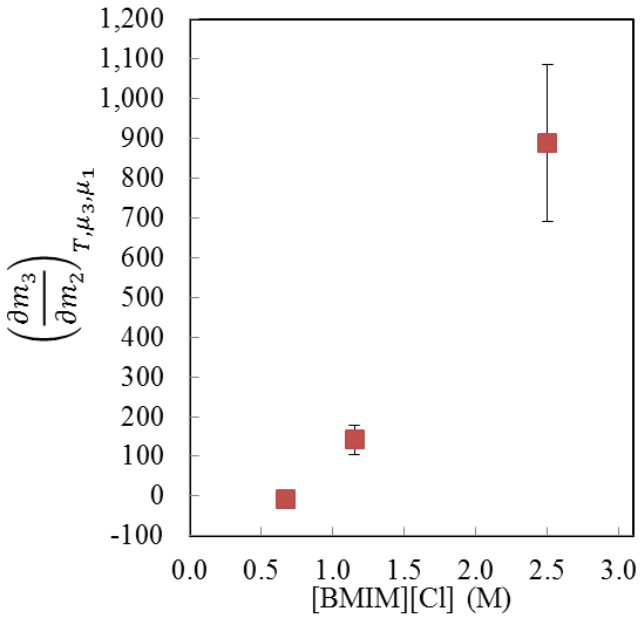

Figure 3.5. Preferential binding of [BMIM][Cl] with chymotrypsin determined at ionic liquid concentrations where the enzyme is presumed to be folded (< 1.2 M, 20 vol %) and largely unfolded (2.5 M, 43 vol% [BMIM][Cl]). The increased binding at higher concentrations of ionic liquid is likely due to increased binding to the unfolded state.

3.3.4 A possible mechanism of [BMIM][Cl] binding and unfolding of chymotrypsin

The data from **Figure 3.5** show convincing evidence of [BMIM][Cl] binding to proteins, and certainly a larger binding to the unfolded states of the protein which would drive denaturation. Here we consider the possible mechanisms of binding. Interactions of histidine in nature provide us with some possible clues. Histidine has a propensity to form π-stacking interactions which are 3-4X stronger when histidine is protonated (imidazolium).[167-170] Fersht et al. found a particular imidazolium interaction of a histidine-tryptophan pair that they determined stabilized Barnase by 1.4 kCal/mol.[171] In light of this, **Figure 3.6A** shows a proposed mechanism by which [BMIM] cations may bind with proteins by cation-π stacking with aromatic amino acids. This would cause unfolding as these aromatics are often buried.[155] Unfolding would increase the exposure, and therefore ability of [BMIM] to bind with these groups. Even in the case of exposed aromatic groups, typically a [BMIM] can only approach from one side, in the unfolded case, perhaps two [BMIM] molecules per aromatic can bind (top and bottom of ring). This is especially plausible considering the calculated 3.7 [BMIM] molecules / residue from the equilibrium dialysis. Another possible mechanism of binding of the cation would be hydrophobic interactions of the butyl chain with hydrophobic amino acid side chains. **Figure 3.6B** highlights possible mechanisms of [BMIM] and [Cl] binding to a polypeptide. While [Cl] likely does not cause unfolding of proteins itself, based on what we know about [Cl] interactions (in NaCl, for example),[95, 96] it is important to consider the total interaction of the salt. This is because counter-ions must bind in the protein domain to maintain electroneutrality. Therefore, no excess [Cl] molecules would mean no excess [BMIM] molecules could bind.

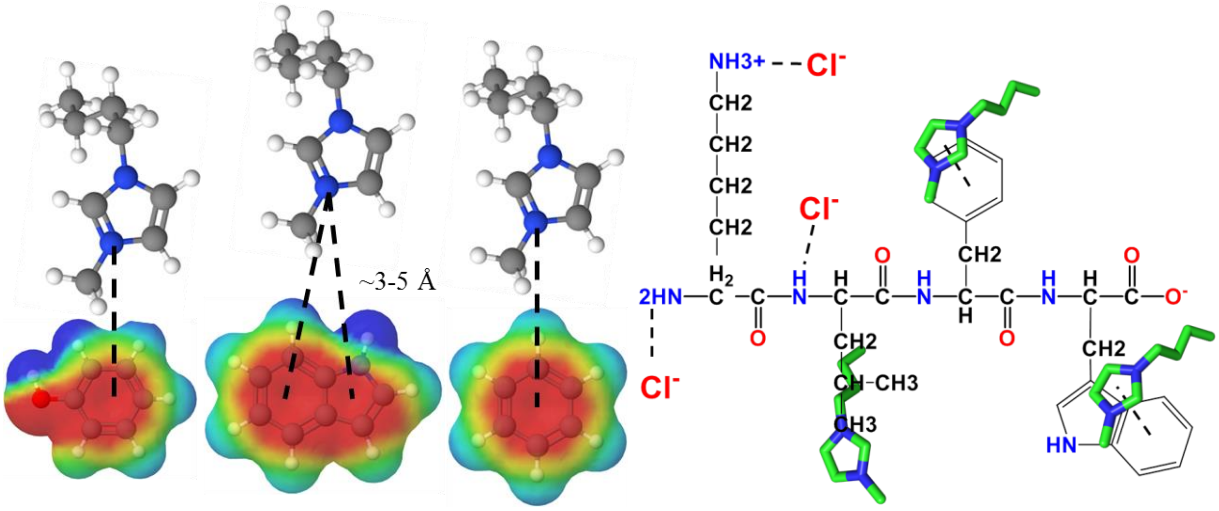

Figure 3.6. Proposed mechanism of [BMIM][Cl] binding is (A) primarily cation-π stacking with aromatic amino acids. Shown are the aromatic portion of Tyr, Trp, and Phe sidechains, respectively, which are typically buried. Binding would increase upon unfolding as a result of increased exposure of these aromatic groups. (B) Other potential contacts [BMIM][Cl] could make with an unfolded peptide include Van der Waals hydrophobic interactions, hydrogen bonding, or electrostatic interactions.

3.3.5 Crystallographic investigation of the mechanism of [BMIM][Cl] binding to chymotrypsin

To ascertain the validity of our conjecture about [BMIM] binding to proteins via stacking and hydrophobic interactions, the crystal structure of CT soaked in [BMIM][Cl] was determined, yielding high resolution structures, even when the IL was soaked into the crystals (< 1.20 Å). Upon resolving the crystal structure of CT, 1 unique [BMIM] molecule was able to be resolved, shown in **Figure 3.7**. Interestingly, the [BMIM] molecule was resolved around a tryptophan, supporting the idea that [BMIM] can bind through cation-π stacking. Also interesting is the fact that there is a lysine so close. One might expect the lysine to repel the [BMIM] cation, but the [BMIM] is resolved at that location nonetheless. Perhaps the electrostatic attraction or repulsion of [BMIM] is weak. Another additional interaction of the [BMIM] may be between the butyl tail and the nearby valine through hydrophobic interactions.

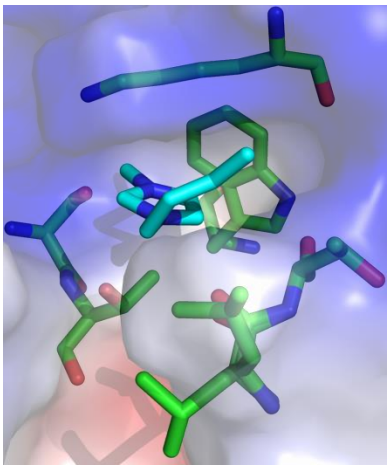

Figure 3.7. Resolving the structure of CT crystals soaked in [BMIM] shows a [BMIM] apparently cation-π stacking with a tryptophan. Also nearby is a valine with which the butyl tail may be interacting. A nearby lysine does not appear to repel the [BMIM] from binding. The surface map highlights positive (blue), negative (red), and non-polar (white) regions. Atoms are colored such that carbon is green, nitrogen is blue, and oxygen is red. Carbons on the [BMIM] are colored teal.

3.4 Conclusions

The goal of this manuscript was to understand in detail the mechanism of [BMIM][Cl] induced enzyme inactivation. Optical density measurements showed that enzyme solubility is retained in solution and is therefore not related to inactivation. Intrinsic tryptophan fluorescence, however, indicated protein unfolding via a redshift in peak maximum and signal loss due to increased [BMIM] quenching of newly exposed tryptophans. This unfolding correlated well with activity loss. Equilibrium dialysis on CT revealed preferential binding, particularly at higher concentrations where CT is thought to be unfolded. This increased binding to the unfolded state will drive denaturation as a function of IL concentration, as described by the Wyman linkage relation.[125] To understand binding modes, CT was also crystallized and soaked in [BMIM][Cl]. High resolution structures (< 1.2 Å) showed [BMIM] binding where it can form a cation-π interaction or a hydrophobic interaction of the butyl tail with the protein. Both aromatic and

hydrophobic amino acids will typically become more exposed upon unfolding, resulting in increased binding of [BMIM] to the denatured state as shown by the equilibrium dialysis.

To design a protein for imidazolium IL tolerance, mutagenesis near high affinity targets to a residue with lower affinity for the IL may favorably alter the total binding to the unfolded and folded states. Specifically, maybe a charged mutation to an exposed residue adjacent (in primary sequence) to a buried tryptophan may reduce the affinity of [BMIM][Cl] to the unfolded state. If [BMIM] is the denaturing ion, positive mutations seem like the natural choice for mutation. However, it has been shown that positive charges are generally deleterious on protein IL tolerance, whereas negative protein variants tend to have higher stability in ILs.[14, 15] As [BMIM] does not seem to have a strong interaction with electrostatic residues, a positive charge may not be very repulsive. This is supported by the crystallographic results showing a [BMIM] stacking with a tryptophan in a pocket with a nearby lysine.

Instead, what may be happening is that negative charges reduce the overall affinity of [BMIM][Cl] for the protein in the vicinity of the amino acid by electrostatically repelling [Cl] and reducing hydrophobic [BMIM]-protein interactions.[172] To maintain electroneutrality in the protein domain, counter ions must also bind, so mediating anion binding may be an effective tool for stabilization despite [BMIM] likely being the main cause for denaturation. Namely, a glutamic acid may reduce the affinity of a [Cl] for the protein more than any slight increases (if any) in affinity the hydrophobic [BMIM] molecule gains. Based on this hypothesis, negative amino acids may reduce total IL binding both in the native and denatured states. As there is a stronger affinity of the IL for the unfolded state, eliminating binding may favor the native state.

3.5 Supplemental

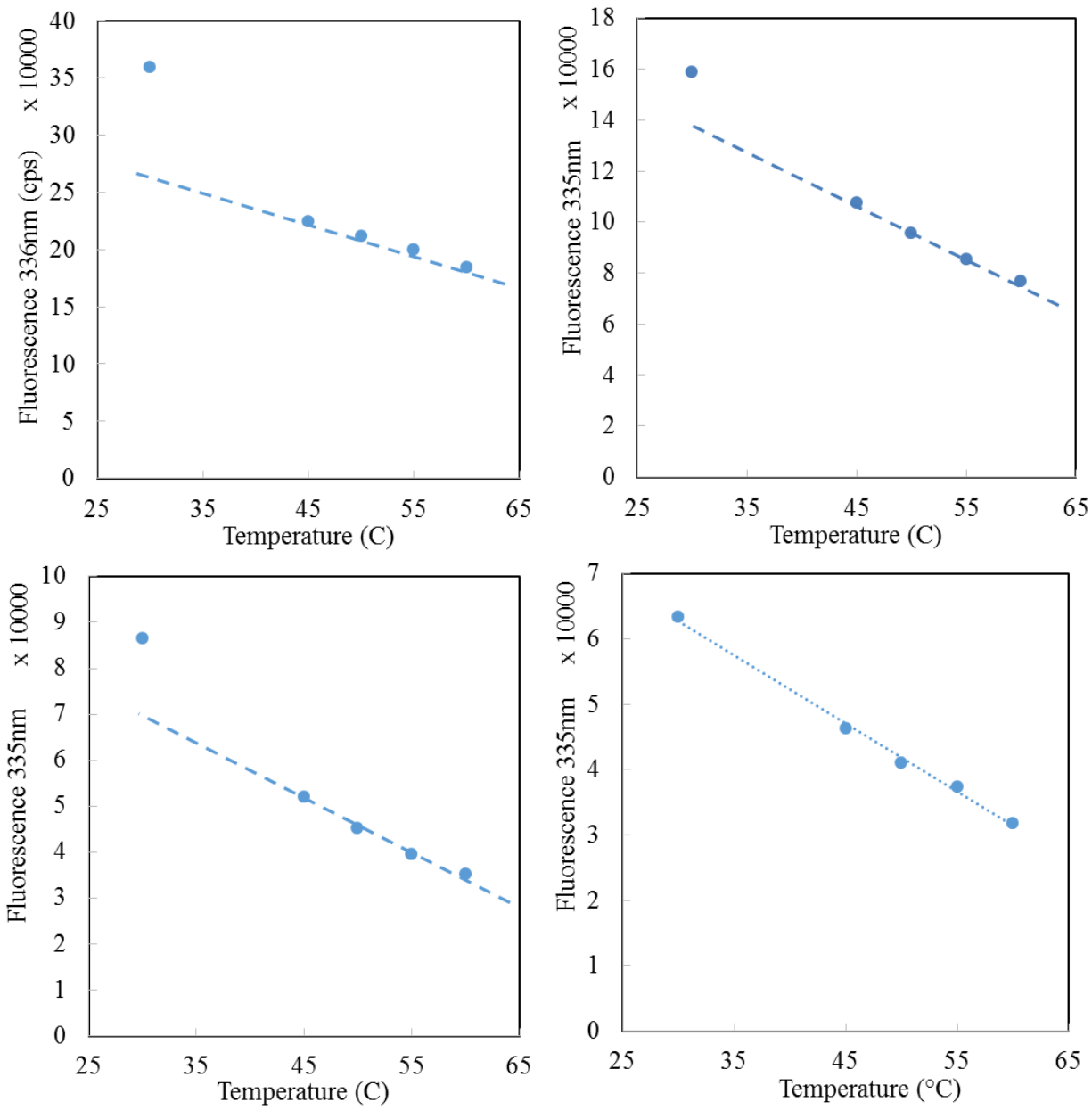

Figure 3.8. Fluorescence as a function of temperature for chymotrypsin (CT) in (A) 10, (B) 20, (C) 30, and (D) 40 vol % [BMIM][Cl]. Perturbations from linearity in concentrations ≤ 30 vol % are thought to be due to enzyme refolding, causing increased tryptophan burial and fluorescence. Increased folding and fluorescence become larger at lower [BMIM][Cl] concentrations (note the scale changes on the plots).

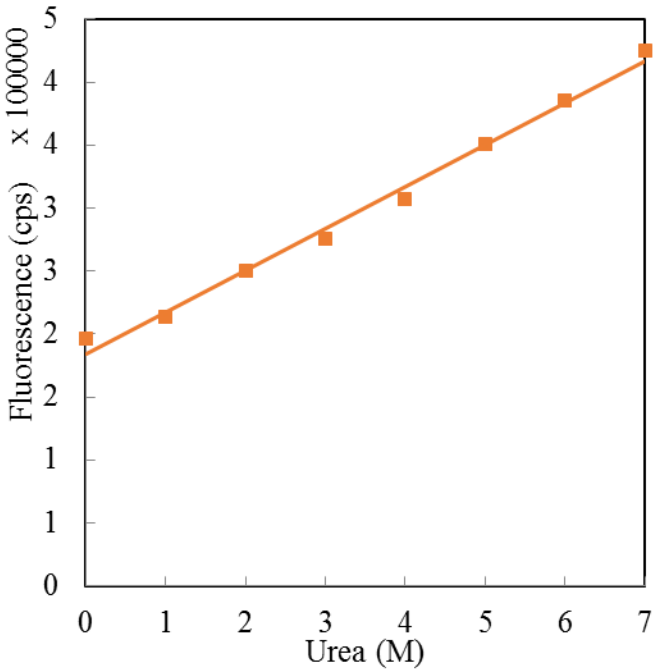

Figure 3.9. Tryptophan fluorescence as a function of urea

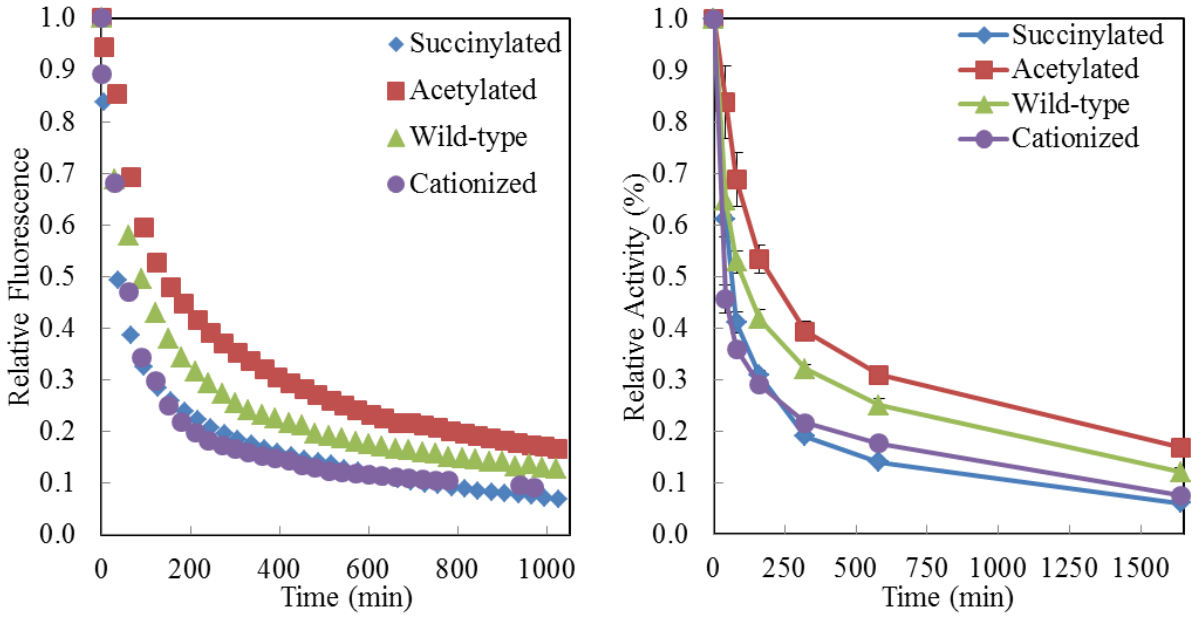

Figure 3.10. The fluorescent decrease with time for charge variants of chymotrypsin matches that of the activity profiles, suggesting the mechanism of increased activity retention is related to retaining structure longer.

3.6 References

3. Kaftzik, N., P. Wasserscheid, and U. Kragl, *Use of ionic liquids to increase the yield and enzyme stability in the beta-galactosidase catalysed synthesis of N-acetyllactosamine.* Organic Process Research & Development, 2002. **6**(4): p. 553-557.
12. Nordwald, E.M., G.S. Armstrong, and J.L. Kaar, *NMR-Guided Rational Engineering of an Ionic-Liquid-Tolerant Lipase.* Acs Catalysis, 2014. **4**(11): p. 4057-4064.
13. Nordwald, E.M., et al., *Charge Engineering of Cellulases Improves Ionic Liquid Tolerance and Reduces Lignin Inhibition.* Biotechnology and Bioengineering, 2014. **111**(8): p. 1541-1549.
14. Nordwald, E.M. and J.L. Kaar, *Stabilization of Enzymes in Ionic Liquids Via Modification of Enzyme Charge.* Biotechnology and Bioengineering, 2013. **110**(9): p. 2352-2360.
15. Nordwald, E.M. and J.L. Kaar, *Mediating Electrostatic Binding of 1-Butyl-3-methylimidazolium Chloride to Enzyme Surfaces Improves Conformational Stability.* Journal of Physical Chemistry B, 2013. **117**(30): p. 8977-8986.
22. Galonde, N., et al., *Use of ionic liquids for biocatalytic synthesis of sugar derivatives.* Journal of Chemical Technology and Biotechnology, 2012. **87**(4): p. 451-471.
24. Ha, S.H., et al., *Lipase-catalyzed biodiesel production from soybean oil in ionic liquids.* Enzyme and Microbial Technology, 2007. **41**(4): p. 480-483.
33. Bose, S., C.A. Barnes, and J.W. Petrich, *Enhanced stability and activity of cellulase in an ionic liquid and the effect of pretreatment on cellulose hydrolysis.* Biotechnology and Bioengineering, 2012. **109**(2): p. 434-443.
41. Constatinescu, D., C. Herrmann, and H. Weingartner, *Patterns of protein unfolding and protein aggregation in ionic liquids.* Physical Chemistry Chemical Physics, 2010. **12**(8): p. 1756-1763.
50. Tee, K.L., et al., *Ionic liquid effects on the activity of monooxygenase P450BM-3.* Green Chemistry, 2008. **10**(1): p. 117-123.
52. Park, S. and R.J. Kazlauskas, *Biocatalysis in ionic liquids - advantages beyond green technology.* Current Opinion in Biotechnology, 2003. **14**(4): p. 432-437.
57. Zhang, K.P., et al., *Penicillium expansum lipase-catalyzed production of biodiesel in ionic liquids.* Bioresource Technology, 2011. **102**(3): p. 2767-2772.
66. Engel, P., et al., *Point by point analysis: how ionic liquid affects the enzymatic hydrolysis of native and modified cellulose.* Green Chemistry, 2010. **12**(11): p. 1959-1966.
68. Baker, G.A. and W.T. Heller, *Small-angle neutron scattering studies of model protein denaturation in aqueous solutions of the ionic liquid 1-butyl-3-methylimidazolium chloride.* Chemical Engineering Journal, 2009. **147**(1): p. 6-12.
69. Baker, S.N., et al., *Fluorescence energy transfer efficiency in labeled yeast cytochrome c: a rapid screen for ion biocompatibility in aqueous ionic liquids.* Physical Chemistry Chemical Physics, 2011. **13**(9): p. 3642-3644.
87. Hofmeister, F., *Zur Lehre von der Wrikung der Salze. Zweite Mittheilung.* Archiv for Expermentelle Pathologie und Pharmakologie, 1888. **24**: p. 247-260.
95. Von Hippel, P.H. and K.Y. Wong, *On the conformational stability of globular proteins. The effects of various electrolytes and nonelectrolytes on the thermal ribonuclease transition.* The Journal of biological chemistry, 1965. **240**(10): p. 3909-23.
96. Von Hippel, P.H. and K.Y. Wong, *Neutral Salts: The Generality of Their Effects on the Stability of Macromolecular Conformations.* Science, 1964. **2**: p. 577-580.

99. Pace, C.N. and K.L. Shaw, *Linear extrapolation method of analyzing solvent denaturation curves.* Proteins-Structure Function and Genetics, 2000: p. 1-7.
109. Timasheff, S.N., *Protein-solvent preferential interactions, protein hydration, and the modulation of biochemical reactions by solvent components.* Proceedings of the National Academy of Sciences of the United States of America, 2002. **99**(15): p. 9721-9726.
111. Tanford, C., *Protein denaturation. C. Theoretical models for the mechanism of denaturation.* Advances in protein chemistry, 1970. **24**: p. 1-95.
112. Casassa, E.F. and H. Eisenberg, *Thermodynamic Analysis of Multicomponent Solutions.* Advances in protein chemistry, 1964. **19**: p. 287-395.
113. Scatchard, G., *Physical chemistry of protein solutions; derivation of the equations for the osmotic pressure.* Journal of the American Chemical Society, 1946. **68**(11): p. 2315-9.
114. Schellman, J.A., *A Simple-Model for Solvation in Mixed-Solvents - Applications to the Stabilization and Destabilization of Macromolecular Structures.* Biophysical Chemistry, 1990. **37**(1-3): p. 121-140.
120. Timasheff, S.N., *Protein hydration, thermodynamic binding, and preferential hydration.* Biochemistry, 2002. **41**(46): p. 13473-13482.
122. Noelken, M.E. and Timashef.Sn, *Preferential Solvation of Bovine Serum Albumin in Aqueous Guanidine Hydrochloride.* Journal of Biological Chemistry, 1967. **242**(21): p. 5080-&.
124. Anderson, C.F., et al., *Generalized derivation of an exact relationship linking different coefficients that characterize thermodynamic effects of preferential interactions.* Biophysical Chemistry, 2002. **101**: p. 497-511.
125. Wyman, J., *Linked Functions and Reciprocal Effects in Hemoglobin - a 2nd Look.* Advances in protein chemistry, 1964. **19**: p. 223-286.
133. Schellman, J.A., *Fifty years of solvent denaturation.* Biophysical Chemistry, 2002. **96**(2-3): p. 91-101.
138. Constantinescu, D., H. Weingartner, and C. Herrmann, *Protein denaturation by ionic liquids and the Hofmeister series: A case study of aqueous solutions of ribonuclease A.* Angewandte Chemie-International Edition, 2007. **46**(46): p. 8887-8889.
143. Jaeger, V., P. Burney, and J. Pfaendtner, *Comparison of Three Ionic Liquid-Tolerant Cellulases by Molecular Dynamics.* Biophysical Journal, 2015. **108**(4): p. 880-892.
144. Burney, P.R., et al., *Molecular dynamics investigation of the ionic liquid/enzyme interface: application to engineering enzyme surface charge.* Proteins: Structure, Function, and Bioinformatics, 2015. **83**(4): p. 670-680.
145. Nordwald, E.M., et al., *Accelerated protein engineering for chemical biotechnology via homologous recombination.* Current Opinion in Biotechnology, 2013. **24**(6): p. 1017-1022.
146. Wei-Wei Gao, Feng-Xiu Zhang, and C.-H. Zhou, *Key factors affecting the activity and stability of enzymes in ionic liquids and novel applications in biocatalysis.* Biochemical engineering journal, 2015. **99**: p. 67-84.
147. Lau, R.M., et al., *Dissolution of Candida antarctica lipase B in ionic liquids: effects on structure and activity.* Green Chemistry, 2004. **6**(9): p. 483-487.
148. Tamura, K., N. Nakamura, and H. Ohno, *Cytochrome c dissolved in 1-allyl-3-methylimidazolium chloride type ionic liquid undergoes a quasi-reversible redox reaction up to 140 degrees C.* Biotechnology and Bioengineering, 2012. **109**(3): p. 729-735.

149. Bekhouche, M., L.J. Blum, and B. Doumeche, *Contribution of Dynamic and Static Quenchers for the Study of Protein Conformation in Ionic Liquids by Steady-State Fluorescence Spectroscopy.* Journal of Physical Chemistry B, 2012. **116**(1): p. 413-423.
150. Hannemann, F., et al., *Unfolding and conformational studies on bovine adrenodoxin probed by engineered intrinsic tryptophan fluorescence.* Biochemistry, 2002. **41**(36): p. 11008-11016.
151. Lakowicz, J.R., *Principles of fluorescence spectroscopy*. 3rd ed2006.
152. Merrill, A.R., L.R. Palmer, and A.G. Szabo, *Acrylamide Quenching of the Intrinsic Fluorescence of Tryptophan Residues Genetically-Engineered into the Soluble Colicin-E1 Channel Peptide - Structural Characterization of the Insertion-Competent State.* Biochemistry, 1993. **32**(27): p. 6974-6981.
153. Monsellier, E. and H. Bedouelle, *Quantitative measurement of protein stability from unfolding equilibria monitored with the fluorescence maximum wavelength.* Protein Engineering Design & Selection, 2005. **18**(9): p. 445-456.
154. Shao, Q., *On the influence of hydrated imidazolium-based ionic liquid on protein structure stability: A molecular dynamics simulation study.* Journal of Chemical Physics, 2013. **139**(11).
155. Alston, R.W., et al., *Contribution of single tryptophan residues to the fluorescence and stability of ribonuclease sea.* Biophysical Journal, 2004. **87**(6): p. 4036-4047.
156. Callis, P.R., *L-1(a) and L-1(b) transitions of tryptophan: Applications of theory and experimental observations to fluorescence of proteins.* Fluorescence Spectroscopy, 1997. **278**: p. 113-150.
157. Chen, Y. and M.D. Barkley, *Toward understanding tryptophan fluorescence in proteins.* Biochemistry, 1998. **37**(28): p. 9976-9982.
158. Kumar, V. and S. Pandey, *Selective Quenching of 2-Naphtholate Fluorescence by Imidazolium Ionic Liquids.* Journal of Physical Chemistry B, 2012. **116**(39): p. 12030-12037.
159. Lai, J.Q., et al., *Specific ion effects of ionic liquids on enzyme activity and stability.* Green Chemistry, 2011. **13**(7): p. 1860-1868.
160. Rawat, K. and H.B. Bohidar, *Universal Charge Quenching and Stability of Proteins in 1-Methyl-3-alkyl (Hexyl/Octyl) Imidazolium Chloride Ionic Liquid Solutions.* Journal of Physical Chemistry B, 2012. **116**(36): p. 11065-11074.
161. Shu, Y., et al., *New Insight into Molecular Interactions of Imidazolium Ionic Liquids with Bovine Serum Albumin.* Journal of Physical Chemistry B, 2011. **115**(42): p. 12306-12314.
162. Moller, M. and A. Denicola, *Protein tryptophan accessibility studied by fluorescence quenching.* Biochemistry and Molecular Biology Education, 2002. **30**(3): p. 175-178.
163. Sontag, B., et al., *Intrinsic Tryptophan Fluorescence of Rat-Liver Elongation-Factor Eef-2 to Monitor the Interaction with Guanylic and Adenylic Nucleotides and Related Conformational-Changes.* Biochemistry, 1993. **32**(8): p. 1976-1980.
164. Moon, C.P. and K.G. Fleming, *Using Tryptophan Fluorescence to Measure the Stability of Membrane Proteins Folded in Liposomes.* Methods in Enzymology: Biothermodynamics, Vol 492, Pt D, 2011. **492**: p. 189-211.
165. Sharma, N.K., et al., *Do ion tethered functional groups affect IL solvent properties? The case of sulfoxides and sulfones.* Chemical Communications, 2006(6): p. 646-648.

166. Myers, J.K., C.N. Pace, and J.M. Scholtz, *Denaturant M-Values and Heat-Capacity Changes - Relation to Changes in Accessible Surface-Areas of Protein Unfolding.* Protein Science, 1995. **4**(10): p. 2138-2148.
167. Churchill, C.D.M. and S.D. Wetmore, *Noncovalent Interactions Involving Histidine: The Effect of Charge on pi-pi Stacking and T-Shaped Interactions with the DNA Nucleobases.* Journal of Physical Chemistry B, 2009. **113**(49): p. 16046-16058.
168. Gallivan, J.P. and D.A. Dougherty, *Cation-pi interactions in structural biology.* Proceedings of the National Academy of Sciences of the United States of America, 1999. **96**(17): p. 9459-9464.
169. Liao, S.M., et al., *The multiple roles of histidine in protein interactions.* Chemistry Central Journal, 2013. **7**.
170. McGaughey, G.B., M. Gagne, and A.K. Rappe, *pi-stacking interactions - Alive and well in proteins.* Journal of Biological Chemistry, 1998. **273**(25): p. 15458-15463.
171. Loewenthal, R., J. Sancho, and A.R. Fersht, *Histidine Aromatic Interactions in Barnase - Elevation of Histidine Pk(a) and Contribution to Protein Stability.* Journal of molecular biology, 1992. **224**(3): p. 759-770.
172. Silva, M., A.M. Figueiredo, and E.J. Cabrita, *Epitope mapping of imidazolium cations in ionic liquid-protein interactions unveils the balance between hydrophobicity and electrostatics towards protein destabilisation.* Physical Chemistry Chemical Physics, 2014. **16**(42): p. 23394-23403.

Chapter 4 Stabilization of enzymes in ionic liquids via modification of enzyme charge

This chapter was adapted from Biotechnology and Bioengineering 110, 2352-2360

4.1 Abstract

Due to the propensity of ionic liquids to inactivate enzymes, the development of strategies to improve enzyme utility in these solvents is critical to fully exploit ionic liquids (ILs) for biocatalysis. We have developed a novel strategy to broadly improve enzyme utility in ILs based on elucidating the effect of charge modifications on the function of enzymes in IL environments. Results of stability studies in aqueous-IL mixtures specifically indicated a clear connection between the ratio of enzyme-containing positive-to-negative sites and enzyme stability in ILs. Stability studies of the effect of [BMIM][Cl] on chymotrypsin specifically found an optimum ratio of enzyme-containing positive-to-negative sites at which the enzyme was most stable. An optimum ratio of positive-to-negative sites was similarly obtained for the effect of [BMIM][Cl] on lipase and papain as well as for the effect of [EMIM][$EtSO_4$] on chymotrypsin. More generally, the results of stability studies found that modifications that reduce the ratio of enzyme-containing positive-to-negative sites improve enzyme stability in ILs. The understanding of the impact of charge modification on enzyme stability in ILs may ultimately be exploited to rationally engineer enzymes for improved function in IL environments.

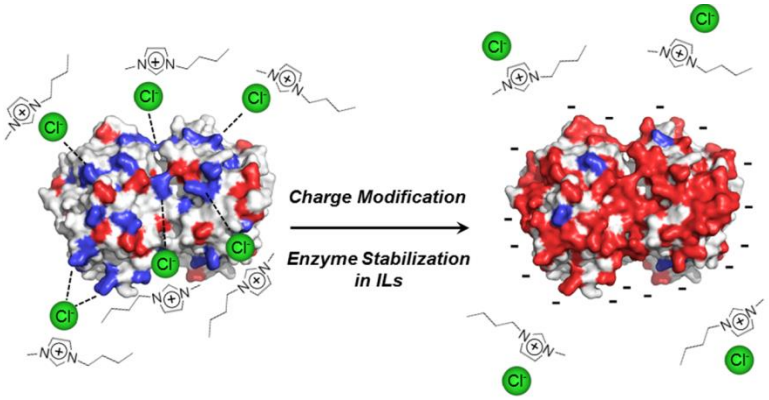

Figure 4.1. Graphical abstract: modifying the charge of an enzyme can potentially mediate ionic liquid-enzyme interactions in a stabilizing manner.

4.2 Introduction

As solvents for anhydrous biocatalysis, ionic liquids (ILs), which have auspicious properties for chemical processing, present considerable opportunities. However, the use of enzymes in ILs has, to date, met with only modest success due to the propensity of ILs to inactivate and destabilize enzymes. The deleterious impact of ILs on the activity and stability of enzymes has, in turn, largely limited the range and thus properties of ILs that may be exploited for biocatalysis. Specifically, outside of dialkylimidazolium ILs with hexafluorophosphate, tetrafluoroborate, trifluoromethylsulfonate, and bis(trifluoromethylsulfonyl)imide anions, few ILs, with the exception of select alkylpyridinium and tetraalkylammonium ILs,[19, 78, 173, 174] have proven useful for biocatalysis. As such, the development of strategies to reduce the impact of ILs on enzyme activity and stability is crucial to the overall utility of ILs as solvents for biocatalytic reactions.

The inactivation and subsequent destabilization of enzymes in ILs, although not well understood, may be attributed to the binding of ILs with enzymes. Structure-activity data from previous work suggests that the interaction of enzymes and ILs is highly anion-dependent.[19, 71, 173] ILs with strongly nucleophilic anions, such as nitrate, thiocyanate, and trifluoroacetate, are found to induce conformational changes.[175] Shu and co-workers[161] recently elucidated the role of electrostatic interactions in mediating the interaction of the ILs dibutylimidazolium chloride, 1-butyl-3-methylimidazolium chloride ([BMIM][Cl]), and 1-butyl-3-methylimidazolium nitrate to the model protein bovine serum albumin in aqueous-IL mixtures, which led to the loss of secondary and tertiary structure. Association of the ILs with albumin also involved hydrophobic interactions between the imidazolium cation and non-polar residues on the protein surface as well as hydrogen bonding interactions. Similarly, non-covalent interactions, involving

electrostatic, hydrophobic, and hydrogen bonding interactions, have been implicated in the formation of other IL-protein complexes in dilute IL solutions.[67, 176, 177] Insight into such interactions has been expanded via molecular simulations, which have, notably, shed light on the relative strength of the respective interaction types in neat ILs.[139, 178] Using simulations, the contribution of electrostatic interactions between anions and proteins as well as hydrophobic interactions between cations and proteins was determined to be largest relative to other interaction types.[178]

Several approaches to enhance the activity and stability of enzymes in bulk ILs and thus the broad utility of ILs for biocatalysis have been explored. Such approaches include adsorption, polyethylene glycol (PEG)-modification, and chemical crosslinking. These approaches have conventionally been employed to prevent deactivating conformational changes in harsh environments, leading to enhanced enzyme activity.[179-181] Using these approaches, the activity and stability of enzymes have been improved in certain ILs with varying degrees of success.[73, 75-78, 174, 182] However, such techniques have, in almost all cases, only proven effective in ILs with cations and anions that can generally be tolerated by enzymes without modification. In this way, the use of these techniques has largely been unsuccessful in expanding the overall range of ILs in which enzymes may function efficiently.

In the present work, we have developed a novel strategy to broadly improve enzyme function in ILs based on investigating the effect of enzyme charge on activity and stability in IL environments. Specifically, we have characterized the impact of chemically modifying the charge state of ionizable residues in an enzyme on the tolerance of enzymes to IL-induced inactivation. We hypothesized that altering the charge state of residues in an enzyme will provide an approach to mediate electrostatic interactions between ILs and enzymes. Moreover, altering

the surface charge of an enzyme may, in principle, also prevent hydrophobic interactions that can influence IL-enzyme binding. The connection between enzyme charge and IL tolerance was recently illuminated by Zhang and co-workers[183] who reported on the tolerance of a halophilic cellulase in highly concentrated IL solutions. In this work, the highly negatively charged cellulase was shown to be remarkably active in ILs in which enzymes with less charge, namely mesophilic enzymes, had little to no activity.

Herein, the effect of enzyme charge on IL tolerance was explored by systematically modifying charged sites, namely primary amines and acid groups, in the model enzyme α-chymotrypsin (CT). The modification chemistries, which enable all possible charge modifications, that were employed include: 1) acetylation, which replaces amines with uncharged acetyl groups, 2) succinylation, which replaces amines with negatively-charged acid groups, 3) cationization, which converts acids to positively-charged amines, and 4) neutralization, which converts acids to neutral ethyl groups (**Figure 4.2**). Enzyme tolerance upon modification was subsequently determined by measuring the activity and stability of CT in solutions of [BMIM][Cl]. To determine if the effect of enzyme charge on IL tolerance was general versus enzyme specific, the enzymes lipase (CRL) and papain (PPI) were similarly modified and characterized in [BMIM][Cl]. Of note, these enzymes had almost no structural homology. Moreover, the effect of enzyme charge was ascertained in 1-ethyl-3-methylimidazolium ethyl sulfate ([EMIM][$EtSO_4$]) to further generalize the apparent impact of charge across ILs. The use of [BMIM][Cl], owing to its high capacity to dissolve cellulose and thus potential use in biomass conversion,[17, 184-186] and [EMIM][$EtSO_4$][147, 187, 188] as biocatalytic solvents have attracted widespread interest.

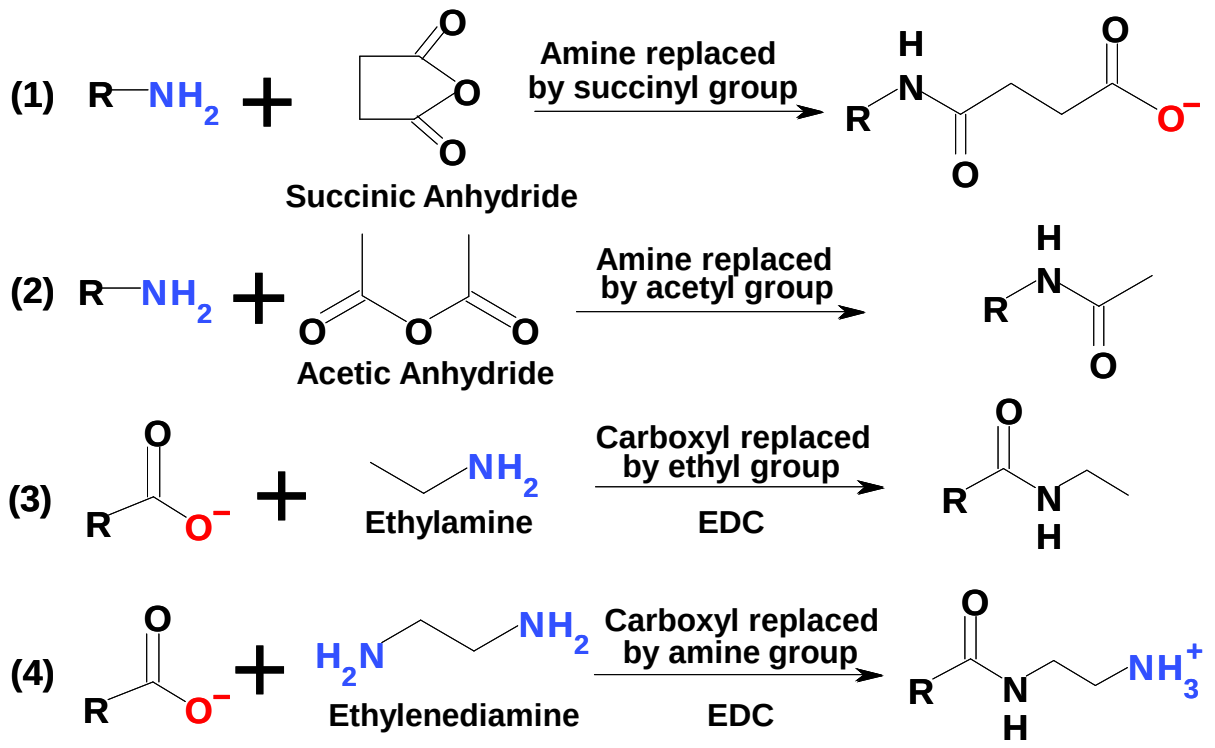

Figure 4.2. Chemistries of the modifications used to create charge variants of enzymes. The modifications used to alter enzyme charge include (1) acetylation, (2) succinylation, (3) cationization, and (4) neutralization.

4.3 Materials and methods

4.3.1 Materials

All enzymes, including CT from bovine pancreas, PPI (*Carica papaya*), and CRL (*Candida rugosa*, type VII) were purchased from Sigma Aldrich (St. Louis, MO) and used without further purification. The enzyme substrates N-succinyl-alanine-alanine-proline-phenylalanine paranitroanalide (SAAPPpNA), benzoyl-D,L-arginine 4-nitroanilide hydrochloride (BApNA), and 4-nitrophenyl butyrate (pNPB) and ILs 1-butyl-3-methylimidazolium chloride ([BMIM][Cl]) and 1-ethyl-3-methylimidazolium ethyl sulfate

([EMIM][$EtSO_4$]) as well as all other reagents were also purchased from Sigma Aldrich and were of the highest purity available.

4.3.2 Enzyme modification

To systematically vary the charge of CT, CRL, and PPI, the enzymes were chemically modified as described by Stoner and co-workers.[189] Briefly, succinylated and acetylated forms of the enzymes were produced by reacting each of the enzymes with succinic anhydride (in 1 M sodium carbonate buffer, pH 8.5) or acetic anhydride (in 100 mM phosphate buffer, pH 7.0), respectively. Succinic or acetic anhydride was added to the enzyme (1 – 10 mg/ml) in solution at a 20:1 molar excess per primary amine sites per sequence. Following the addition of succinic anhydride, which was added incrementally over the course of 2 hrs, the reaction was mixed at room temperature for 1 hr. The reaction with acetic anhydride, which was also added incrementally, was stirred at 4 °C for 1.5 hrs. Residual free succinic anhydride or acetic anhydride was removed via buffer exchange by means of centrifugal filtration after which the enzyme was lyophilized. To cationize the enzymes, the enzymes (1 – 10 mg/ml) were reacted with ethylenediamine dihydrochloride (0.5 M) in buffer (200 mM MES, pH 4.5) containing a 20:1 molar ratio of the crosslinking reagent N-(3-dimethylaminopropyl)-N'-ethylcarbodiimide (EDC)-to-acid sites for 2.5 hrs at room temperature while stirring. Excess diamine and EDC were similarly separated by centrifugal filtration and simultaneous buffer exchange, which was followed by lyophilization of the enzyme. Additionally, acid groups in the enzymes were neutralized via reaction with ethylamine (0.5 M) in buffer (200 mM MES, pH4.5) also using EDC as a crosslinker at a 20:1 molar ratio of EDC-to-acid sites. Like the cationization reaction, the neutralization reaction was stirred for 2.5 hrs at room temperature. Following removal of excess amine and EDC and buffer exchange using a centrifugal filtration device, the neutralized

enzyme was freeze-dried like the other modified forms. The final buffer in which the enzymes were exchanged matched that used for activity measurements. Additionally, the protein concentration of the modified enzymes was determined via measuring absorbance of the modified enzymes at 280 nm (ε_{CT} = 51,840 $M^{-1}cm^{-1}$, ε_{CRL} = 54,650 $M^{-1}cm^{-1}$, ε_{PPI} = 55,010 $M^{-1}cm^{-1}$).

4.3.3 Characterization of enzyme modification

The extent of enzyme modification was determined by titrating the number of amine and carboxylates groups in modified CT, CRL, and PPI. Specifically, the number of primary amines in the modified enzymes was titrated spectrophotometrically at 335 nm with trinitrobenzene sulfonic acid (TNBS) using a Thermo Fisher Scientific (Waltham, MA) Evolution 260 Bio UV/Vis spectrophotometer. The number of carboxylate groups in the modified enzymes was titrated with Woodward's reagent k (N-ethyl-5-phenylisoxazolium-3'-sulfonate), which, upon reaction with a carboxylate group, yields an enol ester. Formation of the enol ester product was also detected spectrophotometrically at 269 nm as described previously.[190] For the titration of enzyme charge variants with Woodward's reagent k, wild-type enzyme was used as a calibration standard.

4.3.4 Measurement of enzyme activity in ionic liquids

Specific activity of wild-type and modified CT, PPI, and CRL were assayed spectrophotometrically using the substrates SAAPPpNA (0.25 mg/mL), BApNA (2 mM), and pNPB (1.25 mg/mL), respectively. In the case of CT, wild-type and modified enzyme were assayed in 50 mM phosphate buffer, pH 7.8 containing 2.5 % (v/v; final concentration) dimethyl sulfoxide. Similarly, wild-type and modified PPI were assayed in 50 mM phosphate buffer, pH

6.5 also containing 2.5 % (v/v; final concentration) dimethyl sulfoxide. Wild-type and modified CRL were assay in 300 mM MES buffer, pH 5.7 containing 2 % (v/v; final concentration) acetonitrile. Aqueous-IL mixtures were prepared by adding IL to buffer containing dimethyl sulfoxide or acetonitrile at the specified pH. For all enzymes, substrate conversion was monitored continuously at 412 nm at room temperature over the initial rate range. One unit of activity was defined as the change in absorbance per second at the specified assay conditions.

4.3.5 Measurement of enzyme stability in ionic liquids

Wild-type and modified CT, CRL, and PPI were incubated in aqueous-IL solutions containing 30 or 40 % (v/v) [BMIM][Cl] at either 25 or 30 °C. The aqueous-IL solutions were prepared in buffer, which matched that used for activity measurements. Enzyme inactivation was followed by removing aliquots (975 μL) periodically and assaying residual enzyme activity in the presence of ILs upon the addition of substrate (25 μL) for up to 60 hrs. For each of the enzymes, the amount of wild-type and modified enzyme used was normalized to have approximately the same initial activity. Additionally, the inactivation of CT in 55 % (v/v) [EMIM][$EtSO_4$] at 35 °C was similarly followed by means of periodically assaying residual enzyme activity. Enzyme half-life was determined by fitting the resulting stability curves to a first order inactivation model.

4.4 Results and discussion

4.4.1 Charge modification of chymotrypsin

To investigate the effect of enzyme charge on the tolerance of enzymes to ILs, CT, a classic model enzyme of known structure that catalyzes alcoholysis reactions in anhydrous

solvents, was initially modified via acetylation, succinylation, cationization, and neutralization. The total number of modifiable primary amines and acid groups in CT based on sequence is 15 and 15, respectively. These groups include the ε-amino groups of lysines, the N-terminal amine, the C-terminal carboxylic acid, and carboxylic acid groups in the side chain of aspartate and glutamate residues. Analysis of the crystal structure of CT revealed that virtually all of the target residues are located on the enzyme's surface, restricting potential modifications to sites on the surface of CT. Based on pK_a prediction, the most reactive acid sites acid are Asp35 and Asp72 and the most reactive amine sites are Lys169, Lys202, and Lys203. In addition to the C and N terminal acid and amine, the side chains of these residues have distinctly low pK_a values compared to the other potential modification sites in CT. These sites, because of their low pK_a value, are likely to be unprotonated and thus nucleophilic under the modification conditions.

Modification of the enzyme resulted in varying degrees of conversion of primary amines and acids, which was quantified via titrating the number of amines and acids in the modified enzyme (**Table 4-1**). Upon modification, the number of primary amines and acids in CT ranged from 3.7 to 23.3 and 5.0 to 28.8, respectively, indicating differences in overall charge between the modified species. Of note, the number of titratable primary amines in wild-type CT was slightly greater than expected based on sequence analysis. This difference is presumably due to the potential cross-reactivity of TNBS, which was used to titrate the number of primary amines, with other residues, namely arginine (wild-type CT contains 3 Arg residues). The total protein charge for CT was also measured by isoelectric focusing (**Figure 4.3**). The neutralized and cationized forms of CT seem to have a pI so high that they did not run appreciably far on the gel. The acetylated and succinylated forms, meanwhile, were both modified to have an isoelectric point < 4.2 on average. The TNBS assay measures the average degree of modification, but

isoelectric focusing does suggest there may be some population heterogeneity as indicated by the band thickness. However, it may be difficult to compare band thickness at a pI of 9.5 to band thickness at a pI of 3.5. Additionally, the impact of the modifications on the specific activity of CT was minimal as confirmed by activity assays, indicating that the aspartate in the active site was not modified. The modifications presumably also do not disrupt the critical interaction between Ile16 and Asp194.[191]

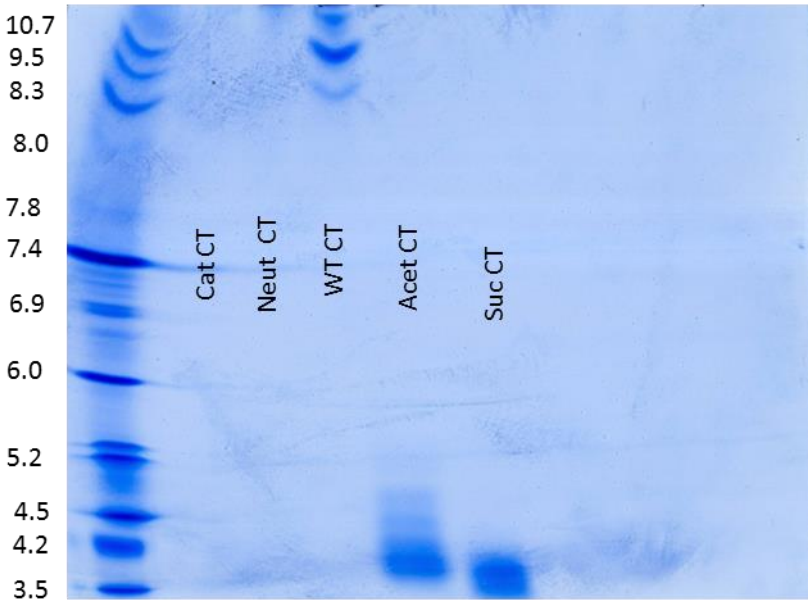

Figure 4.3. Isoelectric focusing of chymotrypsin (CT) and charge variants. The cationized and neutralized forms have a pI > 10.7.

Table 4-1. Extent of reaction of CT upon charge modification. The values for the average number of primary amines and carboxylates represent the average and standard deviation of two independent experiments.

	Average # Primary Amines	Average # Carboxylates	Ratio of Primary Amines:Acids
Wild-type CT	17.5±0.2	15.0±0.0[*]	1.17
Acetylated CT	5.9±0.1	15.0±0.0[†]	0.39
Cationized CT	23.3±0.1	9.2±0.1	2.53
Succinylated CT	3.7±0.1	28.8±0.1	0.13
Neutralized CT	17.5±0.2[‡]	5.0±1.2	3.50

[*]Number is based on theoretical number in enzyme sequence.
[†]Number was assumed to be same as in wild-type enzyme.
[‡]Number was assumed to be same as in wild-type enzyme.

4.4.2 Effect of charge modification on chymotrypsin tolerance to [BMIM][Cl]

Tolerance studies showed little effect of enzyme charge on the activity of CT in [BMIM][Cl] over the range of IL concentrations used (**Figure 4.4A**). Specifically, the activity of the charge variants of CT was similar to that of wild-type CT in aqueous-IL mixtures that contained 0 to 50 % (v/v) [BMIM][Cl]. However, interestingly, significant differences in the apparent stability of CT in [BMIM][Cl] were observed for the different charge variants, including wild-type CT (**Figure 4.4B**). The stability of wild-type and modified CT was measured by monitoring enzyme inactivation in 40 % (v/v) [BMIM][Cl] at 25 ºC. In measuring stability, CT activity was periodically assayed without significantly diluting the concentration of IL, thus preventing potential re-folding of the enzyme after incubation in the IL. Stability studies indicated that the acetylated form of the enzyme was most stable in the IL, retaining approximately 40 % of its initial activity after nearly 10 h. By comparison, wild-type,

succinylated, cationized, and neutralized CT retained 32, 24, 23, and 14 % activity, respectively, over the same time period.

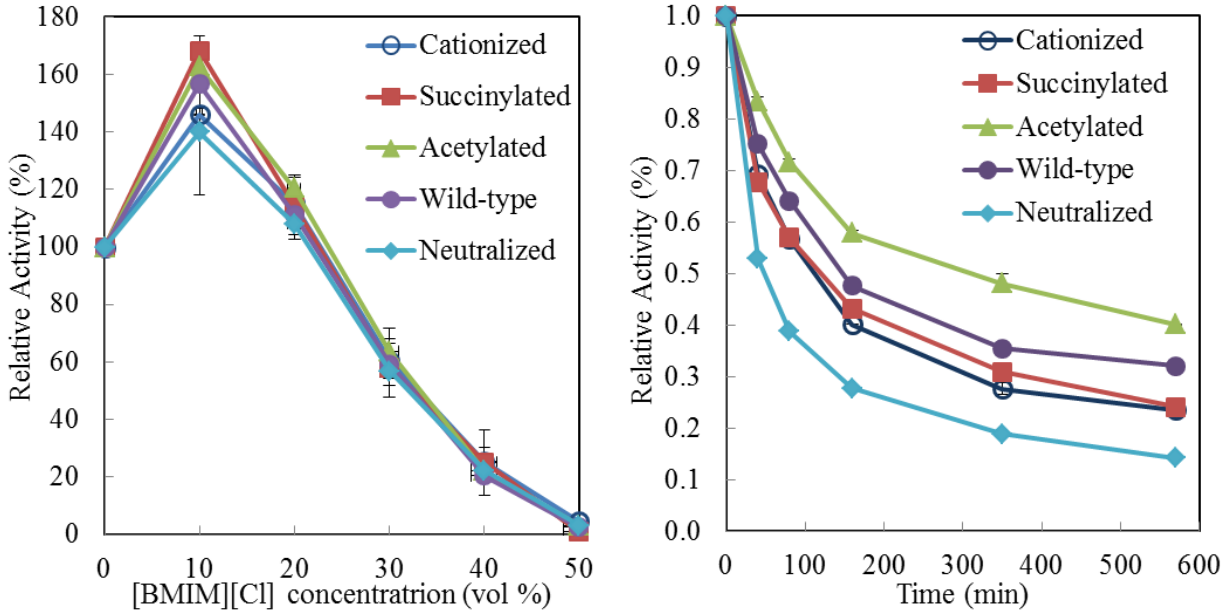

Figure 4.4. Effect of charge on the (A) activity and (B) stability of wild-type (●) and modified (acetylated (▲), succinylated (■), cationized (○), neutralized (♦)) charge variants of CT in 40 % (v/v) [BMIM][Cl] at 25 ºC. Error bars, which in some cases are smaller than the symbols, represent the standard deviation from the mean of two separate experiments.

Differences in stability of variants with a similar number of total primary amines and acids (i.e. acetylated and neutralized CT) suggest that the stability of CT in [BMIM][Cl] is not dependent on net electrostatic potential. The apparent differences in stability may instead presumably be primarily attributed to differences in the ratio of positive-to-negative charged groups of the charge variants. The dependence of stability of CT on this ratio was confirmed by analysis of the enzyme half-life as a function of the molar ratio of primary amine-to-acid groups in CT (**Figure 4.5**). Analysis of the stability of CT in [BMIM][Cl] as a function of the molar ratio of primary amines-to-acids indicated an apparent maximum at an amine-to-acid ratio of 0.39, corresponding to that of the acetylated form of CT. Presumably, at the pH at which stability

of CT was measured (pH 7.8), the amine groups in the enzyme were fully protonated and the acid groups fully deprotonated. Importantly, this presumption does not account for the potential effect of electrostatic interactions with neighboring residues in CT on the protonation state of these groups. Furthermore, the contributions of histidine and arginine residues to enzyme charge were not considered. The likely contributions of histidines and arginines, given their low abundance (there are 2 His and 3 Arg residues in CT), in CT is small, although such contributions may be significant in the case of other enzymes.

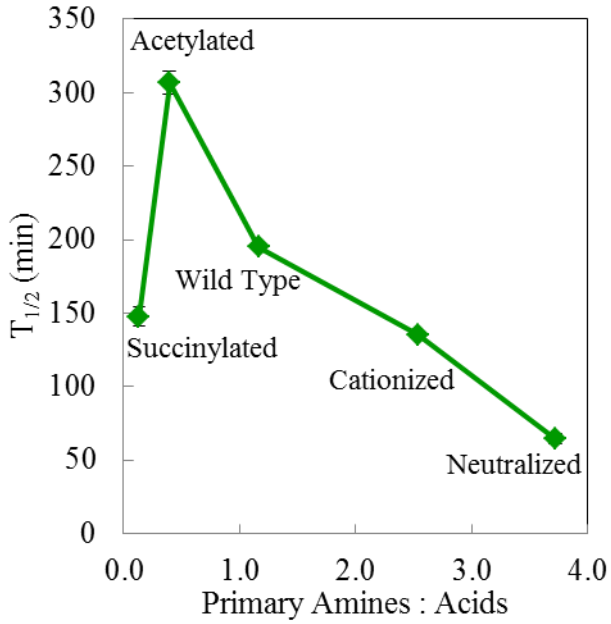

Figure 4.5. Half-life of charge variants of CT in 40 % (v/v) [BMIM][Cl] at 25 ºC as a function of the molar ratio of enzyme-containing primary amine-to-acid groups. Error bars, which in some cases are smaller than the symbols, represent the standard deviation from the mean of two separate experiments.

4.4.3 Effect of charge modification on lipase and papain tolerance to [BMIM][Cl]

Given the results of stabilities studies of CT in [BMIM][Cl], a natural question is to ask if the effect of charge ratio on stability in ILs is enzyme specific or applicable to other enzymes?

Specifically, we were interested in ascertaining if general trends with respect to enzyme stability in ILs as a function of the ratio of primary amines-to-acids exist. To answer this question, the stability of charge modified variants of CRL and PPI were similarly measured in [BMIM][Cl]. CRL and PPI, like CT, have known structures and catalyze industrially important synthetic transformations in the absence of bulk water. The stability of CRL and PPI, which were modified similarly to CT (**Table 4-2**), were assayed upon incubation in 40 and 30 % (v/v) [BMIM][Cl], respectively, at 30 ºC. The concentrations of [BMIM][Cl] used corresponded to the highest concentrations of IL in which the enzyme retained activity. Additionally, wild-type CRL has 18 primary amines and 45 acid groups, including the C-terminal carboxylic acid, while wild-type PPI has 12 primary amines and 16 acid groups, including the C-terminal carboxylic acid. Like in CT, nearly all of the lysines, glutamates, and aspartates in CRL and PPI are situated on the surface of both enzymes. The most likely positions of modification based on pK_a analysis include Asp340, Glu341, Lys 170, Lys274, Lys437, and the N-terminal amine for CRL and Asp6, Asp57, Asp140, Asp158, Lys10, Lys174, the N-terminal amine for PPI. Compared to CT, which has 30 total potential surface modification sites, CRL and PPI have 63 and 28, respectively. The enzymes also largely differ in isoelectric point. The theoretical pI of CRL and PPI is 4.8, and 9.2, respectively, compared to 8.7 for CT.

Results of stability studies with CRL and PPI, like with CT, indicated marked differences between charge variants (**Figure 4.6**). For CRL, the most stable variant was the succinylated form of the enzyme, which had the lowest ratio of primary amines-to-acids amongst the CRL variants (**Table 2**). For PPI, the most stable variant was the acetylated form, which likewise had the lowest ratio of primary amines-to-acids amongst PPI variants. When analyzed in terms of half-life versus primary amine-to-acid ratio, a clear dependence of stability on the ratio of

primary amines-to-acids was observed as with CT (**Figure 4.6C** and **D**). Decreasing the relative ratio of enzyme-containing primary amines-to-acids yielded an increase in half-life of CRL and PPI by as much as 4.0 and 2.4-fold, respectively, compared to wild-type. The trend in half-life associated with increasing and decreasing the primary amine-to-acid ratio in CRL and PPI matches that found for CT, suggesting the effect of this ratio on enzyme stability in ILs is indeed general. Thus, charge modification may be employed as a general strategy to improve the overall stability of enzymes and, more broadly, proteins in general against IL-induced inactivation. Notably, for CRL and PPI, because, as with CT, the trend in stability decreased as the ratio of primary amines-to-acids increased, the cationization was thought to be further disruptive of activity. To this point, the amount of cross-linking reagent for CRL was reduced 2-fold and the cationization and neutralization reaction performed again to yield a more moderate primary amine:acid ratio. As expected, a more moderate amine: acid ratio was achieved than 4.8 but the cationized and neutralized forms of the enzyme still have a lower half-life than the wild-type (**Figure 4.7**). Additionally, because neutralization of PPI led to near complete loss of activity in 30 vol % [BMIM][Cl], the half-life of the neutralized charge variant of PPI was presumed to be zero. Notably, papain did retain activity in plain buffer.

Table 4-2. Extent of reaction of CRL and PPI upon charge modification. The values for the average number of primary amines and carboxylates represent the average and standard deviation of two independent experiments.

	Average # Primary Amines		**Average # Carboxylates**		**Ratio of Primary Amines:Acids**	
	CRL	PPI	CRL	PPI	CRL	PPI
Wild-type	16.6±1.0	19.1±0.4	45.0±0.0*	16±0.0*	0.37	1.19
Acetylated	9.8±0.2	2.4±0.3	45.0±0.0†	16±0.0†	0.22	0.15
Succinylated	4.6±0.2	11.6±1.0	57.0±1.2	23.5±0.9	0.08	0.50
Neutralized	16.6±1.0‡		3.5±0.1		4.80	

*Number is based on theoretical number in enzyme sequence.
†Number was assumed to be same as in wild-type enzyme.
‡Number was assumed to be same as in wild-type enzyme.

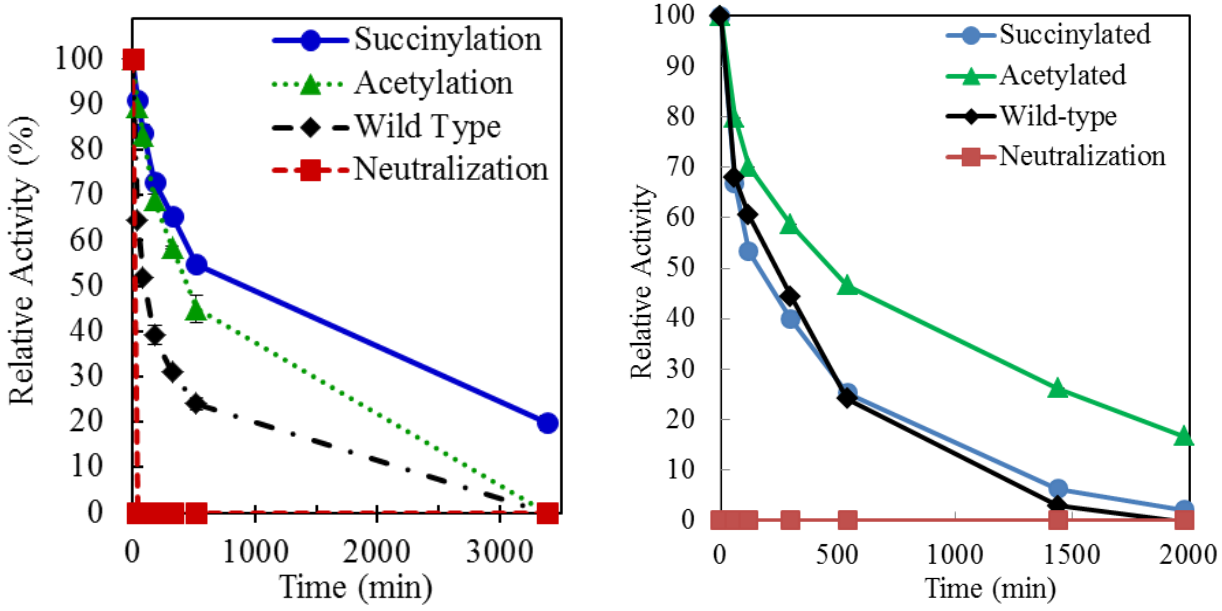

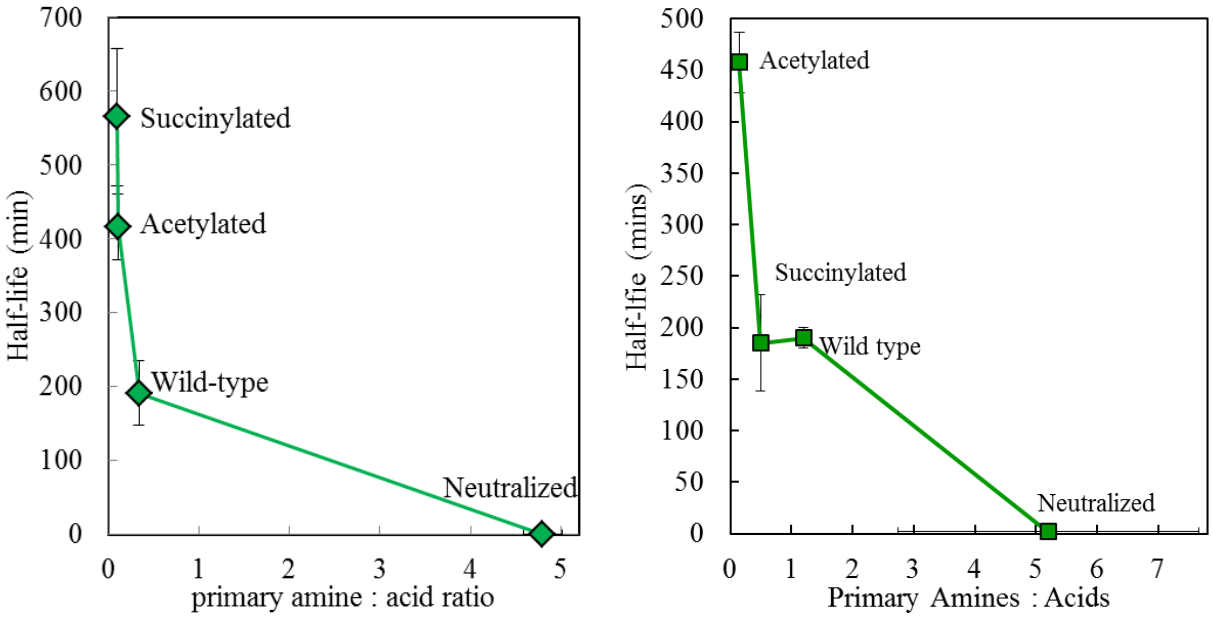

Figure 4.6. Effect of charge on the stability of wild-type (♦) and modified charge variants (acetylated (▲), succinylated (●), neutralized (■)) of (A) CRL and (B) PPI in 40 and 30 % (v/v) [BMIM][Cl], respectively, at 30 ºC. The half-life of (C) CRL and (D) PPI as a function of the molar ratio of enzyme-containing primary amine-to-acid groups is also shown. Error bars, which in some cases are smaller than the symbols, represent the standard deviation from the mean of two separate experiments.

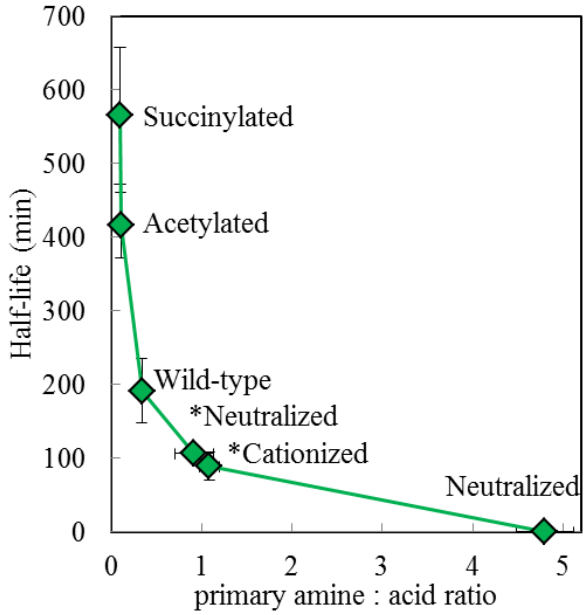

Figure 4.7. The half-life of lipase variants with two extra forms of the enzyme. The *Neutralized and *Cationized forms were made according to the materials and methods except that the cross-linker concentration was reduced 2-fold to decrease the extent of modification.

Although the trend in enzyme half-life as a function of primary amine-to-acid ratio was similar, the apparent optimum ratio for CRL (0.08) and PPI (0.15) was lower than that for CT. This apparent difference may be due to disparities in the number of positively charged arginine and histidine residues in the enzymes (CRL and PPI have 23 and 15 combined arginine and histidines, respectively, compared to CT, which has only 5). Differences in this number, as pointed out above, are overlooked when using the ratio of primary amines-to-acids as a proxy for the ratio of positive-to-negative charged groups in an enzyme. Hence, the optimum ratio of positive-to-negative charged sites for CT, CRL, and PPI may not be directly compared based on the dependence of stability on the primary amines-to-acid ratio. Moreover, the protonation state of charged surface residues may have differed due to different pH's at which the stability of the three enzymes were measured. Of note, isoelectric focusing was attempted for CRL, but the bands were too faint for all forms of the enzyme, yielding meaningless data.

It is also noteworthy that the stabilization of CRL at low primary-amine-to-acid ratios was more dramatic for CRL than PPI or CT. The increased stabilization of CRL may be due CRL having to a greater number of total charged surface sites and thus electrostatic potential relative to the other enzymes. Perhaps the larger number of modification sites led to the enhanced stabilization effects. Also, the net potential charge on an enzyme surface may play a role. As further evidence of this, relative to cationized CT (approximately 32.5 total primary amines and acids), CT that was modified via both neutralization and acetylation (approximately 17 total primary amines and acids) was less stable towards [BMIM][Cl] despite having a similar ratio of enzyme-containing primary amine-to-acid groups (data not shown), although this may simply be the result of reducing the intrinsic stability of the enzyme.

4.4.4 Effect of charge modification on chymotrypsin tolerance to [EMIM][$EtSO_4$]

In addition to determining if the effect of charge modification on stability in [BMIM][Cl] can be applied to multiple enzymes, we also investigated if this effect is significant in other ILs. To generalize the effect of charge modification on enzyme stability in other ILs, the stability of CT variants was assayed in [EMIM][$EtSO_4$] as a function of the ratio of primary amines-to-acids. Reports that [EMIM][$EtSO_4$], which is miscible with water and thus considered hydrophilic, can dissolve proteins indicates that [EMIM][$EtSO_4$] can interact strongly with proteins.[147, 188] Upon incubation in 55 vol % [EMIM][$EtSO_4$] at 35 ºC, the half-life of CT also had a strong dependence on the primary amine-to-acid ratio (**Figure 4.8**). Notably, this dependence mirrored that observed for CT in [BMIM][Cl], exhibiting a maximum stability at a ratio of primary amines-to-acids of 0.39, which matched that found in [BMIM][Cl]. Interestingly, the half-life of succinylated CT, which had a primary amine-to-acid ratio of 0.13, was also considerably greater than that of wild-type CT in [EMIM][$EtSO_4$]. This was unexpected given that, upon incubation in [BMIM][Cl], the half-life of succinylated CT was lower than that of wild-type CT.

The greater half-life of succinylated CT in [EMIM][$EtSO_4$] compared to in [BMIM][Cl] may be related to differences in the concentration of the respective ILs used in stability studies. Specifically, it is plausible that the stabilizing effect of reducing the primary amine-to-acid ratio may be larger at higher IL concentrations, as was used in the case of [EMIM][$EtSO_4$]. It is also plausible that the greater stability of CT in [EMIM][$EtSO_4$] is due to differences with which chloride and sulfate anions interact with the enzyme surface. Chloride anions, because of a weaker exclusion capacity than sulfate anions, may not get excluded by the charged residues to as large of a degree.[192, 193] Ultimately, the results of stabilities studies in [EMIM][$EtSO_4$]

provide evidence for charge modification as a general approach to enhance enzyme stability in imidazolium based ILs.

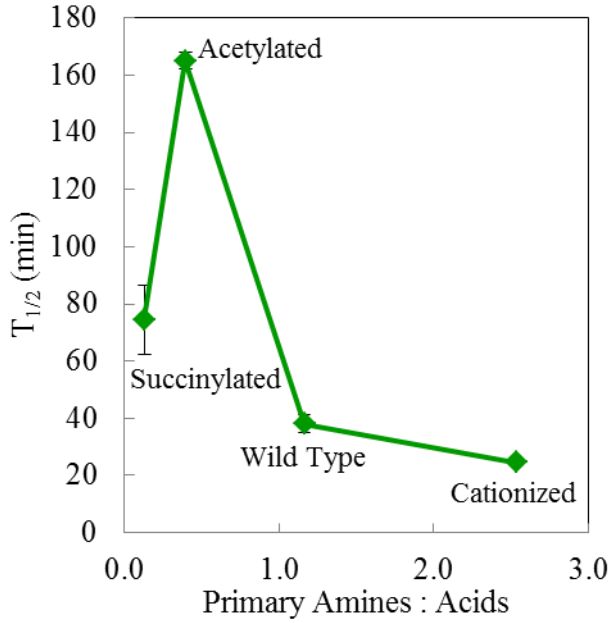

Figure 4.8. Dependence of the half-life of CT as a function of the molar ratio of enzyme-containing primary amine-to-acid groups in 55 vol % [EMIM][$EtSO_4$] at 35 ºC. Error bars, which in some cases are smaller than the symbols, represent the standard deviation from the mean of two separate experiments.

4.4.5 Implications for rationally engineering enzymes for improved function in ionic liquids

Our results overall support a dependence of enzyme stability in ILs on charge modification and, more specifically, the ratio of positive-to-negative charged sites in an enzyme. This dependence also supports the underlying existence of a relationship between the ratio of positive-to-negative charged sites and the extent of solvent-enzyme interactions in ILs. Based on improvements in stability, such interactions were presumably inhibited most strongly via modifications that reduce the ratio of positive-to-negative sites. The addition of negatively charged sites, which lower this ratio, may specifically repel the binding of anions to the enzyme

surface. Such modifications (i.e. acetylation), depending on chemistry, may also remove positive charged sites, which, in turn, eliminates sites for anion association. However, for some enzymes, namely CT, there appears to be a critical ratio below which stabilization is diminished. Diminished stabilization in such cases is likely due to increased repulsion of negatively charged sites, which can lower the intrinsic enzyme stability.[194, 195] Conversely, increasing the ratio of positive-to-negative sites via modification led to a decrease in enzyme stability in both [EMIM][$EtSO_4$] and [BMIM][Cl] for all enzymes tested. In light of this, these results underscore the importance of mediating anion interactions in stabilizing enzymes in ILs.

Protein charge has been shown to be critical to the stability of proteins, including enzymes, in non-related extreme environments. In direct connection with this work, Stoner et al.[189] previously reported on the stabilization of cellulase in the presence of denaturing surfactants via modification of enzyme charge. The stabilization of cellulase upon charge modification was specifically shown to correlate with an increase in electrostatic repulsion of the surfactants from the enzyme. Notably, these results suggest striking similarities with which ILs and charged surfactant molecules presumably interact and denature proteins. Remarkable similarities between the importance of charge on enzyme stability in ILs and the stability of halophilic proteins in hypersaline environments in nature also exist. Structural studies have specifically shown that proteins from halophiles have a markedly higher content of acidic residues relative to related proteins from non-halophilic mesophiles.[141, 196-201] The clustering of acidic residues on the surface of halophilic proteins serves to attract water molecules, which increase protein hydration, and also reduce aggregation, thereby preventing salting-out.[140, 141] Furthermore, certain halophilic proteins have been shown to increase in conformational stability as a function of NaCl and KCl, at even molar quantities, atypical to normal NaCl-protein

effects.[96, 202] Given that ILs are molten salts, it is perhaps not surprising that the distribution of negative charges on the surface of enzymes is similarly important in ILs as in hypersaline environments. Aside from mediating enzyme-IL interactions, it is conceivable that lowering the ratio of enzyme-containing primary amines-to-acids may also improve function in ILs as a result of altering enzyme hydration favorably. Zaccai and Eisenberg suggest that the mechanism of salt stabilization of a halophilic malate dehydrogenase is by coordinating a hydrated salt network resulting in strong binding of water molecules in the native state, but not the unfolded state.[203]

4.5 Conclusions

We have studied the impact of surface charge on enzyme tolerance in ionic liquid. Interestingly, surface charge plays little, if any role in the magnitude of activity as a function of IL concentration. However, upon incubating enzymes at high concentrations of IL, the activity is lost over time, but more slowly for certain charge variants. There is likely interplay between nonspecific and IL specific effects on protein stability that result in increased or decreased half-lives. Likely (and will be explored in the following chapter), charge modification has varying effects on the intrinsic stability of the enzyme. It is interesting, however, that modifying an enzymes' negatively charged amino acids via cationization or neutralization was deleterious in all scenarios. Meanwhile, modification of an enzyme's positive lysines by acetylation was always beneficial and modification of lysines by succinylation was sometimes beneficial. Based on the results, positive charges tend to be deleterious in imidazolium ionic liquids while negative charges can possibly be beneficial. Perhaps the mechanism is based on total salt-binding. If the electrostatic interaction of the anion is indeed stronger than an electrostatic interaction of the cation, perhaps negative charges reduce the total propensity of [BMIM][Cl] to bind to proteins.

That is, the combined interaction of the anion and cation is less with a negative charge than with a positive charge.[172] Whether these effects are purely kinetic (raising the activation barrier for unfolding), thermodynamic (alter the ΔG of unfolding in [BMIM][Cl]), or a combination of the two remains to be seen. If the effect is thermodynamic and specific to ILs, that implies that reducing binding in the unfolded state is greater than binding reduction in the folded state. Nonetheless, non-specific charge modification appears to be a facile strategy for improving activity retention of enzymes in ionic liquids.

4.6 References

17. Pinkert, A., et al., *Ionic Liquids and Their Interaction with Cellulose.* Chemical Reviews, 2009. **109**(12): p. 6712-6728.
19. van Rantwijk, F. and R.A. Sheldon, *Biocatalysis in ionic liquids.* Chemical Reviews, 2007. **107**(6): p. 2757-2785.
67. Singh, T., et al., *Ionic Liquids Induced Structural Changes of Bovine Serum Albumin in Aqueous Media: A Detailed Physicochemical and Spectroscopic Study.* Journal of Physical Chemistry B, 2012. **116**(39): p. 11924-11935.
71. Kaar, J.L., et al., *Impact of ionic liquid physical properties on lipase activity and stability.* Journal of the American Chemical Society, 2003. **125**(14): p. 4125-4131.
73. Persson, M. and U.T. Bornscheuer, *Increased stability of an esterase from Bacillus stearothermophilus in ionic liquids as compared to organic solvents.* J Mol Catal B: Enzym, 2003. **22**(1-2): p. 21-27.
75. Toral, A.R., et al., *Cross-linked Candida antarctica lipase B is active in denaturing ionic liquids.* Enzyme Microb Technol, 2007. **40**(5): p. 1095-1099.
76. Vafiadi, C., et al., *Feruloyl esterase-catalysed synthesis of glycerol sinapate using ionic liquids mixtures.* J Biotechnol, 2009. **139**(1): p. 124-129.
77. van Rantwijk, F., F. Secundo, and R.A. Sheldon, *Structure and activity of Candida antarctica lipase B in ionic liquids.* Green Chem, 2006. **8**(3): p. 282-286.
78. Zhao, H., C.L. Jones, and J.V. Cowins, *Lipase dissolution and stabilization in ether-functionalized ionic liquids.* Green Chem, 2009. **11**(8): p. 1128-1138.
96. Von Hippel, P.H. and K.Y. Wong, *Neutral Salts: The Generality of Their Effects on the Stability of Macromolecular Conformations.* Science, 1964. **2**: p. 577-580.
139. Klahn, M., et al., *On the different roles of anions and cations in the solvation of enzymes in ionic liquids.* Physical Chemistry Chemical Physics, 2011. **13**(4): p. 1649-1662.
140. Elcock, A.H. and J.A. McCammon, *Electrostatic contributions to the stability of halophilic proteins.* Journal of Molecular Biology, 1998. **280**(4): p. 731-748.
141. Frolow, F., et al., *Insights into protein adaptation to a saturated salt environment from the crystal structure of a halophilic 2Fe-2S ferredoxin (vol 3, pg 452, 1996).* Nature Structural Biology, 1996. **3**(12): p. 1055-1055.

147. Lau, R.M., et al., *Dissolution of Candida antarctica lipase B in ionic liquids: effects on structure and activity.* Green Chemistry, 2004. **6**(9): p. 483-487.
161. Shu, Y., et al., *New Insight into Molecular Interactions of Imidazolium Ionic Liquids with Bovine Serum Albumin.* Journal of Physical Chemistry B, 2011. **115**(42): p. 12306-12314.
172. Silva, M., A.M. Figueiredo, and E.J. Cabrita, *Epitope mapping of imidazolium cations in ionic liquid-protein interactions unveils the balance between hydrophobicity and electrostatics towards protein destabilisation.* Physical Chemistry Chemical Physics, 2014. **16**(42): p. 23394-23403.
173. Yang, Z. and W.B. Pan, *Ionic liquids: Green solvents for nonaqueous biocatalysis.* Enzyme and Microbial Technology, 2005. **37**(1): p. 19-28.
174. Schofer, S.H., et al., *Enzyme catalysis in ionic liquids: lipase catalysed kinetic resolution of 1-phenylethanol with improved enantioselectivity.* Chemical Communications, 2001(5): p. 425-426.
175. Figueiredo, A.M., et al., *Protein destabilisation in ionic liquids: the role of preferential interactions in denaturation.* Physical Chemistry Chemical Physics, 2013. **15**(45): p. 19632-19643.
176. Geng, F., et al., *Interaction of bovine serum albumin and long-chain imidazolium ionic liquid measured by fluorescence spectra and surface tension.* Process Biochemistry, 2010. **45**(3): p. 306-311.
177. Singh, T., et al., *Interaction of Gelatin with Room Temperature Ionic Liquids: A Detailed Physicochemical Study.* Journal of Physical Chemistry B, 2010. **114**(25): p. 8441-8448.
178. Micaelo, N.M. and C.M. Soares, *Protein structure and dynamics in ionic liquids. Insights from molecular dynamics simulation studies.* Journal of Physical Chemistry B, 2008. **112**(9): p. 2566-2572.
179. Inada, Y., et al., *Application of Polyethylene Glycol-Modified Enzymes in Biotechnological Processes - Organic Solvent-Soluble Enzymes.* Trends in Biotechnology, 1986. **4**(7): p. 190-194.
180. Arroyo, M., J.M. Sanchez-Montero, and J.V. Sinisterra, *Thermal stabilization of immobilized lipase B from Candida antarctica on different supports: Effect of water activity on enzymatic activity in organic media.* Enzyme and Microbial Technology, 1999. **24**(1-2): p. 3-12.
181. Cao, L.Q., L. van Langen, and R.A. Sheldon, *Immobilised enzymes: carrier-bound or carrier-free?* Current Opinion in Biotechnology, 2003. **14**(4): p. 387-394.
182. Nakashima, K., et al., *Comb-shaped poly(ethylene glycol)-modified subtilisin Carlsberg is soluble and highly active in ionic liquids.* Chemical Communications, 2005(34): p. 4297-4299.
183. Zhang, T., et al., *Identification of a haloalkaliphilic and thermostable cellulase with improved ionic liquid tolerance.* Green Chemistry, 2011. **13**(8): p. 2083-2090.
184. El Seoud, O.A., et al., *Applications of ionic liquids in carbohydrate chemistry: A window of opportunities.* Biomacromolecules, 2007. **8**(9): p. 2629-2647.
185. Swatloski, R.P., et al., *Dissolution of cellose with ionic liquids.* Journal of the American Chemical Society, 2002. **124**(18): p. 4974-4975.
186. Zhao, H., et al., *Improving the enzyme catalytic efficiency using ionic liquids with kosmotropic anions.* Chinese Journal of Chemistry, 2006. **24**(4): p. 580-584.

187. Tavares, A.P., O. Rodriguez, and E.A. Macedo, *Ionic liquids as alternative co-solvents for laccase: study of enzyme activity and stability.* Biotechnology and bioengineering, 2008. **101**(1): p. 201-7.
188. Bihari, M., T.P. Russell, and D.A. Hoagland, *Dissolution and Dissolved State of Cytochrome c in a Neat, Hydrophilic Ionic Liquid.* Biomacromolecules, 2010. **11**(11): p. 2944-2948.
189. Stoner, M.R., et al., *Surfactant-induced unfolding of cellulase: Kinetic studies.* Biotechnology Progress, 2006. **22**(1): p. 225-232.
190. Kosters, H.A. and H.H. de Jongh, *Spectrophotometric tool for the determination of the total carboxylate content in proteins; molar extinction coefficient of the enol ester from Woodward's reagent K reacted with protein carboxylates.* Analytical chemistry, 2003. **75**(10): p. 2512-6.
191. Fersht, A.R., *Conformational Equilibria in Alpha-Chymotrypsin and Delta-Chymotrypsin - Energetics and Importance of Salt Bridge.* Journal of molecular biology, 1972. **64**(2): p. 497-&.
192. Zhang, Y.J. and P.S. Cremer, *Interactions between macromolecules and ions: the Hofmeister series.* Current Opinion in Chemical Biology, 2006. **10**(6): p. 658-663.
193. Danson, M.J. and D.W. Hough, *The structural basis of protein halophilicity.* Comparative Biochemistry and Physiology a-Physiology, 1997. **117**(3): p. 307-312.
194. You, D.J., et al., *Protein thermostabilization requires a fine-tuned placement of surface-charged residues.* Journal of Biochemistry, 2007. **142**(4): p. 507-516.
195. Kohn, W.D., C.M. Kay, and R.S. Hodges, *Protein Destabilization by Electrostatic Repulsions in the 2-Stranded Alpha-Helical Coiled-Coil Leucine-Zipper.* Protein Science, 1995. **4**(2): p. 237-250.
196. Dym, O., M. Mevarech, and J.L. Sussman, *Structural Features That Stabilize Halophilic Malate-Dehydrogenase from an Archaebacterium.* Science, 1995. **267**(5202): p. 1344-1346.
197. Mamat, B., et al., *Crystal structures and enzymatic properties of three formyltransferases from archaea: Environmental adaptation and evolutionary relationship.* Protein Science, 2002. **11**(9): p. 2168-2178.
198. Bieger, B., L.O. Essen, and D. Oesterhelt, *Crystal structure of halophilic dodecin: A novel, dodecameric flavin binding protein from Halobacterium salinarum.* Structure, 2003. **11**(4): p. 375-385.
199. Tadeo, X., et al., *Structural Basis for the Aminoacid Composition of Proteins from Halophilic Archea.* Plos Biology, 2009. **7**(12): p. e1000257.
200. Coquelle, N., et al., *Gradual Adaptive Changes of a Protein Facing High Salt Concentrations.* Journal of Molecular Biology, 2010. **404**(3): p. 493-505.
201. Bracken, C.D., et al., *Crystal structures of a halophilic archaeal malate synthase from Haloferax volcanii and comparisons with isoforms A and G.* Bmc Structural Biology, 2011. **11**.
202. Ortega, G., et al., *Halophilic enzyme activation induced by salts.* Scientific Reports, 2011. **1**.
203. Zaccai, G. and H. Eisenberg, *Halophilic Proteins and the Influence of Solvent on Protein Stabilization.* Trends in biochemical sciences, 1990. **15**(9): p. 333-337.

Chapter 5 Mediating electrostatic interactions of 1-butyl-3-methylmidazolium chloride to enzyme surfaces improves conformational stability

Adapted from Journal of Physical Chemistry, B 117, 8977-8986

5.1 Abstract

We have recently developed a general approach to improve the utility of enzymes in ILs via tuning the ratio of enzyme-containing positive-to-negative surface charges. In this work, the impact of enzyme surface charge ratio on the biophysical interaction of 1-butyl-3-methylimidazolium chloride ([BMIM][Cl]) with chymotrypsin and lipase was investigated to understand this approach at the molecular level. Results of fluorescence quenching assays indicated that the extent of quenching of the [BMIM] cation decreased (7 and 3.5-fold for chymotrypsin and lipase, respectively) as a function of increasing ratio of positive-to-negative surface charges. Chemical urea denaturation assays further indicated that the intrinsic stability in the absence of ionic liquids is highest for the wild-type enzyme. This suggests that kinetic stabilization observed for the variants in ionic liquids is, opposed to a nonspecific effect, perhaps specific to ionic liquid media. Combined, these results provide support that altering the surface charge ratio mediates the organization of IL molecules, namely [BMIM] and [Cl], around the enzymes. Accordingly, these results, more broadly, provide insight into the mechanism of stabilization in ILs via charge modification.

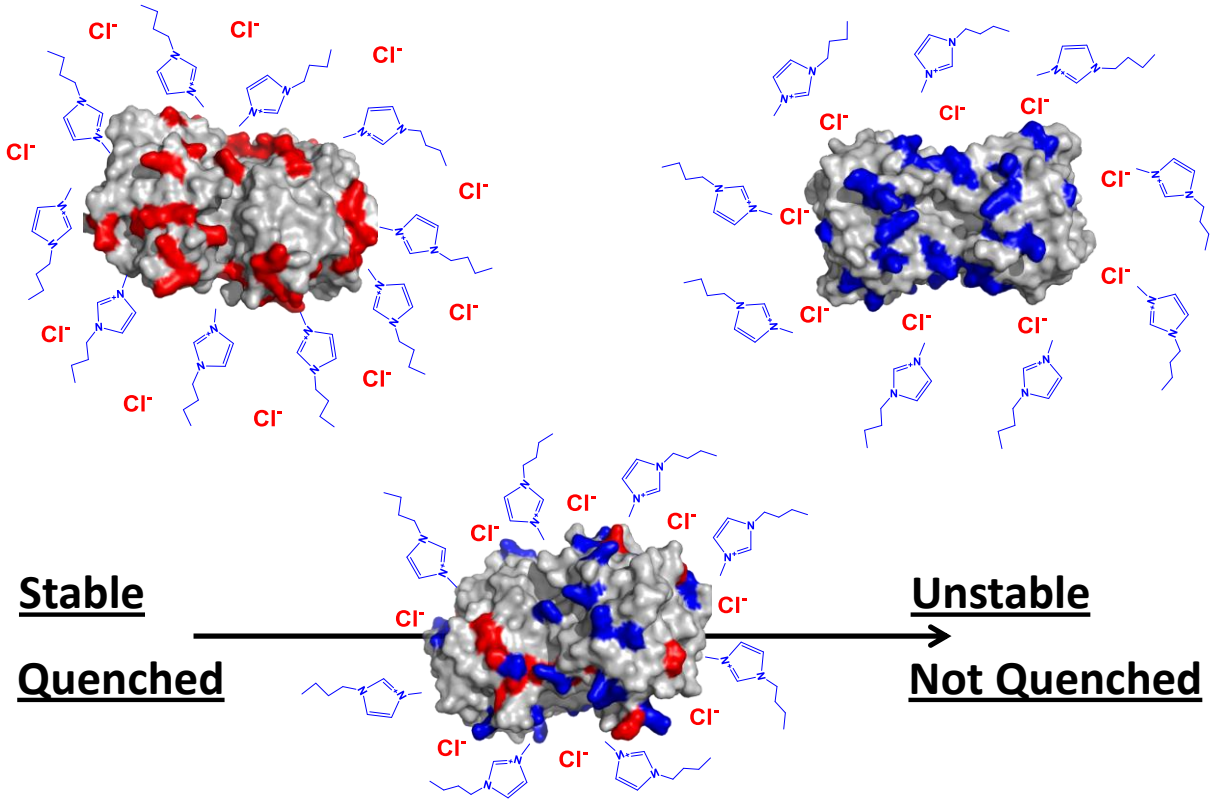

Figure 5.1. Graphical abstract: Stabilizing enzymes in ionic liquids by mediating charged interactions.

5.2 Introduction

Broad interest in ionic liquids (ILs) as solvents for biocatalysis has fueled a need for a mechanistic understanding of the interactions between ILs and enzymes.[19, 65, 204, 205] In lieu of considerable attention, a widely adopted view is that cations interact significantly through hydrophobic interactions, as indicated by crystallographic studies, while anions, which are typically smaller and have high density, interact primarily through electrostatic forces. The, apparent, larger interaction of the two is the electrostatic interaction of the anion. Moreover, enzyme structure-function studies indicate enzyme activity and stability in ILs is strongly anion-dependent.[19, 54, 71, 173, 206] A number of studies have illuminated the connection between electrostatic interactions with ILs, namely imidazolium ILs, with chloride, nitrate, bromide and octylsulfate anions, and conformational changes in enzymes.[67, 159, 161, 176, 177] Moreover, the propensity of the anion species of ILs to associate with enzyme surfaces has been demonstrated via molecular dynamic simulations.[139, 178] While the unfolding of enzymes likely driven by hydrophobic interactions of the cation with the protein core, mediating total binding of 1-butyl-3-methylimidazolium chloride ([BMIM][Cl]) may help preserve the structural stability of enzymes. In particular, it has been shown that the total interaction of the anion and cation seems to be what determines a salts' effect on protein stability.[127] Therefore, if the interaction of anions is indeed stronger, perhaps mediating their interaction will provide a bigger impact on protein function.

We have recently developed a novel method to improve enzyme function in imidazolium ionic liquids via chemical modification of enzyme surface charge, which we hypothesize is related to mediating the organization and total binding of ILs to enzymes.[14] By systematically modifying the surface charge of the model enzymes chymotrypsin (CT), lipase (CRL), and papain, we explored the relationship between the ratio of positive-to-negatively charged surface

groups and enzyme inactivation in aqueous-ILs. In uncovering this relationship, we have previously shown that the half-life of CT, CRL, and papain against IL-induced denaturation was specifically improved in the ILs 1-butyl-3-methylimidazolium chloride ([BMIM][Cl]) and 1-ethyl-3-methylimidazolium ethyl sulfate by modifications that reduce the ratio of positive-to-negative surface charges. The addition of negative surface charges, which lower this ratio, may repel the binding of anions to the enzyme surface by means of electrostatic effects. Modifications that remove positive surface charges may, additionally, eliminate potential binding sites to which anions may associate, contributing to enzyme tolerance to ILs. In this way, such modifications may enhance the structural integrity of enzymes in ILs.

In direct connection with these findings, protein charge has similarly been shown to, notably, be critical to the stability of proteins in hypersaline environments in nature. This connection stems from the observation that proteins from halophilic organisms, which have evolved to be stable in high salt conditions, have an unusually high number of acidic residues.[141, 196-201] Biophysical and structural studies suggest that acidic residues may increase protein function by increasing protein hydration, reducing aggregation propensity, and participating in salt bridges.[140, 141, 196, 207]

In this work, we have investigated the biophysical basis for the apparent impact of charge modification on IL-induced enzyme inactivation in aqueous-IL mixtures. The aim of this investigation was specifically to elucidate the link between the ratio of positive-to-negatively charged surface groups and enzyme inactivation in ILs at the molecular level. To understand this link, we measured the relative quenching of intrinsic tryptophan fluorescence by the cation, [BMIM], with CT and CRL. This quenching with CT and CRL was quantified as a function of

enzyme surface charge. An understanding of these interactions will address a significant gap in our understanding of enzyme stability in ILs.

Enzyme surface charge was varied by acetylation and succinylation of surface lysine residues as well as cationization of carboxylic acid groups with ethylene diamine. Acetylation and succinylation specifically replace positively charged amines with neutral acetyl and acid groups, respectively, while cationization leads to the conversion of acids to amines. The extent of quenching of charge variants of CT and CRL were studied to understand the effect of charge modification on accessibility to [BMIM] and [Cl]. Fluorescence quenching assays have previously been employed to assay the interaction of ILs that contain imidazolium cations to bovine serum albumin.[161, 176] Additionally, the relationship between chemical modification urea chemical stability of CT and CRL in the presence of [BMIM][Cl] was ascertained.

5.3 Materials and methods

5.3.1 Materials

The enzymes CT from bovine pancreas and CRL (*Candida rugosa*, type VII) were purchased from Sigma Aldrich (St. Louis, MO) and used without further purification. Reagents for enzyme modification as well as the enzyme substrates N-succinyl-alanine-alanine-proline-phenylalanine paranitroanalide (SAAPPpNA) and paranitrophenyl butyrate (pNPB) and [BMIM][Cl] were also purchased from Sigma Aldrich. Additionally, trinitrobenzene sulfonic acid (TNBS), urea (ACS grade; 99.8%), and acrylamide (> 99.9%) were obtained from Thermo Fisher Scientific (Waltham, MA).

5.3.2 Modification of enzyme surface charge

Succinylated CT and CRL were prepared by adding succinic anhydride to a solution of enzyme (7.5 mg/ml CT; 1.2 mg/ml CRL) in 1 M sodium carbonate buffer (pH 8.5) in four aliquots over 3 h at room temperature. The final molar ratio of succinic anhydride-to-number of enzyme-containing primary amines was 20:1. Acetylated CT and CRL were similarly prepared by modification with acetic anhydride, which was added in three aliquots over 1.5 h in 100 mM sodium phosphate buffer (pH 7.0). A 20:1 molar excess of acetic anhydride-to-primary amines was also used. To prepare cationized variants of CT and CRL, the enzymes (7.5 mg/ml CT; 1.2 mg/ml CRL) were modified via reaction with ethylenediamine (0.5 M) in buffer (200 mM MES, pH 5) using N-(3-dimethylaminopropyl)-N'-ethylcarbodiimide as a crosslinker. The crosslinker was added to the cationization reaction, which was incubated for 2.5 h at room temperature, in a 20:1 molar excess to the number of enzyme-containing acid sites. Following modification, excess modification reagents were separated by centrifugal filtration or dialysis and the enzymes were subsequently lyophilized.

5.3.3 Characterization of extent of enzyme modification

Extent of modification of CT and CRL charge variants was characterized by titration of enzyme-containing primary amines with TNBS. Briefly, the addition or removal of primary amines upon modification was quantified spectrophotometrically by reacting TNBS with CT and CRL. Reaction of TNBS with CT and CRL was measured at 335 nm using a Thermo Fisher Scientific Evolution 260 Bio UV/Vis spectrophotometer.

5.3.4 Measuring enzyme inactivation in [BMIM][Cl]

Wild-type and modified CT were incubated in 27.5 mM sodium phosphate buffer (pH 7.5) with 2.6 M (or 45 % (v/v)) [BMIM][Cl] at 25 °C. Enzyme inactivation was followed by

periodically removing aliquots (975 μL) and assaying residual enzyme activity by measuring the CT-catalyzed hydrolysis of SAAPPpNA (0.25 mg/mL final concentration), which was prepared in DMSO (2.5 % (v/v) final concentration). The initial rate of SAAPPpNA hydrolysis was assayed spectrophotometrically by continuously monitoring the release of paranitroanalide at 412 nm at room temperature. Similarly, the time-course of inactivation of wild-type and charge variants of CRL was followed by incubation of the enzyme in 120 mM MES buffer (pH 5.7) with 2.3 M (or 40 % (v/v)) [BMIM][Cl] at 30 °C. The residual activity of aliquots (980 μL) of the enzyme was assayed periodically by measuring the initial rate hydrolysis of pNPB (0.6 mg/ml final concentration) by CRL based on the release of paranitrophenyl at 412 nm at room temperature in incubation buffer containing acetonitrile (2.0 % (v/v) final concentration). The half-life ($T_{1/2}$) of the different forms of CT and CRL were determined by fitting the stability profiles to a first-order inactivation model by means of non-linear regression.

5.3.5 Fluorescence quenching measurements

Quenching of the intrinsic fluorescence of wild-type and modified CT (0.4 mg/mL) and CRL (0.2 or 0.3 mg/mL) was measured by titrating [BMIM][Cl] (0 – 0.6 M or 0 – 10 % (v/v)) or acrylamide (0 – 0.85 M) into enzyme in buffer (50 mM sodium phosphate) at pH 7.5 (CT) or 7.0 (CRL). Upon addition of quencher, fluorescence emission was monitored between 300 – 370 nm via excitation at 291 and 285 nm for CT and CRL, respectively, at 22 °C. The maximum fluorescence intensity at each IL concentration was plotted and subsequently fit to the Stern-Volmer equation to quantify the extent of quenching (Equation 1).

$$F_0/F = (1 + K_{exposed}Q)/(1 + K_{exposed}Q(1 - f)) \qquad (1)$$

In this equation, F is the observed maximum fluorescence intensity as a function of quencher concentration (Q), F_o is the fluorescence intensity in the absence of quencher, f is the fraction of solvent exposed intrinsic fluorophores, and $K_{exposed}$ is the Stern-Volmer quenching constant. The value of f was determined from analysis of the wild-type enzyme and assumed constant for charge variants of CT and CRL. Using the value of f from wild-type CT or CRL, $K_{exposed}$ was determined via a least squares minimization. The mean and standard deviation of $K_{exposed}$ was determined from three and four independent experiments with acrylamide and [BMIM][Cl], respectively.

5.3.6 Urea equilibrium denaturation

Urea-induced denaturation of wild-type and modified CT and CRL in buffer containing IL (0 – 0.6 M or 0 – 10 % (v/v)) was monitored by recording changes in intrinsic tryptophan fluorescence. Specifically, changes in the fluorescence was monitored between 300 – 370 nm upon excitation at 291 and 285 nm for CT and CRL, respectively, at 22 °C. Prior to measuring fluorescence, CT (0.2 – 0.5 mg/mL) and CRL (0.6 – 2.0 mg/mL) were incubated with urea and IL in buffer (50 mM sodium phosphate) at pH 7.5 (for CT) or 7.0 (for CRL) for at least 13 hours at room temperature to ensure unfolding to reach equilibrium. Control experiments confirmed that the fluorescence signal did not change upon incubation between 10 – 20 h. Two separate trials, totaling 36-39 data points, were overlaid and used to determine the pre-transition, post-transition, and transition regions of the unfolding curve.

Fluorescence denaturation curves were fit to a conventional two-state folding model (i.e. $N \leftrightarrow D$), to quantify apparent free energy of unfolding (ΔG_{D-N}) of CT. Of note, the authors do not wish to claim the model follows a perfect two-state unfolding mechanism. However, in

addition to analyzing the denaturation curves in terms of urea unfolding midpoints, this analysis provides an interesting secondary level of analysis to corroborate. The equilibrium constant (K_{eq}) of the unfolding reaction was determined as a function of the fraction of folded enzyme at a given urea concentration using Equation 2:

$$K_{eq} = (\lambda_N - \lambda)/(\lambda - \lambda_U) \quad (2)$$

where λ is the fluorescence emission maximum wavelength and λ_N and λ_U are the respective signals of the folded and unfolded enzyme at that concentration of urea. The values of λ_N and λ_U were determined by extrapolation of the linear-dependence of the pre- and post-transition regions on urea concentration. Using the values of K_{eq} in the transition region, ΔG_{D-N} was subsequently determined using Equation 3 in which R is the gas constant and T is temperature:

$$\Delta G_{D-N} = -RT \ln(K_{eq}) \quad (3)$$

The data was then fit to Equation 4 to yield the free energy of unfolding in the absence of urea (ΔG^o_{D-N}):

$$\Delta G_{D-N} = -m[Urea] + \Delta G^o_{D-N} \quad (4)$$

A theoretical unfolding curve was determined for the denaturation data by combining and rearranging Equations 2, 3, and 4. Analysis of the correlation coefficient for all of the theoretical curves confirmed that the data closely fit the predicted model.

5.4 Results and discussion

5.4.1 Characterization of surface charge of wild-type and modified CT and CRL

Interaction and organization of ILs to enzymes as a function of surface charge was investigated by systematically modifying the charge of the surface of CT and CRL via chemical modification. Surface charge of the enzymes was specifically varied by means of acetylation,

succinylation, and cationization of reactive primary amine and carboxylic acid groups. Notably, wild-type CT contains 15 primary amine and 15 carboxylic acid groups, including those in amino acid side chains and the N- and C-terminal amine and acid. Wild-type CRL contains, in total, 18 primary amines and 45 carboxylic acid groups as sites of possible modification.

Titration of the number of primary amines and acids post-modification indicated that the resulting charge state of CT and CRL varied considerably (**Table 5-1**). The extent of modification, which was expressed as a ratio of the resulting primary amine-to-carboxylic acid groups, varied from 0.20 to 2.01 for CT and 0.08 to 0.49 for CRL. The ratio of primary amines-to-acids, having previously been shown to correlate with enzyme kinetic stability in ILs,[14] provides a proxy for the ratio of positive-to-negative charged sites in an enzyme. Although useful as a proxy measure of the charge ratio, the ratio of primary amines-to-acids does not take into account the charge of other ionizable residues (i.e. histidines and arginines) or protonation state. All amine and acid groups are assumed to be fully protonated and deprotonated, respectively, at the pH of subsequent biophysical and stability measurements. Additionally, we have noted previously that the most reactive sites, besides the enzyme termini, within CT are Asp35, Asp72, Lys169, Lys202, and Lys203 and within CRL are Asp340, Glu341, Lys170, Lys274, Lys437, which are surface exposed.[14] The specific activity of the modified variants of CT and CRL was, furthermore, measured to confirm that the modifications did not result in the inactivation of enzymes.

Table 5-1. Fluorescence quenching constants and half-life of wild-type and modified CT and CRL in presence of [BMIM][Cl]. The fluorescence quenching constant $K_{exposed}$, was determined from Stern-Volmer analysis.

	CT			CRL		
	Primary Amines:Acids	$K_{exposed}$ **(M^{-1})**	$T_{1/2}$ **(min)***	**Primary Amines:Acids**	$K_{exposed}$ **(M^{-1})**	$T_{1/2}$ **(min)†**
Succinylated	0.20 ± 0.00	15.0 ± 1.5	107 ± 8	0.08 ± 0.00	15.3 ± 0.6	686 ± 55
Acetylated	0.28 ± 0.02	7.5 ± 1.0	232 ± 31	0.09 ± 0.00	10.2 ± 0.9	511 ± 56
Wild-type	1.04 ± 0.00	5.6 ± 0.1	141 ± 14	0.37 ± 0.02	6.8 ± 0.5	235 ± 49
Cationized	2.01 ± 0.05	2.2 ± 0.2	58 ± 2	0.49 ± 0.07	4.5 ± 0.4	187 ± 5

The values of the ratio of primary amines:acids as well as $T_{1/2}$ represent the average and standard deviation of two independent experiments.
The value of $K_{exposed}$ represents the average and standard deviation of four independent experiments.
*The $T_{1/2}$ of CT was measured in 2.6 M (or 45 % (v/v)) [BMIM][Cl].
†The $T_{1/2}$ of CRL was measured in 2.3 M (or 40 % (v/v)) [BMIM][Cl].

5.4.2 Fluorescence quenching of wild-type and modified CT and CRL by [BMIM][Cl]

Upon modification, the relative accessibility of [BMIM] to the tryptophans of CT and CRL as a function of enzyme surface charge was measured by means of fluorescence quenching assays. The basis for quenching in this context is the transfer of electrons from the excited state of tryptophan residues to the imidazolium cation of the IL upon interaction of the IL and enzymes.[149, 158, 161, 176, 208-210] Photoinduced electron transfer (PET) to the IL is directly proportional to the rate of collision of the IL with the enzyme, which is dependent upon the exposure of the fluorophore to quenching molecule as well as the affinity of the IL to the enzyme surface near the tryptophans. Shu and co-workers[161] previously determined the apparent Stern-Volmer constants of the interaction of [BMIM][Cl] as well as the related imidazolium ILs 1,3-

dibutylimidazolium chloride and 1-butyl-3-methylimidazolium nitrate with bovine serum albumin by measuring imidazolium fluorescence quenching of tryptophan residues. In this work, fluorescence quenching studies found the Stern-Volmer constants of the ILs were around 10^2 M^{-1}, suggesting that the affinity or exposure of tryptophans with the ILs was quite low. A similar Stern-Volmer constant was also obtained for 1-tetradecyl-3-methylimidazolium bromide quenching of bovine serum albumin.[176]

Figure 5.2 shows the fluorescence spectra of wild-type and modified CT as a function of [BMIM][Cl] concentration. The quenching data clearly show that the fluorescence intensity of the intrinsic fluorophores within the enzymes decreases with increasing IL concentration. The concentration range of [BMIM][Cl] (0 – 0.6 M or 0 – 10 % (v/v)) that was used in quenching assays was below that which is thought to induce unfolding of CT and CRL as indicated by previous activity and stability studies.[14] Also, the titration occurs over the course of minutes, whereas CT and CRL were observed to lose < 1% activity over the course of two hours at 25 °C. The starting emission of wavelength was 335 nm for all of the variants. This suggests that the average exposure of tryptophans to solvent is the same between the different variants. To this point, circular dichroism observed no gross structural changes between the charge variants (**Figure 5.3**). As [BMIM][Cl] is added, the emission actually blue shifts. This blue shift may occur as a result of increased burial of tryptophans or as a result of larger quenching of the more exposed tryptophans, making the more buried tryptophans larger contributors of the total fluorescence. Nonetheless, the largest blue shift happens for the variant (succinylated) that gets quenched the most, suggesting quenching is not only a result of differences in tertiary structure between the variants that occur at increasing concentrations of [BMIM][Cl]. A similar argument can be made about dynamics, if the time averaged exposure of a tryptophan to solvent is more

significant for one variant resulting in larger quenching, a red shift would be expected, which is the opposite of what is observed. This, in turn, suggests that changes in fluorescence are due to altering solvent interactions with the enzymes. The background fluorescence from the IL did not interfere with the measurement of the enzyme signal.

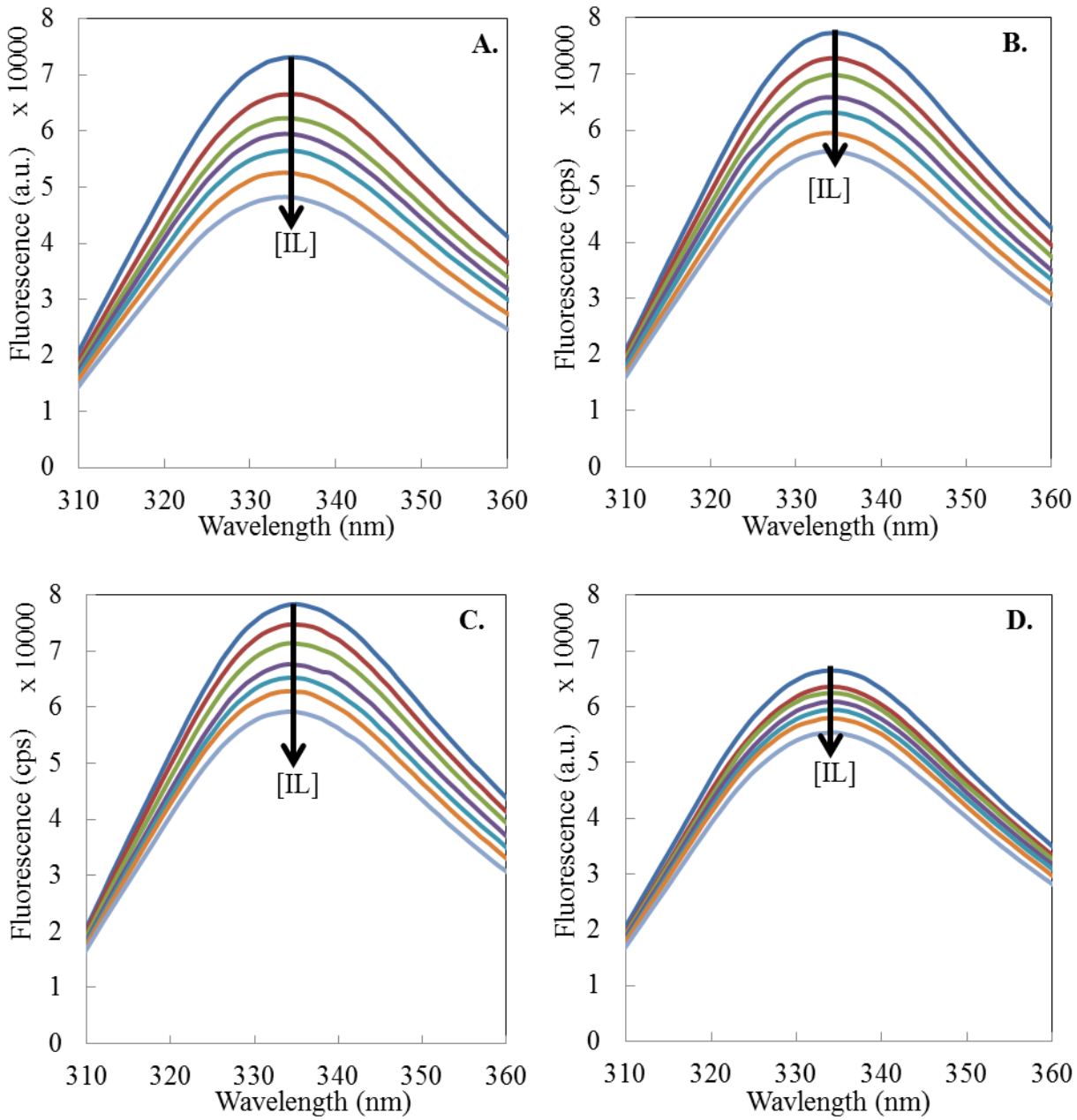

Figure 5.2. Fluorescence quenching of CT in 0 – 0.6 M (0 – 10 % (v/v)) [BMIM][Cl] when excited at 291 nm for (A) succinylated (B) acetylated (C) wild-type and (D) cationized charge variants. Fluorescence values are the average of four independent experiments.

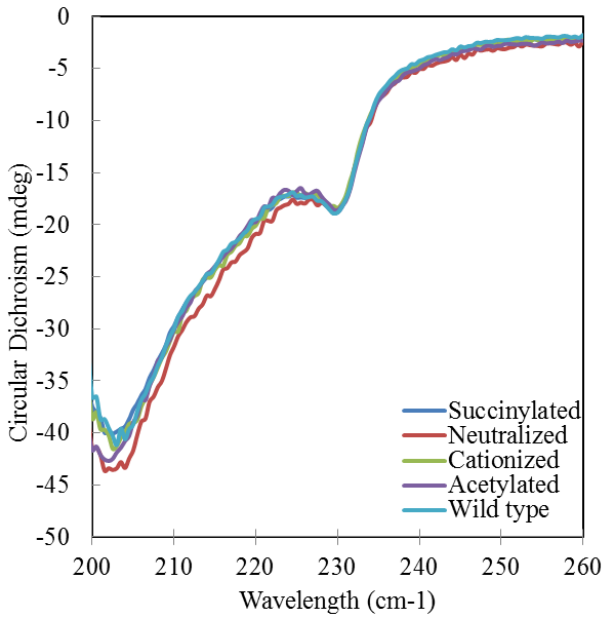

Figure 5.3. Circular dichroism of charge variants of chymotrypsin indicating no change in secondary structure.

To quantify the differences in interaction of [BMIM] with the CT and CRL charge variants, the extent of quenching from the fluorescence spectra was determined via Stern-Volmer analysis. Stern-Volmer plots were specifically created by plotting the ratio of the fluorescence maximum in the absence of [BMIM][Cl] to the fluorescence maximum at each IL concentration (**Figure 5.4A** and **B**). As evident from the Stern-Volmer plots, the extent of quenching was greatest for the succinylated forms of CT and CRL, suggesting that [BMIM] interacts most directly to these forms. Differences in quenching among the charge variants were examined by determination of the quenching constant $K_{exposed}$ from the Stern-Volmer plots. In this analysis, $K_{exposed}$ is analogous to the Stern-Volmer quenching constant K_{SV}. The value of $K_{exposed}$ was specifically found by fitting the ratio of fluorescence intensities at each concentration of [BMIM][Cl] to the Stern-Volmer equation. Due to the negative curvature of this ratio as a function of IL concentration, the conventional Stern-Volmer equation for two populations of

tryptophan residues was used. Such curvature specifically suggests that there are a fraction of tryptophans that are exposed as well as a fraction that are buried. Buried tryptophans were considered inaccessible and, as such, were assumed to have an insignificant quenching constant (i.e. $K_{buried} = 0$). The fractions of exposed and buried tryptophans in the modified forms of CT and CRL were assumed to be similar as in wild-type CT and CRL, respectively.

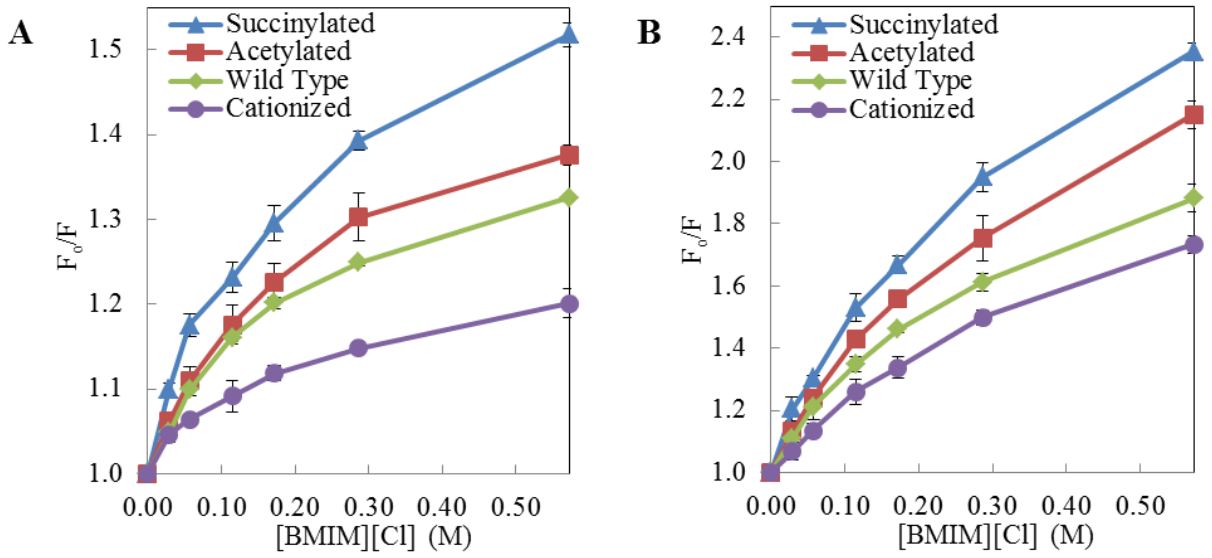

Figure 5.4. Stern-Volmer plots for succinylated (▲), acetylated (■), wild-type (♦), and cationized (●) charge variants of (A) chymotrypsin (0.4 mg/ml) and (B) lipase (0.3 mg/ml) in the presence of [BMIM][Cl]. Data values and error bars represent the mean and standard deviation of four independent experiments.

Comparison of $K_{exposed}$ for the charge variants of CT and CRL found a distinct trend between quenching and enzyme amine : acid ratio (**Table 5-1**). Interestingly, a decrease in $K_{exposed}$ as the ratio of enzyme-containing positive-to-negatively charged sites increased was observed. The apparent decrease in $K_{exposed}$ was approximately 7-fold and 3.5-fold, respectively, over the range of the ratio of primary amine-to-acid surface groups for CT and CRL. This trend is consistent with that expected based on the presumed impact of adding or removing positive and negative surface charges on the interaction of the positively-charged

[BMIM] cation. Namely, the addition of positive charges would presumably increase the electrostatic repulsion of [BMIM] and, in turn, reduce the affinity of the positive [BMIM] head for the enzyme surface. Conversely, removing positive charges would presumably reduce the repulsion of [BMIM] and, particularly, when converted to negative charges, enhance the Coulombic attraction of [BMIM].

However, crystallographic evidence suggests Coulombic binding is not that strong for [BMIM]. In fact, [BMIM] was observed stacking with a tyrosine despite being near two positively charged arginines salt bridging with an aspartic acid. In light of this notion, perhaps orienting the cation may also be important as the imidazolium quenching of tryptophan happens through PET at the positively charged head of the cation. Interactions of the uncharged butyl tail likely would not produce any quenching. Another interpretation could also be that anions crowd the surface of a positively charged enzyme, blocking accessibility of the [BMIM] to the tryptophan through excluded volume effects. In this situation, attracting the [BMIM] with a negative charge is not necessarily important, but repelling [Cl] which allows [BMIM] more direct access to the now more accessible tryptophans results in higher quenching. Additionally, despite the lack of red-shift, perhaps there is a folding state difference that occurs only upon addition of [BMIM][Cl] resulting in this experimental artifact. Barring experimental artifacts, it is interesting that altering the charge of a certain residue can apparently impact either the solvent structuring or the direct interaction of [BMIM] at a nearby, different residue (Trp). Of important note, considering an intermediate population (i.e. a partially accessible fraction) with the quenching constant $K_{intermediate}$ did not result in significant changes in $K_{exposed}$. Moreover, the trends in both $K_{exposed}$ and $K_{intermediate}$ when considering three populations were consistent with that of $K_{exposed}$ when analyzed with only two populations.

The dependence of $K_{exposed}$ on the ratio of positive-to-negative enzyme surface charges correlated with that of CT and CRL kinetic stability in the presence of [BMIM][Cl]. Specifically, the trend in $K_{exposed}$ followed that of the $T_{1/2}$ of CT and CRL, which was measured by monitoring enzyme inactivation in 2.6 (or 45 % (v/v)) and 2.3 M (or 40 % (v/v)) [BMIM][Cl], respectively (**Table 5-1**). Deviation of this correlation in the case of succinylated CT may be related to the decreasing the kinetic barrier for unfolding. Lowering the activation energy required to reach the inactive state would thereby increase the inactivation kinetics. Succinylation could also potentially alter the ΔG of unfolding unfavorably resulting in faster unfolding. Perhaps, even if succinylation is favorably mediating the interaction with [BMIM][Cl], the intrinsic stability was lowered enough to overcompensate any beneficial effects of mediating the enzyme-IL interaction. The correlation between $T_{1/2}$ and quenching suggests a link between, namely, cation interactions and enzyme stability in aqueous-IL mixtures. In this work, the $T_{1/2}$ of CT was determined in a higher concentration of [BMIM][Cl] than in our previous work while that of CRL was measured at the same IL concentration.[14]

5.4.3 Fluorescence quenching of wild-type and modified CT and CRL by acrylamide

To further probe if the apparent quenching of CT and CRL by [BMIM][Cl] was based on solvent exposure, quenching was also quantified using a quencher that is uncharged. **Figure 5.5** shows the Stern-Volmer plots for the quenching of wild-type and modified CT (**A**) and CRL (**B**) fluorescence by the neutral quencher acrylamide. As anticipated, the Stern-Volmer plots for wild-type and modified CT as well as for wild-type and modified CRL are virtually indistinguishable. The values of $K_{exposed}$ for succinylated, acetylated, wild-type, and cationized CT were 2.00, 1.99, 2.01, and 2.00 M^{-1}, respectively, and CRL were 14.2, 13.4, 13.5, and 13.1

M^{-1}, respectively. Identical Stern-Volmer plots in both cases indicate that, unlike with [BMIM][Cl] as a quencher, the extent of quenching of the charge variants of CT as well as of CRL was equivalent. Accordingly, the Stern-Volmer plots, moreover, suggest that the accessibility in tryptophans is similar between the charge variants of CT and CRL.

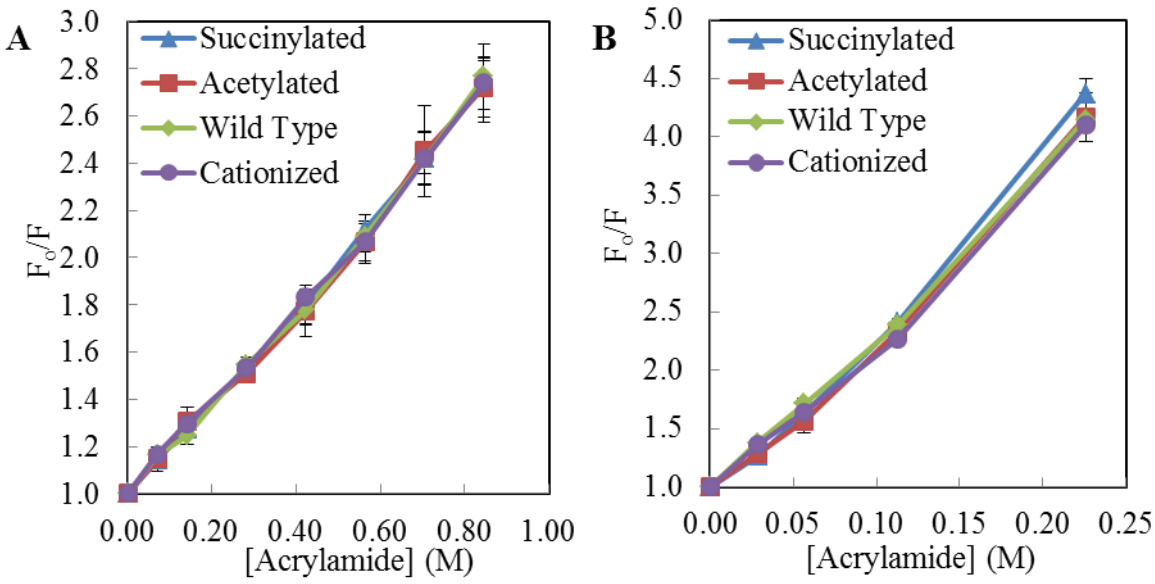

Figure 5.5. Stern-Volmer plots for succinylated (▲), acetylated (■), wild-type (♦), and cationized (●) charge variants of (A) chymotrypsin (0.4 mg/ml) and (B) lipase (0.2 mg/ml) in the presence of the neutral quencher acrylamide. Data values and error bars represent the mean and standard deviation of three independent experiments.

5.4.4 Impact of charge modification on the chemical stability of CT

Despite the apparent connection between enzyme stability in ILs and charge ratio, it is reasonable to assume that the charge modifications have a general effect on enzyme stability. Presumably, one would expect that modifications that enhance the general stability of enzymes would lead to the apparent stabilization of enzymes in extreme environments, including ILs. To ascertain if this was indeed the case, or if the effect of charge ratio on stability is specific to in ILs, the urea chemical stability of wild-type and modified CT in buffer was measured.

Equilibrium urea denaturation was studied by following the fluorescence as a function of urea concentration (**Figure 5.6**). In equilibrium urea denaturation studies, CT was equilibrated with urea in solution overnight prior to measuring fluorescence. It was found that the fluorescent profile did not change between 10-20 hours.

Contrary to the modifications having a general effect, unfolding curves for both wild-type and modified CT (**Figure 5.6**) indicated that the charge variants are less stable than wild-type. The lower thermodynamic stability of the charge variants may be due disrupting salt bridges, or repulsive intramolecular interactions between like surface charges, which are introduced via modification. Such repulsive interactions may destabilize the enzyme, particularly in low ionic strength environments, which has been observed previously.[194, 195, 211] A number of ways can be used to analyze the stability of CT in **Figure 5.6**, the most conservative being strictly looking at the midpoint of urea induced unfolding. This analysis suggests that wild-type CT is the most stable, having a midpoint of 4.6 M urea, while the acetylated form is marginally less stable and the cationized and succinylated appear significantly less stable. However, this analysis does not include the dependence of conformational stability, ΔG^{o}_{D-N} on denaturant concentration. In particular, the slope of the transition region for unfolding is slightly steeper for the wild-type enzyme than the charge variants. Fitting the data to a two state unfolding model and assuming that the pre and post-transition baselines are the same between each variant allows for calculation of the ΔG^{o}_{D-N}. This analysis more convincingly shows that wild-type CT is the most stable at 25.2 kJ/mol compared to 18.3, 17.6 and 16.5 kJ/mol for the acetylated, succinylated, and cationized variants. Perhaps this is not surprising that a modification of the enzyme generally lowered its stability. Also, the calculated conformational stability of wild-type CT closely matches that as reported previously.[130]

In order to calculate a ΔG^{o}_{D-N}, it is important to discuss the validity of the two state model for unfolding and the reversibility of unfolding. Under these conditions, CT was refolded and regained more than half of native signal and activity. This shows, not surprisingly, that the assumptions are not perfect. However, calculation of an *apparent* ΔG^{o}_{D-N} should be valid for comparisons sake. Examination of the fluorescence profile in **Figure 5.6** shows that the pre and post-transition fluorescence values are increasing slightly. This is in line with what Pace et al. reports, suggesting tryptophan fluorescence increases as a function of urea concentration.[212, 213] Moreover, the dependence of tryptophan fluorescence on urea was tested with and without [BMIM][Cl] present (**Figure 5.7**) and was found to increase with urea concentration with a similar slope as the pre and post-transition data points in **Figure 5.6**.

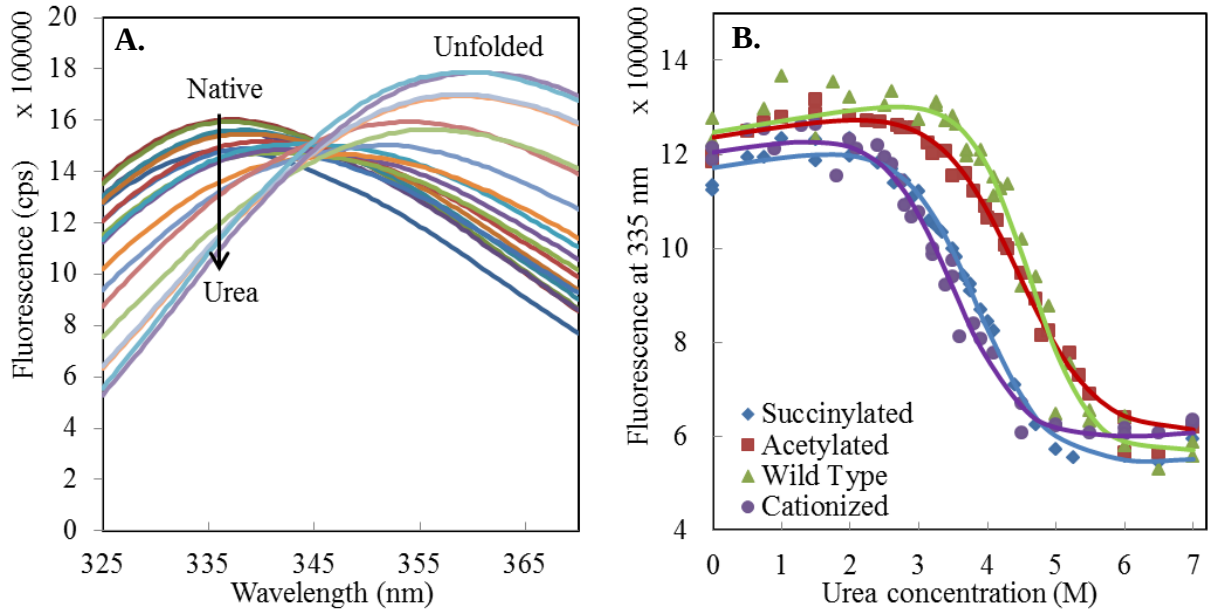

Figure 5.6. Representative urea-induced fluorescence denaturation of wild-type (A) CT (0.2 mg/ml) and 50 mM sodium phosphate buffer, pH 7.5, in the absence of ionic liquid. (B) The corresponding unfolding curves were created from the fluorescence denaturation data for succinylated (♦), acetylated (■), wild-type (▲), and cationized (●) charge variants of CT.

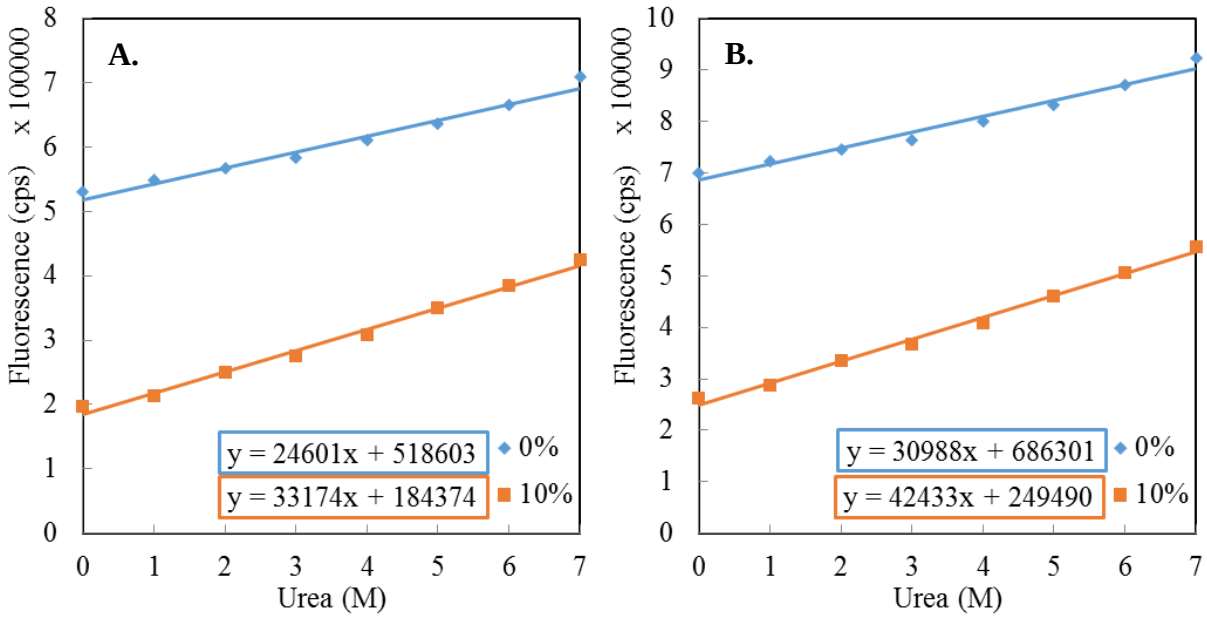

Figure 5.7. Tryptophan fluorescence as a function of urea concentration with and without 10 vol % [BMIM][Cl] measured at (A) 335 nm and (B) 355 nm.

The urea chemical stability of CT was also tested in 10 and 20 vol % [BMIM][Cl] (0.6 and 1.1 M). At 10 vol %, increasing the concentration of urea caused a decrease in signal accompanied by a red shift in peak maximum. The reason for the signal decrease is presumably due to increased quenching of [BMIM] with the more highly exposed tryptophan residues. Notably, at the end of the spectra there is an increase in fluorescent signal, this increase in signal is thought to be due to increasing tryptophan fluorescence caused by adding urea. Again, the baseline for the post-transition region does approximately match the control of free tryptophan (only amino acid in solution) fluorescence increasing with urea concentration under identical solution conditions. In **Figure 5.8**, we see that the urea unfolding midpoint is now highest for the acetylated form. Also, the slopes of unfolding in the transition region for each of the variants are quite different than in buffer. The IL may be altering the ability of urea to bind to CT. Also, if the slope is related to the difference in denaturant molecules that bind upon unfolding, adding a

molecule that binds more to the unfolded than folded states may be expected to change this apparent value. This may convolute interpretation of apparent ΔG^{o}_{D-N} from fitting the curves. Moreover, there is apparently specific binding of [BMIM][Cl] to enzymes like CT found through crystallographic studies as well as non-specific binding at higher IL concentrations seen through equilibrium dialysis. This will likely disrupt the two state unfolding assumption, making the resulting thermodynamic parameters imperfect. Although, as all charge variants of CT were treated the same and induced to unfold under the same conditions, the apparent values resulting from fitting their denaturation curves may give insight into the impact of charge on conformational stability in ionic liquids as best as we can get. Fitting the curves to a two-state unfolding model yielded the apparent thermodynamic parameters reported in **Table 5-2**.

The increased stability of the succinylated enzyme over the wild-type, despite a lower kinetic stability at higher [BMIM][Cl] concentrations may highlight fallacies in the type of analysis, namely deviation from two-state unfolding. However, the urea unfolding midpoints should be a fair analysis to get a rough perspective on relative stability between the different variants. Interestingly, the unfolding midpoint lowers upon addition of [BMIM][Cl] for wild-type and cationized CT but not for acetylated and succinylated CT. Moreover, the acetylated form appears to be the most stable based on unfolding midpoint (albeit, within error).

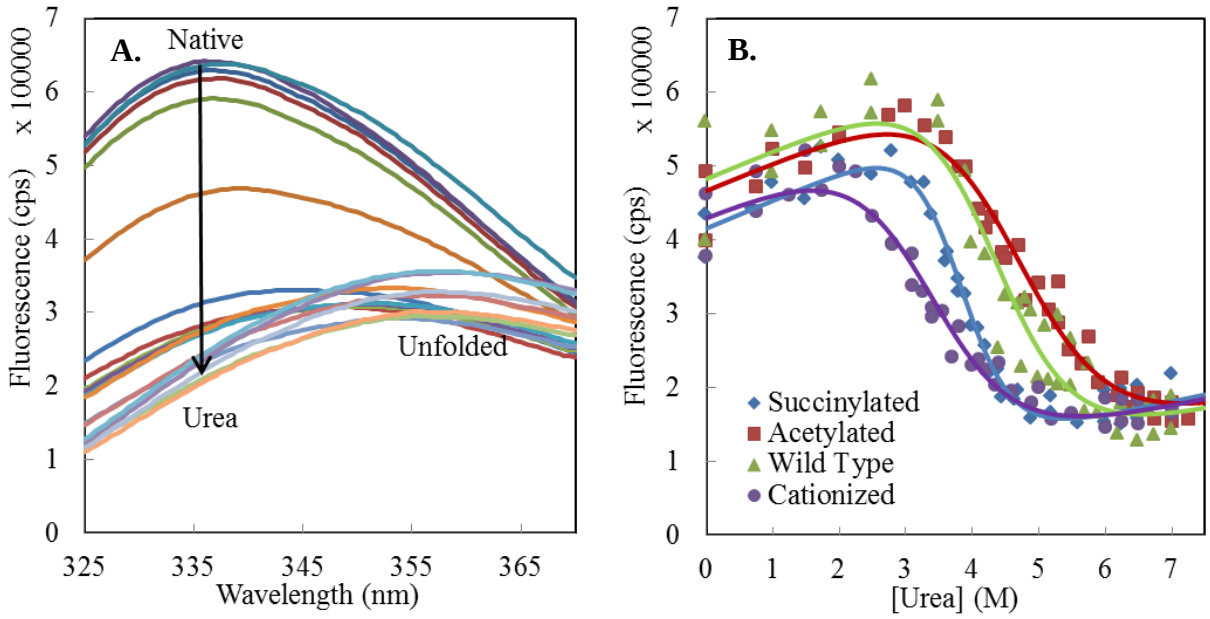

Figure 5.8. Representative urea-induced fluorescence denaturation of wild-type (A) CT (0.5 mg/ml) and 50 mM sodium phosphate buffer, pH 7.5, in 10 vol % [BMIM][Cl]. (B) The corresponding unfolding curves were created from the fluorescence denaturation data for succinylated (♦), acetylated (■), wild-type (▲), and cationized (●) charge variants of CT.

Table 5-2. Apparent thermodynamic unfolding data for CT in 0 – 0.6 M [BMIM][Cl] from equilibrium urea denaturation studies.

	m (kJ/mol-M)	ΔG^{o}_{D-N} (kJ/mol)	$[Urea]_{1/2}$ (M)	$\Delta\Delta G^{o}_{D-N}$ (kJ/mol)
0 M [BMIM][Cl]				
Succinylated	4.61 ± 0.13	17.6 ± 0.5	3.8 ± 0.1	-7.6 ± 1.6
Acetylated	4.13 ± 0.17	18.3 ± 0.7	4.4 ± 0.2	-7.0 ± 1.7
Wild Type	5.49 ± 0.37	25.2 ± 1.5	4.6 ± 0.4	
Cationized	4.77 ± 0.22	16.5 ± 0.7	3.5 ± 0.2	-8.7 ± 1.7
0.6 M [BMIM][Cl]				
Succinylated	6.46 ± 0.69	24.6 ± 2.8	3.8 ± 0.4	6.0 ± 3.2
Acetylated	3.63 ± 0.24	16.9 ± 1.2	4.6 ± 0.3	-1.7 ± 1.9
Wild Type	4.31 ± 0.31	18.6 ± 1.5	4.3 ± 0.4	
Cationized	3.92 ± 0.21	13.1 ± 0.8	3.3 ± 0.2	-5.6 ± 1.7

At 20 vol % (1.1 M) [BMIM][Cl], the chemical stability data became quite noisy and was hard to interpret based on fluorescence decrease. The increase in tryptophan fluorescence as a result of increasing urea concentration combined with the decrease in fluorescence as a result of increased tryptophan exposure to [BMIM] upon unfolding created data difficult to interpret. Therefore, the data was not analyzed according to a two-state unfolding model.

5.4.5 Impact of charge modification on the chemical stability of CRL

The chemical stability of CRL was also attempted to try and understand if the stabilizing of effects are specific to ILs or not. Due to lower solubility than CT, there were more inherent difficulties in getting accurate spectra of CRL. The fluorescence spectra did not have a clear decrease in fluorescent signal as a function of urea that could be accurately fit to a two-state

unfolding model. However, there is a clear red shift between the unfolded and folded spectra. In an effort to understand how each variant's spectra are perturbed by urea, the wavelength of maximum emission was followed as a function of urea. This allowed us to look at the urea unfolding midpoint for all the different variants. This type of analysis revealed unfolding midpoints of 4.3, 4.0, 3.9, and 3.1 for the wild-type, acetylated, cationized, and succinylated variants. This, like with CT, indicates that the wild-type is the most chemically stable of all the variants. Interestingly enough, the succinylated form is the least stable to urea unfolding in buffer, despite having the highest activity retention in high concentrations of [BMIM][Cl]. This provides strong evidence that the kinetic stabilization of enzymes in imidazolium ILs seen upon surface charge modification is specific to IL-media, and not a generic effect.

5.4.6 Proposed mechanism of enzyme IL-stabilization by surface charge alterations

The fluorescence quenching results indicate that surface charge can globally alter the interaction of [BMIM] with proteins which correlates with a more kinetically stable enzyme in the IL [BMIM][Cl]. Mechanistically, the connection between [BMIM][Cl] binding and stability may be explained in the context of structuring the IL around the surface of the enzymes. Perhaps the charges exclude the anion form the surface while orienting the head of the [BMIM] moiety, organizing the IL around the enzyme in a micellar fashion (**Figure 5.9**). Consequently, modifications that lower the ratio of positive-to-negative surface charges may shield the enzyme surface from the [Cl] anion, thereby altering the microenvironment of the enzyme. For modifications that increase the ratio of positive-to-negative surface charges, the converse (i.e. the crowding of the enzyme surface by [Cl] and preferential exclusion of [BMIM]) seemingly occurs. In addition to the affinity of the cation, exclusion of the anion from the enzyme surface is likely dependent on the size and nucleophilicity of the anion.

While it is still unclear, if increases in $T_{1/2}$ of enzymes in aqueous-ILs is a conformational effect, strictly kinetic effect, or both, urea unfolding studies suggest it is specific to IL environments, and not a result of enhancing the intrinsic stability of the enzyme. Nonetheless, we propose a mechanism of stabilization based on altering the thermodynamic stability of protein in ILs. The strength of charged interactions is thought to be considerably weaker for [BMIM] than [Cl] (or most IL anions) due to greater charge delocalization of the imidazole ring compared to that of the anion.[139, 143] In light of this, perhaps negative charges exclude anions stronger than they bind cations. The fluorescence quenching data suggests altering surface charge can globally alter the interaction of [BMIM][Cl] with an enzyme surface. Particularly, the [BMIM] interaction at certain residues (tryptophans) appears to be affected by the amino acid properties (namely charge) of nearby residues. If a negative amino acid can affect the interaction of [BMIM][Cl] across the surface area of a native protein, it can presumably affect the interaction of [BMIM][Cl] across the surface area of a denatured protein. Moreover, a denatured protein has more surface area for a negative amino acid to exert its influence. If electrostatic interactions of anions are stronger than cations, perhaps the net effect of a negative charge is a slight total exclusion of the salt [BMIM][Cl]. In the unfolded peptide, there may be larger exclusion as a result of larger surface area. While exclusion is actually energetically unfavorable, if it is more unfavorable (larger exclusion) for the unfolded state, this would result in a net stabilization between the folded and unfolded states.

In light of the proposed mechanism of enzyme stabilization, it is interesting to consider the impact of charge modification in neat or anhydrous ILs as well as in other ILs. Altering the charge state of ionizable residues on enzyme surfaces, as in aqueous-IL mixtures, may also lead to preferential exclusion of [Cl] ions in neat ILs. Charge modification could also prevent

aggregation and increase the hydration shell of enzymes in neat ILs, which may further enhance activity. In the case of other ILs, the effect of anion exclusion would likely increase with increasing polarity of the anion as the electrostatic interaction of the anion becomes stronger. To determine how charge modification impacts enzyme stability in ILs with varying properties (i.e. polarity, LogP, viscosity), stability studies in other ILs are required.

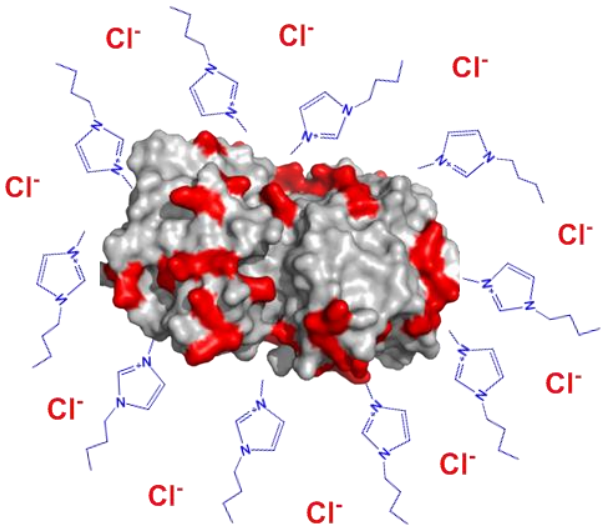

Figure 5.9. Proposed mechanism of exclusion of [Cl] from the surface of CT as a result of altering the solvent environment. The image was created using pymol (PDB code: 1YPH).

5.5 Conclusions

The objective of this work was to elucidate the molecular basis for the connection between enzyme surface charge ratio and the apparent stability against IL-induced deactivation. Chemical denaturation studies using urea suggest that all charge variants are less stable in buffer than the wild-type enzymes. This suggests that stabilization based on charge modification is specific to the IL-milieu. Additionally, it was found that modification of the ratio of amines-to-acids on enzyme surfaces directly impacted the extent of [BMIM] quenching to CT and CRL via fluorescence quenching studies. The most important suggestion of the quenching data is that

charge modification can affect the global interaction of the ionic liquid with the enzyme. That is, at certain residues, namely tryptophans, there appears to be an altered interaction with [BMIM] as a result of modifying the charge state of a different residue. As it has been shown that total salt binding is important, perhaps negative charges result in a slight exclusion of the salt [BMIM][Cl] as the repulsion of [Cl] is stronger than any modest attraction that [BMIM] feels. This exclusion may be larger in the unfolded state due to larger surface area for the negative charge to exert its influence over.

5.6 References

14. Nordwald, E.M. and J.L. Kaar, *Stabilization of Enzymes in Ionic Liquids Via Modification of Enzyme Charge.* Biotechnology and Bioengineering, 2013. **110**(9): p. 2352-2360.
19. van Rantwijk, F. and R.A. Sheldon, *Biocatalysis in ionic liquids.* Chemical Reviews, 2007. **107**(6): p. 2757-2785.
54. Kamiya, N., et al., *Enzymatic in situ saccharification of cellulose in aqueous-ionic liquid media.* Biotechnology Letters, 2008. **30**(6): p. 1037-1040.
65. Yang, Z., *Hofmeister effects: an explanation for the impact of ionic liquids on biocatalysis.* Journal of Biotechnology, 2009. **144**(1): p. 12-22.
67. Singh, T., et al., *Ionic Liquids Induced Structural Changes of Bovine Serum Albumin in Aqueous Media: A Detailed Physicochemical and Spectroscopic Study.* Journal of Physical Chemistry B, 2012. **116**(39): p. 11924-11935.
71. Kaar, J.L., et al., *Impact of ionic liquid physical properties on lipase activity and stability.* Journal of the American Chemical Society, 2003. **125**(14): p. 4125-4131.
127. Arakawa, T. and S.N. Timasheff, *Protein Stabilization and Destabilization by Guanidinium Salts.* Biochemistry, 1984. **23**(25): p. 5924-5929.
130. Greene, R.F. and C.N. Pace, *Urea and Guanidine-Hydrochloride Denaturation of Ribonuclease, Lysozyme, Alpha-Chymotrypsin, and Beta-Lactoglobulin.* Journal of Biological Chemistry, 1974. **249**(17): p. 5388-5393.
139. Klahn, M., et al., *On the different roles of anions and cations in the solvation of enzymes in ionic liquids.* Physical Chemistry Chemical Physics, 2011. **13**(4): p. 1649-1662.
140. Elcock, A.H. and J.A. McCammon, *Electrostatic contributions to the stability of halophilic proteins.* Journal of Molecular Biology, 1998. **280**(4): p. 731-748.
141. Frolow, F., et al., *Insights into protein adaptation to a saturated salt environment from the crystal structure of a halophilic 2Fe-2S ferredoxin (vol 3, pg 452, 1996).* Nature Structural Biology, 1996. **3**(12): p. 1055-1055.
143. Jaeger, V., P. Burney, and J. Pfaendtner, *Comparison of Three Ionic Liquid-Tolerant Cellulases by Molecular Dynamics.* Biophysical Journal, 2015. **108**(4): p. 880-892.

149. Bekhouche, M., L.J. Blum, and B. Doumeche, *Contribution of Dynamic and Static Quenchers for the Study of Protein Conformation in Ionic Liquids by Steady-State Fluorescence Spectroscopy.* Journal of Physical Chemistry B, 2012. **116**(1): p. 413-423.
158. Kumar, V. and S. Pandey, *Selective Quenching of 2-Naphtholate Fluorescence by Imidazolium Ionic Liquids.* Journal of Physical Chemistry B, 2012. **116**(39): p. 12030-12037.
159. Lai, J.Q., et al., *Specific ion effects of ionic liquids on enzyme activity and stability.* Green Chemistry, 2011. **13**(7): p. 1860-1868.
161. Shu, Y., et al., *New Insight into Molecular Interactions of Imidazolium Ionic Liquids with Bovine Serum Albumin.* Journal of Physical Chemistry B, 2011. **115**(42): p. 12306-12314.
173. Yang, Z. and W.B. Pan, *Ionic liquids: Green solvents for nonaqueous biocatalysis.* Enzyme and Microbial Technology, 2005. **37**(1): p. 19-28.
176. Geng, F., et al., *Interaction of bovine serum albumin and long-chain imidazolium ionic liquid measured by fluorescence spectra and surface tension.* Process Biochemistry, 2010. **45**(3): p. 306-311.
177. Singh, T., et al., *Interaction of Gelatin with Room Temperature Ionic Liquids: A Detailed Physicochemical Study.* Journal of Physical Chemistry B, 2010. **114**(25): p. 8441-8448.
178. Micaelo, N.M. and C.M. Soares, *Protein structure and dynamics in ionic liquids. Insights from molecular dynamics simulation studies.* Journal of Physical Chemistry B, 2008. **112**(9): p. 2566-2572.
194. You, D.J., et al., *Protein thermostabilization requires a fine-tuned placement of surface-charged residues.* Journal of Biochemistry, 2007. **142**(4): p. 507-516.
195. Kohn, W.D., C.M. Kay, and R.S. Hodges, *Protein Destabilization by Electrostatic Repulsions in the 2-Stranded Alpha-Helical Coiled-Coil Leucine-Zipper.* Protein Science, 1995. **4**(2): p. 237-250.
196. Dym, O., M. Mevarech, and J.L. Sussman, *Structural Features That Stabilize Halophilic Malate-Dehydrogenase from an Archaebacterium.* Science, 1995. **267**(5202): p. 1344-1346.
197. Mamat, B., et al., *Crystal structures and enzymatic properties of three formyltransferases from archaea: Environmental adaptation and evolutionary relationship.* Protein Science, 2002. **11**(9): p. 2168-2178.
198. Bieger, B., L.O. Essen, and D. Oesterhelt, *Crystal structure of halophilic dodecin: A novel, dodecameric flavin binding protein from Halobacterium salinarum.* Structure, 2003. **11**(4): p. 375-385.
199. Tadeo, X., et al., *Structural Basis for the Aminoacid Composition of Proteins from Halophilic Archea.* Plos Biology, 2009. **7**(12): p. e1000257.
200. Coquelle, N., et al., *Gradual Adaptive Changes of a Protein Facing High Salt Concentrations.* Journal of Molecular Biology, 2010. **404**(3): p. 493-505.
201. Bracken, C.D., et al., *Crystal structures of a halophilic archaeal malate synthase from Haloferax volcanii and comparisons with isoforms A and G.* Bmc Structural Biology, 2011. **11**.
204. Moniruzzaman, M., N. Kamiya, and M. Goto, *Activation and stabilization of enzymes in ionic liquids.* Organic & biomolecular chemistry, 2010. **8**(13): p. 2887-99.
205. Patel, D.D. and J.M. Lee, *Applications of ionic liquids.* Chemical Record, 2012. **12**(3): p. 329-355.

206. Zhao, H., et al., *Designing enzyme-compatible ionic liquids that can dissolve carbohydrates.* Green Chemistry, 2008. **10**(6): p. 696-705.
207. Dalhus, B., et al., *Structural basis for thermophilic protein stability: Structures of thermophilic and mesophilic malate dehydrogenases.* Journal of molecular biology, 2002. **318**(3): p. 707-721.
208. Willaert, K. and Y. Engelborghs, *The Quenching of Tryptophan Fluorescence by Protonated and Unprotonated Imidazole.* European Biophysics Journal, 1991. **20**(3): p. 177-182.
209. Jayabharathi, J., et al., *Fluorescence investigation of the interaction of 2-(4-fluoropheny1)-1-pheny1-1H-phenanthro [9,10-d] imidazole with bovine serum albumin.* Journal of Photochemistry and Photobiology B-Biology, 2012. **117**: p. 222-227.
210. Bose, S., D.W. Armstrong, and J.W. Petrich, *Enzyme-Catalyzed Hydrolysis of Cellulose in Ionic Liquids: A Green Approach Toward the Production of Biofuels.* Journal of Physical Chemistry B, 2010. **114**(24): p. 8221-8227.
211. Gribenko, A.V., et al., *Rational stabilization of enzymes by computational redesign of surface charge-charge interactions.* Proceedings of the National Academy of Sciences of the United States of America, 2009. **106**(8): p. 2601-6.
212. Pace, C.N., D.V. Laurents, and J.A. Thomson, *Ph-Dependence of the Urea and Guanidine-Hydrochloride Denaturation of Ribonuclease-a and Ribonuclease-T1*. Biochemistry, 1990. **29**(10): p. 2564-2572.
213. Pace, C.N., D.V. Laurents, and R.E. Erickson, *Urea Denaturation of Barnase - Ph-Dependence and Characterization of the Unfolded State.* Biochemistry, 1992. **31**(10): p. 2728-2734.

Chapter 6 Charge engineering of cellulases improves ionic liquid tolerance and reduces lignin inhibition

Adapted from Biotechnology and Bioengineering, 111, 1541-1549

6.1 Abstract

We report a novel approach to concurrently improve the tolerance to ionic liquids (ILs) as well as reduce lignin inhibition of *Trichoderma reesei* cellulase via engineering enzyme charge. Succinylation of the cellulase enzymes led to a nearly 2-fold enhancement in cellulose conversion in 15 % (v/v) 1-butyl-3-methylimidazolium chloride ([BMIM][Cl]). Additionally, modeling analysis of progress curves of Avicel hydrolysis in buffer indicated that succinylation had a negligible impact on the apparent V_{max} and K_M of cellulase. As evidence of reducing lignin inhibition of *T. reesei* cellulase, succinylation resulted in a greater than 2-fold increase in Avicel conversion after 170 h in buffer with 1 wt % lignin. The impact of succinylation on lignin inhibition of cellulase further led to the reduction in apparent K_M of the enzyme cocktail for Avicel by 2.7-fold. These results provide evidence that naturally evolved cellulases with highly negative surface charge densities may similarly repel lignin, resulting in improved cellulase activity. Ultimately, these results underscore the potential of rational charge engineering as a means of enhancing cellulase function and thus conversion of whole biomass in ILs.

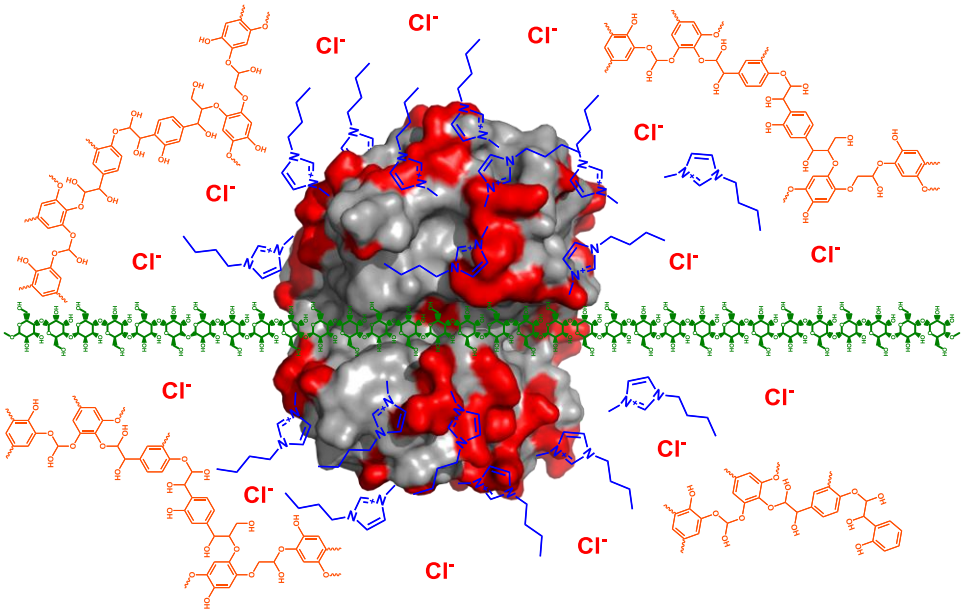

Figure 6.1. Graphical abstract: modification of the density of negative surface charges on the *Trichoderma reesei* cellulase increases the conversion of cellulose by mediating denaturing interactions with ionic liquids and reducing lignin inhibition.

6.2 Introduction

Engineering robust cellulases that are highly active and stable represents a major challenge in the biocatalytic conversion of biomass and, in turn, is crucial to the efficient production of renewable fuels and chemicals. This challenge stems from the inherent recalcitrant nature of biomass, which hinders the efficient hydrolysis of cellulose to fermentable sugars, necessitating extreme conditions. Cellulose hydrolysis is specifically limited by the physical barrier created by insoluble matrix components within biomass (i.e., hemicellulose and lignin) as well as the microfibril structure of cellulose.[214, 215] The latter of these barriers is the result of internal cohesive forces, namely hydrogen bonding, that cause cellulose to self-aggregate.[216-218] In the crystalline state, these interactions are so strong that the tightly packed aggregates are impenetrable by most solvents, including water. Conventional solvent systems that can dissolve cellulose, which contain inorganic salts, acids and bases, and metal complexes, are largely toxic and environmentally polluting.[219]

The realization that ionic liquids (ILs) may be used as alternative solvents to improve the biocatalytic rate of cellulose hydrolysis by dissolving biomass has paved new opportunities for the conversion of cellulosic materials. Specifically, with the appropriate selection of cation and anion, ILs can be rationally tuned to dissolve high concentrations (i.e., 20 – 30 % w/v) of untreated crystalline cellulose.[17, 184, 220, 221] The formation of hydrogen bonds between the IL and cellulose disrupts the internal hydrogen bonding network that causes the cellulose chains to pack tightly. In addition to lowering the degree of crystallinity of cellulose, select ILs can, moreover, loosen the matrix components within biomass that add to the overall recalcitrance of cellulose.[21, 33] Furthermore, owing to their thermal stability and negligible vapor pressure, ILs constitute an environmentally attractive solution to the need for cleaner media for cellulose processing.[17, 25, 32,

[36] However, the attractive properties of ILs are negated by the broad inactivation of cellulases in these solvents.[33, 66, 185] Consequently, for ILs to be fully exploited for processing whole biomass, the solvent effects of ILs on cellulases must be effectively mediated.

One approach to circumvent the inactivation of cellulases by ILs is to rinse the IL from the biomass following dissolution or precipitate the treated biomass from the IL.[21, 25, 29, 36, 66] Wu et al.[222] previously demonstrated that high conversion of cellulose by *T. reesei* cellulases was attainable after dissolution and precipitation from 1-ethyl-3-methylimidazolium acetate. While this approach has met with partial success, residual IL associated with the biomass after rinsing or precipitation can lead to cellulase inactivation, requiring extensive washing and removal of the IL prior to biocatalytic hydrolysis. Following rinsing or precipitation, residual IL concentrations can exceed 10 - 15 % (v/v),[66] which is sufficient to inhibit cellulases.

Cellulase inactivation by even residual or trace amounts of ILs highlights the need to engineer cellulases for improved stability in ILs for the use of ILs for biomass conversion. We have recently demonstrated an approach to potentially mediate the interaction of the cation and anion of ILs with enzymes at the molecular level via engineering enzyme charge.[14, 15] This work broadly suggests that the relative density of negative to positive enzyme surface charges is critical to mediating salt binding and thus the inactivation of enzymes in ILs. In this work, enzyme surface charge was varied via chemical modification of reactive primary amine and carboxylate functional groups on the enzyme's surface. Engineering of enzyme surface charge via chemical modification presents a facile strategy to broaden the utility of enzymes in IL environments.

The goal of this work was to explore the use of surface charge modification as a means of rationally engineering cellulase for improved biomass hydrolysis in the presence of ILs.

Specifically, in this work, the ratio of negative to positive surface charges of the cellulase cocktail from *T. reesei* was increased by succinylation and acetylation of primary amine groups. The effects of charge modification on cellulase stability in buffer with [BMIM][Cl] were subsequently determined by measuring progress curves of the conversion of microcrystalline cellulose (Avicel). Furthermore, the hydrolysis of Avicel upon charge modification was monitored with varying amounts of lignin to ascertain the effect of surface charge on cellulase inhibition by lignin. Lignin, which is a major component of plant biomass, can non-productively absorb to cellulases via hydrophobic and electrostatic interactions,[223-227] which we hypothesized would be disrupted by charge modification.

6.3 Materials and methods

6.3.1 Materials

The cellulase cocktail from *Trichoderma reesei* (TRC), [BMIM][Cl], Avicel, Kraft lignin, and reagents for enzyme modification and determination of glucose production were purchased from Sigma Aldrich (St. Louis, MO). Trinitrobenzene sulfonic acid (TNBS) for determination of amine content was obtained from Thermo Fisher Scientific (Waltham, MA).

6.3.2 Modification of enzyme surface charge

Succinylated TRC was prepared by adding succinic anhydride to the enzyme cocktail (3 mg/mL, determined by Bradford assay) in 1 M sodium carbonate buffer (pH 8.5) in four aliquots over 3 h at room temperature.. Acetylated TRC was similarly prepared by modification with acetic anhydride, which was added in three aliquots over 1.5 h in 100 mM sodium phosphate buffer (pH 7.0). The final molar ratio of succinic or acetic anhydride to number of enzyme containing primary amines was approximately 30:1. Following modification, excess reagents

were separated by centrifugal filtration using a polyethersulfone membrane with a 10 kDa cutoff at 4 °C. The resulting modified enzyme cocktail was subsequently lyophilized prior to use and characterized via TNBS assay for determination of residual primary amines.

6.3.3 Monitoring of progress curves of Avicel hydrolysis

Wild-type and modified TRC were incubated at 40 °C in 50 mM citric acid buffer (pH 4.5) shaking at 175 rpm with 1 wt % Avicel, 0 or 15 % (v/v) [BMIM][Cl], and 0, 0.25, 0.5, or 1 wt % lignin. The concentration of wild-type and modified TRC was 0.029, 0.023, and 0.021 mg/mL, as determined by Bradford assay, resulting in enzyme loadings of 2.9, 2.3, and 2.1 mg total enzyme per gram of Avicel for succinylated, acetylated, and wild type TRC, respectively. The progress of Avicel hydrolysis was assayed by quantifying the number of soluble reducing sugars in the mixture using the DNS assay described by Miller.[228]

6.3.4 Modeling of progress curves

Progress curves of Avicel hydrolysis were modeled based on Michaelis-Menten kinetics with competitive product inhibition as well as first-order IL-induced inactivation. The model, which is given in Equation 2 where v is reaction velocity, V_{max} is maximum reaction velocity, $[S]$ is substrate concentration, $[P]$ is product concentration, K_M is the Michaelis-Menten constant, $k_{1/2}$ is the constant for first order inactivation, t is time, and K_I is the constant for competitive product inhibition, was integrated numerically.

$$v = V_{max}[S]\exp\left(-k_{1/2}t\right)/(K_M + (K_M/K_I)[P] + [S]) \qquad (2)$$

The value of K_I, which was assumed constant for all TRC charge variants, was determined by least square analysis of the wild-type progress curve in buffer only. Notably, differences in the

extent of product inhibition and thus K_I for conditions with buffer, buffer and [BMIM][Cl], and buffer and lignin were assumed to be negligible. Similarly, the values of K_M and V_{max} were determined by independently fitting the progress curves at different conditions. For progress curves with [BMIM][Cl], the values of $k_{1/2}$ and V_{max} were determined using the value of K_M determined in buffer only. In this way, it was assumed that the addition IL had a negligible effect on the apparent K_M of the enzyme cocktail. For progress curves with buffer only and buffer and lignin, the apparent effect of charge modification on K_M was determined while assuming $k_{1/2}$ was negligible and constant V_{max}. In this case, the value of V_{max} in buffer only was used for all progress curves in the absence of IL such that it was assumed only K_M was affected.

6.4 Results and discussion

6.4.1 Charge modification of *Trichoderma reesei* cellulase

The cellulase preparation engineered in this study consisted of the well-characterized fungal cellulase cocktail from *T. reesei*. The commercial TRC cellulase cocktail is composed primarily of the cellobiohydrolases Cel7A (CBH I) and Cel6A (CBH II), which contain approximately 11 primary amine and 32 acid groups each, and the endoglucanases Cel7B (EG I) and Cel5A (EG II), which contain approximately 11 primary amine and 33 acid groups each. These enzymes collectively make up approximately 95 % of the total enzyme content of the cocktail and thus are the most likely targets for modification.[229] Although of low abundance, the prominent β-glucosidases in the cocktail, which include Cel1A and Cel3A, presumably may also be modified. To investigate the effect of altering surface charge density on TRC activity in ILs, the cellulase cocktail was separately modified via succinylation and acetylation. Succinylation

and acetylation result in the conversion of positively-charged primary amine groups to negatively-charged acid and neutral acetyl groups, respectively.

Titration of the residual number of primary amines in TRC after modification confirmed that the density of positive-to-negative surface charges had been lowered (**Table 6-1**). As evidence of the alteration of this density, succinylation and acetylation, respectively, resulted in the modification of approximately 29 % and 58 % of the primary amines in TRC. These values represent the ensemble weighted average of the extent of modification for the entire TRC cocktail. Although characterization of succinylated and acetylated TRC confirmed the decrease in density of positive-to-negative surface charges, the exact ratio of positive-to-negative surface charges could not be determined due to uncertainty associated with the precise composition (i.e., concentration of individual enzymes) of the enzyme cocktail. Nevertheless, the activity of succinylated and acetylated TRC in ILs could be directly compared to that of wild-type TRC to broadly ascertain the impact of altering the ratio of surface charges.

Table 6-1. Extent of reaction of TRC upon charge modification. For determination of primary amine content, protein concentration was measured via Bradford assay. Error bars for the number of primary amines per protein concentration represent the standard deviation from the mean of two separate experiments.

	Moles Primary Amines / (g total protein) × 10^4
Wild-type TRC	3.8 ± 0.2
Acetylated TRC	1.6 ± 0.2
Succinylated TRC	2.7 ± 0.1

6.4.2 Impact of charge modification on Avicel hydrolysis by *Trichoderma reesei* cellulase in presence of [BMIM][Cl]

Upon modification, the activity of succinylated, acetylated, and wild-type TRC were initially measured in buffer only by measuring progress curves of Avicel hydrolysis. Importantly, both of the modified forms of TRC were active towards Avicel, indicating that succinylation and acetylation did not abolish the binding of TRC to insoluble cellulose. The activity of wild-type and succinylated and acetylated TRC was subsequently normalized based on overall activity on Avicel, resulting in overlapping progress curves (**Figure 6.2A**). By normalizing the activity of the variants, including wild-type TRC, we were able to directly investigate the effect of charge modification upon adding IL on Avicel conversion.

Progress curves of normalized Avicel conversion with 15 % (v/v) [BMIM][Cl] in buffered media are shown in **Figure 6.2B**. While the conversion of Avicel by acetylated TRC was similar to that of wild-type TRC, succinylated TRC was notably more active in the presence of the IL. The conversion of Avicel after 170 h at the conditions used by succinylated TRC was approximately 1.6-fold greater than by wild-type TRC. More broadly, the improvement in TRC activity by succinylation indicates that the addition of negative charges presumably mediates the interaction of ILs with TRC as has been observed previously with other model enzymes.[14] Such improvement in TRC activity may potentially be further enhanced by optimizing the surface charge for each enzyme in TRC individually. In principle, efficient cellulose hydrolysis in ILs may be achieved via optimizing the surface charge for only one endoglucanase (i.e., EG I or EG II) and a β-glucosidase (i.e., Cel1A or Cel3A), which work in concert. Of note, the concentration of [BMIM][Cl] employed in these studies is representative of that encountered following precipitation of biomass from ILs. To solubilize appreciable amounts of cellulose, significantly higher concentrations of IL would be required. An understanding of the site-specific nature of the interaction of ILs with cellulases may be used to more effectively stabilize cellulases in ILs,

thereby increasing the tolerance of cellulases to higher concentrations of ILs. Moreover, although Avicel conversion was lower with [BMIM][Cl] than without, ILs can bolster the hydrolysis of cellulose from whole biomass by more than 50-fold.[36] Thus, in the case of whole biomass as opposed to Avicel, we anticipate cellulose conversion by TRC upon charge modification would be greater with IL present relative to in non-IL conditions.

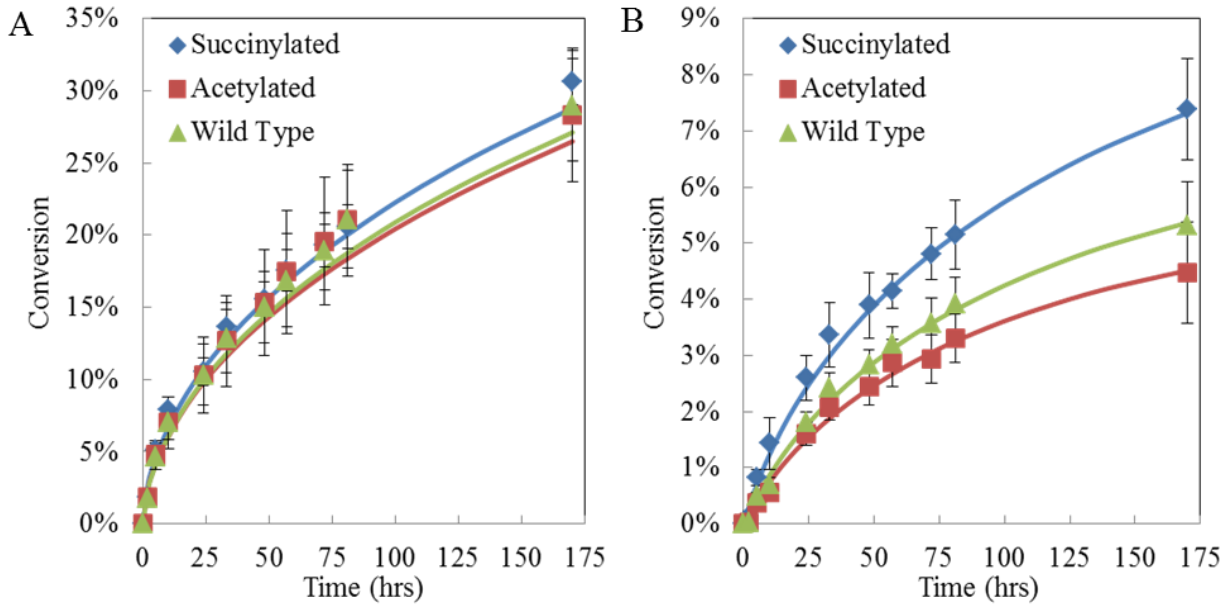

Figure 6.2. Progress curves for the hydrolysis of Avicel for succinylated (♦), acetylated (■), and wild type (▲) TRC at 40 °C in (A) 50 mM citric acid buffer (pH 4.5) and (B) 50 mM citric acid buffer (pH 4.5) with 15 % (v/v) [BMIM][Cl]. Enzyme loadings were 2.9, 2.3, and 2.1 mg/g Avicel for succinylated, acetylated, and wild type TRC, respectively. Error bars represent the standard deviation from the mean for five independent experiments in buffer and four independent experiments in the presence of [BMIM][Cl].

6.4.3 Impact of charge engineering on the inhibition of *Trichoderma reesei* cellulase by lignin

In light of the effect of succinylation on TRC activity in ILs, an interesting question that arises is if succinylation may impact the non-productive adsorption of lignin to TRC? Non-productive adsorption of lignin, which is a highly heterogeneous phenolic polymer, to cellulase

represents a major challenge in the saccharification of whole biomass. The adsorption of cellulases to insoluble lignin may specifically inhibit enzyme function by blocking binding to cellulose and potentially leading to cellulase denaturation.[223-227, 230] Interestingly, it was previously found that modification of lignin with negatively-charged acid groups reduced the extent of cellulase inhibition by lignin, suggesting adsorption is at least in part electrostatically driven.[231-233] Lou and co-workers[234] similarly showed that decreasing the protonation state of lignin as well as cellulase by increasing pH (from 4.8 to 5.5) led to a marked decrease in lignin adsorption to cellulases. The apparent decrease in lignin adsorption presumably was the result of electrostatic repulsion between the negatively-charged lignin and negatively-charge cellulase. Based on this, we thus hypothesized that the increase in negative charge of TRC via succinylation, in addition to increasing stability in [BMIM][Cl], would reduce lignin adsorption.

The impact of succinylation on lignin adsorption to TRC was ascertained by monitoring Avicel hydrolysis by TRC in the presence of various amounts of Kraft lignin (0 – 1 wt %). Progress curves of Avicel hydrolysis showed that succinylated TRC, as anticipated, was profoundly more active at all concentrations of lignin than wild-type and acetylated TRC (**Figure 6.3 A-C**). For comparison of progress curves, the activity of succinylated, acetylated, and wild-type TRC was normalized as previously based on comparing progress curves in buffer only. Interestingly, the decrease in conversion for wild-type and acetylated TRC was greatest in the presence of 0.25 wt % lignin and appears to level off for higher lignin concentrations (**Figure 6.3D**), indicating the apparent saturation of theoretical binding sites on TRC by lignin. Such saturation was not observed for succinylated TRC, which presumably was due to repulsion and thus lower binding affinity to lignin imparted by the addition of negatively charged sites. The results of activity assays in the presence of lignin ultimately support the utility of charge

engineering, namely succinylation, as a means to mediate non-productive lignin adsorption. These results also support the potential advantage of alternative cellulases that intrinsically have high negative surface charge densities such those from *Limnoria quadripunctata* and *Halorhabdus utahensis*, which presumably are less susceptible to lignin inhibition as a result of natural evolution.[183, 235] Importantly, due to the heterogeneity of the structure and composition of lignin, the extent of inhibition of lignin adsorption may differ with lignin from other sources. The exact extent to which such differences exist upon charge modification of cellulases remains to be determined.

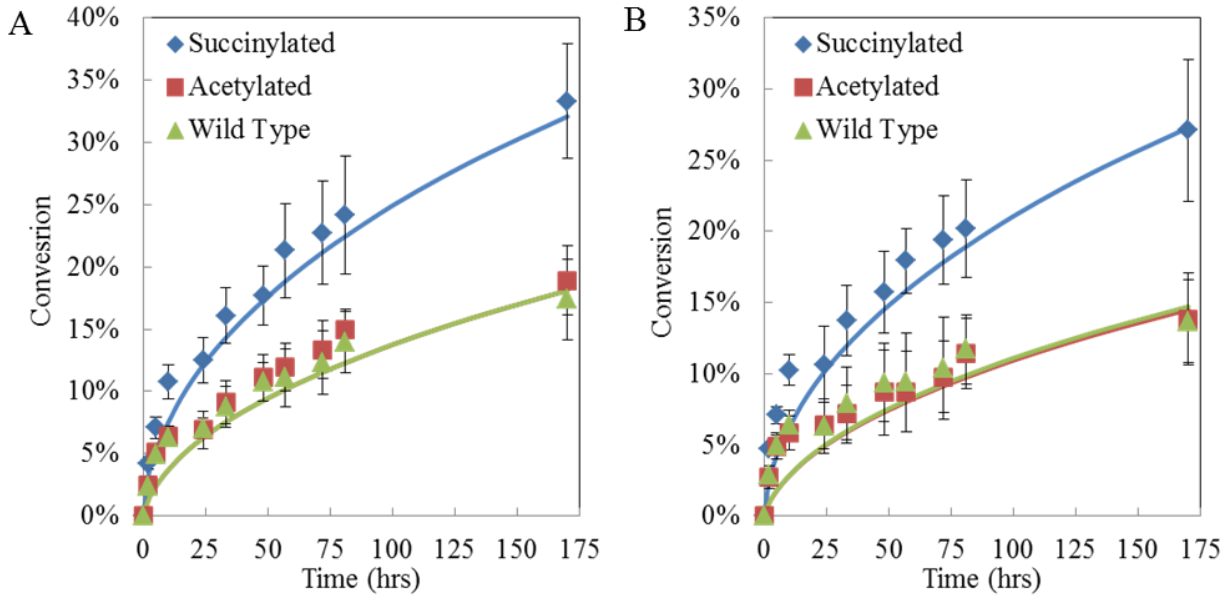

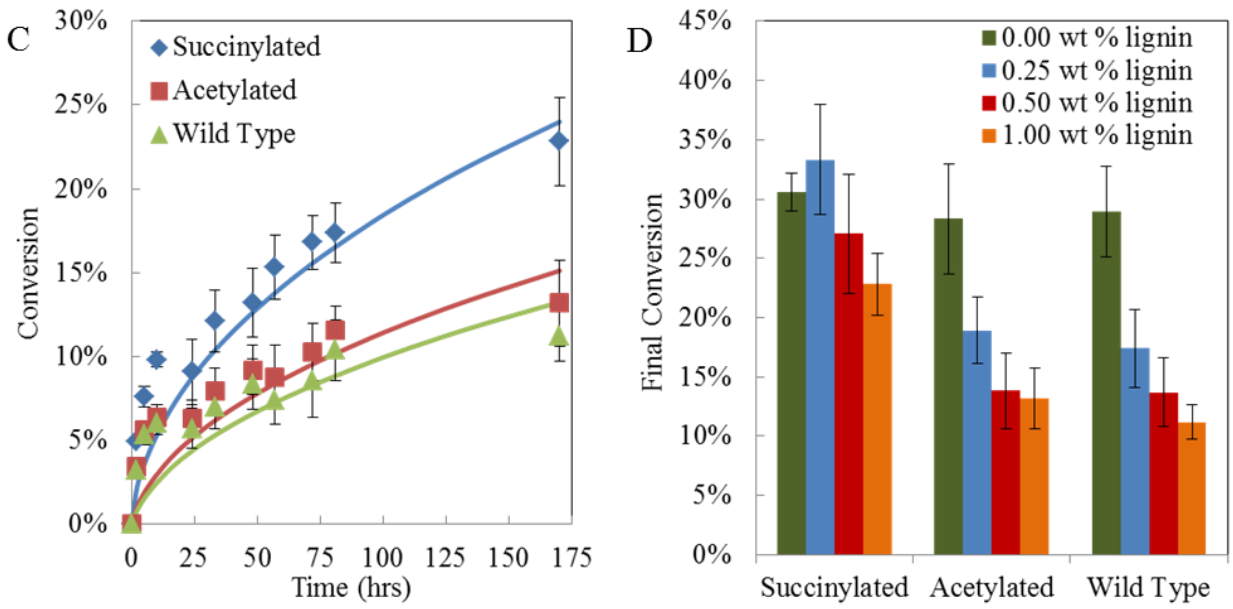

Figure 6.3. Progress curves for succinylated (♦), acetylated (■), and wild-type (▲) charge variants of TRC with (A) 0.25, (B) 0.5, and (C) 1 wt % lignin in 50 mM citric acid buffer (pH 4.5). (D) Direct comparison of the final conversion of Avicel at 170 h for succinylated, acetylated, and wild-type TRC at each concentration of lignin is also shown. Enzyme loadings were 2.9, 2.3, and 2.1 mg/g Avicel for succinylated, acetylated, and wild type TRC. Error bars represent the standard deviation from the mean for five independent experiments for 0 wt % lignin and four independent experiments for 0.25 - 1 wt % lignin.

6.4.4 Michaelis-Menten analysis of progress curves of Avicel hydrolysis by engineered *Trichoderma reesei* cellulase

Progress curves of Avicel digestion were modeled using Michaelis-Menten kinetics to further understand the effect of charge modification on the mechanism of TRC activity. Specifically, modeling of the progress curves was used to determine the relative impact of charge modification on the overall apparent kinetic parameters V_{max} and K_M of TRC. Additionally, model analysis was employed to examine how charge modification impacted V_{max} and K_M of TRC in the presence of [BMIM][Cl] and lignin. To account for the inhibition of TRC by products of Avicel conversion, including, glucose and cellobiose, the Michaelis-Menten model with competitive product inhibition was used. Because presumably there are multiple types of

product inhibition given that there are multiple enzymes in TRC, the inhibition constant K_I is representative of an overall inhibition constant. A first-order inactivation term ($k_{1/2}$) was also included in the model to capture the inactivation of TRC by [BMIM][Cl] for curves in which the IL was present. Of note, the model does not perfectly capture the exact mechanism by which this heterogeneous enzyme cocktail adsorbs to and deconstructs cellulose. It does, however, give useful apparent constants for understanding apparent inactivation and inhibition.

Michaelis-Menten kinetics have previously been used to model the conversion of insoluble cellulose by cellulase, demonstrating that cellulases follow Michaelis-Menten kinetics.[236-239] Of direct relevance to this work, Bezzerra and co-workers[237] modeled progress curves of Cel7A-catalyzed hydrolysis of Avicel using Michaelis-Menten kinetics, enabling direct determination of V_{max} and K_M as well as the constant for product inhibition. This work ultimately provides precedence for using Michaelis-Menten kinetics to model progress curves of TRC activity. Notably, their model did not include a term for the inactivation of Cel7A, which was assumed stable in the assay buffer used, which was the same buffer used in this work.

Values of V_{max} and K_M for progress curves for Avicel hydrolysis by wild-type and modified TRC in plain buffer are shown in

Table 6-2. Interestingly, results of the modeling analysis found that charge modification had very little overall impact on V_{max} and K_M of TRC. Accordingly, comparison of V_{max} and K_M of wild-type and modified TRC indicated that, namely, succinylation did not significantly alter binding of TRC to cellulose or cellulose turnover. In 15 % (v/v) [BMIM][Cl], the apparent V_{max} of wild-type and modified TRC was lower than in buffer only. Importantly, for analysis of progress curves in 15 % (v/v) [BMIM][Cl], the values of K_M for each form of TRC from progress curves in buffer only was used. Use of the values of K_M from buffer only conditions

was based on the assumption that the presence of [BMIM][Cl] did not impact substrate binding. In support of this assumption, when allowed to vary, K_M did not differ significantly between the presence and absence of [BMIM][Cl]. While the values of V_{max} were very similar between wild-type and acetylated TRC, the value of V_{max} for succinylated TRC was approximately 59 % greater than the other forms of TRC. Additionally, the value of $k_{1/2}$ was approximately 25 % lower for succinylated TRC compared to wild-type and acetylated TRC, which is consistent with the enhancement in stability of succinylated TRC in the presence of [BMIM][Cl]. The apparent enhancement in activity and stability upon succinylation is presumably the result of mediating interaction of [BMIM][Cl] and TRC at the molecular level.

Table 6-2. Michaelis-Menten kinetic parameters for wild-type and modified TRC in buffer (50 mM citric acid, pH 4.5) in the absence and presence of 15 % (v/v) [BMIM][Cl]. The value of $\boldsymbol{K_I}$ was fixed at 0.94 for all conditions. Error bars for kinetic constants in buffer and buffer with IL represent the standard deviation from the mean of five and four separate experiments, respectively.

	Buffer		**15 % (v/v) [BMIM][Cl]**	
	$\boldsymbol{V_{max}}$ **(mM-hr^{-1})**	$\boldsymbol{K_M}$ **(mM)**	$\boldsymbol{V_{max}}$ **(mM-hr^{-1})**	$\boldsymbol{k_{1/2}}$ **(hr^{-1})**
Wild-type	1.96 ± 0.19	103 ± 30	0.17 ± 0.02	0.0052 ± 0.0016
Acetylated	2.48 ± 0.56	138 ± 70	0.18 ± 0.02	0.0060 ± 0.0020
Succinylated	2.39 ± 0.83	111 ± 33	0.27 ± 0.05	0.0039 ± 0.0005

In analyzing progress curves with lignin, it was assumed that the adsorption of lignin, which presumably acts as a competitive inhibitor, impacts the apparent K_M of TRC only. Accordingly, the value of V_{max} was held constant, using the value determined from the buffer only conditions. This assumption was validated by the close fit of the model to the progress curves. Notably, for wild-type and acetylated TRC, the value of K_M increased with increasing concentration of lignin, which is consistent with that expected for a competitive inhibitor (**Figure**

6.4). However, increasing concentrations of lignin resulted in only a marginal increase on the apparent K_M of succinylated TRC. For comparison, the apparent K_M of succinylated TRC at 1 wt % lignin was approximately 31 % lower than that of wild-type TRC at 0.25 wt % lignin. The resulting difference in K_M highlights the potential utility of charge engineering to reduce lignin adsorption to cellulases. In this way, charge engineering may be exploited to prevent cellulase inactivation during the conversion of whole biomass, leading to improvements in the efficiency of biomass conversion.

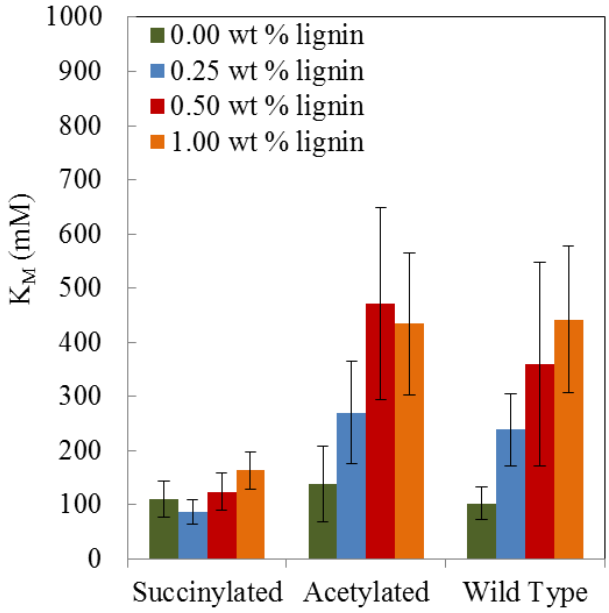

Figure 6.4. Effect of lignin on the apparent $\boldsymbol{K_M}$ of wild-type and modified TRC from progress curves in the presence of 0 – 1 wt % lignin. Error bars represent the standard deviation from the mean of four separate experiments for 0.25 – 1 wt % lignin and five separate experiments for 0 wt % lignin.

6.5 Conclusions

Our results demonstrate the potential of rational charge engineering to enhance TRC function in ILs. Specifically, we found that succinylation of the commercial TRC cellulase

cocktail led to a marked improvement in cellulase activity in aqueous solutions containing the IL [BMIM][Cl]. Importantly, succinylation had a negligible impact on the substrate affinity and turnover of TRC towards Avicel, suggesting the catalytic mechanism of the enzyme was unaffected. We have also shown that the addition of negative charges via succinylation of TRC reduced lignin adsorption to TRC during cellulose conversion, which improved cellulase activity. These results provide evidence that naturally evolved cellulases with highly negative surface charge densities may similarly repel lignin. Further studies are required to determine if charge engineering of individual cellulase enzymes may further enhance IL tolerance as well as reduce cellulase inhibition by lignin.

6.6 References

14. Nordwald, E.M. and J.L. Kaar, *Stabilization of Enzymes in Ionic Liquids Via Modification of Enzyme Charge.* Biotechnology and Bioengineering, 2013. **110**(9): p. 2352-2360.
15. Nordwald, E.M. and J.L. Kaar, *Mediating Electrostatic Binding of 1-Butyl-3-methylimidazolium Chloride to Enzyme Surfaces Improves Conformational Stability.* Journal of Physical Chemistry B, 2013. **117**(30): p. 8977-8986.
17. Pinkert, A., et al., *Ionic Liquids and Their Interaction with Cellulose.* Chemical Reviews, 2009. **109**(12): p. 6712-6728.
21. Brandt, A., et al., *The effect of the ionic liquid anion in the pretreatment of pine wood chips.* Green Chemistry, 2010. **12**(4): p. 672-679.
25. Alvira, P., et al., *Pretreatment technologies for an efficient bioethanol production process based on enzymatic hydrolysis: A review.* Bioresource Technology, 2010. **101**(13): p. 4851-4861.
29. Shill, K., et al., *Ionic Liquid Pretreatment of Cellulosic Biomass: Enzymatic Hydrolysis and Ionic Liquid Recycle.* Biotechnology and Bioengineering, 2011. **108**(3): p. 511-520.
32. Turner, M.B., et al., *Ionic liquid salt-induced inactivation and unfolding of cellulase from Trichoderma reesei.* Green Chemistry, 2003. **5**(4): p. 443-447.
33. Bose, S., C.A. Barnes, and J.W. Petrich, *Enhanced stability and activity of cellulase in an ionic liquid and the effect of pretreatment on cellulose hydrolysis.* Biotechnology and Bioengineering, 2012. **109**(2): p. 434-443.
36. Li, C.L., et al., *Comparison of dilute acid and ionic liquid pretreatment of switchgrass: Biomass recalcitrance, delignification and enzymatic saccharification.* Bioresource Technology, 2010. **101**(13): p. 4900-4906.
66. Engel, P., et al., *Point by point analysis: how ionic liquid affects the enzymatic hydrolysis of native and modified cellulose.* Green Chemistry, 2010. **12**(11): p. 1959-1966.

183. Zhang, T., et al., *Identification of a haloalkaliphilic and thermostable cellulase with improved ionic liquid tolerance.* Green Chemistry, 2011. **13**(8): p. 2083-2090.
184. El Seoud, O.A., et al., *Applications of ionic liquids in carbohydrate chemistry: A window of opportunities.* Biomacromolecules, 2007. **8**(9): p. 2629-2647.
185. Swatloski, R.P., et al., *Dissolution of cellose with ionic liquids.* Journal of the American Chemical Society, 2002. **124**(18): p. 4974-4975.
214. Himmel, M.E., et al., *Biomass recalcitrance: Engineering plants and enzymes for biofuels production.* Science, 2007. **315**(5813): p. 804-807.
215. Vinzant, T.B., et al., *Simultaneous saccharification and fermentation of pretreated hardwoods - Effect of native lignin content.* Applied Biochemistry and Biotechnology, 1997. **62**(1): p. 99-104.
216. Nishiyama, Y., P. Langan, and H. Chanzy, *Crystal structure and hydrogen-bonding system in cellulose 1 beta from synchrotron X-ray and neutron fiber diffraction.* Journal of the American Chemical Society, 2002. **124**(31): p. 9074-9082.
217. Nishiyama, Y., et al., *Crystal structure and hydrogen bonding system in cellulose 1(alpha), from synchrotron X-ray and neutron fiber diffraction.* Journal of the American Chemical Society, 2003. **125**(47): p. 14300-14306.
218. Beckham, G.T., et al., *Molecular-Level Origins of Biomass Recalcitrance: Decrystallization Free Energies for Four Common Cellulose Polymorphs.* Journal of Physical Chemistry B, 2011. **115**(14): p. 4118-4127.
219. Zhang, H., et al., *1-Allyl-3-methylimidazolium chloride room temperature ionic liquid: a new and powerful nonderivatizing solvent for cellulose.* Macromolecules, 2005. **38**: p. 8272-8277.
220. Lopes, A.M.D., et al., *Pretreatment and Fractionation of Wheat Straw Using Various Ionic Liquids.* Journal of Agricultural and Food Chemistry, 2013. **61**(33): p. 7874-7882.
221. Guo, J., et al., *Probing anion-cellulose interactions in imidazolium-based room temperature ionic liquids: a density functional study.* Carbohydrate research, 2010. **345**(15): p. 2201-5.
222. Wu, H., et al., *Facile Pretreatment of Lignocellulosic Biomass at High Loadings in Room Temperature Ionic Liquids.* Biotechnology and Bioengineering, 2011. **108**(12): p. 2865-2875.
223. Rahikainen, J.L., et al., *Inhibitory effect of lignin during cellulose bioconversion: The effect of lignin chemistry on non-productive enzyme adsorption.* Bioresource Technology, 2013. **133**: p. 270-278.
224. Rahikainena, J.L., et al., *Cellulase–lignin interactions—The role of carbohydrate-binding module and pH in non-productive binding.* Enzyme and Microbial Technology, 2013. **53**(5): p. 315-321.
225. Rahikainena, J.L., et al., *Effect of temperature on lignin-derived inhibition studied with three structurally different cellobiohydrolases.* Bioresource Technology, 2013. **146**: p. 118-125.
226. Rahikainen, J., et al., *Inhibition of Enzymatic Hydrolysis by Residual Lignins From Softwood-Study of Enzyme Binding and Inactivation on Lignin-Rich Surface.* Biotechnology and Bioengineering, 2011. **108**(12): p. 2823-2834.
227. Martin-Sampedro, R., et al., *Preferential Adsorption and Activity of Monocomponent Cellulases on Lignocellulose Thin Films with Varying Lignin Content.* Biomacromolecules, 2013. **14**(4): p. 1231-1239.

228. Miller, G.L., *Use of Dinitrosalicylic Acid Reagent for Determination of Reducing Sugar*. Analytical Chemistry, 1959. **31**(3): p. 426-428.
229. Seiboth, B., C. Ivanova, and V. Seidl-seiboth, *Trichoderma reesei: A Fungal Enzyme Producer for Cellulosic Biofuels*, in *Biofuel Production-Recent Developments and Prospects*, M.A.d.S. Bernardes, Editor 2011, InTech. p. 309-340.
230. Rajakumara, E., et al., *Crystallization and preliminary X-ray crystallographic investigations on several thermostable forms of a Bacillus subtilis lipase.* Acta Crystallographica Section D-Biological Crystallography, 2004. **60**: p. 160-162.
231. Kumar, L., R. Chandra, and J. Saddler, *Influence of Steam Pretreatment Severity on Post-Treatments Used to Enhance the Enzymatic Hydrolysis of Pretreated Softwoods at Low Enzyme Loadings.* Biotechnology and Bioengineering, 2011. **108**(10): p. 2300-2311.
232. Nakagame, S., et al., *Enhancing the Enzymatic Hydrolysis of Lignocellulosic Biomass by Increasing the Carboxylic Acid Content of the Associated Lignin.* Biotechnology and Bioengineering, 2011. **108**(3): p. 538-548.
233. Zhu, J.Y., et al., *Sulfite pretreatment (SPORL) for robust enzymatic saccharification of spruce and red pine.* Bioresource Technology, 2009. **100**(8): p. 2411-2418.
234. Lou, H.M., et al., *pH-Induced Lignin Surface Modification to Reduce Nonspecific Cellulase Binding and Enhance Enzymatic Saccharification of Lignocelluloses.* Chemsuschem, 2013. **6**(5): p. 919-927.
235. Kern, M., et al., *Structural characterization of a unique marine animal family 7 cellobiohydrolase suggests a mechanism of cellulase salt tolerance.* Proceedings of the National Academy of Sciences of the United States of America, 2013. **110**(25): p. 10189-10194.
236. Zhang, Y., et al., *Cellulase deactivation based kinetic modeling of enzymatic hydrolysis of steam-exploded wheat straw*. Bioresource Technology, 2010. **101**(21): p. 8261-8266.
237. Bezerra, R.M.F. and A.A. Dias, *Discrimination among eight modified Michaelis-Menten kinetics models of cellulose hydrolysis with a large range of substrate/enzyme ratios.* Applied Biochemistry and Biotechnology, 2004. **112**(3): p. 173-184.
238. Brown, R.F., F.K. Agbogbo, and M.T. Holtzapple, *Comparison of mechanistic models in the initial rate enzymatic hydrolysis of AFEX-treated wheat straw*. Biotechnology for Biofuels, 2010. **3**.
239. Bansal, P., et al., *Modeling cellulase kinetics on lignocellulosic substrates.* Biotechnology Advances, 2009. **27**(6): p. 833-848.

Chapter 7 NMR-guided rational engineering of an ionic-liquid-tolerant lipase

Adapted from ACS Catalysis, 4, 4057-4064

7.1 Abstract

Biocatalysis in ionic liquids (ILs) is largely limited by the instabilities of enzymes in these solvents, thus negating their auspicious solvent properties. Here, we have engineered an IL tolerant variant of lipase A (lipA) from *Bacillus subtilis* by examining the site-specific interactions of lipA with 1-butyl-3-methylimidazolium chloride ([BMIM][Cl]). Results of NMR analysis found that [BMIM][Cl] induced structural perturbations near the active site of lipA, underscoring the importance of mediating direct ion interactions with the IL in this region. Mutation of G158 near the active site to glutamic acid resulted in a 2.5-fold improvement in tolerance of lipA to 2.9 M (or 50 % v/v) [BMIM][Cl], which correlated with the retention of active site structure. The effect of the G158E mutation was likely the result of inhibition of hydrophobic interactions with the [BMIM] cation. Further analysis of the electrostatic surface of lipA led to the mutation of K44 to glutamic acid to diminish the attraction of chloride anions, which also improved lipA tolerance to [BMIM][Cl]. Beneficial point mutations, which had an additive effect of lipA stability, were combined, resulting in a super stable lipA quadruple mutant (G158E/K44E/R57E/Y49E) with a 7-fold improvement in stability. In comparison, non-specific modification via acetylation and succinylation resulted in only a 1.2 and 1.9-fold improvement in stability, respectively, over wild-type lipA. Ultimately, these results, while providing insight into

the nature of the structural effects of ILs on enzymes, highlight the utility of combining NMR and charge engineering to rationally optimize enzyme stability for biocatalysis in ILs.

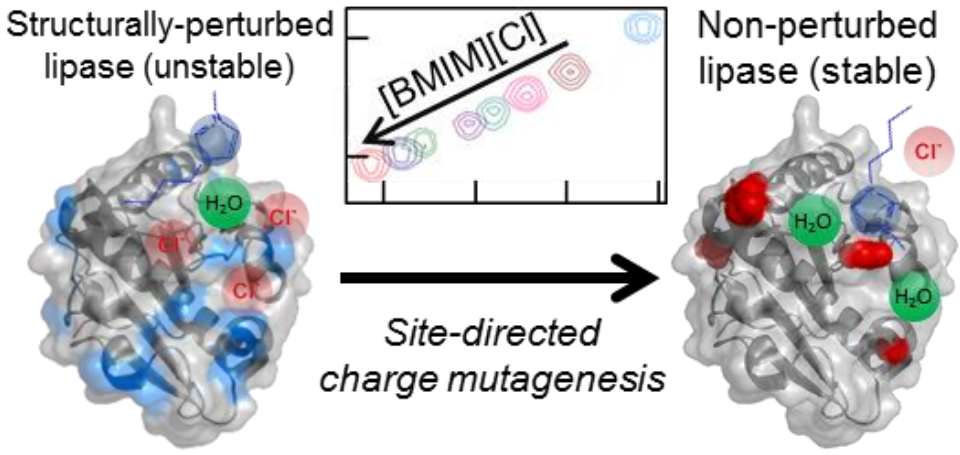

Figure 7.1. Graphical abstract: Adding ionic liquid causes perturbations around various residues. Mutagenesis around these residues to negatively charged amino acids results in increased stability, and mitigated perturbations.

7.2 Introduction

Despite the immense potential of ionic liquids (ILs) as solvents for biocatalysis for producing pharmaceuticals,[3, 22, 50] biofuels,[24, 33, 36, 57] and other fine chemicals,[52] rational approaches to improve enzyme tolerance to ILs are inherently needed. Biocatalytic reactions in neat ILs as well as aqueous-IL mixtures are largely limited due to the denaturation of enzymes by ILs, thus negating the excellent solvent properties of ILs.[19, 68-71, 138] While many approaches to improve the stability of enzymes in ILs have been investigated, conventional approaches, including immobilization, polyethylene glycol modification, and chemical crosslinking have been, in virtually all cases, unsuccessful in expanding the scope of biocatalysis in IL media.[72-78]

In earlier work, we reported that altering the surface charge of enzymes can markedly enhance the kinetic stability of enzymes in the presence of the IL 1-butyl-3-methylimidazolium chloride ([BMIM][Cl]).[14, 15] Enhancements in stability specifically correlated with the ratio of positive-to-negative charged groups on the enzyme surface. In these studies, the impact of changing this ratio was studied by chemically modifying the enzyme surface using non-specific reactions that randomly target primary amines and carboxylate groups. Lowering this ratio, in particular, led to increased kinetic stability, which also correlated with the apparent exclusion of the chloride anion from the enzyme surface.

The stabilization of enzymes against IL-induced denaturation via charge modification presents considerable opportunities for improving the efficiency of biocatalytic reactions in IL environments. As evidence of such opportunities, we have shown that a range of enzymes, including chymotrypsin, lipase, papain, and cellulase can be stabilized from inactivation in aqueous-IL solutions via altering surface charge.[13-15] In the case of cellulase, the enzyme preparation (*Trichoderma reesei*) that was modified consisted of a mixture of cellulolytic

enzymes, which, upon modification, also showed improved resistance towards lignin inhibition.[13] However, such enhancements in stability by charge modification may be significantly improved with a more detailed understanding of the specific sites in enzymes that are structurally perturbed by ILs. An understanding of the propensity of the constituent cation and anion to perturb specific sites may be used to inform or guide the mutation of these sites to site-specifically mediate changes in solvent environment. Importantly, by site-specifically mediating cation and anion-induced changes in enzyme structure, functionally important residues and motifs may be more effectively shielded from the denaturing effects of ILs than via non-specific modifications. Moreover, through site-specific charge engineering, deleterious modifications as well as even neutral modifications, which have a negligible effect on enzyme stability, may also be prevented. The ability to probe direct ion interactions involving ILs with specific sites on protein surfaces was recently demonstrated by Figueiredo and co-workers[175] using NMR spectroscopy.

Herein, we have uniquely combined NMR spectroscopy with charge engineering to rationally engineer the industrially important enzyme lipase A (lipA) from *Bacillus subtilis* for improved tolerance to [BMIM][Cl]. In this approach, two-dimensional heteronuclear single quantum coherence (15N/1H HSQC) NMR was employed to identify residues on the surface of lipA that experience a change in local chemical environment in the presence of [BMIM][Cl]. Analysis of chemical shift perturbations due to changes in solvent environment was used to mutate specific residues to charged amino acids to locally inhibit direct ion interactions with the cation and anion. Furthermore, analysis of the electrostatic map of lipA was used to discern additional residues as candidates for mutation that are potential sites around which chloride may cluster due to strong Coulombic interactions. Upon screening mutants with single point

mutations by measuring enzyme half-life ($T_{1/2}$), beneficial mutations were combined to optimize lipA stability and relate lipA stability to sequence and structure. Notably, lipA, like other lipases, catalyzes industrial biotransformations that entail the hydrolysis, formation, and rearrangement of ester bonds in aqueous and non-aqueous media.[240-242] Despite previous attempts to improve enzyme tolerance to ILs via directed evolution,[51, 243, 244] this work represents, to the best of our knowledge, the first attempt to rationally engineer an enzyme for improved biocatalysis in IL environments.

7.3 Materials and methods

7.3.1 Materials

Genomic DNA from *Bacillus subtilis* containing the lipA gene was kindly donated by Robert Batey (University of Colorado, Boulder). The QuickChange lightning mutagenesis kit for site-directed mutation of lipA was purchased from Agilent (Santa Clara, CA). All other chemicals, including [BMIM][Cl] (>98%), 4-nitrophenyl butyrate (pNPB), and N_{15} labeled ammonium chloride (98 atom %) were purchased from Sigma Aldrich (St. Louis, MO) and used as supplied.

7.3.2 Enzyme expression, purification, and mutagenesis

To produce recombinant lipA, the gene for lipA (without the pelB leader sequence) was initially PCR amplified from genomic *Bacillus subtilis* DNA and cloned into pET21b, using NdeI and SacI restriction sites. The forward and reverse primers used for amplification were 5'-GATATACATATGGCTGAACACAATCCAGTCGTTATG-3' and 5'-GATATTGAGCTCTCATTAATTCGTATTCTGGCCCCC-3', respectively. Upon cloning, the pET21b lipA vector was transformed into BL21 (DE3) *Escherichia coli*, which was grown in

growth media (Luria broth) at 37 °C and 200 rpm with 100 mg/L ampicillin. Expression of lipA was induced via the addition of 1 mM isopropyl β-D-1-thiogalactopyranoside also at 37 °C. After 1.5 days, soluble lipA that was secreted during expression was collected and dialyzed against 50 mM MES buffer (pH 6.8) prior to use in stability assays without further purification.

For 15N/1H HSQC experiments, lipA was expressed in M9 minimal media with N_{15} ammonium chloride as the sole nitrogen source and purified from insoluble cell lysate. Following an induction period of 2.5 days, cells were harvested via centrifugation and lysed using a PandaPlus 2000 (GEA Inc, Columbia, MD) homogenizer. To purify lipA, the insoluble portion of the lysate was dissolved in 6 M GnHCl, which was subsequently diluted 20-fold with 10 mM sodium phosphate (pH 5.5) to promote re-folding of the enzyme. The re-folded enzyme was separated via centrifugation at 15,000 g for 15 min and finally purified by cation exchange chromatography. The resulting purified enzyme was dialyzed against 10 mM sodium phosphate buffer (pH 7.0) concentrated to 8 mg/ml, and was estimated quantitatively to be >98 % pure by SDS-PAGE.

For site-directed mutagenesis, lipA was mutated by using the QuickChange lightning mutagenesis kit. The correct insertion of all mutations was verified by sequencing.

7.3.3 Stability assay of lipase A

Stability to IL-induced inactivation was assayed by incubating wild-type or mutant lipA (0.01 mg/ml) in 20 mM MES buffer with 2.9 M or (50 % v/v) [BMIM][Cl] (final pH 6.5) at 35°C with constant shaking (100 rpm). Inactivation of lipA was followed by periodically removing aliquots (735 μL) and assaying residual lipA activity by measuring the enzymatic hydrolysis of pNPB (3 mM), which was prepared in acetonitrile (2 % v/v final concentration). The initial rate of pNPB hydrolysis was assayed spectrophotometrically by continuously

monitoring the release of 4-nitrophenyl at 412 nm at room temperature. To determine $T_{1/2}$, the resulting stability curves were fit to a first-order, reversible (N⇔U) unfolding model.

7.3.4 NMR experiments

15N/1H HSQC spectra of wild-type and G158E lipA (400 μM) were recorded at 298 K for 30 mins using a 900 MHz DD2 spectrometer with a cryogenic probe (Agilent Technologies). For sample preparation, 0 – 0.29 M (or 5 % v/v) [BMIM][Cl] was added to the enzyme in 10 mM sodium phosphate (final pH 7.0) with 5 % v/v D_2O. Peak assignments, which were previously reported by Augustyniak and co-workers,[245] were transferred from the Biological Magnetic Resonance Bank (entry 18574). Of the 171 residues for which peak assignments were reported, 165 of the residues in the spectra of lipA were easily assignable based on overlapping peak resonances. The remaining 6 peaks could not be assigned with confidence due to weak signal-to-noise or because of uncertainty in the peak position. For determination of chemical shift perturbations (Δ chemical shift), the combined ΔH_1 and ΔN_{15} perturbation was calculated using the following equation:

$$\Delta \text{ chemical shift} = ((\Delta H_1)^2+(\alpha\, \Delta N_{15})^2)^{0.5}$$

In the above equation, ΔH_1 and ΔN_{15} are the H_1 and N_{15} chemical shift perturbations (in ppm), respectively, and α is a scaling factor for which a value of 0.17 was used.[246, 247] In the analysis of Δ chemical shift, a minimum cutoff of 0.05 ppm was used as the threshold for significance.

7.4 Results and discussion

7.4.1 15N/1H HSQC analysis of ionic liquid-induced chemical shift perturbations in lipase

With the goal of rationally enhancing IL tolerance of lipA, specific residues that are structurally perturbed by the addition of [BMIM][Cl] due to local changes in solvent

environment were initially determined by 15N/1H HSQC NMR. Local changes in enzyme and, more broadly, protein structure can be probed using 15N/1H HSQC NMR via analysis of perturbations in the peak resonances of individual residues within the enzyme. In analogous studies, Figueiredo and co-workers[175] previously used 15N/1H HSQC NMR to examine IL-induced structural changes in a model four-bundle helix protein by [BMIM][Cl] along with other ILs, demonstrating the applicability of this technique for our purpose. Notably, their results identified a number of charged as well as nonpolar residues that experienced significant chemical shift perturbations, implicating electrostatic as well as hydrophobic ion interactions. Hydrophobic ion interactions may specifically arise from interactions involving the alkyl side chain of the [BMIM] cation with non-polar residues and regions on the protein surface. Additionally, 15N/1H HSQC NMR has been also used to examine the effects of organic solvents on enzyme and protein structure, including for a thermostabile lipase mutant also from *B. subtilis*.[248-250]

Results of 15N/1H HSQC analysis of lipA with [BMIM][Cl] found multiple peak perturbations involving surface residues that are likely involved in direct ion interactions with the IL. The perturbation of select residues are readily apparent in **Figure 7.2A**, which shows an overlay of 15N/1H HSQC spectra for lipA with 0 – 0.29 M (or 5 % v/v) [BMIM][Cl]. Of important note, at the concentrations of IL used, the global structure of the enzyme was retained, resulting in shifts of only residues thought to be perturbed as a result of direct ion interactions. Residues that experienced the largest shifts include the catalytic residue H156 and G158 (see **Figure 7.2B** for an enlarge view of the spectral shifts of H156 and G158), which are part of a patch of residues involving V154, G155 and I157 that are also perturbed. The magnitude of the perturbations of the residues in this patch is shown in **Figure 7.2C**, which shows the chemical

shift perturbations for all residues in lipA with 0.29 M [BMIM][Cl]. Due to the non-polar nature of many of the residues in this patch, these residues are presumably perturbed by the cation through hydrophobic interactions with the butyl chain of [BMIM]. To confirm that these residues were perturbed by ion interactions and not changes in pH, which alter the ionization state of H156, control spectra were collected at pH 6.9 (at the largest IL concentration, the addition of [BMIM][Cl] reduced the solution pH 0.05 units from pH 7). In the control spectra, residues V154-G158 did not appear to shift, verifying the role of direct ion interactions between lipA and the IL in perturbing this patch on the enzyme surface (data not shown). Additionally, around the active site region, G11, G13, and residues V136-Y139 as well as the other residues of the catalytic triad S77 and D133 are also perturbed. Notably, residues V136-139 are situated close to the positively-charged residues R107 and R142, which may attract the chloride anion to this region.

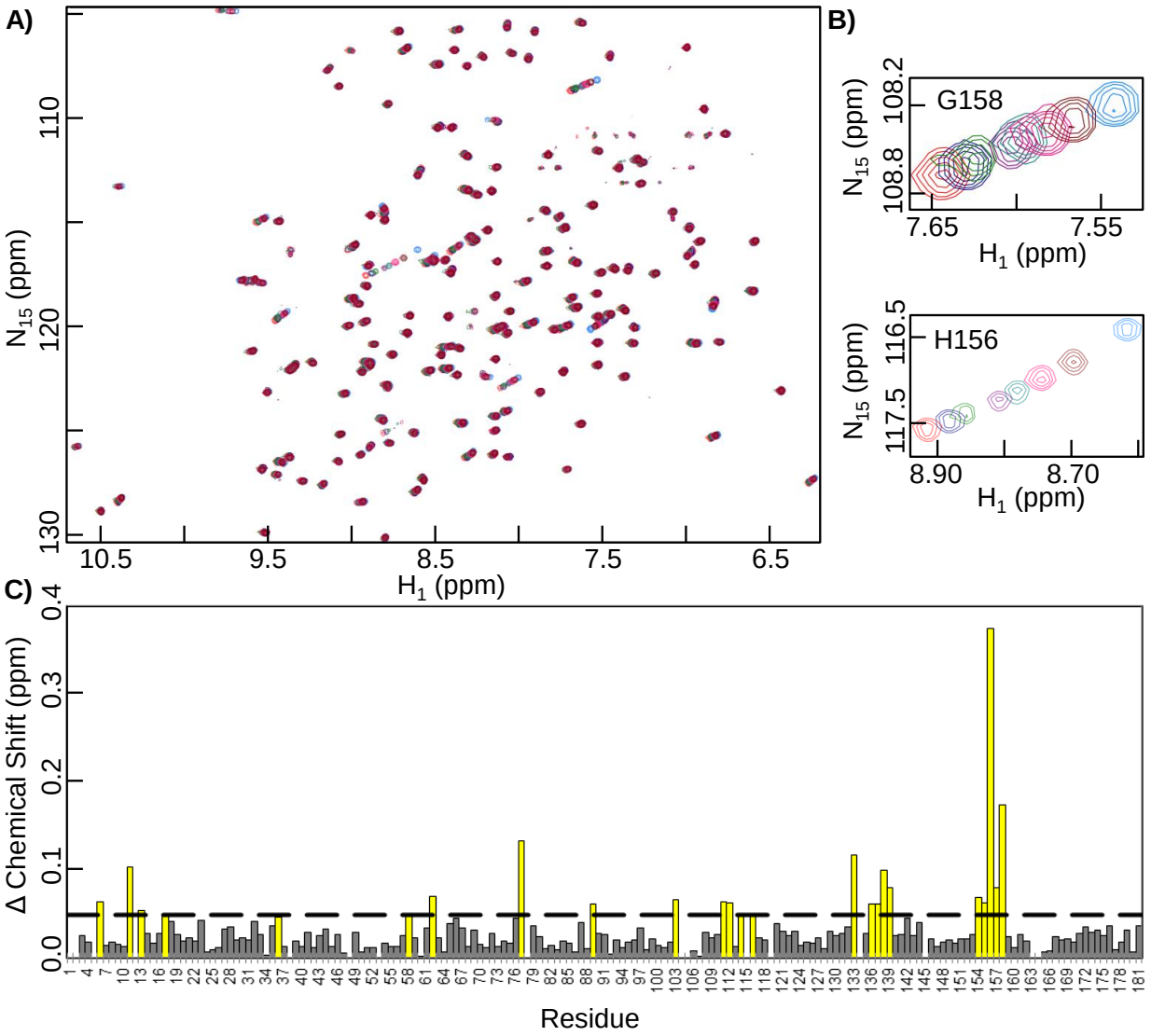

Figure 7.2. 15N/1H HSQC spectra of wild-type lipA in the presence of [BMIM][Cl]. (A) Overlay of spectra with 0 (light blue), 0.029 (brown), 0.057 (pink), 0.086 (cyan), 0.11 (purple), 0.17 (green), 0.23 (navy), and 0.29 (red) M [BMIM][Cl]. (B) Enlarged views of spectral changes to residues G158 and H156, which experienced the largest chemical shift perturbations in lipA upon titration with [BMIM][Cl]. (C) Chemical shift perturbations with 0.29 M (or 5 v/v %) [BMIM][Cl] for all residues in lipA. The dashed line at 0.05 ppm represents the threshold used for significance of chemical shift perturbations. All residues with significant chemical shift perturbations are represented by yellow bars. For unassigned residues, bars representing chemical shift perturbations were omitted.

While it is interesting to consider perturbations near the active site, which may directly contribute to the loss of enzyme activity, shifts in other regions of lipA may similarly be

important for IL tolerance. A patch of surface residues that are distant from the active site that encompasses N89, G111, K112, L114, and G116 also experience significant chemical shifts (**Figure 7.2C**). Shifts in this patch may be attributed to chloride interactions due to the presence of neighboring positively-charged residues (K88, R107, and K122). Also hydrophobic interactions of the [BMIM] cation with L114 may be important. Several other non-polar residues in different locations throughout the enzyme are also perturbed, including V6, F17, F58, V62, and G103. Interestingly, of the total 23 residues that were perturbed in lipA by [BMIM][Cl], the majority of these residues (13) are located in flexible loop regions as opposed to structured β-sheets (1) or α-helices (9). Because of the inherent flexibility of these residues, these residues may be more susceptible to structural perturbations at low IL concentrations. To better understand the location, exposure, secondary structure and proximity of the residues that are perturbed, the structurally perturbed residues were mapped onto the crystal structure of lipA (**Figure 7.3**).

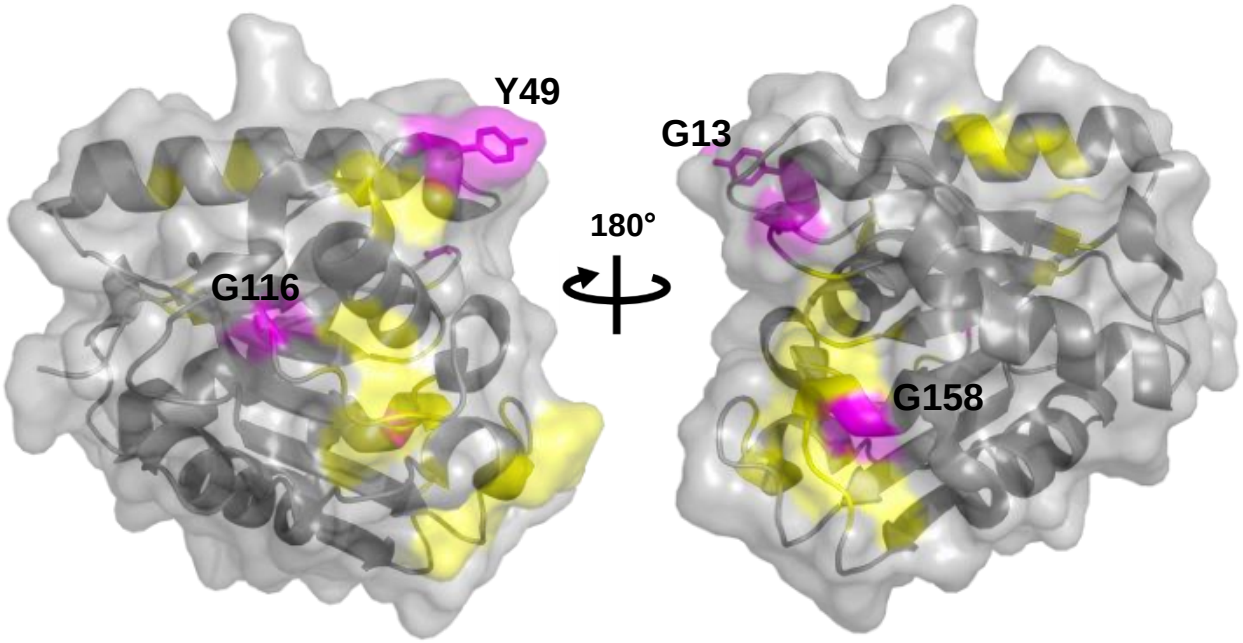

Figure 7.3. Structure of lipA (PDB code: 1ISP) with map of chemical shift perturbations due to direct ion interactions with [BMIM][Cl]. Residues that experienced significant chemical shift perturbations (≥ 0.05 ppm) with the addition of 0.29 M (5 v/v %) IL are colored yellow. The

residues in magenta with side chains showing represent sites that were mutated to glutamic acid to inhibit direct ion interactions with the IL by site-directed mutagenesis.

7.4.2 Impact of site-directed mutagenesis on ionic liquid tolerance of lipase A

Based on proximity to structurally perturbed sites, residues on the surface of lipA were subsequently considered for site-directed mutagenesis. The goal of mutagenesis in this case was to inhibit direct ion interactions with the cation and anion by altering the local electrostatic environment through mutating candidate residues to glutamic acid. We hypothesized that substitution of glutamic acid would, as suggested previously,[15] lead to exclusion of the chloride ion through repulsive Coulombic interactions. Furthermore, we predicted that glutamic acid mutations would weaken hydrophobic interactions with the butyl chain of [BMIM] by disrupting the hydrophobicity of non-polar regions on the surface of lipA. In principle, the mutation of surface residues to aspartic acid would exert a similar effect. The residues that were mutated were G13, Y49, G116, and G158, which are themselves structurally perturbed (G13, G116, G158) or in close proximity to structurally perturbed sites (Y49) in lipA (**Figure 7.3**). Although not significantly perturbed itself, residue Y49 is nearby the perturbed residue N89, which was not directly mutated due to potential steric clashes with neighboring residues (namely Y85). In addition to their proximity to perturbed sites, the mutated residues are highly solvent exposed and non-hydrogen bonding in the crystal structure of lipA.

To determine the effect of G13E, Y49E, G116E, and G158E substitutions on lipA tolerance to [BMIM][Cl], individual variants with each point mutation were prepared by site-directed mutagenesis. Tolerance of wild-type and mutant lipA to [BMIM][Cl] was measured by assaying residual enzyme activity over time upon incubation in buffer containing 2.9 M (50 %

v/v) [BMIM][Cl]. With the exception of G116E, all of the mutations resulted in a significant increase in the $T_{1/2}$ of lipA relative to wild-type lipA, thereby improving the tolerance of lipA to [BMIM][Cl] (**Figure 7.4**). The most significant increase in $T_{1/2}$ was observed for the G158E mutant ($T_{1/2}$ = 183 min), which extended the $T_{1/2}$ of lipA relative to wild-type ($T_{1/2}$ = 74 min) by nearly 2.5-fold. Substitution of glutamic acid at this position presumably alters the polarity around V154-G158, reducing the propensity of [BMIM] interactions in this region and, furthermore, preventing structural perturbations to the catalytic H156, D133, and S77. Given the large impact of the G158 mutation on $T_{1/2}$, the results of stability studies suggest that the interactions with [BMIM] in this region may be particularly denaturing and thus critical to lipA stability. For the Y49E ($T_{1/2}$ = 108 min) and G13E ($T_{1/2}$ = 105 min) mutations, improvements in $T_{1/2}$ of lipA of approximately 1.5-fold were observed for each. Due to the proximity of G13 to the active site, the mutation of this residue to glutamic acid likely also leads to the retention of active site structure while preventing cation and anion interactions. In the case of the G116E mutation, substitution of G116 to glutamic acid resulted in destabilization of lipA, perhaps by disrupting local hydrogen bonding and nearby salt bridges.

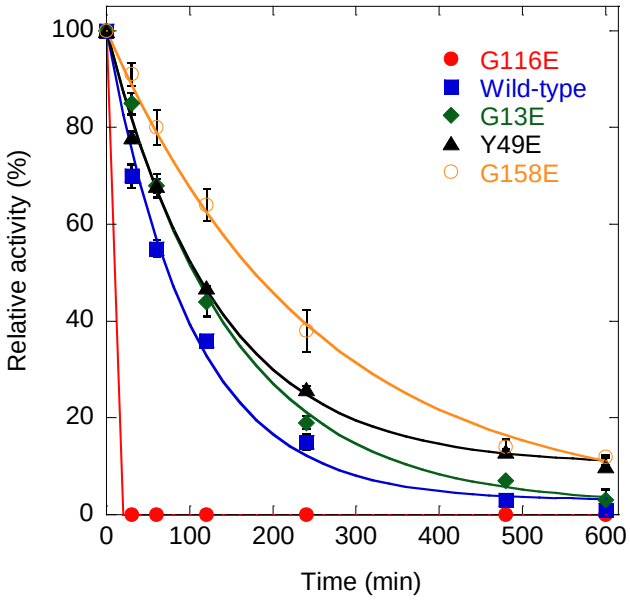

Figure 7.4. Activity retention profiles for wild-type (■), G116E (●), G13E (♦), Y49E (▲), and G158E (○) lipA in 20mM MES buffer and 2.9 M (50 v/v %) [BMIM][Cl] (pH 6.5) at 35 °C.

Because the glutamic acid mutations alter enzyme charge, an alternative explanation for the observed improvements in stability of lipA G13E, Y49E, and G158E variants is that the added negative charge prevents IL-induced salting out of the enzyme. Specifically, it is plausible that the charge mutations lead to increased solubility of lipA in the presence of [BMIM][Cl], which, in turn, leads to an increase in $T_{1/2}$. To confirm that the stabilization of lipA upon mutation was due to the inhibition of IL-induced unfolding rather than salting out, lipA solubility in the presence of [BMIM][Cl] was directly measured. For measuring salting out, the concentration of soluble lipA in the presence of [BMIM][Cl] was monitored over time by monitoring absorbance of lipA at 280 nm. The concentration of [BMIM][Cl] used for salting out assays was the equivalent to that used in the above stability studies. Notably, at this concentration of IL, the absorbance of wild-type lipA decreased by a negligible amount (< 5 %) over one week, indicating minimal if any precipitation of lipA occurred. Given the lack of precipitation of wild-type lipA over this period, it is highly unlikely that salting-out, although not measured for lipA variants, was the cause of lipA inactivation in stability studies. Additionally, inhibition studies of lipA activity as a function of varying [BMIM][Cl] concentration showed little difference between the variants and wild-type lipA. Based on this, the mutations appear to affect only the kinetic stability of the enzyme and, conversely, do not alter the specific activity of lipA in the presence of [BMIM][Cl].

7.4.3 Effect of G158E on structural perturbations in the active site of lipase A

Of the glutamic acid mutations that stabilize lipA, the G158E mutation is of particular interest due to the magnitude of its stabilizing effect and proximity to the active site. The structural basis for the stabilization of lipA upon mutation of G158 to glutamic acid was elucidated by 15N/1H HSQC analysis of G158E lipA with [BMIM][Cl]. Peak assignments for G158E lipA were inferred based on the juxtaposition of resonances relative to that in the spectra of wild-type lipA. Although the spectra of the G158E lipA was not assigned directly, the majority of the resonance peaks in G158E could be identified, including namely around the active site (155 of 171 residues were assigned for G158E lipA). As for wild-type lipA, the resonance peaks in the spectra of G158E lipA were distinct and well-dispersed, which facilitated the identification of peak resonances. Importantly, all of the residues in G158E lipA that are perturbed shift in the same direction as in the spectra of wild-type lipA with [BMIM][Cl]. While many of the residues around the mutation site could be assigned, changes in the chemical shift upon mutation prevented the assignment of E158 in the spectra of the mutant lipA.

Analysis of the active site region of lipA in the 15N/1H HSQC spectra of G158E lipA with 0 – 0.29 M (or 5 % v/v) [BMIM][Cl], like with wild-type lipA, showed obvious perturbations (**Figure 7.5A**). However, the magnitude of the chemical shift perturbations for residues in the active site region overall were significantly weaker than that for wild-type lipA with equivalent [BMIM][Cl] concentrations. In particular, perturbations in H156 are markedly smaller in the mutant lipA (**Figure 7.5B**). In addition to the magnitude of the shifts being weaker, the dependence of the observed shifts on IL concentration in G158E lipA was diminished relative to those in wild-type lipA. The dependence of chemical shifts for all residues within 10 Å of residue 158 that are structurally perturbed by [BMIM][Cl] was determined for wild-type (**Figure 7.6A**) and G158E (**Figure 7.6B**) lipA. Accordingly, structural perturbations in

the active site region of G158E lipA were less sensitive to IL concentration than in the active site region of wild-type lipA. To analyze the sensitivity of chemical shifts on IL concentration, the shifts were normalized to the theoretical maximum shift at each site by fitting the shifts to a Langmuir isotherm model as described previously.[175] Because E158 could not be assigned in the 15N/1H HSQC spectra, analysis of chemical shift perturbations of the mutated residue was omitted from the structural characterization of G158E lipA. Ultimately, the 15N/1H HSQC results provide evidence that the G158E mutation stabilizes lipA from inactivation by [BMIM][Cl] via increasing the retention of active site structure.

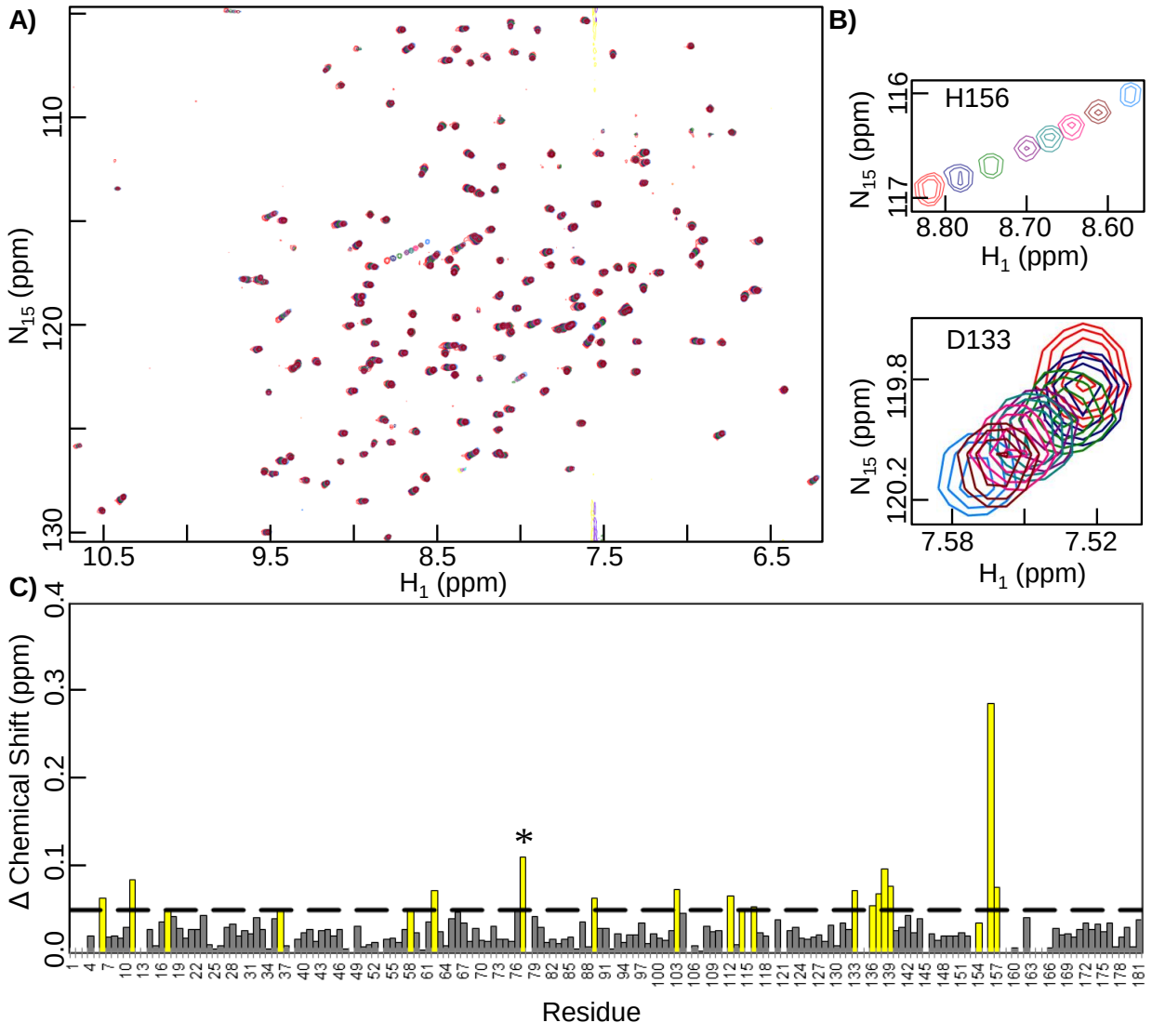

Figure 7.5. 15N/1H HSQC spectra of G158E lipA in the presence of [BMIM][Cl]. (A) Overlay of spectra with 0 (light blue), 0.029 (brown), 0.057 (pink), 0.086 (cyan), 0.11 (purple), 0.17 (green), 0.23 (navy), and 0.29 (red) M [BMIM][Cl]. (B) Enlarged views of spectral changes to residues H156 and D133 upon titration with [BMIM][Cl]. (C) Chemical shift perturbations with 0.29 M (or 5 v/v %) [BMIM][Cl] for all residues in lipA. The dashed line at 0.05 ppm represents the threshold used for significance of chemical shift perturbations. Yellow bars represent residues that experienced a significant chemical shift perturbation in wild-type lipA. For unassigned residues, bars representing chemical shift perturbations were omitted. (*) Due to weak signal at 0.29 M [BMIM][Cl], the chemical shift perturbation for S77 was determined using the 0.23 M [BMIM][Cl] sample.

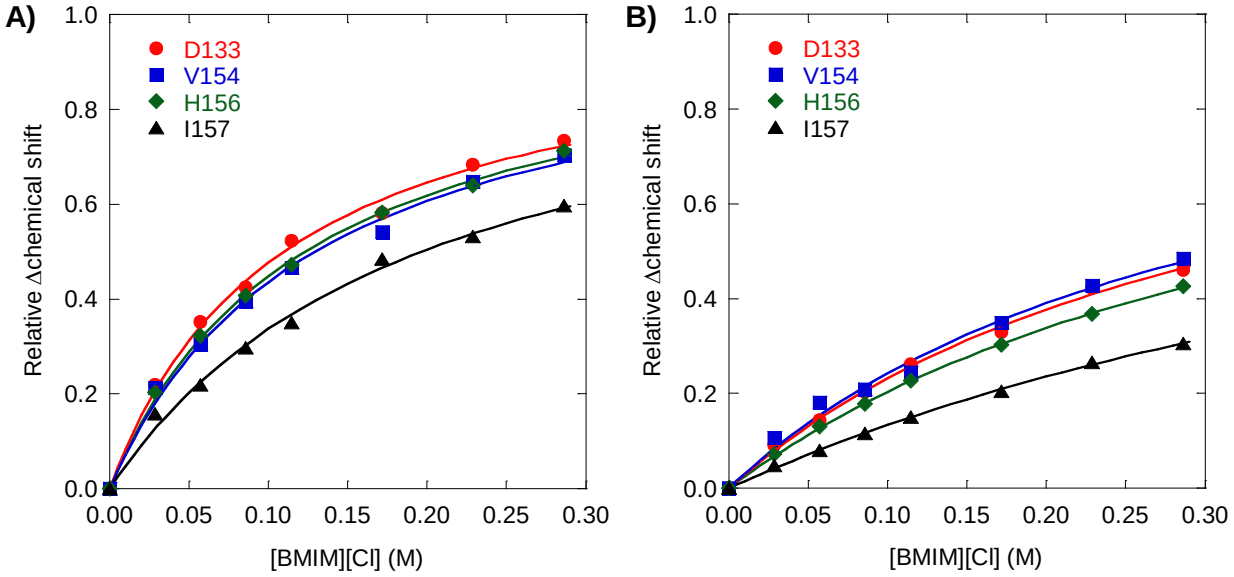

Figure 7.6. Dependence of chemical shift perturbations on [BMIM][Cl] concentration for residues D133 (●), V154 (■), H156 (♦), and I157 (▲) in (A) wild-type and (B) G158E lipA. All of the residues analyzed are within 10 Å of amino acid 158 and experienced a Δ chemical shift ≥ 0.05 ppm in wild-type lipA with the addition of 0.29 M (5 % v/v) [BMIM][Cl]. Curves were fit to a Langmuir isotherm model to determine the theoretical maximum shift at each site for normalization of the perturbations at each IL concentration.

7.4.4 Analysis of electrostatic surface of lipase A

The electrostatic map of the surface of lipA was analyzed to complement the use of NMR to identify surface exposed residues in lipA involved in direct ion interactions. Analysis of the electrostatic map of lipA specifically revealed two residues that point out from the enzyme

surface, which are highly-positively charged. These residues, K44 and R57, although not in the active site, may attract chloride anions to the enzyme surface, resulting in destabilization of the tertiary structure of lipA (**Figure 7.7A**). Interestingly, K44 is located in a flexible loop that is adjacent to G11 and G13, which were structurally perturbed by [BMIM][Cl] in 15N/1H HSQC analysis. It is thus plausible that the perturbation of G11 and G13 is the indirect result of attraction of chloride anions to this region of the enzyme by K44. The role of K44 in direct ion interactions with chloride was investigated by mutation of K44 to glutamic acid, which resulted in a 2.9-fold improvement in the $T_{1/2}$ of lipA in IL tolerance assays (**Figure 7.7B**). Mutation of R57, which is nearby the perturbed residues F58 and V62, had only a minimal, although still beneficial (1.2-fold improvement in $T_{1/2}$), impact on lipA stability in the presence of [BMIM][Cl].

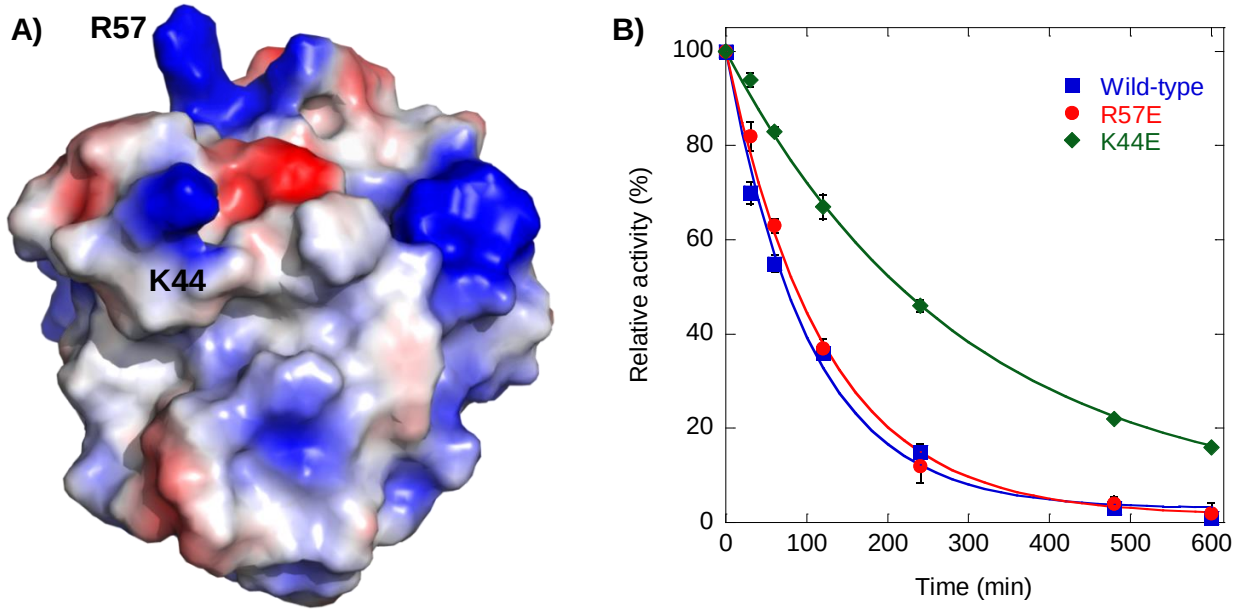

Figure 7.7. Effect of glutamic acid mutations based on analysis of surface electrostatics. (A) Electrostatic map of the surface of lipA, indicating the positions of the positive-charged K44 and R57, which are highly exposed. (B) Activity retention profiles for wild-type (■), R57E (●), and K44E (♦) lipA in 20mM MES buffer and 2.9 M (50 v/v %) [BMIM][Cl] (pH 6.5) at 35 °C.

7.4.5 Combinatorial optimization of lipase A ionic liquid tolerance

Individual single point mutations that had beneficial effects on lipA tolerance to [BMIM][Cl] were combined to optimize lipA stability for biocatalysis in IL environments. By combining mutations, a super stable lipA quadruple mutant (G158E/K44E/R57E/Y49E) was created, which was over 7-times more tolerant to [BMIM][Cl] than wild-type lipA (**Figure 7.8A** and **B**). Notably, the super stable G158E/K44E/R57E/Y49E quadruple mutant retained approximately 20 % activity after nearly 1.5 days and appeared to reach an equilibrium state. In all cases, the effect of combining beneficial mutations on lipA tolerance to [BMIM][Cl] was additive, suggesting that effect of each mutation is individual from one another. The additive nature of the mutations is perhaps not surprising given that the mutations that were combined are distant from one another in lipA and thus presumably would not interact. In optimizing the IL tolerance of lipA, the G13E and K44E mutations were not combined due to the proximity of G13 and K44 in the folded state of lipA. It was presumed that the simultaneous mutation of both residues would result in repulsion between the neighboring glutamic acids, which would have a deleterious effect on lipA stability. Although the combined mutations improved the stability of lipA in the presence of [BMIM][Cl], the melting temperatures of the quadruple mutant and wild-type lipA were nearly identical in the absence of IL, suggesting that the impact of the mutations on stability was specific to in ILs.

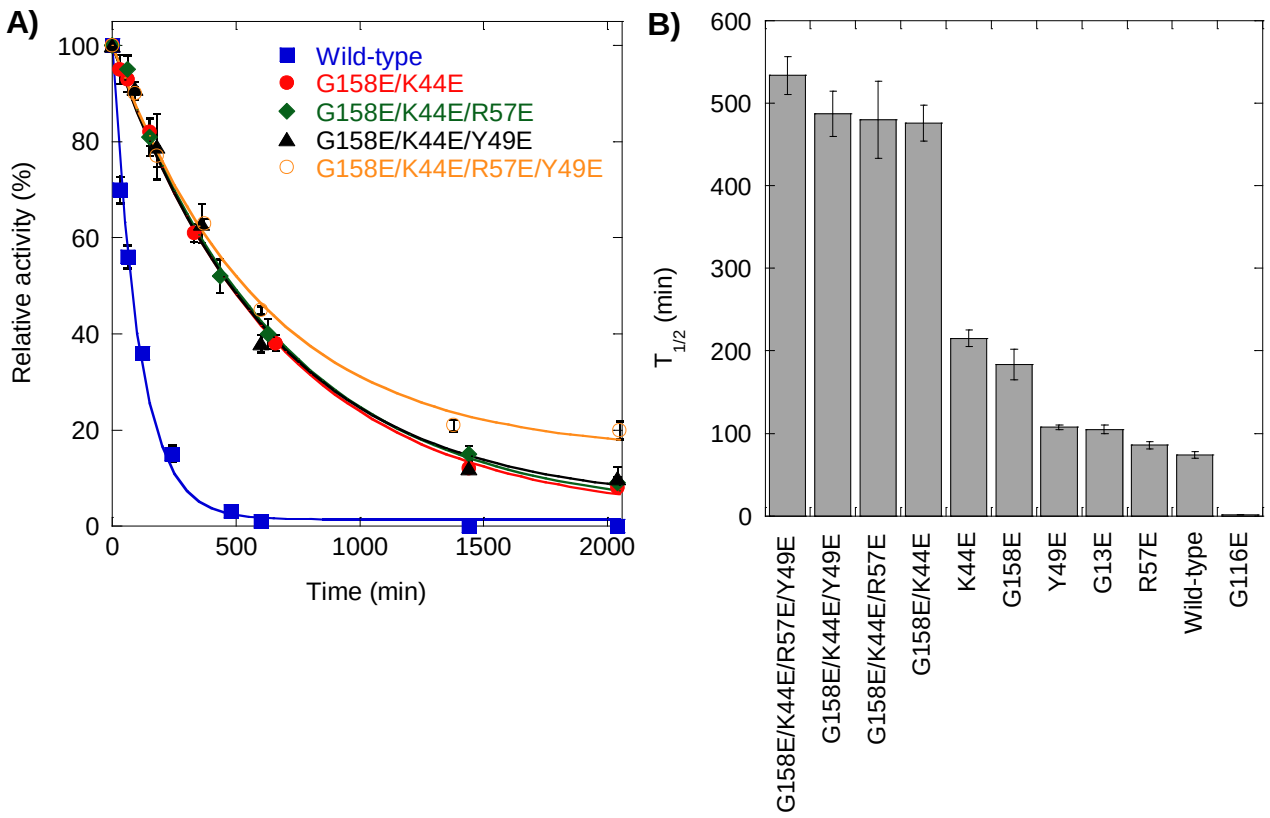

Figure 7.8. Optimization of lipA tolerance to [BMIM][Cl] by combining beneficial glutamic acid mutations. (A) Activity retention profiles for wild-type (■), G158E/K44E (●), G158E/K44E/R57E (♦), G158E/K44E/Y49E (▲), and G158E/K44E/R57E/Y49E (○) lipA in 20mM MES buffer and 2.9 M (50 v/v %) [BMIM][Cl] (pH 6.5) at 35 °C. (B) The $T_{1/2}$ values for wild-type and all lipA variants based on activity retention profiles, assuming reversible, first-order unfolding.

To underscore the improvement in stability afforded by this site-specific approach, lipA was also modified by acetylation and succinylation as a means of non-specific charge engineering. Having previously been shown to mediate direct anion interactions involving ILs in our earlier work,[15] acetylation and succinylation provide a simple route to replace the positive charge of amines with neutral and acid groups, respectively. In comparison to the super stable G158E/K44E/R57E/Y49E quadruple mutant, acetylation and succinylation resulted in only a 1.2 and 1.9-fold improvement in $T_{1/2}$, respectively, over wild-type lipase A. This drastic difference in

stabilizing effects upon site-specific versus random charge engineering highlight the importance of mediating ion interactions with functionally important residues.

7.5 Conclusions

We have engineered an IL tolerant lipA through site-directed mutagenesis of surface residues to charged amino acids, which are thought to mediate direct ion interactions with the solvent. Mutation of surface residues to glutamic acid in structurally perturbed regions of lipA, including near the active site, improved lipA tolerance to [BMIM][Cl] by as much as 2.5-fold. Substitution of glutamic acid was found to have a large effect on lipA stability upon mutation of, in particular, G158, which is located within a hydrophobic region near the active site of lipA. This effect, which correlated with the retention of active site structure, was likely the result of the inhibition of hydrophobic interactions with the [BMIM] cation. However, the electrostatic map also indicates a slight positive dipole where the [Cl] can potentially bind. Tolerance of lipA to [BMIM][Cl] was also significantly enhanced via similar mutation of positively-charged surface residues (i.e., K44) that may attract chloride ions to glutamic acid. When combined, the effects of beneficial mutations were additive, resulting in a super stable lipA quadruple mutant (G158E/K44E/R57E/Y49E), which had a 7-fold improvement in stability relative to wild-type lipA. These results ultimately shed light on the effect of direct ion interactions on enzyme stability in ILs and the impact of mediating these interactions site-specifically via charge engineering. The combination of NMR and charge engineering to site-specifically visualize and mediate direct ion interactions represents a powerful approach to improve enzyme stability to ILs.

7.6 References

3. Kaftzik, N., P. Wasserscheid, and U. Kragl, *Use of ionic liquids to increase the yield and enzyme stability in the beta-galactosidase catalysed synthesis of N-acetyllactosamine.* Organic Process Research & Development, 2002. **6**(4): p. 553-557.
13. Nordwald, E.M., et al., *Charge Engineering of Cellulases Improves Ionic Liquid Tolerance and Reduces Lignin Inhibition.* Biotechnology and Bioengineering, 2014. **111**(8): p. 1541-1549.
14. Nordwald, E.M. and J.L. Kaar, *Stabilization of Enzymes in Ionic Liquids Via Modification of Enzyme Charge.* Biotechnology and Bioengineering, 2013. **110**(9): p. 2352-2360.
15. Nordwald, E.M. and J.L. Kaar, *Mediating Electrostatic Binding of 1-Butyl-3-methylimidazolium Chloride to Enzyme Surfaces Improves Conformational Stability.* Journal of Physical Chemistry B, 2013. **117**(30): p. 8977-8986.
19. van Rantwijk, F. and R.A. Sheldon, *Biocatalysis in ionic liquids.* Chemical Reviews, 2007. **107**(6): p. 2757-2785.
22. Galonde, N., et al., *Use of ionic liquids for biocatalytic synthesis of sugar derivatives.* Journal of Chemical Technology and Biotechnology, 2012. **87**(4): p. 451-471.
24. Ha, S.H., et al., *Lipase-catalyzed biodiesel production from soybean oil in ionic liquids.* Enzyme and Microbial Technology, 2007. **41**(4): p. 480-483.
33. Bose, S., C.A. Barnes, and J.W. Petrich, *Enhanced stability and activity of cellulase in an ionic liquid and the effect of pretreatment on cellulose hydrolysis.* Biotechnology and Bioengineering, 2012. **109**(2): p. 434-443.
36. Li, C.L., et al., *Comparison of dilute acid and ionic liquid pretreatment of switchgrass: Biomass recalcitrance, delignification and enzymatic saccharification.* Bioresource Technology, 2010. **101**(13): p. 4900-4906.
50. Tee, K.L., et al., *Ionic liquid effects on the activity of monooxygenase P450BM-3.* Green Chemistry, 2008. **10**(1): p. 117-123.
51. Liu, H.F., et al., *Directed laccase evolution for improved ionic liquid resistance.* Green Chemistry, 2013. **15**(5): p. 1348-1355.
52. Park, S. and R.J. Kazlauskas, *Biocatalysis in ionic liquids - advantages beyond green technology.* Current Opinion in Biotechnology, 2003. **14**(4): p. 432-437.
57. Zhang, K.P., et al., *Penicillium expansum lipase-catalyzed production of biodiesel in ionic liquids.* Bioresource Technology, 2011. **102**(3): p. 2767-2772.
68. Baker, G.A. and W.T. Heller, *Small-angle neutron scattering studies of model protein denaturation in aqueous solutions of the ionic liquid 1-butyl-3-methylimidazolium chloride.* Chemical Engineering Journal, 2009. **147**(1): p. 6-12.
69. Baker, S.N., et al., *Fluorescence energy transfer efficiency in labeled yeast cytochrome c: a rapid screen for ion biocompatibility in aqueous ionic liquids.* Physical Chemistry Chemical Physics, 2011. **13**(9): p. 3642-3644.
70. Heller, W.T., et al., *Characterization of the Influence of the Ionic Liquid 1-Butyl-3-methylimidazolium Chloride on the Structure and Thermal Stability of Green Fluorescent Protein.* Journal of Physical Chemistry B, 2010. **114**(43): p. 13866-13871.
71. Kaar, J.L., et al., *Impact of ionic liquid physical properties on lipase activity and stability.* Journal of the American Chemical Society, 2003. **125**(14): p. 4125-4131.
72. Nakashima, K., et al., *Comb-shaped poly(ethylene glycol)-modified subtilisin Carlsberg is soluble and highly active in ionic liquids.* Chem Commun, 2005. **34**(34): p. 4297-4299.

73. Persson, M. and U.T. Bornscheuer, *Increased stability of an esterase from Bacillus stearothermophilus in ionic liquids as compared to organic solvents.* J Mol Catal B: Enzym, 2003. **22**(1-2): p. 21-27.
74. Schofer, S.H., et al., *Enzyme catalysis in ionic liquids: lipase catalysed kinetic resolution of 1-phenylethanol with improved enantioselectivity.* Chem Commun, 2001. **5**(5): p. 425-426.
75. Toral, A.R., et al., *Cross-linked Candida antarctica lipase B is active in denaturing ionic liquids.* Enzyme Microb Technol, 2007. **40**(5): p. 1095-1099.
76. Vafiadi, C., et al., *Feruloyl esterase-catalysed synthesis of glycerol sinapate using ionic liquids mixtures.* J Biotechnol, 2009. **139**(1): p. 124-129.
77. van Rantwijk, F., F. Secundo, and R.A. Sheldon, *Structure and activity of Candida antarctica lipase B in ionic liquids.* Green Chem, 2006. **8**(3): p. 282-286.
78. Zhao, H., C.L. Jones, and J.V. Cowins, *Lipase dissolution and stabilization in ether-functionalized ionic liquids.* Green Chem, 2009. **11**(8): p. 1128-1138.
138. Constantinescu, D., H. Weingartner, and C. Herrmann, *Protein denaturation by ionic liquids and the Hofmeister series: A case study of aqueous solutions of ribonuclease A.* Angewandte Chemie-International Edition, 2007. **46**(46): p. 8887-8889.
175. Figueiredo, A.M., et al., *Protein destabilisation in ionic liquids: the role of preferential interactions in denaturation.* Physical Chemistry Chemical Physics, 2013. **15**(45): p. 19632-19643.
240. Adlercreutz, P., *Immobilisation and application of lipases in organic media.* Chem Soc Rev, 2013. **42**(15): p. 6406-6436.
241. Nagarajan, S., *New tools for exploring "old friends-microbial lipases".* Appl Biochem Biotechnol, 2012. **168**(5): p. 1163-1196.
242. Stergiou, P.Y., et al., *Advances in lipase-catalyzed esterification reactions.* Biotechnol Adv, 2013. **31**(8): p. 1846-1859.
243. Lehmann, C., et al., *Ionic liquid and deep eutectic solvent-activated CelA2 variants generated by directed evolution.* Appl Microbiol Biotechnol, 2014. **98**(12): p. 5775-5785.
244. Chen, Z.W., et al., *Improved Activity of a Thermophilic Cellulase, Cel5A, from Thermotoga maritima on Ionic Liquid Pretreated Switchgrass.* Plos One, 2013. **8**(11).
245. Augustyniak, W., et al., *Biophysical characterization of mutants of Bacillus subtilis lipase evolved for thermostability: Factors contributing to increased activity retention.* Protein Science, 2012. **21**(4): p. 487-497.
246. Farmer, B.T., *Localizing the NADP(+) binding site on the MurB enzyme by NMR.* Nature Structural Biology, 1996. **3**(12): p. 995-997.
247. Williamson, M.P., *Using chemical shift perturbation to characterise ligand binding.* Progress in Nuclear Magnetic Resonance Spectroscopy, 2013. **73**: p. 1-16.
248. Byerly, D.W., C.A. McElroy, and M.P. Foster, *Mapping the surface of Escherichia coli peptide deformylase by NMR with organic solvents.* Protein Sci, 2002. **11**(7): p. 1850-1853.
249. McLachlan, G.D., et al., *High-resolution NMR characterization of a spider-silk mimetic composed of 15 tandem repeats and a CRGD motif.* Protein Sci, 2009. **18**(1): p. 206-216.
250. Kamal, M.Z., et al., *Lipase in aqueous-polar organic solvents: activity, structure, and stability.* Protein Sci, 2013. **22**(7): p. 904-915.

Chapter 8 Crystallographic investigation of imidazolium ionic liquid unfolding and stabilization mechanisms

This chapter will be submitted to Angewandte Chemie International Edition

Imidazolium based ionic liquids are a class of salts with unique properties containing the potential to open up additional biocatalytic reactions (production of biofuels,[24, 33, 36] pharmaceuticals,[50]and fine chemicals[3, 22]). However, lack of understanding of IL-enzyme effects limits these potential reactions. Much data suggests many ILs, in particular 1-butyl-3-methylimidazolium chloride ([BMIM][Cl]), denatures enzymes.[68, 69] Work by our lab, and others, has proposed that this is related to a binding mechanism.[15, 175] Moreover, we have recently shown via 2D HSQC NMR that binding sites can be visualized via chemical shift perturbations.[12] Mitigating these perturbations with mutagenesis correlates with being able to stabilize lipase against [BMIM][Cl] induced inactivation. Four mutations (K44E/Y49E/R57E/G158E) were made that additively contributed to a more than 7 fold stabilization. Of note, K44E and R57E were not made based on [BMIM][Cl] induced NMR-perturbations but on a hypothesis that negative amino acids could non-specifically exclude the IL. In an effort to better understand the perturbations and stabilization mechanism of the mutations, we have crystallized the wild-type and mutant lipase A (lipA) from *Bacillus subtilis* and then soaked the crystals in varying concentrations of [BMIM][Cl]. We are able to see differences in binding at mutation sites 49 and 158 between the wild-type and mutant enzyme. Moreover, we are able to see local ion binding throughout both the mutant and wild-type lipA giving immense information on the denaturation mechanism of imidazolium ionic liquids. This knowledge will enhance the ability to rationally design proteins for imidazolium IL tolerance.

Upon examining the structures, it was found there was no difference between the wild-type and mutant lipase. Also, as the IL soaking concentration increased, (0, 5, 10, 20 % v/v [BMIM][Cl]) no noticeable local or gross structural perturbations were observed (**Figure 8.1**). At 20 % v/v [BMIM][Cl], structural changes may not be observed as a result of stabilizing crystal contacts. Also, lipase is not observed to lose activity over time until concentrations >30 % v/v [BMIM][Cl] (albeit the activity measurements were performed in different buffer conditions). Notably, at 30 % v/v the crystals for wild-type lipase dissolved, suggesting strong enzyme-[BMIM][Cl] interactions. Interestingly, although no structural perturbations were observed, the space-group of the wild-type lipase changed from $P2_12_12_1$ to $P432_12$ at 20 % IL. As many of the [BMIM] molecules are binding at contacts between lipase, perhaps this is not so surprising. The resolution at the 20 % v/v soaking concentration did also drop significantly for the wild-type lipA (1.9 Å) while the IL did not change the space group or largely affect the resolution of mutant lipA.

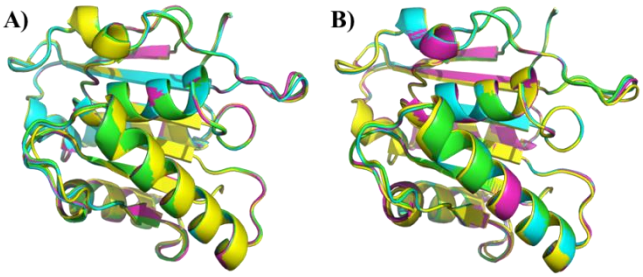

Figure 8.1. (A) Wild-type and (B) mutant lipA with 0 (green), 5 (teal), 10 (magenta), and 20 (yellow) % v/v [BMIM][Cl] soaked into the crystals.

The solvent molecules resolved in wild-type and mutant lipA are reported in **Table 8-1**. Of note, there were two lipA molecules in the asymmetric unit for wild-type lipA but only one for mutant lipA. While there are 7 unique [BMIM] molecules resolved in wild-type lipase, some are ambiguous as to whether the binding was a result of crystal-crystal contacts (i.e. binding

between molecules) vs binding to a specific site on lipase. Resolution differences also make it difficult to directly compare the number of solvent molecules *resolved* between the wild-type and mutant lipase. Inherently, lower resolution, as in the case of wild-type lipase (1.5 – 2.0 Å) compared with mutant lipase (1.3 – 1.4 Å) will result in less solvent molecules confidently resolved. Nonetheless, it is interesting to see several [BMIM] molecules resolved binding to both forms of lipA despite the lack of structural changes observed.

Table 8-1. Solvent molecules resolved in wild-type and mutant lipA as a function of soaking condition.

Molecule[a]	H_2O	[Cl]	[BMIM]
Wild-type			
0%	476	0	0
5%	502	1	2
10%	397	1	3
20%	233	4	7
Mutant			
0%	264	0	0
5%	250	1	1
10%	357	1	1
20%	239	2	5

The aim of the mutations was to stabilize the enzyme based on mitigating preferential binding. Activity measurements show a clear stabilization of the mutant over the wild-type enzyme. NMR experiments further showed that chemical shift perturbations surrounding residue 158 (glycine in wild-type, glutamic acid in the mutant) had smaller chemical shift perturbations, indicating decreased [BMIM][Cl] binding in the area. Surrounding residue G158 there was a

tightly bound [Cl] and a [BMIM] nearby under the 20 % v/v soaking condition (**Figure 8.2A**). Meanwhile, at E49 in the mutant enzyme, no [BMIM] was resolved and the [Cl] was resolved further way from the mutation site (**Figure 8.2B**). Perhaps the negatively charged amino acid electrostatically repels the [Cl]. Moreover, the charged glutamic acid may reduce the hydrophobicity of the area resulting in decreased propensity of [BMIM] to bind through hydrophobic interactions. Thus, the crystallography data is very consistent with the previously measured NMR HSQC data. Specifically, it was observed that G158 and surrounding residues had large perturbations in chemical shift upon addition of [BMIM][Cl]. Crystallographic resolution of [BMIM] and [Cl] molecules in the vicinity support the perturbations being related to specific IL binding. Moreover, mutation at G158 to reduce the binding resulted in decreased NMR perturbations and decreased binding by crystallographic resolution of [BMIM] and [Cl] molecules. Importantly, the resolution of the mutant lipA was higher than wild-type, meaning lack of IL molecules is not an artifact of not having enough resolution.

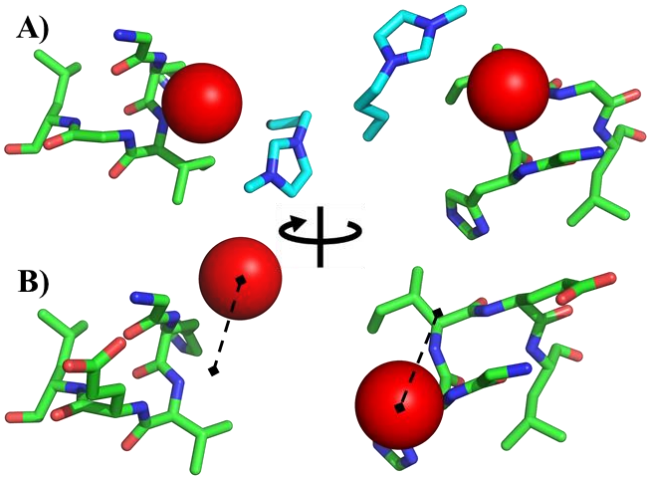

Figure 8.2. (A) G158 (wild-type) and (B) E158 (mutant) with 20 % v/v [BMIM][Cl] soaked into the structures showing two views. A [BMIM] (teal) is resolved at G158 and a [Cl] (red sphere) nearby. At E158 there are no [BMIM]s and the [Cl] is resolved further away, shown by the dashed line.

One of the clearest crystallographic depictions of reduced binding was at residue Y49 (E49 in the mutant). **Figure 8.3A**, shows a [BMIM] molecule, modelled in two orientations, binding at Y49 in the wild-type enzyme, and perhaps hydrogen bonding at a nearby asparagine. Meanwhile, in the mutant enzyme, there were no [BMIM] molecules resolved at residue E49 (**Figure 8.3B**). This suggests that the stacking interaction of the cation is more favorable than an electrostatic interaction of an acid with the dispersed positive charge at the imidazolium head. A reason for stabilization based on reducing binding is because binding is even more reduced in the denatured state. For example, at Y49, the other side of the residue is buried. Perhaps in the unfolded state, two [BMIM]s (either side) may bind to the residue. Mutating this residue may, therefore reduce one [BMIM] bound to the native state, but two in the unfolded state, resulting in relative stabilization. At G158, there are many surrounding hydrophobic residues, in primary sequence, that could tightly bind to the butyl tail in [BMIM] upon unfolding. Mutation at residue 158 to a charged amino acid may disrupt this hydrophobic binding, decreasing denatured state binding even more largely than the apparent decrease in binding shown in **Figure 8.2**.

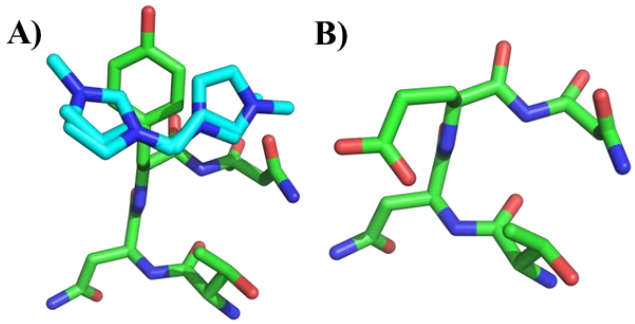

Figure 8.3. (A) Y49 (wild-type) and (B) E49 (mutant) with 20 % v/v [BMIM][Cl] soaked into the structures. A [BMIM] (teal) is resolved at Y49 but not at E49.

The other two mutation sites, K44E and R57E, were made in hopes of non-specifically excluding the IL [BMIM][Cl]. That is, it was hoped that a negative charge would repel the [Cl] more than it attracts the [BMIM] molecules, resulting in a total salt exclusion, as it is known that

salt-pair binding defines the overall thermodynamic effect on proteins.[127] This is akin to non-specifically excluded osmolytes such as sucrose and trehalose stabilizing proteins. Crystallographic resolution of wild-type lipA soaked in [BMIM][Cl] found no [BMIM] molecules bound at either K44 or R57, as expected. It is possible that one of the modelled water molecules around these residues is actually a [Cl], but could not be distinguished based on the electron density. The [Cl]s that were chosen had electron density too high to be a water, even at complete occupancy and low B-factor. There may have been missed [Cl]s that did not produce high enough signal to suggest it cannot be a water molecule. The number of water molecules surrounding these residues were also analyzed, but were too convoluted by resolution changes to be able to accurately draw conclusions.

There were some commonalities of IL binding between the mutant and wild-type enzyme, which helps elucidate the binding mechanism of [BMIM][Cl] to enzymes. Shown in **Figure 8.4A**, is a [BMIM] bound in the hydrophobic active site of lipA, evolved to bind fatty substrates. Under all soaking concentrations in the wild-type enzyme, a [BMIM] was resolved in the active site, suggesting that this hydrophobic interaction is quite relevant. There were also many cations bound in the active site of the mutant, although not under all soaking conditions. Given the propensity of the cation to bind to hydrophobic regions, it is reasonable to think that imidazolium cations, particularly with long alkyl side chains, may reduce the hydrophobic effect enough to cause enzyme unfolding. It has been found by Constinanteau et al. that increasing the side-chain length of imidazolium ILs results in a more destabilizing IL based on T_m measurements. In the unfolded state, more hydrophobic side-chains will be exposed, allowing for stronger [BMIM]-enzyme binding, potentially driving unfolding.

Figure 8.4B shows a cation-π stacking interaction of [BMIM] with a tryptophan. At this location, there seems to be no significant interaction of [BMIM] with the protein aside from this stacking interaction (i.e. hydrophobic interactions with the butyl tail), as both these residues are quite exposed. Interestingly, in the 0 % v/v soaked structure (yellow), His 3 appears to be stacking with this Trp. However, the [BMIM] cation is able to out-compete the residue for stacking with Trp. Based on His-Trp stacking interactions in nature, cation-π interactions of imidazoliums from His are thought to be ~3-4X stronger than π-π interactions in the neutral, imidazole, form.[155, 167-169] Moreover, Fersht and co-workers[171] have found that a particular Trp-imidazolium (His) interaction contributed 1.4 kCal/mol to protein stability, ~14% of the total stability of most proteins for a single interaction. Accordingly, as [BMIM] has a permanent positive charge on the imidazolium moiety, perhaps it can form stronger stacking interactions than neutrally charged histidines.

Figure 8.4C shows, perhaps, the most tightly bound [BMIM] molecules resolved in the entire study, based on clarity of electron density at only 5 % v/v [BMIM][Cl]. Shown in the supplemental is unbiased (before modelling in the [BMIM]) electron density surrounding this [BMIM], even the hole in the imidazolium moiety is resolved. Here, hydrophobic binding of the butyl tail surrounding a valine and phenylalanine is combined with a cation-π stacking interaction at the head of the imidazolium moiety. It is interesting to note that rotation of the [BMIM] 90° about the first carbon of the butyl tail would lead to an appropriate distance for a salt-bridge between the positive imidazolium head and glutamic acid 65. However, no electron density is resolved in this orientation; it seems the [BMIM] prefers a stacking interaction instead.

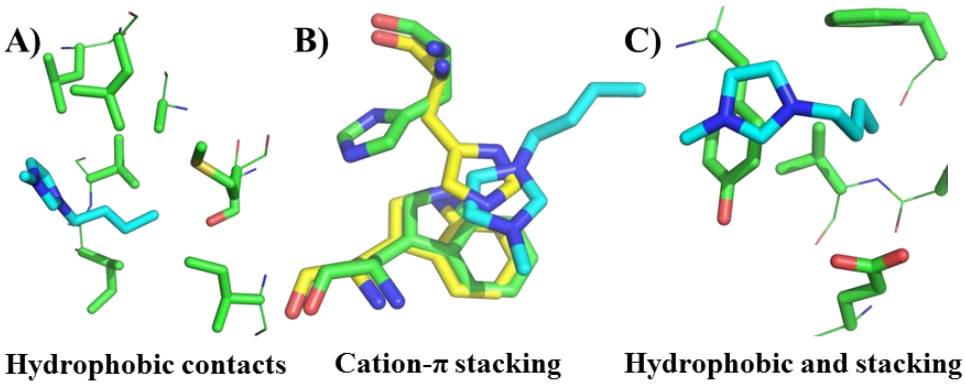

Figure 8.4. The specific binding sites of [BMIM] with lipase. (A) hydrophobic residues such as in the binding pocket of lipA strongly bind the butyl chain of [BMIM]. Elements are colored green for carbon, blue for nitrogen, red for oxygen, and gold for sulfur. The carbons of [BMIM] are teal. Contacting residues are 2 leucines, 2 isoleucines, 1 valine, 1 alanine, and a methionine. (B) The 0 % v/v [BMIM][Cl] soaked structure (yellow carbons) shows His3 stacking with Trp31, however, upon soaking in 20 % v/v [BMIM][Cl], a [BMIM] outcompetes His3 for the stacking interaction. (C) The most clearly resolved [BMIM] involved both hydrophobic contacts and a stacking interaction. It is interesting the stacking interaction takes precedence over salt-bridging with glutamic acid.

The overall contacts made with amino acids and all the [BMIM] molecules in this study at the highest soaking concentration (20 % v/v) are depicted in **Figure 8.5**. The butyl tail participates strongly in contacts with hydrophobic and aromatic (which are also hydrophobic) amino acids, then there are very few polar and positively charged contacts and no negatively charged contacts (**Figure 8.5A**). The [BMIM] contact with the positively charged residue is at a carbon on a lysine. Perhaps part of the butyl carbon chain of lysines can interact weakly with the butyl tail of [BMIM] despite the positively charged amine at the lysine end. The imidazolium head (**Figure 8.5B**), however, has mostly contacts with aromatic amino acids followed by hydrophobic amino acids. Moreover, 7 of the 12 [BMIM] molecules appear to be forming a cation-π stacking interaction. **Figure 8.5B** also shows that there are more contacts of the imidazolium head with positively charged residues than negatively charged ones. Our conclusion from this is that the electrostatic attraction or repulsion of the [BMIM] cation must be weak.

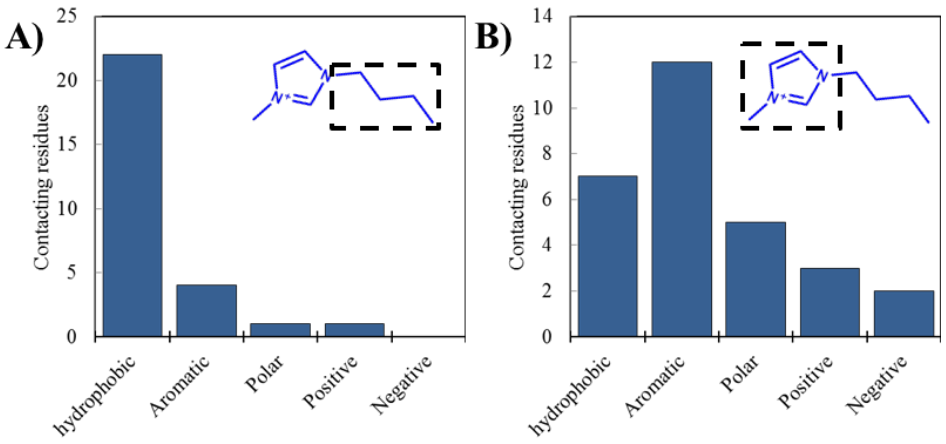

Figure 8.5. The contacting amino acid residue types with all the resolved [BMIM] molecules at the 20 % v/v [BMIM][Cl] soaking condition for the (A) butyl side chain and (B) imidazolium head.

Other mechanisms of IL binding may be based on ion pair binding. There are instances where the [Cl] anion is found nearby a [BMIM] molecule in a somewhat hydrophobic region. Conceivably, in a region with no acid groups, if there is a [BMIM] molecule bound, the counter ion has a greater propensity to bind nearby to maintain local electroneutrality. That is, bound cations may recruit anions to the surface. Therefore, mediating total salt binding to folded and unfolded states is important towards enzyme stabilization.

The goal of this manuscript was to further understand the relationship between [BMIM][Cl] and enzyme binding in the context of stabilizing mechanisms. Wild-type and an IL-stable mutant (G158E/Y49E/K44E/R57E) lipA were crystallized and soaked in [BMIM][Cl]. There was a bound [BMIM] near Y49 which was not present for the mutant enzyme at E49. Moreover, near G158, there was a [Cl] and [BMIM] resolved while no [BMIM] was resolved at E158 and the resolved [Cl] was further away. This is consistent with previous NMR data showing reduced chemical shift perturbations surrounding residue 158 for the mutant enzyme compared to the wild-type enzyme. The other two mutation sites, which were mutated based on a

hypothesis of non-specific IL exclusion, did not resolve [BMIM] or [Cl] ions. To maintain electroneutrality in the protein domain, counter ions must also bind, so mediating anion binding may be an effective tool for stabilization despite [BMIM] likely being the main cause for denaturation. Given the low affinity of [BMIM] for charged groups, and that [Cl] is a purely electrostatic atom, negative charges may decrease the total [BMIM][Cl] that can bind locally. Namely, a glutamic acid may reduce the affinity of the [Cl] for the protein more than any slight increases (if any) in affinity the [BMIM] molecule gains. This non-specific exclusion mechanism may be similar to other non-specifically excluded osmolytes, such as certain sugars.

High resolution structures (1.2-1.9 Å) show several binding modes of [BMIM] with enzymes. [BMIM] appears to have a preference for aromatic and hydrophobic amino acids, both of which should become more exposed upon unfolding. Meanwhile, there were no ions resolved at negative amino acids. Perhaps at residues such as Y49, [BMIM] can cation-π stack from one side of the molecule in the native state but two in the unfolded state. Therefore, eliminating this binding site results in an overall stabilization. Similarly, at G158 there are many hydrophobic residues nearby in primary sequence which could bind more strongly upon unfolding. Mutation at G158 to an acid group may disrupt the hydrophobic binding.

8.1 Experimental section

8.1.1 Materials

Genomic DNA from *Bacillus subtilis* containing the lipA gene was donated by Robert Batey (University of Colorado, Boulder). The QuickChange lightning mutagenesis kit for site-directed mutation of lipA was purchased from Agilent (Santa Clara, CA). All other chemicals, including [BMIM][Cl] (> 98%), were purchased from Sigma Aldrich (St. Louis, MO) and used as supplied.

8.1.2 Enzyme expression and purification

Following Nordwald et al.,[12] both wild-type and mutant lipA with no tag were grown in Luria broth at 37 °C and 200 rpm with 100 mg/L ampicillin. Expression of lipA was induced via the addition of 1 mM isopropyl β-D-1-thiogalactopyranoside at 37 °C. After 1.5 days, soluble lipA that was secreted during expression was collected and purified over a phenyl sepharose hydrophobic exchange column using 500 mM NaCl with 50 mM ammonium sulfate as the loading buffer and deionized water as the elution buffer. The wild-type protein formed aggregates on the column that had to be bumped off with 6M GnCl. Next, the protein was exchanged into 5 mM $NaPO_4$ buffer, pH 7.0 (refolded in the case of wild-type lipase) and flowed over an anion exchange column. Neither wild-type nor mutant lipA sticks, therefore the flow-through is collected and is of higher purity. Next, lipA was purified over a cation exchange column, loaded with the same 5 mM $NaPO_4$ buffer. The mutant lipase does not stick to this column either, but the wild-type does and can be eluted with 500 mM NaCl and 10 mM $NaPO_4$ buffer, pH 7.0. The resulting procedure typically yielded 30 mg of > 99 % pure lipase by SDS gel analysis per liter of culture.

8.1.3 Crystallography

Wild-type and mutant lipA were crystallized as described previously[230, 251] using the hanging drop method at room temperature with a 1 ml reservoir solution containing 0.1M ethanolamine, 20mM Na_2SO_4, pH 9.5 with 35 wt/v % PEG 3350 and 10 mM $ZnCl_2$. The enzymes were dialyzed into 0.1M ethanolamine and 20mM 20mM Na_2SO_4, pH 9.5, titrated with sulfuric acid. Then the enzymes were concentrated to 10 mg/ml, and 3 µL of enzyme solution was mixed with 3 µL of reservoir solution. Crystals appeared within 24 hours.

Crystals were soaked in mother liquor (but no $ZnCl_2$) containing 0, 5, 10, or 20 % v/v [BMIM][Cl] for 5-10 mins followed by freezing in liquid nitrogen. Data collection was performed on either a Rigaku R-axis IV++ image plate system (wild-type buffer condition) or on synchrotron beam line 8.2.2 at Lawrence Berkeley Laboratory Advanced Light Source (ALS). Merging data for the reflections is shown in **Table 8-2**.

Table 8-2. Merging statistics. Note that all space-group and Laue group probabilities > 0.91. Space group was primitive tetragonal $P4_32_12$ for the WT 20% sample. All other samples were primitive orthorhombic $P2_12_12_1$. Parenthesis indicates data in the highest resolution shell.

	Wild-type				Mutant			
	0%	**5%**	**10%**	**20%**	**0%**	**5%**	**10%**	**20%**
Bin (Å)	30.3-1.63 (1.72-1.63)	39.4-1.49 (1.57-1.49)	41.4-1.75 (1.84-1.75)	47.9-1.90 (1.93-1.90)	27.9-1.29 (1.36-1.29)	28.0-1.40 (1.48-1.40)	27.9-1.24 (1.31-1.24)	31.7-1.29 (1.36-1.29)
R_{meas}	0.058 (0.265)	0.053 (0.167)	0.079 (0.182)	0.122 (0.000)	0.048 (0.194)	0.075 (0.126)	0.054 (0.072)	0.056 (0.088)
R_{merge}	0.046 (0.205)	0.040 (0.126)	0.063 (0.145)	0.063 (0.568)	0.040 (0.153)	0.070 (0.119)	0.042 (0.056)	0.030 (0.068)
I/σ	15.2 (4.7)	16.9 (7.2)	12.5 (6.3)	14.5 (1.0)	13.5 (5.4)	24.8 (17.4)	18.2 (12.5)	15.7 (8.9)
%Complete	99.7 (99.7)	99.4 (96.9)	99.4 (98.7)	100.0 (100.0)	99.3 (99.5)	99.1 (100.0)	92.1 (98.5)	96.5 (97.2)
a (Å)	39.25	39.44	39.27	74.9	48.09	48.14	48.21	47.72
b (Å)	82.62	83.16	82.78	74.9	55.69	55.9	55.95	56.81
c (Å)	95.12	95.82	95.5	112.35	64.56	64.41	64.42	64.09
Observations	149,193 (20,700)	183,074 (24,632)	32,167 (4,608)	25,866 (1,241)	144,094 (19,740)	455,416 (69,316)	154,296 (23,091)	144,653 (20,377)

The data were indexed and integrated using imosflm[252] and the structure was determined by molecular replacement using Phenix.[253] Positional and individual B-factor (isotropic) refinement was carried out initially. Manual real-space refinement of the data was performed followed by refinement in Phenix and automatic water picking. Next ligand replacement was performed and accepted only if the R_{free} decreased as a result of adding the ligand and removing any water molecules placed in the density by Phenix. Note that the [BMIM] near His3 in the 20 % [BMIM][Cl] soak of the mutant lipA was removed and an alternate conformation of His3 was placed there instead. This, however, caused a significant increase in the R_{free} and was therefore

rejected. Nearly all the density around the [BMIM] molecules seemed unambiguous. In some cases, the hole in the imidazolium ring could even be resolved.

The chloride molecules were picked by difference peak analysis of the model vs. the data. Typically a water molecule with signal too high, even at complete occupancy and low B-factor, was replaced by a [Cl], resulting in a decrease in R_{free}. The final step was anisotropic B-factor refinement on the solvent and protein structure for crystals with resolution ≤ 1.40 Å and just on the protein structure for crystals with max resolution ≤ 1.75 Å but ≥ 1.40 Å. This was successful, particularly for higher resolution data, as determined by significant decreases in the R_{free}. Final refinement statistics are reported in **Table 8-3**.

Table 8-3. Final refinement parameters.

	Wild-type				Mutant			
	0%	**5%**	**10%**	**20%**	**0%**	**5%**	**10%**	**20%**
R_{work}	0.139	0.126	0.128	0.191	0.125	0.119	0.109	0.121
R_{free}	0.175	0.156	0.173	0.229	0.143	0.148	0.135	0.138
rms angle (°)	1.26	1.20	1.25	1.17	1.22	1.23	1.29	1.30
rms bonds (Å)	0.010	0.009	0.010	0.011	0.009	0.010	0.009	0.008
Reflections[1]	37,229 (2,000)	50,537 (2,000)	30,129 (2,000)	23,817 (2,000)	42,064 (2,000)	32,544 (2,000)	43,807 (2,000)	40,464 (2,000)

[1]Working set (test set)

8.1.4 Model structure analysis

Pymol and Coot were used to analyze and visualize binding sites of the ionic liquid to lipase. Note that for all situations, all adjacent symmetry molecules to the binding sites were considered.

8.2 Supplemental figures

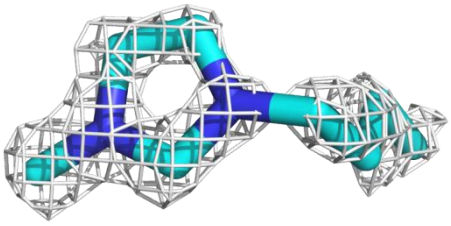

Figure 8.6. Unbiased electron density maps for [BMIM] contoured at 1.0 RMSD.

8.3 References

3. Kaftzik, N., P. Wasserscheid, and U. Kragl, *Use of ionic liquids to increase the yield and enzyme stability in the beta-galactosidase catalysed synthesis of N-acetyllactosamine.* Organic Process Research & Development, 2002. **6**(4): p. 553-557.
12. Nordwald, E.M., G.S. Armstrong, and J.L. Kaar, *NMR-Guided Rational Engineering of an Ionic-Liquid-Tolerant Lipase.* Acs Catalysis, 2014. **4**(11): p. 4057-4064.
15. Nordwald, E.M. and J.L. Kaar, *Mediating Electrostatic Binding of 1-Butyl-3-methylimidazolium Chloride to Enzyme Surfaces Improves Conformational Stability.* Journal of Physical Chemistry B, 2013. **117**(30): p. 8977-8986.
22. Galonde, N., et al., *Use of ionic liquids for biocatalytic synthesis of sugar derivatives.* Journal of Chemical Technology and Biotechnology, 2012. **87**(4): p. 451-471.
24. Ha, S.H., et al., *Lipase-catalyzed biodiesel production from soybean oil in ionic liquids.* Enzyme and Microbial Technology, 2007. **41**(4): p. 480-483.
33. Bose, S., C.A. Barnes, and J.W. Petrich, *Enhanced stability and activity of cellulase in an ionic liquid and the effect of pretreatment on cellulose hydrolysis.* Biotechnology and Bioengineering, 2012. **109**(2): p. 434-443.
36. Li, C.L., et al., *Comparison of dilute acid and ionic liquid pretreatment of switchgrass: Biomass recalcitrance, delignification and enzymatic saccharification.* Bioresource Technology, 2010. **101**(13): p. 4900-4906.
50. Tee, K.L., et al., *Ionic liquid effects on the activity of monooxygenase P450BM-3.* Green Chemistry, 2008. **10**(1): p. 117-123.
68. Baker, G.A. and W.T. Heller, *Small-angle neutron scattering studies of model protein denaturation in aqueous solutions of the ionic liquid 1-butyl-3-methylimidazolium chloride.* Chemical Engineering Journal, 2009. **147**(1): p. 6-12.
69. Baker, S.N., et al., *Fluorescence energy transfer efficiency in labeled yeast cytochrome c: a rapid screen for ion biocompatibility in aqueous ionic liquids.* Physical Chemistry Chemical Physics, 2011. **13**(9): p. 3642-3644.
127. Arakawa, T. and S.N. Timasheff, *Protein Stabilization and Destabilization by Guanidinium Salts.* Biochemistry, 1984. **23**(25): p. 5924-5929.
155. Alston, R.W., et al., *Contribution of single tryptophan residues to the fluorescence and stability of ribonuclease sea.* Biophysical Journal, 2004. **87**(6): p. 4036-4047.

167. Churchill, C.D.M. and S.D. Wetmore, *Noncovalent Interactions Involving Histidine: The Effect of Charge on pi-pi Stacking and T-Shaped Interactions with the DNA Nucleobases.* Journal of Physical Chemistry B, 2009. **113**(49): p. 16046-16058.
168. Gallivan, J.P. and D.A. Dougherty, *Cation-pi interactions in structural biology.* Proceedings of the National Academy of Sciences of the United States of America, 1999. **96**(17): p. 9459-9464.
169. Liao, S.M., et al., *The multiple roles of histidine in protein interactions.* Chemistry Central Journal, 2013. **7**.
171. Loewenthal, R., J. Sancho, and A.R. Fersht, *Histidine Aromatic Interactions in Barnase - Elevation of Histidine Pk(a) and Contribution to Protein Stability.* Journal of molecular biology, 1992. **224**(3): p. 759-770.
175. Figueiredo, A.M., et al., *Protein destabilisation in ionic liquids: the role of preferential interactions in denaturation.* Physical Chemistry Chemical Physics, 2013. **15**(45): p. 19632-19643.
230. Rajakumara, E., et al., *Crystallization and preliminary X-ray crystallographic investigations on several thermostable forms of a Bacillus subtilis lipase.* Acta Crystallographica Section D-Biological Crystallography, 2004. **60**: p. 160-162.
251. van Pouderoyen, G., et al., *The crystal structure of Bacillus subtilis lipase: A minimal alpha/beta hydrolase fold enzyme.* Journal of molecular biology, 2001. **309**(1): p. 215-226.
252. Leslie, A.G.W. and H.R. Powell, *Processing diffraction data with MOSFLM.* Evolving Methods for Macromolecular Crystallography, 2007. **245**: p. 41-51.
253. Adams, P.D., et al., *PHENIX: a comprehensive Python-based system for macromolecular structure solution.* Acta Crystallographica Section D-Biological Crystallography, 2010. **66**: p. 213-221.

Chapter 9 Possible stabilization mechanisms

The reason for the large increase in half-life of the quadruple mutant lipase over the wild-type is possibly the most interesting discussion of this thesis. Lipase is the most well-behaved, pure enzyme used in this thesis. Moreover, mutagenesis provides a homogeneous variant unlike the chemical modification approach, which has some uncertainty in modification position and homogeneity. Also, the stabilization was large enough that we may be able to make better speculations about stabilization mechanisms than comparing variants with minute differences in stability.

9.1 Generic or ionic liquid specific stabilization?

Is the mutant enzyme generally more stable than the wild-type which may translate to many extreme environments, or is this increased stability only a result of the ionic liquid environment? To test this variable, we melted wild-type and mutant lipA and found the apparent T_m's to be virtually indistinguishable (**Figure 9.1**). If anything, the mutant enzyme had a slightly lower apparent T_m. Moreover, the nature of the melting curve is exactly the same. This suggests that the dependence of stability on temperature is similar, if not the same, such that the stability at 35 °C, the activity retention assay temperature, is the same as well. The dependence of ΔG on temperature can be described by the Van 't Hoff equation.

$$\Delta G(T) = \Delta H_m \left(1 - \frac{T}{T_m}\right) - \Delta C_p \left(T_m - T + T ln\left(\frac{T}{T_m}\right)\right)$$

The change in heat capacity (ΔC_p) upon unfolding should be quite similar for the mutant as all the mutated residues are exposed, and will also be exposed in the unfolded state. Pace et al. previously performed a series of charge mutations on highly exposed residues and found that, in all cases, the ΔC_p negligibly changed, and increases or decreases in the melting temperature of each variant directly resulted in corresponding increases or decreases, respectively, of the protein's ΔG at 25 °C.[254] Also, the high degree of similarity in the unfolding curves suggests that the enthalpy is not largely perturbed either. Importantly, while the reversible two-state unfolding mechanism is not perfect as aggregates form upon melting, a portion of the lipase does refold quite nicely to have the same structure (by CD) and specific activity.

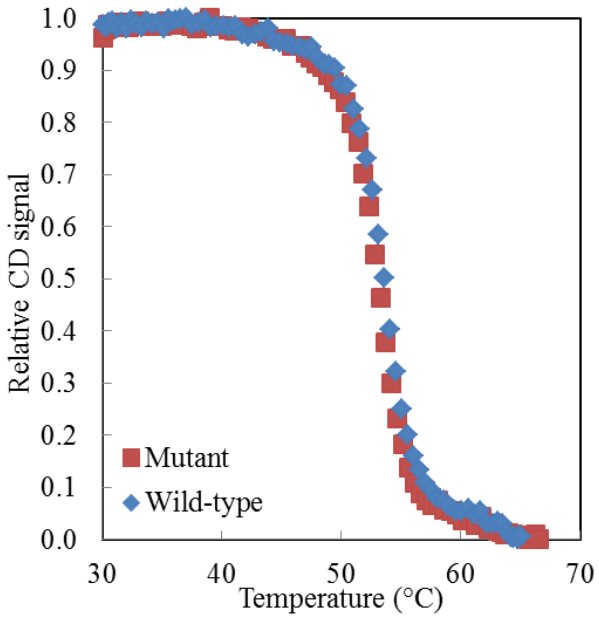

Figure 9.1. Temperature induced unfolding of wild-type and quadruple mutant lipase A. The melting temperature of the mutant lipase is marginally lower.

9.2 Is the stabilization a strictly kinetic effect, thermodynamic effect, or both?

The time for which an enzyme retains its activity is its kinetic stability. In an equilibrium unfolding experiment, the kinetic stability is impacted by the size of the activation barrier for unfolding, as well as the difference in free energy between the folded and unfolded states, or the conformational stability. **Figure 9.2** shows a reaction coordinate for the reaction N↔U, labelling the native state free energy, unfolded free energy, and activation energy. Solving the mass balance of N↔U, the relative activity can be defined as:

$$Relative\ Activity = \frac{k_2}{k_2 + k_1} + \frac{k_1}{k_2 + k_1}\exp(-(k_2 + k_1)t)$$

Where k_2 is the rate constant for refolding and k_1 is the rate constant for unfolding. The ratio of these two is related to the thermodynamic stability.

$$\Delta G = -RTln(K) = -RTln\left(\frac{k_1}{k_2}\right)$$

Of note, the relative activity model, does assume two states only, an active and inactive one which may not be a perfect assumption. By fitting the relative activity equation to the activity profiles in **Figure 9.3**, we are able to gain some insight into the roles of altering the activation barrier for unfolding (strictly kinetic effect) and changes in the thermodynamic stability. Raw inspection of the relative activity profile shows an equilibrium in inactivation at the end of the profile. This was supported by melting the proteins at 50 °C, measuring no activity, then cooling to 25 °C and watching the activity of the enzyme be regained at 40 and 50 vol % [BMIM][Cl]. Equilibrium in activity loss suggests a thermodynamic stabilization of the enzyme. This is, of course, supported by fitting the activity equation and extracting the ΔG. Interestingly, the values of k_1 between the wild-type and mutant enzyme also suggest a slight increase in the inactivation

barrier, which would provide additional kinetic stabilization aside from the thermodynamic stabilization.

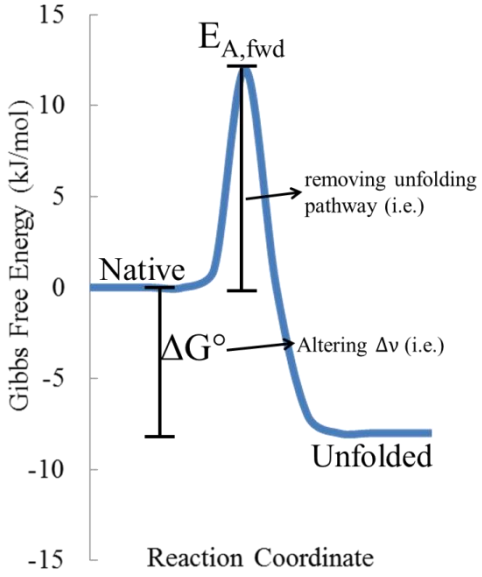

Figure 9.2. A hypothetical reaction coordinate for protein unfolding in [BMIM][Cl]. The thermodynamic stability is defined by the free energy difference between the folded and unfolded states. The activation energy barrier is the free energy difference between the folded state and transition state of enzyme unfolding.

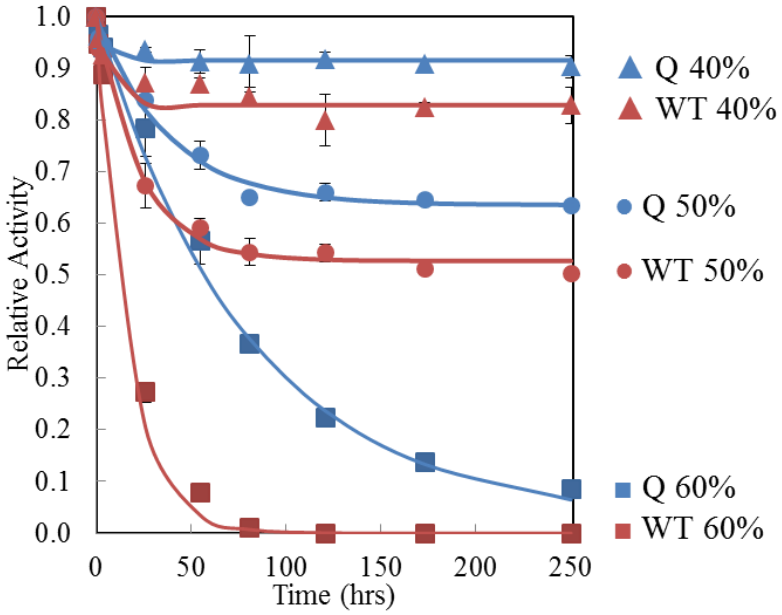

Figure 9.3. Inactivation profiles for wild-type (WT) and quadruple mutant (Q) lipase A at various concentrations of [BMIM][Cl] and 25 °C. The 50 and 40 vol % samples were melted by increasing temperature at the end of the experiment, and their activity regained by lowering the

temperature back to 25 °C, to confirm equilibrium, which is higher for the mutant enzyme than the wild-type at both 40 and 50 vol % [BMIM][Cl].

Equilibrium dialysis on the mutant and wild-type enzyme after 5 days indicates that there is vastly less binding of the mutant than the wild-type at ~55 vol % [BMIM][Cl]. Assuming equilibrium has been achieved, either the mutant has a larger amount folded, resulting in lower binding, or the unfolded form of the mutant enzyme has greatly less binding than wild-type lipA. An enzyme having a higher fraction folded at equilibrium in a denaturation experiment indicates a more stable enzyme (dG=-RTlnK). Also, having vastly less binding to the unfolded state indicates the denaturant (IL) is less denaturing to the mutant than wild-type lipA. The decreased binding of mutant lipase compared to wild-type lipase is consistent at lower concentrations of [BMIM][Cl], where the enzymes are both presumed to be primarily folded. As described in Chapter 2, the author believes that charged mutations are reducing the binding of [BMIM][Cl] in the folded state, but more so in the unfolded state.

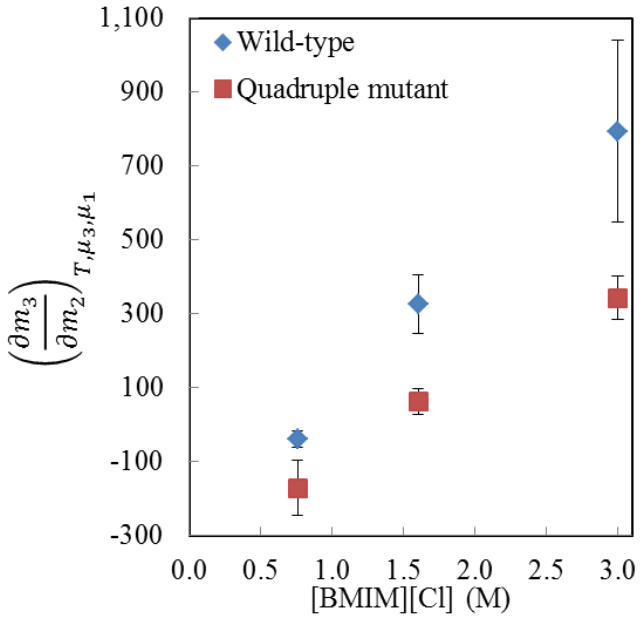

Figure 9.4. Preferential binding of [BMIM][Cl] to wild-type and mutant lipase A. Increased binding at higher concentrations is thought to be a result of unfolding. At the low concentrations

where the enzyme should be primarily folded, there appears to be a larger amount of preferential exclusion for the mutant than the wild-type enzyme.

9.3 References

254. Shaw, K.L., et al., *The effect of net charge on the solubility, activity, and stability of ribonuclease Sa.* Protein Science, 2001. **10**(6): p. 1206-1215.

Chapter 10 Outlook and conclusions

10.1 Conclusions

Aim 1: Explore the cause of enzyme inactivation in [BMIM][Cl] and the role of folding state on activity.

- Enzymes are inactivated in [BMIM][Cl] and show structural losses in [BMIM][Cl] indicated by fluorescence studies. Both inactivation and unfolding increase at higher concentrations of ionic liquid and are highly correlated (**Figure 3.4**). Solubility losses do not appear to play a role in inactivation (**Figure 3.1**).

Aim 2: Study the mechanism of [BMIM][Cl] induced enzyme unfolding.

- The cation, [BMIM], binds to aromatic and hydrophobic residues as shown by resolving crystal structures soaked in [BMIM][Cl] (**Figure 3.7**, **Figure 8.4**, **Figure 8.5**). These residues should become more exposed in the unfolded state.
- Equilibrium dialysis shows increased [BMIM][Cl] binding to enzymes at high concentrations where the enzyme is expected to be unfolded (**Figure 3.5** and **Figure 9.4**).

Aim 3: Investigate non-specific and site-specific approaches to prevent preferential [BMIM][Cl] binding and improve enzyme activity.

- Consistent across four enzymes (chymotrypsin, *Candida rugose* lipase, papain, and *Bacillus subtilis* lipase) chemical modifying enzymes by removing positive charges for a neutral moiety is beneficial while removing negative charges for a neutral moiety is deleterious. (**Figure 4.5**, **Figure 4.6**, **Figure 4.7**).

- [BMIM][Cl] causes perturbations in HSQC NMR spectra, interpreted as enzyme-IL binding sites (**Figure 7.2**). This is supported by crystallographic studies showing [Cl] and [BMIM] binding near perturbation sites.
- Mutagenesis to a negative charge at perturbed residues resulting in smaller perturbations correlates with enhanced kinetic stability, suggesting binding reduction (**Figure 7.6** and **Figure 7.8**).
- Crystallographic resolution of [BMIM] molecules at Y49 and G158 in the mutant enzyme but not near the E49 and E158 mutation sites indicate decreased IL binding (**Figure 8.2** and **Figure 8.3**).
- Equilibrium dialysis suggests a larger preferential exclusion of [BMIM][Cl] for the native state of wild-type and mutant lipA (**Figure 9.4**).
- The IL stable mutant lipase A (or charge variants of model enzymes) is not more stable in buffer than the wild-type enzyme, as measured by thermal melting (urea chemical denaturation for the charge variants), disagreeing with notion that the enzyme is generally more stable (**Figure 9.1** and **Figure 5.6**).
- Kinetic measurements showing an equilibrium in activity being approached that is higher for the IL-stable mutant than wild-type lipase suggests enhanced thermodynamic stability is, in part, responsible for kinetic stabilization (**Figure 9.3**).

10.2 Proposed mechanisms of stabilization

1. *A non-specific effect*: The negative charge reduces the overall affinity of the salt [BMIM][Cl] for the enzyme. [Cl] is repelled more than [BMIM] (if at all) is attracted. In the unfolded state there is more surface area for a negative charge to exert its influence

resulting in greater overall reduction in binding than in the native state. This mechanism is akin to other non-specifically excluded molecules, like sucrose, that stabilize enzymes.

2. *A site-specific effect*: As in the case of the G158E mutation, this residue is surrounded in primary sequence by hydrophobic amino acids that are mostly buried in the folded state. In the unfolded state [BMIM][Cl] may bind strongly to these now exposed resides unless binding is disrupted by an amino acid for which [BMIM][Cl] has low affinity.

10.3 Outlook

Much ground has been gained in understanding [BMIM][Cl]-enzyme effects. Based on the proposed denaturation mechanism, the [BMIM][Cl] stable mutant lipase may have enhanced function in most imidazolium-based ionic liquids. In neat ionic liquids like [BMIM][BF_4], where esterification and transesterification reactions are possible using lipase, the IL-stable mutant shows greatly enhanced stability over the wild-type enzyme (**Figure 10.1**). Much work still needs to be done to fully understand the stabilization effects and be able to design proteins for IL-tolerance. One idea would be to explore the difference in thermodynamic stability of the wild-type and mutant enzyme as a function of [BMIM][Cl] at low and high concentrations. Perhaps DSC between the two variants can achieve this result. Another interesting avenue to explore would be to do saturation mutagenesis at the four mutation sites in the IL-stable quadruple mutant lipase. This will increase confidence in the role negative amino acids play in altering preferential binding. The ultimate goal of an engineer is to be able to design, without need for experimental guide. Being able to recapitulate the results computationally could lead to designing other enzymes with applications in ionic liquids, such as cellulases, for optimum IL tolerance. Pathways of enzymes may even be designed. In the production of ethanol from cellulase, instead of requiring yeast to ferment the sugar post breakdown of cellulose, the ethanol

production pathway along with the appropriate cellulases could be designed for IL-tolerance to convert biomass to ethanol directly.

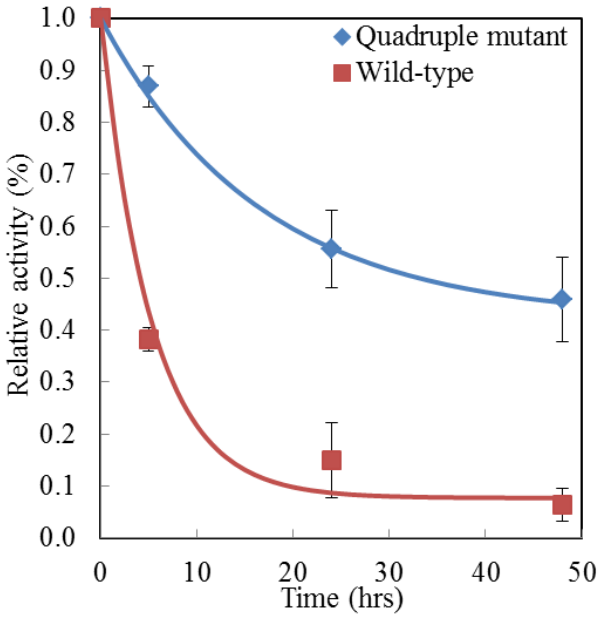

Figure 10.1. Activity retention of quadruple mutant and wild-type lipase A in anhydrous [BMIM][PF_6]. Activity was assayed by following the transesterification of 2-ethylhexanol with methylmethacrylate at 55 °C.

Chapter 11 Bibliography

1. Ke, T., C.R. Wescott, and A.M. Klibanov, *Prediction of the solvent dependence of enzymatic prochiral selectivity by means of structure-based thermodynamic calculations.* Journal of the American Chemical Society, 1996. **118**(14): p. 3366-3374.
2. Sheldon, R., *Catalytic reactions in ionic liquids.* Chemical Communications, 2001(23): p. 2399-2407.
3. Kaftzik, N., P. Wasserscheid, and U. Kragl, *Use of ionic liquids to increase the yield and enzyme stability in the beta-galactosidase catalysed synthesis of N-acetyllactosamine.* Organic Process Research & Development, 2002. **6**(4): p. 553-557.
4. Klibanov, A.M., *Improving enzymes by using them in organic solvents.* Nature, 2001. **409**(6817): p. 241-246.
5. Schmid, A., et al., *Industrial biocatalysis today and tomorrow.* Nature, 2001. **409**(6817): p. 258-268.
6. Halling, P.J., *Thermodynamic Predictions for Biocatalysis in Nonconventional Media - Theory, Tests, and Recommendations for Experimental-Design and Analysis.* Enzyme and Microbial Technology, 1994. **16**(3): p. 178-206.
7. Klibanov, A.M., *Enzyme Memory - What Is Remembered and Why.* Nature, 1995. **374**(6523): p. 596-596.
8. Pace, C.N., *Energetics of protein hydrogen bonds.* Nature Structural & Molecular Biology, 2009. **16**(7): p. 681-682.
9. Koskinen, A. and A.M. Klibanov, *Enzymatic reactions in organic media*1996.
10. Pace, C.N., et al., *Protein structure, stability and solubility in water and other solvents.* Philosophical Transactions of the Royal Society of London Series B-Biological Sciences, 2004. **359**(1448): p. 1225-1234.
11. Griebenow, K. and A.M. Klibanov, *On protein denaturation in aqueous-organic mixtures but not in pure organic solvents.* Journal of the American Chemical Society, 1996. **118**(47): p. 11695-11700.
12. Nordwald, E.M., G.S. Armstrong, and J.L. Kaar, *NMR-Guided Rational Engineering of an Ionic-Liquid-Tolerant Lipase.* Acs Catalysis, 2014. **4**(11): p. 4057-4064.
13. Nordwald, E.M., et al., *Charge Engineering of Cellulases Improves Ionic Liquid Tolerance and Reduces Lignin Inhibition.* Biotechnology and Bioengineering, 2014. **111**(8): p. 1541-1549.
14. Nordwald, E.M. and J.L. Kaar, *Stabilization of Enzymes in Ionic Liquids Via Modification of Enzyme Charge.* Biotechnology and Bioengineering, 2013. **110**(9): p. 2352-2360.
15. Nordwald, E.M. and J.L. Kaar, *Mediating Electrostatic Binding of 1-Butyl-3-methylimidazolium Chloride to Enzyme Surfaces Improves Conformational Stability.* Journal of Physical Chemistry B, 2013. **117**(30): p. 8977-8986.
16. Zhao, H., *Methods for stabilizing and activating enzymes in ionic liquids - a review.* Journal of Chemical Technology and Biotechnology, 2010. **85**(7): p. 891-907.
17. Pinkert, A., et al., *Ionic Liquids and Their Interaction with Cellulose.* Chemical Reviews, 2009. **109**(12): p. 6712-6728.
18. Sheldon, R.A., et al., *Biocatalysis in ionic liquids.* Green Chemistry, 2002. **4**(2): p. 147-151.

19. van Rantwijk, F. and R.A. Sheldon, *Biocatalysis in ionic liquids.* Chemical Reviews, 2007. **107**(6): p. 2757-2785.
20. Freire, M.G., et al., *An overview of the mutual solubilities of water-imidazolium-based ionic liquids systems.* Fluid Phase Equilibria, 2007. **261**(1-2): p. 449-454.
21. Brandt, A., et al., *The effect of the ionic liquid anion in the pretreatment of pine wood chips.* Green Chemistry, 2010. **12**(4): p. 672-679.
22. Galonde, N., et al., *Use of ionic liquids for biocatalytic synthesis of sugar derivatives.* Journal of Chemical Technology and Biotechnology, 2012. **87**(4): p. 451-471.
23. Carda-Broch, S., A. Berthod, and D.W. Armstrong, *Solvent properties of the 1-butyl-3-methylimidazolium hexafluorophosphate ionic liquid.* Analytical and Bioanalytical Chemistry, 2003. **375**(2): p. 191-199.
24. Ha, S.H., et al., *Lipase-catalyzed biodiesel production from soybean oil in ionic liquids.* Enzyme and Microbial Technology, 2007. **41**(4): p. 480-483.
25. Alvira, P., et al., *Pretreatment technologies for an efficient bioethanol production process based on enzymatic hydrolysis: A review.* Bioresource Technology, 2010. **101**(13): p. 4851-4861.
26. Groff, D., et al., *Acid enhanced ionic liquid pretreatment of biomass.* Green Chemistry, 2013. **15**(5): p. 1264-1267.
27. Klein-Marcuschamer, D., B.A. Simmons, and H.W. Blanch, *Techno-economic analysis of a lignocellulosic ethanol biorefinery with ionic liquid pre-treatment.* Biofuels Bioproducts & Biorefining-Biofpr, 2011. **5**(5): p. 562-569.
28. Li, Q., et al., *Improving enzymatic hydrolysis of wheat straw using ionic liquid 1-ethyl-3-methyl imidazolium diethyl phosphate pretreatment.* Bioresource Technology, 2009. **100**(14): p. 3570-3575.
29. Shill, K., et al., *Ionic Liquid Pretreatment of Cellulosic Biomass: Enzymatic Hydrolysis and Ionic Liquid Recycle.* Biotechnology and Bioengineering, 2011. **108**(3): p. 511-520.
30. Zhang, J.M., et al., *NMR spectroscopic studies of cellobiose solvation in EmimAc aimed to understand the dissolution mechanism of cellulose in ionic liquids.* Physical Chemistry Chemical Physics, 2010. **12**(8): p. 1941-1947.
31. Fu, D.B. and G. Mazza, *Optimization of processing conditions for the pretreatment of wheat straw using aqueous ionic liquid.* Bioresource Technology, 2011. **102**(17): p. 8003-8010.
32. Turner, M.B., et al., *Ionic liquid salt-induced inactivation and unfolding of cellulase from Trichoderma reesei.* Green Chemistry, 2003. **5**(4): p. 443-447.
33. Bose, S., C.A. Barnes, and J.W. Petrich, *Enhanced stability and activity of cellulase in an ionic liquid and the effect of pretreatment on cellulose hydrolysis.* Biotechnology and Bioengineering, 2012. **109**(2): p. 434-443.
34. Datta, S., et al., *Ionic liquid tolerant hyperthermophilic cellulases for biomass pretreatment and hydrolysis.* Green Chemistry, 2010. **12**(2): p. 338-345.
35. Park, J.I., et al., *A Thermophilic Ionic Liquid-Tolerant Cellulase Cocktail for the Production of Cellulosic Biofuels.* Plos One, 2012. **7**(5).
36. Li, C.L., et al., *Comparison of dilute acid and ionic liquid pretreatment of switchgrass: Biomass recalcitrance, delignification and enzymatic saccharification.* Bioresource Technology, 2010. **101**(13): p. 4900-4906.
37. Rinaldi, R., et al., *An Integrated Catalytic Approach to Fermentable Sugars from Cellulose.* Chemsuschem, 2010. **3**(10): p. 1151-1153.

38. Uju, et al., *Peracetic acid-ionic liquid pretreatment to enhance enzymatic saccharification of lignocellulosic biomass.* Bioresource Technology, 2013. **138**: p. 87-94.
39. Akdogan, Y. and D. Hinderberger, *Solvent-Induced Protein Refolding at Low Temperatures.* Journal of Physical Chemistry B, 2011. **115**(51): p. 15422-15429.
40. Buchfink, R., et al., *Ionic liquids as refolding additives: Variation of the anion.* Journal of Biotechnology, 2010. **150**(1): p. 64-72.
41. Constatinescu, D., C. Herrmann, and H. Weingartner, *Patterns of protein unfolding and protein aggregation in ionic liquids.* Physical Chemistry Chemical Physics, 2010. **12**(8): p. 1756-1763.
42. Noritomi, H., et al., *Thermal stability of proteins in the presence of aprotic ionic liquids.* Journal of biomedical science and engineering, 2011. **4**: p. 94-99.
43. Attri, P., P. Venkatesu, and A. Kumar, *Activity and stability of alpha-chymotrypsin in biocompatible ionic liquids: enzyme refolding by triethyl ammonium acetate.* Physical Chemistry Chemical Physics, 2011. **13**(7): p. 2788-2796.
44. Lange, C., G. Patil, and R. Rudolph, *Ionic liquids as refolding additives: N '-alkyl and N '-(omega-hydroxyalkyl) N-methylimidazolium chlorides.* Protein Science, 2005. **14**(10): p. 2693-2701.
45. Summers, C.A. and R.A. Flowers, *Protein renaturation by the liquid organic salt ethylammonium nitrate.* Protein Science, 2000. **9**(10): p. 2001-2008.
46. Weaver, K.D., et al., *Structure and function of proteins in hydrated choline dihydrogen phosphate ionic liquid.* Physical Chemistry Chemical Physics, 2012. **14**(2): p. 790-801.
47. Rodrigues, J.V., et al., *Protein stability in an ionic liquid milieu: on the use of differential scanning fluorimetry.* Physical Chemistry Chemical Physics, 2011. **13**(30): p. 13614-13616.
48. Kuper, J., et al., *The role of active-site Phe87 in modulating the organic co-solvent tolerance of cytochrome P450 BM3 monooxygenase.* Acta Crystallographica Section F-Structural Biology and Crystallization Communications, 2012. **68**: p. 1013-1017.
49. Munro, A.W., et al., *P450 BM3: the very model of a modern flavocytochrome.* Trends in biochemical sciences, 2002. **27**(5): p. 250-257.
50. Tee, K.L., et al., *Ionic liquid effects on the activity of monooxygenase P450BM-3.* Green Chemistry, 2008. **10**(1): p. 117-123.
51. Liu, H.F., et al., *Directed laccase evolution for improved ionic liquid resistance.* Green Chemistry, 2013. **15**(5): p. 1348-1355.
52. Park, S. and R.J. Kazlauskas, *Biocatalysis in ionic liquids - advantages beyond green technology.* Current Opinion in Biotechnology, 2003. **14**(4): p. 432-437.
53. Fu, D.B. and G. Mazza, *Aqueous ionic liquid pretreatment of straw.* Bioresource Technology, 2011. **102**(13): p. 7008-7011.
54. Kamiya, N., et al., *Enzymatic in situ saccharification of cellulose in aqueous-ionic liquid media.* Biotechnology Letters, 2008. **30**(6): p. 1037-1040.
55. Hwang, H.T., et al., *Lipase-catalyzed process for biodiesel production: Protein engineering and lipase production.* Biotechnology and Bioengineering, 2013.
56. De Diego, T., et al., *A recyclable enzymatic biodiesel production process in ionic liquids.* Bioresource Technology, 2011. **102**(10): p. 6336-6339.
57. Zhang, K.P., et al., *Penicillium expansum lipase-catalyzed production of biodiesel in ionic liquids.* Bioresource Technology, 2011. **102**(3): p. 2767-2772.

58. Lozano, P., et al., *One-Phase Ionic Liquid Reaction Medium for Biocatalytic Production of Biodiesel.* Chemsuschem, 2010. **3**(12): p. 1359-1363.
59. Yang, R.L., N. Li, and M.H. Zong, *Using ionic liquid cosolvents to improve enzymatic synthesis of arylalkyl beta-D-glucopyranosides.* Journal of Molecular Catalysis B-Enzymatic, 2012. **74**(1-2): p. 24-28.
60. Ee, G.C.L., et al., *Pellitorine, a Potential Anti-Cancer Lead Compound against HL60 and MCT-7 Cell Lines and Microbial Transformation of Piperine from Piper Nigrum.* Molecules, 2010. **15**(4): p. 2398-2404.
61. Ley, J.P., et al., *Stereoselective enzymatic synthesis of cis-pellitorine, a taste active alkamide naturally occurring in tarragon.* European Journal of Organic Chemistry, 2004(24): p. 5135-5140.
62. Jacobson, M., *Pellitorine Isomers .2. The Synthesis of N-Isobutyl-Trans-2,Trans-4-Decadienamide.* Journal of the American Chemical Society, 1953. **75**(11): p. 2584-2586.
63. Weingartner, H., C. Cabrele, and C. Herrmann, *How ionic liquids can help to stabilize native proteins.* Physical Chemistry Chemical Physics, 2012. **14**(2): p. 415-426.
64. Byrne, N., et al., *Reversible folding-unfolding, aggregation protection, and multi-year stabilization, in high concentration protein solutions, using ionic liquids.* Chemical Communications, 2007(26): p. 2714-2716.
65. Yang, Z., *Hofmeister effects: an explanation for the impact of ionic liquids on biocatalysis.* Journal of Biotechnology, 2009. **144**(1): p. 12-22.
66. Engel, P., et al., *Point by point analysis: how ionic liquid affects the enzymatic hydrolysis of native and modified cellulose.* Green Chemistry, 2010. **12**(11): p. 1959-1966.
67. Singh, T., et al., *Ionic Liquids Induced Structural Changes of Bovine Serum Albumin in Aqueous Media: A Detailed Physicochemical and Spectroscopic Study.* Journal of Physical Chemistry B, 2012. **116**(39): p. 11924-11935.
68. Baker, G.A. and W.T. Heller, *Small-angle neutron scattering studies of model protein denaturation in aqueous solutions of the ionic liquid 1-butyl-3-methylimidazolium chloride.* Chemical Engineering Journal, 2009. **147**(1): p. 6-12.
69. Baker, S.N., et al., *Fluorescence energy transfer efficiency in labeled yeast cytochrome c: a rapid screen for ion biocompatibility in aqueous ionic liquids.* Physical Chemistry Chemical Physics, 2011. **13**(9): p. 3642-3644.
70. Heller, W.T., et al., *Characterization of the Influence of the Ionic Liquid 1-Butyl-3-methylimidazolium Chloride on the Structure and Thermal Stability of Green Fluorescent Protein.* Journal of Physical Chemistry B, 2010. **114**(43): p. 13866-13871.
71. Kaar, J.L., et al., *Impact of ionic liquid physical properties on lipase activity and stability.* Journal of the American Chemical Society, 2003. **125**(14): p. 4125-4131.
72. Nakashima, K., et al., *Comb-shaped poly(ethylene glycol)-modified subtilisin Carlsberg is soluble and highly active in ionic liquids.* Chem Commun, 2005. **34**(34): p. 4297-4299.
73. Persson, M. and U.T. Bornscheuer, *Increased stability of an esterase from Bacillus stearothermophilus in ionic liquids as compared to organic solvents.* J Mol Catal B: Enzym, 2003. **22**(1-2): p. 21-27.
74. Schofer, S.H., et al., *Enzyme catalysis in ionic liquids: lipase catalysed kinetic resolution of 1-phenylethanol with improved enantioselectivity.* Chem Commun, 2001. **5**(5): p. 425-426.
75. Toral, A.R., et al., *Cross-linked Candida antarctica lipase B is active in denaturing ionic liquids.* Enzyme Microb Technol, 2007. **40**(5): p. 1095-1099.

76. Vafiadi, C., et al., *Feruloyl esterase-catalysed synthesis of glycerol sinapate using ionic liquids mixtures.* J Biotechnol, 2009. **139**(1): p. 124-129.
77. van Rantwijk, F., F. Secundo, and R.A. Sheldon, *Structure and activity of Candida antarctica lipase B in ionic liquids.* Green Chem, 2006. **8**(3): p. 282-286.
78. Zhao, H., C.L. Jones, and J.V. Cowins, *Lipase dissolution and stabilization in ether-functionalized ionic liquids.* Green Chem, 2009. **11**(8): p. 1128-1138.
79. Ansorge-Schumacher, M.B. and O. Thum, *Immobilised lipases in the cosmetics industry.* Chemical Society Reviews, 2013. **42**(15): p. 6475-6490.
80. Kirchner, G., M.P. Scollar, and A.M. Klibanov, *Resolution of Racemic Mixtures Via Lipase Catalysis in Organic-Solvents.* Journal of the American Chemical Society, 1985. **107**(24): p. 7072-7076.
81. Zaks, A. and D.R. Dodds, *Application of biocatalysis and biotransformations to the synthesis of pharmaceuticals.* Drug Discovery Today, 1997. **2**(12): p. 513-531.
82. Carrea, G. and S. Riva, *Properties and synthetic applications of enzymes in organic solvents.* Angewandte Chemie-International Edition, 2000. **39**(13): p. 2226-2254.
83. Akkara, J.A., M.S.R. Ayyagari, and F.F. Bruno, *Enzymatic synthesis and modification of polymers in nonaqueous solvents.* Trends in Biotechnology, 1999. **17**(2): p. 67-73.
84. Karl, U. and A. Simon, *BASF's ChiPros (R) chiral building blocks The cornerstones of your API syntheses!* Chimica Oggi-Chemistry Today, 2009. **27**(5): p. 66-69.
85. Solano, D.M., et al., *Industrial biotransformations in the synthesis of building blocks leading to enantiopure drugs.* Bioresource Technology, 2012. **115**: p. 196-207.
86. Gill, I. and R. Patel, *Biocatalytic ammonolysis of (5S)-4,5-dihydro-1H-pyrrole-1,5-dicarboxylic acid, 1-(1,1-dimethylethyl)-5-ethyl ester: Preparation of an intermediate to the dipeptidyl peptidase IV inhibitor Saxagliptin.* Bioorganic & Medicinal Chemistry Letters, 2006. **16**(3): p. 705-709.
87. Hofmeister, F., *Zur Lehre von der Wrikung der Salze. Zweite Mittheilung.* Archiv for Expermentelle Pathologie und Pharmakologie, 1888. **24**: p. 247-260.
88. Timasheff, S.N., *Solvent effects on protein stability.* Current Opinion in Structural Biology, 1992. **2**(1): p. 35-39.
89. Pegram, L.M. and M.T. Record, *Hofmeister salt effects on surface tension arise from partitioning of anions and cations between bulk water and the air-water interface.* Journal of Physical Chemistry B, 2007. **111**(19): p. 5411-5417.
90. Baldwin, R.L., *How Hofmeister ion interactions affect protein stability.* Biophysical Journal, 1996. **71**(4): p. 2056-2063.
91. Pegram, L.M. and M.T. Record, *Thermodynamic origin of Hofmeister ion effects.* Journal of Physical Chemistry B, 2008. **112**(31): p. 9428-9436.
92. Nandi, P.K. and D.R. Robinson, *Effects of Urea and Guanidine-Hydrochloride on Peptide and Nonpolar Groups.* Biochemistry, 1984. **23**(26): p. 6661-6668.
93. Moelbert, S., B. Normand, and P.D. Rios, *Kosmotropes and chaotropes: modelling preferential exclusion, binding and aggregate stability.* Biophysical Chemistry, 2004. **112**(1): p. 45-57.
94. Plumridge, T.H. and R.D. Waigh, *Water structure theory and some implications for drug design.* Journal of Pharmacy and Pharmacology, 2002. **54**(9): p. 1155-1179.
95. Von Hippel, P.H. and K.Y. Wong, *On the conformational stability of globular proteins. The effects of various electrolytes and nonelectrolytes on the thermal ribonuclease transition.* The Journal of biological chemistry, 1965. **240**(10): p. 3909-23.

96. Von Hippel, P.H. and K.Y. Wong, *Neutral Salts: The Generality of Their Effects on the Stability of Macromolecular Conformations.* Science, 1964. **2**: p. 577-580.
97. Becktel, W.J. and J.A. Schellman, *Protein Stability Curves.* Biopolymers, 1987. **26**(11): p. 1859-1877.
98. Schellman, J.A. and R.B. Hawkes, *Protein Stability from Thermal and Solvent Denaturation Curves.* Hoppe-Seylers Zeitschrift Fur Physiologische Chemie, 1979. **360**(8): p. 1015-1015.
99. Pace, C.N. and K.L. Shaw, *Linear extrapolation method of analyzing solvent denaturation curves.* Proteins-Structure Function and Genetics, 2000: p. 1-7.
100. Tadeo, X., M. Pons, and O. Millet, *Influence of the Hofmeister anions on protein stability as studied by thermal denaturation and chemical shift perturbation.* Biochemistry, 2007. **46**(3): p. 917-23.
101. Bye, J.W. and R.J. Falconer, *Thermal stability of lysozyme as a function of ion concentration: A reappraisal of the relationship between the Hofmeister series and protein stability.* Protein Science, 2013. **22**(11): p. 1563-1570.
102. Courtenay, E.S., M.W. Capp, and M.T. Record, *Thermodynamics of interactions of urea and guanidinium salts with protein surface: Relationship between solute effects on protein processes and changes in water-accessible surface area.* Protein Science, 2001. **10**(12): p. 2485-2497.
103. Lin, T.Y. and S.N. Timasheff, *On the role of surface tension in the stabilization of globular proteins.* Protein Science, 1996. **5**(2): p. 372-381.
104. Arakawa, T., R. Bhat, and S.N. Timasheff, *Why Preferential Hydration Does Not Always Stabilize the Native Structure of Globular-Proteins.* Biochemistry, 1990. **29**(7): p. 1924-1931.
105. Donald Voet, Judith G. Voet, and C.W. Pratt, *Fundamentals of Biochemistry*. 3rd ed2008.
106. Schellman, J.A., *Solvent Denaturation.* Biopolymers, 1978. **17**(5): p. 1305-1322.
107. Schellman, J.A., *Selective binding and solvent denaturation.* Biopolymers, 1987. **26**(4): p. 549-59.
108. Timasheff, S.N., *In disperse solution, "osmotic stress" is a restricted case of preferential interactions.* Proceedings of the National Academy of Sciences of the United States of America, 1998. **95**(13): p. 7363-7367.
109. Timasheff, S.N., *Protein-solvent preferential interactions, protein hydration, and the modulation of biochemical reactions by solvent components.* Proceedings of the National Academy of Sciences of the United States of America, 2002. **99**(15): p. 9721-9726.
110. Arakawa, T. and S.N. Timasheff, *Preferential Interactions of Proteins with Salts in Concentrated-Solutions.* Biochemistry, 1982. **21**(25): p. 6545-6552.
111. Tanford, C., *Protein denaturation. C. Theoretical models for the mechanism of denaturation.* Advances in protein chemistry, 1970. **24**: p. 1-95.
112. Casassa, E.F. and H. Eisenberg, *Thermodynamic Analysis of Multicomponent Solutions.* Advances in protein chemistry, 1964. **19**: p. 287-395.
113. Scatchard, G., *Physical chemistry of protein solutions; derivation of the equations for the osmotic pressure.* Journal of the American Chemical Society, 1946. **68**(11): p. 2315-9.
114. Schellman, J.A., *A Simple-Model for Solvation in Mixed-Solvents - Applications to the Stabilization and Destabilization of Macromolecular Structures.* Biophysical Chemistry, 1990. **37**(1-3): p. 121-140.

115. Schellman, J.A., *The Relation between the Free-Energy of Interaction and Binding.* Biophysical Chemistry, 1993. **45**(3): p. 273-279.
116. Timasheff, S.N., *Thermodynamic binding and site occupancy in the light of the Schellman exchange concept.* Biophysical Chemistry, 2002. **101**: p. 99-111.
117. Timasheff, S.N., *Water as Ligand - Preferential Binding and Exclusion of Denaturants in Protein Unfolding.* Biochemistry, 1992. **31**(41): p. 9857-9864.
118. Courtenay, E.S., et al., *Vapor pressure osmometry studies of osmolyte-protein interactions: Implications for the action of osmoprotectants in vivo and for the interpretation of "osmotic stress" experiments in vitro.* Biochemistry, 2000. **39**(15): p. 4455-4471.
119. Anderson, C.F., E.S. Courtenay, and M.T. Record, *Thermodynamic expressions relating different types of preferential interaction coefficients in solutions containing two solute components.* Journal of Physical Chemistry B, 2002. **106**(2): p. 418-433.
120. Timasheff, S.N., *Protein hydration, thermodynamic binding, and preferential hydration.* Biochemistry, 2002. **41**(46): p. 13473-13482.
121. Arakawa, T., R. Bhat, and S.N. Timasheff, *Preferential Interactions Determine Protein Solubility in 3-Component Solutions - the Mgcl2 System.* Biochemistry, 1990. **29**(7): p. 1914-1923.
122. Noelken, M.E. and Timashef.Sn, *Preferential Solvation of Bovine Serum Albumin in Aqueous Guanidine Hydrochloride.* Journal of Biological Chemistry, 1967. **242**(21): p. 5080-&.
123. Arakawa, T. and S.N. Timasheff, *Mechanism of Protein Salting in and Salting out by Divalent-Cation Salts - Balance between Hydration and Salt Binding.* Biochemistry, 1984. **23**(25): p. 5912-5923.
124. Anderson, C.F., et al., *Generalized derivation of an exact relationship linking different coefficients that characterize thermodynamic effects of preferential interactions.* Biophysical Chemistry, 2002. **101**: p. 497-511.
125. Wyman, J., *Linked Functions and Reciprocal Effects in Hemoglobin - a 2nd Look.* Advances in protein chemistry, 1964. **19**: p. 223-286.
126. Timasheff, S.N., *Control of protein stability and reactions by weakly interacting cosolvents: The simplicity of the complicated.* Advances in Protein Chemistry, Vol 51, 1998. **51**: p. 355-432.
127. Arakawa, T. and S.N. Timasheff, *Protein Stabilization and Destabilization by Guanidinium Salts.* Biochemistry, 1984. **23**(25): p. 5924-5929.
128. Lopez-Garcia, J.J., C. Grosse, and J. Horno, *On the use of the hypothesis of local electroneutrality in colloidal suspensions for the calculation of their dielectric properties.* Journal of Physical Chemistry B, 2005. **109**(12): p. 5808-5815.
129. Hill, T.L., *A. Fundamental studies on the theory of the Donnan membrane equilibrium.* Discussions of the Faraday Society, 1955. **21**: p. 31-45.
130. Greene, R.F. and C.N. Pace, *Urea and Guanidine-Hydrochloride Denaturation of Ribonuclease, Lysozyme, Alpha-Chymotrypsin, and Beta-Lactoglobulin.* Journal of Biological Chemistry, 1974. **249**(17): p. 5388-5393.
131. Pace, C.N., *Measuring and Increasing Protein Stability.* Trends in Biotechnology, 1990. **8**(4): p. 93-98.
132. Pace, C.N., *Determination and analysis of urea and guanidine hydrochloride denaturation curves.* Methods in enzymology, 1986. **131**: p. 266-80.

133. Schellman, J.A., *Fifty years of solvent denaturation.* Biophysical Chemistry, 2002. **96**(2-3): p. 91-101.
134. Schellman, J.A., *The Thermodynamic Stability of Proteins.* Annual Review of Biophysics and Biophysical Chemistry, 1987. **16**: p. 115-137.
135. Schellman, J.A., *Macromolecular Binding.* Biopolymers, 1975. **14**(5): p. 999-1018.
136. Schellman, J.A., *The Thermodynamics of Solvent Exchange.* Biopolymers, 1994. **34**(8): p. 1015-1026.
137. Johnson, C.M. and A.R. Fersht, *Protein Stability as a Function of Denaturant Concentration - the Thermal-Stability of Barnase in the Presence of Urea.* Biochemistry, 1995. **34**(20): p. 6795-6804.
138. Constantinescu, D., H. Weingartner, and C. Herrmann, *Protein denaturation by ionic liquids and the Hofmeister series: A case study of aqueous solutions of ribonuclease A.* Angewandte Chemie-International Edition, 2007. **46**(46): p. 8887-8889.
139. Klahn, M., et al., *On the different roles of anions and cations in the solvation of enzymes in ionic liquids.* Physical Chemistry Chemical Physics, 2011. **13**(4): p. 1649-1662.
140. Elcock, A.H. and J.A. McCammon, *Electrostatic contributions to the stability of halophilic proteins.* Journal of Molecular Biology, 1998. **280**(4): p. 731-748.
141. Frolow, F., et al., *Insights into protein adaptation to a saturated salt environment from the crystal structure of a halophilic 2Fe-2S ferredoxin (vol 3, pg 452, 1996).* Nature Structural Biology, 1996. **3**(12): p. 1055-1055.
142. Rao, J.K.M. and P. Argos, *Structural Stability of Halophilic Proteins.* Biochemistry, 1981. **20**(23): p. 6536-6543.
143. Jaeger, V., P. Burney, and J. Pfaendtner, *Comparison of Three Ionic Liquid-Tolerant Cellulases by Molecular Dynamics.* Biophysical Journal, 2015. **108**(4): p. 880-892.
144. Burney, P.R., et al., *Molecular dynamics investigation of the ionic liquid/enzyme interface: application to engineering enzyme surface charge.* Proteins: Structure, Function, and Bioinformatics, 2015. **83**(4): p. 670-680.
145. Nordwald, E.M., et al., *Accelerated protein engineering for chemical biotechnology via homologous recombination.* Current Opinion in Biotechnology, 2013. **24**(6): p. 1017-1022.
146. Wei-Wei Gao, Feng-Xiu Zhang, and C.-H. Zhou, *Key factors affecting the activity and stability of enzymes in ionic liquids and novel applications in biocatalysis.* Biochemical engineering journal, 2015. **99**: p. 67-84.
147. Lau, R.M., et al., *Dissolution of Candida antarctica lipase B in ionic liquids: effects on structure and activity.* Green Chemistry, 2004. **6**(9): p. 483-487.
148. Tamura, K., N. Nakamura, and H. Ohno, *Cytochrome c dissolved in 1-allyl-3-methylimidazolium chloride type ionic liquid undergoes a quasi-reversible redox reaction up to 140 degrees C.* Biotechnology and Bioengineering, 2012. **109**(3): p. 729-735.
149. Bekhouche, M., L.J. Blum, and B. Doumeche, *Contribution of Dynamic and Static Quenchers for the Study of Protein Conformation in Ionic Liquids by Steady-State Fluorescence Spectroscopy.* Journal of Physical Chemistry B, 2012. **116**(1): p. 413-423.
150. Hannemann, F., et al., *Unfolding and conformational studies on bovine adrenodoxin probed by engineered intrinsic tryptophan fluorescence.* Biochemistry, 2002. **41**(36): p. 11008-11016.
151. Lakowicz, J.R., *Principles of fluorescence spectroscopy*. 3rd ed2006.

152. Merrill, A.R., L.R. Palmer, and A.G. Szabo, *Acrylamide Quenching of the Intrinsic Fluorescence of Tryptophan Residues Genetically-Engineered into the Soluble Colicin-E1 Channel Peptide - Structural Characterization of the Insertion-Competent State.* Biochemistry, 1993. **32**(27): p. 6974-6981.
153. Monsellier, E. and H. Bedouelle, *Quantitative measurement of protein stability from unfolding equilibria monitored with the fluorescence maximum wavelength.* Protein Engineering Design & Selection, 2005. **18**(9): p. 445-456.
154. Shao, Q., *On the influence of hydrated imidazolium-based ionic liquid on protein structure stability: A molecular dynamics simulation study.* Journal of Chemical Physics, 2013. **139**(11).
155. Alston, R.W., et al., *Contribution of single tryptophan residues to the fluorescence and stability of ribonuclease sea.* Biophysical Journal, 2004. **87**(6): p. 4036-4047.
156. Callis, P.R., *L-1(a) and L-1(b) transitions of tryptophan: Applications of theory and experimental observations to fluorescence of proteins.* Fluorescence Spectroscopy, 1997. **278**: p. 113-150.
157. Chen, Y. and M.D. Barkley, *Toward understanding tryptophan fluorescence in proteins.* Biochemistry, 1998. **37**(28): p. 9976-9982.
158. Kumar, V. and S. Pandey, *Selective Quenching of 2-Naphtholate Fluorescence by Imidazolium Ionic Liquids.* Journal of Physical Chemistry B, 2012. **116**(39): p. 12030-12037.
159. Lai, J.Q., et al., *Specific ion effects of ionic liquids on enzyme activity and stability.* Green Chemistry, 2011. **13**(7): p. 1860-1868.
160. Rawat, K. and H.B. Bohidar, *Universal Charge Quenching and Stability of Proteins in 1-Methyl-3-alkyl (Hexyl/Octyl) Imidazolium Chloride Ionic Liquid Solutions.* Journal of Physical Chemistry B, 2012. **116**(36): p. 11065-11074.
161. Shu, Y., et al., *New Insight into Molecular Interactions of Imidazolium Ionic Liquids with Bovine Serum Albumin.* Journal of Physical Chemistry B, 2011. **115**(42): p. 12306-12314.
162. Moller, M. and A. Denicola, *Protein tryptophan accessibility studied by fluorescence quenching.* Biochemistry and Molecular Biology Education, 2002. **30**(3): p. 175-178.
163. Sontag, B., et al., *Intrinsic Tryptophan Fluorescence of Rat-Liver Elongation-Factor Eef-2 to Monitor the Interaction with Guanylic and Adenylic Nucleotides and Related Conformational-Changes.* Biochemistry, 1993. **32**(8): p. 1976-1980.
164. Moon, C.P. and K.G. Fleming, *Using Tryptophan Fluorescence to Measure the Stability of Membrane Proteins Folded in Liposomes.* Methods in Enzymology: Biothermodynamics, Vol 492, Pt D, 2011. **492**: p. 189-211.
165. Sharma, N.K., et al., *Do ion tethered functional groups affect IL solvent properties? The case of sulfoxides and sulfones.* Chemical Communications, 2006(6): p. 646-648.
166. Myers, J.K., C.N. Pace, and J.M. Scholtz, *Denaturant M-Values and Heat-Capacity Changes - Relation to Changes in Accessible Surface-Areas of Protein Unfolding.* Protein Science, 1995. **4**(10): p. 2138-2148.
167. Churchill, C.D.M. and S.D. Wetmore, *Noncovalent Interactions Involving Histidine: The Effect of Charge on pi-pi Stacking and T-Shaped Interactions with the DNA Nucleobases.* Journal of Physical Chemistry B, 2009. **113**(49): p. 16046-16058.
168. Gallivan, J.P. and D.A. Dougherty, *Cation-pi interactions in structural biology.* Proceedings of the National Academy of Sciences of the United States of America, 1999. **96**(17): p. 9459-9464.

169. Liao, S.M., et al., *The multiple roles of histidine in protein interactions.* Chemistry Central Journal, 2013. **7**.
170. McGaughey, G.B., M. Gagne, and A.K. Rappe, *pi-stacking interactions - Alive and well in proteins.* Journal of Biological Chemistry, 1998. **273**(25): p. 15458-15463.
171. Loewenthal, R., J. Sancho, and A.R. Fersht, *Histidine Aromatic Interactions in Barnase - Elevation of Histidine Pk(a) and Contribution to Protein Stability.* Journal of molecular biology, 1992. **224**(3): p. 759-770.
172. Silva, M., A.M. Figueiredo, and E.J. Cabrita, *Epitope mapping of imidazolium cations in ionic liquid-protein interactions unveils the balance between hydrophobicity and electrostatics towards protein destabilisation.* Physical Chemistry Chemical Physics, 2014. **16**(42): p. 23394-23403.
173. Yang, Z. and W.B. Pan, *Ionic liquids: Green solvents for nonaqueous biocatalysis.* Enzyme and Microbial Technology, 2005. **37**(1): p. 19-28.
174. Schofer, S.H., et al., *Enzyme catalysis in ionic liquids: lipase catalysed kinetic resolution of 1-phenylethanol with improved enantioselectivity.* Chemical Communications, 2001(5): p. 425-426.
175. Figueiredo, A.M., et al., *Protein destabilisation in ionic liquids: the role of preferential interactions in denaturation.* Physical Chemistry Chemical Physics, 2013. **15**(45): p. 19632-19643.
176. Geng, F., et al., *Interaction of bovine serum albumin and long-chain imidazolium ionic liquid measured by fluorescence spectra and surface tension.* Process Biochemistry, 2010. **45**(3): p. 306-311.
177. Singh, T., et al., *Interaction of Gelatin with Room Temperature Ionic Liquids: A Detailed Physicochemical Study.* Journal of Physical Chemistry B, 2010. **114**(25): p. 8441-8448.
178. Micaelo, N.M. and C.M. Soares, *Protein structure and dynamics in ionic liquids. Insights from molecular dynamics simulation studies.* Journal of Physical Chemistry B, 2008. **112**(9): p. 2566-2572.
179. Inada, Y., et al., *Application of Polyethylene Glycol-Modified Enzymes in Biotechnological Processes - Organic Solvent-Soluble Enzymes.* Trends in Biotechnology, 1986. **4**(7): p. 190-194.
180. Arroyo, M., J.M. Sanchez-Montero, and J.V. Sinisterra, *Thermal stabilization of immobilized lipase B from Candida antarctica on different supports: Effect of water activity on enzymatic activity in organic media.* Enzyme and Microbial Technology, 1999. **24**(1-2): p. 3-12.
181. Cao, L.Q., L. van Langen, and R.A. Sheldon, *Immobilised enzymes: carrier-bound or carrier-free?* Current Opinion in Biotechnology, 2003. **14**(4): p. 387-394.
182. Nakashima, K., et al., *Comb-shaped poly(ethylene glycol)-modified subtilisin Carlsberg is soluble and highly active in ionic liquids.* Chemical Communications, 2005(34): p. 4297-4299.
183. Zhang, T., et al., *Identification of a haloalkaliphilic and thermostable cellulase with improved ionic liquid tolerance.* Green Chemistry, 2011. **13**(8): p. 2083-2090.
184. El Seoud, O.A., et al., *Applications of ionic liquids in carbohydrate chemistry: A window of opportunities.* Biomacromolecules, 2007. **8**(9): p. 2629-2647.
185. Swatloski, R.P., et al., *Dissolution of cellose with ionic liquids.* Journal of the American Chemical Society, 2002. **124**(18): p. 4974-4975.

186. Zhao, H., et al., *Improving the enzyme catalytic efficiency using ionic liquids with kosmotropic anions.* Chinese Journal of Chemistry, 2006. **24**(4): p. 580-584.
187. Tavares, A.P., O. Rodriguez, and E.A. Macedo, *Ionic liquids as alternative co-solvents for laccase: study of enzyme activity and stability.* Biotechnology and bioengineering, 2008. **101**(1): p. 201-7.
188. Bihari, M., T.P. Russell, and D.A. Hoagland, *Dissolution and Dissolved State of Cytochrome c in a Neat, Hydrophilic Ionic Liquid.* Biomacromolecules, 2010. **11**(11): p. 2944-2948.
189. Stoner, M.R., et al., *Surfactant-induced unfolding of cellulase: Kinetic studies.* Biotechnology Progress, 2006. **22**(1): p. 225-232.
190. Kosters, H.A. and H.H. de Jongh, *Spectrophotometric tool for the determination of the total carboxylate content in proteins; molar extinction coefficient of the enol ester from Woodward's reagent K reacted with protein carboxylates.* Analytical chemistry, 2003. **75**(10): p. 2512-6.
191. Fersht, A.R., *Conformational Equilibria in Alpha-Chymotrypsin and Delta-Chymotrypsin - Energetics and Importance of Salt Bridge.* Journal of molecular biology, 1972. **64**(2): p. 497-&.
192. Zhang, Y.J. and P.S. Cremer, *Interactions between macromolecules and ions: the Hofmeister series.* Current Opinion in Chemical Biology, 2006. **10**(6): p. 658-663.
193. Danson, M.J. and D.W. Hough, *The structural basis of protein halophilicity.* Comparative Biochemistry and Physiology a-Physiology, 1997. **117**(3): p. 307-312.
194. You, D.J., et al., *Protein thermostabilization requires a fine-tuned placement of surface-charged residues.* Journal of Biochemistry, 2007. **142**(4): p. 507-516.
195. Kohn, W.D., C.M. Kay, and R.S. Hodges, *Protein Destabilization by Electrostatic Repulsions in the 2-Stranded Alpha-Helical Coiled-Coil Leucine-Zipper.* Protein Science, 1995. **4**(2): p. 237-250.
196. Dym, O., M. Mevarech, and J.L. Sussman, *Structural Features That Stabilize Halophilic Malate-Dehydrogenase from an Archaebacterium.* Science, 1995. **267**(5202): p. 1344-1346.
197. Mamat, B., et al., *Crystal structures and enzymatic properties of three formyltransferases from archaea: Environmental adaptation and evolutionary relationship.* Protein Science, 2002. **11**(9): p. 2168-2178.
198. Bieger, B., L.O. Essen, and D. Oesterhelt, *Crystal structure of halophilic dodecin: A novel, dodecameric flavin binding protein from Halobacterium salinarum.* Structure, 2003. **11**(4): p. 375-385.
199. Tadeo, X., et al., *Structural Basis for the Aminoacid Composition of Proteins from Halophilic Archea.* Plos Biology, 2009. **7**(12): p. e1000257.
200. Coquelle, N., et al., *Gradual Adaptive Changes of a Protein Facing High Salt Concentrations.* Journal of Molecular Biology, 2010. **404**(3): p. 493-505.
201. Bracken, C.D., et al., *Crystal structures of a halophilic archaeal malate synthase from Haloferax volcanii and comparisons with isoforms A and G.* Bmc Structural Biology, 2011. **11**.
202. Ortega, G., et al., *Halophilic enzyme activation induced by salts.* Scientific Reports, 2011. **1**.
203. Zaccai, G. and H. Eisenberg, *Halophilic Proteins and the Influence of Solvent on Protein Stabilization.* Trends in biochemical sciences, 1990. **15**(9): p. 333-337.

204. Moniruzzaman, M., N. Kamiya, and M. Goto, *Activation and stabilization of enzymes in ionic liquids.* Organic & biomolecular chemistry, 2010. **8**(13): p. 2887-99.
205. Patel, D.D. and J.M. Lee, *Applications of ionic liquids.* Chemical Record, 2012. **12**(3): p. 329-355.
206. Zhao, H., et al., *Designing enzyme-compatible ionic liquids that can dissolve carbohydrates.* Green Chemistry, 2008. **10**(6): p. 696-705.
207. Dalhus, B., et al., *Structural basis for thermophilic protein stability: Structures of thermophilic and mesophilic malate dehydrogenases.* Journal of molecular biology, 2002. **318**(3): p. 707-721.
208. Willaert, K. and Y. Engelborghs, *The Quenching of Tryptophan Fluorescence by Protonated and Unprotonated Imidazole.* European Biophysics Journal, 1991. **20**(3): p. 177-182.
209. Jayabharathi, J., et al., *Fluorescence investigation of the interaction of 2-(4-fluoropheny1)-1-pheny1-1H-phenanthro [9,10-d] imidazole with bovine serum albumin.* Journal of Photochemistry and Photobiology B-Biology, 2012. **117**: p. 222-227.
210. Bose, S., D.W. Armstrong, and J.W. Petrich, *Enzyme-Catalyzed Hydrolysis of Cellulose in Ionic Liquids: A Green Approach Toward the Production of Biofuels.* Journal of Physical Chemistry B, 2010. **114**(24): p. 8221-8227.
211. Gribenko, A.V., et al., *Rational stabilization of enzymes by computational redesign of surface charge-charge interactions.* Proceedings of the National Academy of Sciences of the United States of America, 2009. **106**(8): p. 2601-6.
212. Pace, C.N., D.V. Laurents, and J.A. Thomson, *Ph-Dependence of the Urea and Guanidine-Hydrochloride Denaturation of Ribonuclease-a and Ribonuclease-T1.* Biochemistry, 1990. **29**(10): p. 2564-2572.
213. Pace, C.N., D.V. Laurents, and R.E. Erickson, *Urea Denaturation of Barnase - Ph-Dependence and Characterization of the Unfolded State.* Biochemistry, 1992. **31**(10): p. 2728-2734.
214. Himmel, M.E., et al., *Biomass recalcitrance: Engineering plants and enzymes for biofuels production.* Science, 2007. **315**(5813): p. 804-807.
215. Vinzant, T.B., et al., *Simultaneous saccharification and fermentation of pretreated hardwoods - Effect of native lignin content.* Applied Biochemistry and Biotechnology, 1997. **62**(1): p. 99-104.
216. Nishiyama, Y., P. Langan, and H. Chanzy, *Crystal structure and hydrogen-bonding system in cellulose 1 beta from synchrotron X-ray and neutron fiber diffraction.* Journal of the American Chemical Society, 2002. **124**(31): p. 9074-9082.
217. Nishiyama, Y., et al., *Crystal structure and hydrogen bonding system in cellulose 1(alpha), from synchrotron X-ray and neutron fiber diffraction.* Journal of the American Chemical Society, 2003. **125**(47): p. 14300-14306.
218. Beckham, G.T., et al., *Molecular-Level Origins of Biomass Recalcitrance: Decrystallization Free Energies for Four Common Cellulose Polymorphs.* Journal of Physical Chemistry B, 2011. **115**(14): p. 4118-4127.
219. Zhang, H., et al., *1-Allyl-3-methylimidazolium chloride room temperature ionic liquid: a new and powerful nonderivatizing solvent for cellulose.* Macromolecules, 2005. **38**: p. 8272-8277.
220. Lopes, A.M.D., et al., *Pretreatment and Fractionation of Wheat Straw Using Various Ionic Liquids.* Journal of Agricultural and Food Chemistry, 2013. **61**(33): p. 7874-7882.

221. Guo, J., et al., *Probing anion-cellulose interactions in imidazolium-based room temperature ionic liquids: a density functional study.* Carbohydrate research, 2010. **345**(15): p. 2201-5.
222. Wu, H., et al., *Facile Pretreatment of Lignocellulosic Biomass at High Loadings in Room Temperature Ionic Liquids.* Biotechnology and Bioengineering, 2011. **108**(12): p. 2865-2875.
223. Rahikainen, J.L., et al., *Inhibitory effect of lignin during cellulose bioconversion: The effect of lignin chemistry on non-productive enzyme adsorption.* Bioresource Technology, 2013. **133**: p. 270-278.
224. Rahikainena, J.L., et al., *Cellulase–lignin interactions—The role of carbohydrate-binding module and pH in non-productive binding.* Enzyme and Microbial Technology, 2013. **53**(5): p. 315-321.
225. Rahikainena, J.L., et al., *Effect of temperature on lignin-derived inhibition studied with three structurally different cellobiohydrolases.* Bioresource Technology, 2013. **146**: p. 118-125.
226. Rahikainen, J., et al., *Inhibition of Enzymatic Hydrolysis by Residual Lignins From Softwood-Study of Enzyme Binding and Inactivation on Lignin-Rich Surface.* Biotechnology and Bioengineering, 2011. **108**(12): p. 2823-2834.
227. Martin-Sampedro, R., et al., *Preferential Adsorption and Activity of Monocomponent Cellulases on Lignocellulose Thin Films with Varying Lignin Content.* Biomacromolecules, 2013. **14**(4): p. 1231-1239.
228. Miller, G.L., *Use of Dinitrosalicylic Acid Reagent for Determination of Reducing Sugar.* Analytical Chemistry, 1959. **31**(3): p. 426-428.
229. Seiboth, B., C. Ivanova, and V. Seidl-seiboth, *Trichoderma reesei: A Fungal Enzyme Producer for Cellulosic Biofuels*, in *Biofuel Production-Recent Developments and Prospects*, M.A.d.S. Bernardes, Editor 2011, InTech. p. 309-340.
230. Rajakumara, E., et al., *Crystallization and preliminary X-ray crystallographic investigations on several thermostable forms of a Bacillus subtilis lipase.* Acta Crystallographica Section D-Biological Crystallography, 2004. **60**: p. 160-162.
231. Kumar, L., R. Chandra, and J. Saddler, *Influence of Steam Pretreatment Severity on Post-Treatments Used to Enhance the Enzymatic Hydrolysis of Pretreated Softwoods at Low Enzyme Loadings.* Biotechnology and Bioengineering, 2011. **108**(10): p. 2300-2311.
232. Nakagame, S., et al., *Enhancing the Enzymatic Hydrolysis of Lignocellulosic Biomass by Increasing the Carboxylic Acid Content of the Associated Lignin.* Biotechnology and Bioengineering, 2011. **108**(3): p. 538-548.
233. Zhu, J.Y., et al., *Sulfite pretreatment (SPORL) for robust enzymatic saccharification of spruce and red pine.* Bioresource Technology, 2009. **100**(8): p. 2411-2418.
234. Lou, H.M., et al., *pH-Induced Lignin Surface Modification to Reduce Nonspecific Cellulase Binding and Enhance Enzymatic Saccharification of Lignocelluloses.* Chemsuschem, 2013. **6**(5): p. 919-927.
235. Kern, M., et al., *Structural characterization of a unique marine animal family 7 cellobiohydrolase suggests a mechanism of cellulase salt tolerance.* Proceedings of the National Academy of Sciences of the United States of America, 2013. **110**(25): p. 10189-10194.
236. Zhang, Y., et al., *Cellulase deactivation based kinetic modeling of enzymatic hydrolysis of steam-exploded wheat straw.* Bioresource Technology, 2010. **101**(21): p. 8261-8266.

237. Bezerra, R.M.F. and A.A. Dias, *Discrimination among eight modified Michaelis-Menten kinetics models of cellulose hydrolysis with a large range of substrate/enzyme ratios.* Applied Biochemistry and Biotechnology, 2004. **112**(3): p. 173-184.
238. Brown, R.F., F.K. Agbogbo, and M.T. Holtzapple, *Comparison of mechanistic models in the initial rate enzymatic hydrolysis of AFEX-treated wheat straw.* Biotechnology for Biofuels, 2010. **3**.
239. Bansal, P., et al., *Modeling cellulase kinetics on lignocellulosic substrates.* Biotechnology Advances, 2009. **27**(6): p. 833-848.
240. Adlercreutz, P., *Immobilisation and application of lipases in organic media.* Chem Soc Rev, 2013. **42**(15): p. 6406-6436.
241. Nagarajan, S., *New tools for exploring "old friends-microbial lipases".* Appl Biochem Biotechnol, 2012. **168**(5): p. 1163-1196.
242. Stergiou, P.Y., et al., *Advances in lipase-catalyzed esterification reactions.* Biotechnol Adv, 2013. **31**(8): p. 1846-1859.
243. Lehmann, C., et al., *Ionic liquid and deep eutectic solvent-activated CelA2 variants generated by directed evolution.* Appl Microbiol Biotechnol, 2014. **98**(12): p. 5775-5785.
244. Chen, Z.W., et al., *Improved Activity of a Thermophilic Cellulase, Cel5A, from Thermotoga maritima on Ionic Liquid Pretreated Switchgrass.* Plos One, 2013. **8**(11).
245. Augustyniak, W., et al., *Biophysical characterization of mutants of Bacillus subtilis lipase evolved for thermostability: Factors contributing to increased activity retention.* Protein Science, 2012. **21**(4): p. 487-497.
246. Farmer, B.T., *Localizing the NADP(+) binding site on the MurB enzyme by NMR.* Nature Structural Biology, 1996. **3**(12): p. 995-997.
247. Williamson, M.P., *Using chemical shift perturbation to characterise ligand binding.* Progress in Nuclear Magnetic Resonance Spectroscopy, 2013. **73**: p. 1-16.
248. Byerly, D.W., C.A. McElroy, and M.P. Foster, *Mapping the surface of Escherichia coli peptide deformylase by NMR with organic solvents.* Protein Sci, 2002. **11**(7): p. 1850-1853.
249. McLachlan, G.D., et al., *High-resolution NMR characterization of a spider-silk mimetic composed of 15 tandem repeats and a CRGD motif.* Protein Sci, 2009. **18**(1): p. 206-216.
250. Kamal, M.Z., et al., *Lipase in aqueous-polar organic solvents: activity, structure, and stability.* Protein Sci, 2013. **22**(7): p. 904-915.
251. van Pouderoyen, G., et al., *The crystal structure of Bacillus subtilis lipase: A minimal alpha/beta hydrolase fold enzyme.* Journal of molecular biology, 2001. **309**(1): p. 215-226.
252. Leslie, A.G.W. and H.R. Powell, *Processing diffraction data with MOSFLM.* Evolving Methods for Macromolecular Crystallography, 2007. **245**: p. 41-51.
253. Adams, P.D., et al., *PHENIX: a comprehensive Python-based system for macromolecular structure solution.* Acta Crystallographica Section D-Biological Crystallography, 2010. **66**: p. 213-221.
254. Shaw, K.L., et al., *The effect of net charge on the solubility, activity, and stability of ribonuclease Sa.* Protein Science, 2001. **10**(6): p. 1206-1215.

Chapter 12 Appendix

12.1 The binding polynomial

There are many models and assumptions we can make to derive the binding polynomial. To start, we shall begin with the independent site-binding model. Here we can write for the native state binding to ligand, x:

$$(1.1)\ N + x \leftrightarrow [Nx]$$

Adding another ligand at an independent site gives:

$$(1.2)\ [Nx] + x \leftrightarrow [Nx_2]$$

This can be extended for any number of ligands. Let $k_{j,N}$ be the binding constant at binding site "j".

$$(1.3)\ k_{j,N} = \frac{[Nx_j]}{[x][N]}$$

For 3 ligand sites, we can write that the total amount of protein

$$(1.4)\ N_T = N\left[1 + k_{1,N}[x] + k_{2,N}[x] + k_{3,N}[x] + k_{1,N}k_{2,N}[x]^2 + k_{1,N}k_{3,N}[x]^2 + k_{2,N}k_{3,N}[x]^2 + k_{1,N}k_{2,N}k_{3,N}[x]^3\right]$$

Which is simply the amount free in solution, N, times the amount in complex with 0, 1, 2, or 3 ligands at the different binding sites. This can be re-written as:

$$(1.5)\ N_T = N\prod_{1}^{3}(1 + k_{j,N}\,x)$$

A similar expression can be written for the total amount of denatured protein (D_T), allowing us to write an expression for the equilibrium constant for unfolding with "j" and "i" ligands bound to the unfolded and folded state.

$$(1.6)\ K = D\prod_{1}^{j}(1 + k_{j,D}\,x)/N\prod_{1}^{i}(1 + k_{i,N}\,x) = k_o\prod_{1}^{j}(1 + k_{j,D}\,x)/\prod_{1}^{i}(1 + k_{i,N}\,x)$$

Where k_o is the equilibrium constant in the absence of denaturant. One last assumption one can make is that the binding sites have equivalent affinity, but that there is a different number of binding sites between the folded and unfolded states. This reduces the above equation to:

$$(1.7)\ K = k_o\frac{(1 + kx)^{n_D}}{(1 + kx)^{n_N}}$$

Where n_D and n_N are the amount of binding sites in the unfolded and folded states. Alternatively, if one does not make the assumption of equivalent binding sites, or that ligands bind consecutively the equilibrium constant can be written as:

$$(1.8)\ K = k_o\frac{\sum k'_{j,D}x^j}{\sum k'_{i,N}x^i}$$

Summed from 0 to j or i, and the zeroth term (i.e. $k'_{0,D}$) is 1. Note that the equilibrium constants here represent macroscopic apparent binding values for a certain number of ligands bound, rather than at a particular site. These polynomials are referred to as the 'binding polynomials' for the denatured and native states.

12.2 The Wyman linkage relation

The total amount of ligand bound to the denatured state, ν_D is:

$$(1.9)\ \nu_D = \frac{\text{Total Bound Ligand}}{\text{Total Macromolecule}} = \frac{\sum j[Dx_j]}{\sum[Dx_j]} = \frac{\sum jk_{j,D}x^j}{\sum k_{j,D}x^j} = \frac{\partial \ln\left(\sum k_{j,D}x^j\right)}{\partial \ln(x)}$$

where x represents the concentration of ligand. An equivalent expression can be written for the number of molecules bound to the native state, ν_N. Taking the logarithm of Equation 1.8 yields:

$$(1.10)\ \ln(K) = \ln(k_o) + \ln\left(\sum k_{j,D}x^j\right) - \ln\left(\sum k_{i,N}x^i\right)$$

Taking the derivative with respect to ligand concentration (more accurately, activity) and noting that k_o is not a function of ligand concentration gives the Wyman linkage relation.

$$(1.11)\ \frac{d\ln(K)}{d\ln x} = \Delta\nu$$

12.3 Linearity of ΔG with ligand concentration

We are now in position to analyze the effects of ligands on the conformational stability of a protein, ΔG, in terms of a binding polynomial.[115, 134] Experimentally, it has been observed that the ΔG is linear with denaturant concentration.[130]

$$(1.12)\ \Delta G = m[x] + \Delta G^o$$

We know that

$$(1.13)\ \Delta G = -RT\ln(K)$$

where K is the equilibrium constant for unfolding. We can use Equation 1.7 to write

$$(1.14)\ \Delta G = \Delta G^o - RT\ln(1 + kx)^{\Delta n} = \Delta G^o - \Delta nRT\ln(1 + kx)$$

A Taylor series expansion of $\ln(1 + kx)$ about 0 gives:

$$(1.15)\ \ln(1) + \frac{kx}{1 + k(0)} - \frac{k^2x^2}{2} + \cdots$$

Truncating to the first term, we see that

$$(1.16)\ \ln(1 + kx) \approx kx$$

Substituting Equation 1.16 into Equation 1.14, we find:

$$(1.17)\ \Delta G = \Delta G^o - \Delta nRTkx$$

Thus, the m-value is proportional to the increase in number of molecules that bind upon unfolding and is linear with concentration (activity, actually) of the ligand.

12.4 How does binding strength affect the Gibbs free energy at various denaturant activities?

Schellman shows the chemical potential of macromolecule can be written in units of molality as:[107]

$$(1.18)\ \mu_2 = \mu_2^o + \mathrm{RTln}(m_2) + \mathrm{RT}\beta$$

Here, m_2 is the total concentration of macromolecule and RTβ is the excess chemical potential as a result of ligand binding. Note that we assume macromolecule non-idealities do not play a role (i.e. infinite dilution). The change in energy as a result of binding can be written in relation to the binding polynomial.

$$(1.19)\ \mathrm{RT}\beta = \text{-}\mathrm{RTln}\left(\sum k_i {a_3}^i\right)$$

Here Scatchard notation is used for the activity of water, protein, and ligand (a_1, a_2, a_3, respectively). Combining Equations 1.18 and 1.19:

$$(1.20)\ \ \mu_2 = \mu_2^o + \mathrm{RTln}(m_2) \text{-}\mathrm{RTln}\left(\sum k_i {a_3}^i\right)$$

Recalling our binding relationships:

$$(1.21)\ \Gamma_{2,3} \equiv \left(\frac{\partial m_3}{\partial m_2}\right)_{\mu_3,T,P} = \text{-}\frac{\partial \mu_2}{\partial \mu_3} = \nu$$

and noting that

$$(1.22)\ \ \mu_3 = \mu_3^o + \mathrm{RTln}(a_3)$$

$$(1.23)\ \text{-}\frac{\partial \mu_2}{\partial \mu_3} = \frac{\text{-}a_3}{\mathrm{RT}}\frac{\partial \mu_2}{\partial a_3}$$

Expanding the binding polynomial as follows

$$(1.24)\ \sum_{0}^{j} k_i {a_3}^i = 1 + \sum_{1}^{j} k_i {a_3}^i$$

where the index changes to start at 1 makes it clear that, from Equations 1.23 and 1.21:

$$(1.25)\ \Gamma_{2,3} = \frac{\sum i k_i {a_3}^i}{1 + \sum k_i {a_3}^i}$$

which much resembles the Hill equation. This shows that at 0 activity (no ligand in solution) there is also no molecules bound. As the concentration (and activity) of ligand increase the number of molecules bound increase until a point of saturation, just like the traditional ligand vs. occupancy curves reported in most biochemistry textbooks. **Figure 12.1** shows 5 ligand binding sites for (A) weak binding (k_d = 100 mM) and (B) moderate binding (k_d = 100 μM). Notice that for weak binding, the curves increase linearly and the separation is still increasing, even at high activities of ligand (~0.1). For the moderate binding scenario, saturation is achieved immediately.

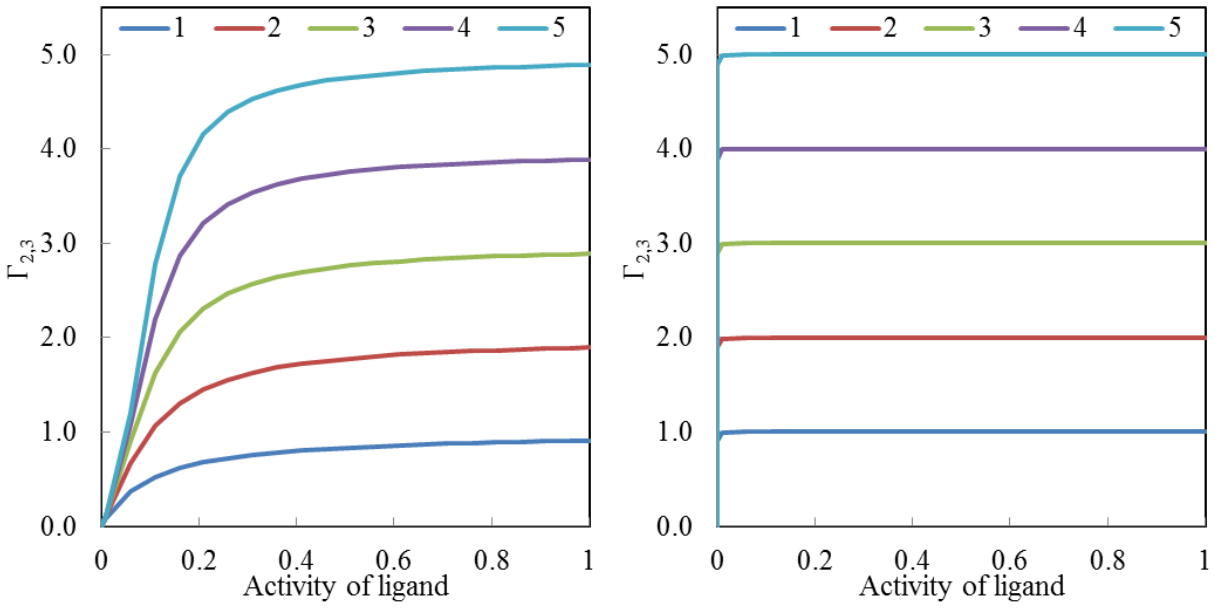

Figure 12.1. Preferential binding of 1, 2, 3, 4, or 5 ligands as a function of ligand activity for (A) weak binding (k_d = 100 mM) and (B) moderate binding (k_d = 100 μM). Model was created assuming independent site binding.

In the case of solvent denaturation, where are we on the occupancy vs concentration of ligand curve? Are we near saturation or is occupancy, or amount bound, still increasing? First we note that:

$$(1.26)\ \frac{\mathrm{dln(K)}}{\mathrm{dlnx}} = \Delta\nu = -\frac{1}{\mathrm{RT}}\frac{\mathrm{d}\Delta\mathrm{G}}{\mathrm{dlnx}} = \frac{-\mathrm{x}}{\mathrm{RT}}\frac{\mathrm{d}\Delta\mathrm{G}}{\mathrm{dx}}$$

Also we know, experimentally, solvent denaturation with urea and GnCl shows that ΔG is linear with concentration of denaturation, even at molar quantities. Two interesting situations to consider are 1. nearing saturation and 2. linear increase with concentration. If we are at saturation, Δν is constant with activity of ligand, this would result in a nonlinear function of dG with activity by equation 1.26. However, if we have extremely weak binding, where Δν increases linearly with activity, so does ΔG. Using this model, the ΔG as a function of ligand concentration for extremely weak binding (~0.75 M = k_d) and moderate binding (10 μM) binding for a Δν of 30 was calculated. **Figure 12.2** shows that for the moderate binding condition, the ΔG of unfolding becomes largely negative at very small activities of ligand, and then starts to level off. The ΔG of unfolding for the weak binding condition is decreasing across the entire range of activities and shows that it would take a high concentration of ligand to induce unfolding. This model, however, is not without flaw. Nonetheless, this type of analysis is useful for instructive purposes.

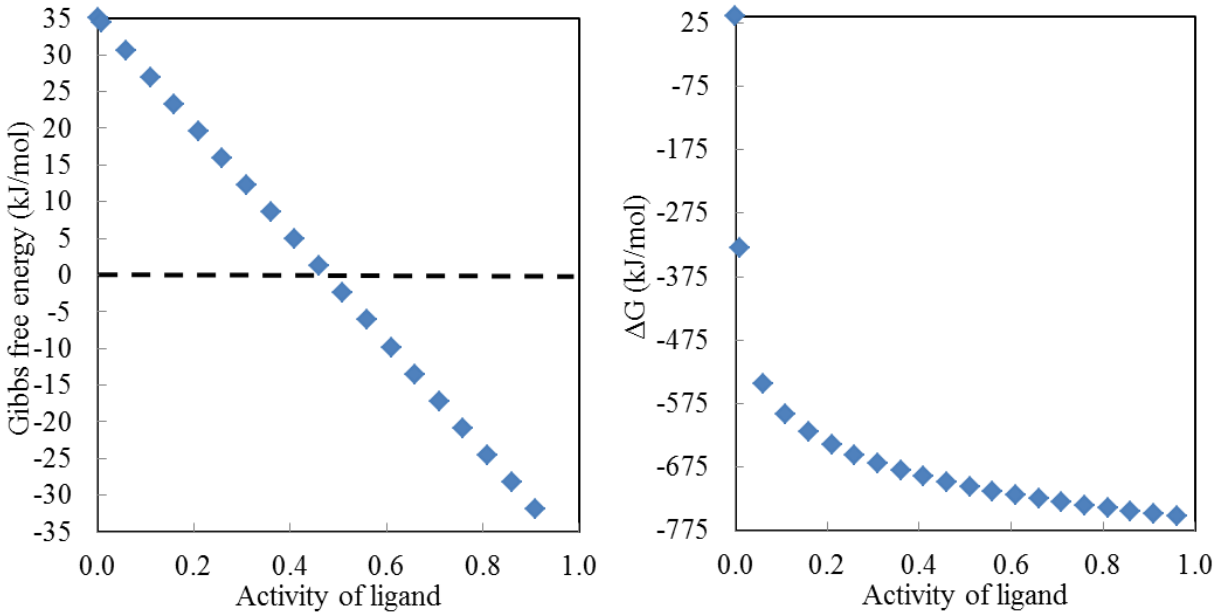

Figure 12.2. ΔG of unfolding as a function of ligand activity for an increase in ligand binding sites of 30 upon unfolding and a binding constant at all sites of (A) ~750 mM and (B) ~10 µM.

12.5 References

107. Schellman, J.A., *Selective binding and solvent denaturation.* Biopolymers, 1987. 26(4): p. 549-59.
115. Schellman, J.A., *The Relation between the Free-Energy of Interaction and Binding.* Biophysical Chemistry, 1993. 45(3): p. 273-279.
130. Greene, R.F. and C.N. Pace, *Urea and Guanidine-Hydrochloride Denaturation of Ribonuclease, Lysozyme, Alpha-Chymotrypsin, and Beta-Lactoglobulin.* Journal of Biological Chemistry, 1974. 249(17): p. 5388-5393.
134. Schellman, J.A., *The Thermodynamic Stability of Proteins.* Annual Review of Biophysics and Biophysical Chemistry, 1987. 16: p. 115-137.